THE BIODEGRADATION OF NEPHELINE BY ASPERGILLUS NIGER

by

Andrew King, B.Sc.(Hons.)

A thesis submitted for the degree of Doctor of Philosophy of the University of London, and for the Diploma of the Imperial College

Department of Mineral Resources Engineering,
Mineral Technology Section,
Royal School of Mines,
Imperial College of Science and Technology,
University of London.

February 1985

ABSTRACT

A literature review of factors influencing acid production and mineral degradation by filamentous fungi has been carried out with particular reference to the biodegradation of nepheline by Aspergillus niger.

Preliminary mineral and fungal appraisal tests were carried out to determine the combination of mineral and fungus suitable for a detailed study. These tests indicated that high grade nepheline was readily attacked by Aspergillus niger (CMI strain 31821). When grown under optimum conditions citric acid yields in excess of 90% (based on sucrose consumed) were obtained. By manipulation of the growth environment oxalic acid yields of up to 60% were obtained.

The kinetics of nepheline leaching by different acids and the biosynthesis of citric acid by Aspergillus niger were studied in detail. These data were combined (by means of a computer program) in a model to optimise the fermentation conditions for simultaneous maximum rates of acid production and mineral leaching. These conditions were checked experimentally. The nepheline leaching rate in acid solutions was directly related to the concentration of hydrogen ions. The reaction rate was controlled by a silica gel product layer coating reacting grains, and could be described by the Crank leaching model. Hydrogen and metal ions had an inhibitory effect on acid biosynthesis. This was attributed to the deactivation of cell wall functions and was adequately described by the Leudking and Piret model. The computer model indicated an equilibrium pH during leaching of 3.1± 0.5 which was consistent with physical reality and that above a nepheline concentration of 35 g/l acid biosynthesis would cease. In practice this value was 14 g/l. The break down of the model at high nepheline loadings was attributed to the extrapolation of sensitive data. Optimum leaching was obtained at nepheline loadings of the order of 8-10 g/l.

Semi-continuous fermentation-leaching apparatus was designed, built and operated under a range of conditions determined by the computer predictions. For an inlet nepheline concentration of 8 g/l and a dilution rate (flow/reactor volume) of 0.006 hr^{-1} , approximately 90% of added nepheline was leached to form sodium, potassium and aluminium citrates and silica gel. The fraction of nepheline reacted decreased with increasing dilution rate, until at a value of 0.05 hr^{-1}, the fraction of nepheline reacted was only 0.25.

A general economic assessment of the leaching process indicated that if oriented to the production of carboxylic acid metal salts, under certain conditions, it might be profitable.

ACKNOWLEDGEMENTS

My sincere thanks are expressed to the following:

Dr. A.W.L. Dudeney for his valued suggestions and advice given over the past three years,

Prof. H.E. Cohen for instigating the research into fungal leaching,

Dr M. Carlile, Mr. D. Shillam, Mr R. Shaw, Mrs E. Lewis, Mrs. J. Heeley and Mr. V. Harris for their helpful technical assistance and advice,

the Mineral Resources Engineering analytical services laboratory for chemical analyses and engineering workshop for the construction of leaching equipment,

the Department of Biochemistry for the use of autoclaves and other specialised equipment,

the Geology, Metallurgy and Petroleum Engineering Departments for the use of chromatographic, image analysis, electron microprobe and electron microscope equipment,

the Commonwealth Mycological Institute for identifying unknown fungi,

and finally to the Science and Engineering Research Council for financing this research including a visit to the Nephton district of Ontario.

LIST OF CONTENTS

	Page
ABSTRACT	i
ACKNOWLEDGEMENTS	ii
LIST OF CONTENTS	iii
CHAPTER 1 INTRODUCTION AND LITERATURE SURVEY	1
1.1 Introduction	1
1.1.1 Bacterial leaching	2
Sulphur and iron oxidising bacteria	3
Mineral leaching by bacteria producing organic acids	5
1.1.2 Fungal leaching	6
Mineral leaching by fungi producing organic acids	7
Mineral leaching due to metal absorption	8
1.1.3 Mineral degradation by other microorganisms	8
1.1.4 Aims of the project	9
1.2 Literature Survey	11
1.2.1 Growth and development of fungi	11
Spore production	11
Vegetative growth	12
1.2.2 Structure of hyphae	14
1.2.3 Sites of action of inhibitors	15
Intracellular	15
Cell surface	15
Extracellular	17
1.2.4 Other factors affecting chemical inhibition	17
Hydrogen ion concentration	17
Temperature	17
1.2.5 Growth kinetics of filamentous fungi	18
Lag/acceleration phases	18
Unrestricted growth phase	18
Restricted growth phase	22
Stationary/declining phases	23
Kinetic models taking account of differentiation along hyphae	24
Kinetic models of the complete growth cycle	25
Product formation	26
1.2.6 Metabolism in fungi	28
Primary pathways	29
Secondary pathways	29
Energy production	31
Mechanism of acid production by A.niger	33

Page

1.2.7 Cultivation of filamentous fungi to produce organic acids 36
Fungi used in commercial acid fermentations 36
A.niger 38
Other Aspergillus species 38
Penicillia 38
Rhizopus 38
Other fungi 38
1.2.8 Chemical and physical conditions affecting growth and acid production 39
Chemical environment 39
Alkali metals 39
Aluminium 41
Arsenic 41
Barium 41
Boron 42
Calcium 42
Cobalt 42
Copper 42
Halogens 43
Heavy metals 43
Iron 44
Magnesium 44
Manganese 45
Molybdenum 45
Strontium 46
Vanadium 46
Zinc 46
Nitrogen 47
Phosphorus 48
Sulphur 48
Silicon 49
Low molecular weight alcohols 49
Carbohydrates 50
Lipids 50
Carboxylic acids 51
Physical environment 51
Aeration 51
pH 54
Temperature 55
Agitation 56
1.2.9 Mineral degradation by fungi 56
Mineral alteration due to metal adsorption 57
Silicate leaching 57
Non-silicate leaching 58
Mechanism of silicate leaching 59

CHAPTER 2 ANALYTICAL, MINERALOGICAL AND BIOCHEMICAL METHODS 62

2.1 Analytical Methods 62

Page

2.1.1 Atomic absorption/emission spectroscopy 62
2.1.2 Gas-liquid chromatography 64
2.1.3 Electron microprobe (EMA) and scanning electron microscopy (SEM) 66
2.1.4 Omnicon image analysis 72
2.1.5 X-ray diffraction 75
2.1.6 Classical wet chemical analyses of saccharides 76
Titrimetric analysis of glucose and sucrose 76
Sucrose hydrolysis 79
2.1.7 Gravimetric analysis of citric acid 80
2.1.8 Determination of oxalic acid 81
2.1.9 Other analytical methods 82

2.2 Selection and Appraisal of Nepheline Bearing Samples 83

2.2.1 Preliminary mineral appraisal 89
2.2.2 Estimation of liberation sizes 91
2.2.3 Scheme of elemental and mineralogical analysis 94
2.2.4 Elemental analysis by fusion/EMA and by acid leach/AA 97
2.2.5 Mineralogical analysis by electron microprobe 99
2.2.6 Physical/chemical separations 104

2.3 Selection and Appraisal of Fungal Systems 112

2.3.1 Preparation of cultures and inocula 115
2.3.2 Typical fermentation procedure 119
2.3.3 Comparative fermentations producing carboxylic acids 121
2.3.4 Fermentations of A.niger CMI 31821 and A.niger CMI 243400 on nepheline discs 125
2.3.5 Optimisation of growth media for acid biosynthesis by A.niger 31821 133
2.3.6 Effect of chemical additives on citric and oxalic acid biosynthesis by A.niger 31821 138
Tests with methanol, sodium arsenite and sodium ferrocyanide 139
Tests with copper 142
Production of mycelium 143
Preparation of adsorption standards 144
Adsorption tests

2.4 General Conclusions 149

CHAPTER 3 MECHANISM OF NEPHELINE BIODEGRADATION WITH A.NIGER 31821 151

3.1 Rate of Reaction of Nepheline With Citric, Oxalic and Hydrochloric acids 152

Page

3.1.1 Preliminary experimental work 153
3.1.2 Typical experimental procedure 154
3.1.3 Results and discussion 155
Stoichiometry 155
Calculation of rate constants 159
Effect of sucrose on rate constants 164
Comparison of experimental and computer predicted curves of fraction of nepheline reacted with time for citric acid 167
Reaction mechanism 170

3.2 The Effect of Aluminium, Sodium, Potassium, Silicon and Hydrogen Ions on the Biosynthesis of Citric Acid By A.niger 177

3.2.1 Theoretical basis of calculation of K1 and K2 178
Theory of determination of μ1 and t1 180
Theory of determination of t2, kt1 and x2 during Ø1 182
Theory of determination of t2, kt2, x2 and x3 during Ø2 183
Theory of determination of K1 and K2 from dP/dt, dx2/dt and x2 186
3.2.2 Experimental procedure for the determination of K1 and K2 187
Fermentations 187
Calculation of K1 and K2 188
3.2.3 Results and discussion 190
Validity of growth, acid and deactivated cells 204

3.3 A Computer Model of Nepheline Leaching By A.niger 206

3.3.1 Prediction of acid produced, nepheline leached and pH with time 207
3.3.2 Results and discussion 218
Batch and continuous leaching 225
Bases for assumptions used in the model 229
3.3.3 Fermentations in the presence of nepheline 225
Results and discussion 232

3.4 General Conclusions 238

CHAPTER 4 SEMI-CONTINUOUS FERMENTATION-LEACHING OF NEPHELINE 240

4.1 Process Appraisal and Equipment Design 241

4.1.1 System appraisal 241
Fermenter 243
Leaching equipment 245
Product recovery 247

		Page
4.1.2	Design analysis	250
	Fluidised bed fermenter	250
	Recirculation pump	255
	Leach (buffer) tank	256
	Ion-exchange apparatus	257
	General specification of fermentation/ leaching equipment	258
4.2	Experimental Testwork	260
4.2.1	Typical operating procedure	261
4.2.2	Results and discussion	262
	Equipment performance	266
	Physical interaction of hyphae with mineral surfaces	267
4.3	Economic Evaluation of Fungal Leaching Processes	274
	Capital and operating costs of leaching equipment	278
REFERENCES		284
APPENDIX 1	Computer programs	302
APPENDIX 2	Estimation of nepheline grain size required for leaching apparatus	313
APPENDIX 3	Estimation of gas flow rate required for fermentation	314
APPENDIX 4	Operating and capital cost data	315
APPENDIX 5	Results of fermentations in the presence of nepheline	316
NOMENCLATURE		328

CHAPTER 1 INTRODUCTION AND LITERATURE SURVEY.

1.1 Introduction.

Microorganisms comprise viruses, bacteria, protozoa and fungi and algae. Ecologically they are a highly successful group of lifeforms as is shown by their ability to colonise diverse environments hostile to higher life forms. They are capable of very high metabolic growth rates. This is made possible by their large surface area to volume ratios and the short path lengths for diffusion of nutrients and products. Bacteria have been recovered from subsea volcanoes where pressures and temperatures are of the order of 260 atm and 105 C (1).

Microorganisms were first studied seriously after Pasteur and others discovered that bacteria could cause disease in man (2). Our dependence on an adequate food supply gave impetus to the study of plant diseases and soil fertility, which established the importance of microbes in the cycles of carbon, nitrogen, phosphorus and sulphur (3). Medical and agricultural microbiology continue to be important areas studied today.

The wider occurrence and characteristics of microorganisms have been studied in much less detail. Thus when samples of soil are studied to assess microbe populations there are always a significant number of unknown species. On this basis Hartley estimated that no more than 1% of microorganisms have been adequately recorded (4).

In recent years it has been demonstrated that microorganisms have a significant impact on the environment. Thus Silverman (5) indicated that the first inhabitants of freshly exposed rocks were photoautotrophic microorganisms which gained a firm foothold on otherwise sterile silicates. Heterotrophic microorganisms (mainly species of bacteria and fungi) could colonise silicates in numbers as high as 1.5×10^{5} /g of rock and one must assume that they benefit from this attachment. Jacks (6) concluded from numerous observations that the finer particles of mineral soils could not have been produced by purely mechanical action and were not produced by inorganic chemical weathering. He postulated that they might be produced by the action of living organisms on massive rocks and by subsequent decomposition of the organism leaving a clay-humus residue.

Of the microorganisms mentioned above bacteria and fungi appear to be the most effective mineral weathering agents and will receive greatest attention here.

1.1.1. Bacterial Leaching.

Bacteria are microscopic (averaging 0.5-2.0 µm in diameter) single-celled organisms of varied form (7). Bacteria which are able to assist in mineral leaching can be categorised into two groups. The first includes those deriving energy for growth from oxidation of mineral sulphides or inorganic ions in solution. In this case mineral leaching occurs either by direct attack on a sulphide in acid medium or indirect attack by a lixivant

such as aqueous Fe^{3+} generated by bacterial oxidation of Fe^{2+}. The second category includes those deriving energy for growth from the oxidation of organic compounds and producing organic acids as ancillary byproducts.

Sulphur and iron oxidising bacteria. Bacterial decomposition of sulphides is a natural phenomenon unknowingly harnessed by man for centuries in the recovery of copper from ores by weathering (8). The leaching of sulphide ores using sulphur bacteria has developed in recent times from an academic curiosity into a practical tool for the recovery of metals from low grade ores (9). There are now many bacterially assisted sulphide leaching operations which are used to recover copper or uranium (10-11). Other processes have been investigated, notably those making use of the desulphurisation properties of the bacteria to upgrade high sulphur coals and auriferous pyrite (12-13).

The sulphur bacterium of greatest commercial importance is Thiobacillus ferrooxidans (T.ferrooxidans). It is a rod shaped organism 0.5-0.8 µm in diameter and 1.0-2.0 µm long (Fig 1.1). Kelly (8) indicated that it can oxidise sulphides, ferrous iron, sulphur, soluble sulphur compounds (such as thiosulphate and tetrathionate) and possibly cuprous and stannous ions. The mechanism by which thiobacilli oxidise inorganic compounds is not fully understood. It is certain that the oxidation process furnishes the bacteria with metabolic energy (14), and must as a consequence be directly linked to metabolic processes within the cell. T.ferrooxidans is reported to leach

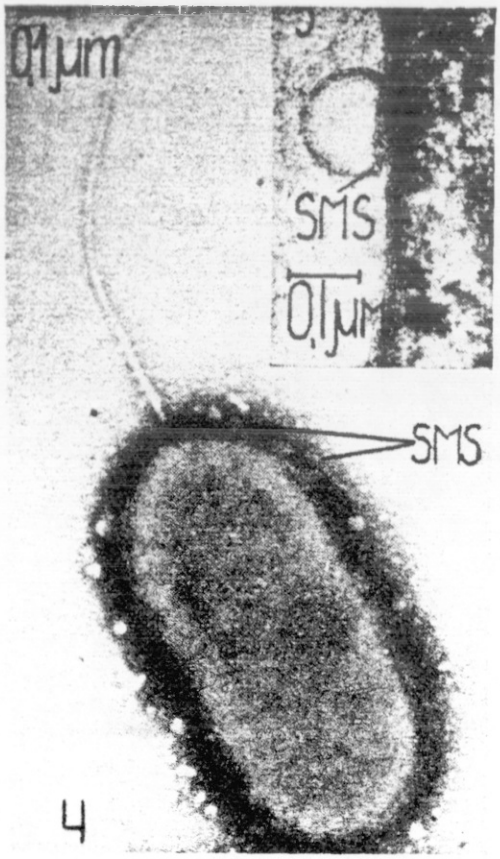


Fig 1.1 Electron photomicrograph of Thiobacillus ferrooxidans (14).

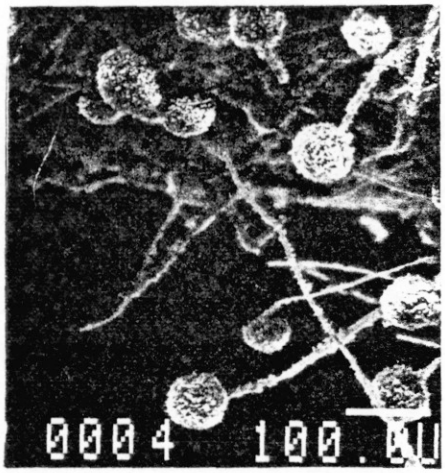


Fig 1.2



Fig 1.3

Electron and optical photomicrographs of the filamentous fungi Aspergillus niger.

sulphide and/or metal ions directly from their mineral lattice (8), onto which the bacterium becomes preferentially attached (14-16).

Commercial leaching processes can be based on direct or indirect oxidation of sulphides. Examples of the direct attack of T.ferrooxidans on sulphides are (3,8,9):

$$CuS + 2O_2 = CuSO_4 \quad (1.1)$$

$$2FeS_2 + 7O_2 + 2H_2O = 2FeSO_4 + 2H_2SO_4 \quad (1.2)$$

$$2Cu_2S + O_2 + 2H_2SO_4 = 2CuS + 2CuSO_4 + 2H_2O \quad (1.3)$$

Oxidation reactions catalysed by T.ferrooxidans and used for indirect attack of sulphides are (8):

$$4FeSO_4 + O_2 + 2H_2SO_4 = 2Fe_2(SO_4)_3 + 2H_2O \quad (1.4)$$

$$H_2S + 2O_2 = H_2SO_4 \quad (1.5)$$

$$2S^0 + 3O_2 + 2H_2O = 2H_2SO_4 \quad (1.6)$$

Sulphuric acid and ferric iron can dissolve sulphide and oxide minerals independently of thiobacilli and regenerate oxidisable substrates in Eqns (1.4)-(1.6):

$$Cu_2S + 2Fe_2(SO_4)_3 = 2CuSO_4 + 4FeSO_4 + S^0 \quad (1.7)$$

$$FeS_2 + Fe_2(SO_4)_3 = 3FeSO_4 + 2S^0 \quad (1.8)$$

$$UO_2 + Fe_2(SO_4)_3 = UO_2SO_4 + 2FeSO_4 \quad (1.9)$$

Mineral leaching by bacteria producing organic acids. Although a considerable body of literature is available concerning the production of organic acids by bacteria,

little is directly relevant to mineral leaching.

Duff et al. (17) used Pseudonomas fluorescens to convert glucose to 2-ketogluconic acid. They showed that the acid could be used to leach metals from a wide variety of soils, minerals and insoluble salts.

Bulgarian workers (18-19) have suggested that soil bacteria, particularly species of Bacillus, can secrete fatty and carboxylic acids which are able to degrade silicate minerals. A feature of silicate bacteria is their ability to form mucilaginous silicate capsules around growing cells, and it has been suggested that they require silicon for normal growth (20). Similar phenomena have been recognised in the adsorption of iron and manganese onto sheathed bacteria (Chlamydobacteriales) and Gallionella (3). It has been suggested that the accumulation of iron and manganese in sheaths and stalks of Gallionella is due to a build up of the end product of enzymic iron and manganese oxidation (21-23).

French workers showed that bacterial cultures grown on liquid media based on oatmeal, fish or blood could solubilise gold from gold bearing minerals (24). Bacterial lixivants responsible for leaching the gold were not reported. However other workers have suggested amino acids may be responsible (25,26). At present there are no industrial processes employing bacteria in this category.

1.1.2. Fungal Leaching.

Fungi are heterotrophic organisms, whose vegetative bodies are either composed of microscopic filaments called

hyphae, or form discrete cells, when they are termed yeasts (Figs 1.2-1.3) (27). Fungi are of global occurrence, surviving above the snowline, in desert regions and in the oceans (28). They are among the most fecund of all living organisms. Individuals of the species Lycoperdon giganteum can each produce $>10^9$ spores (29). They find wide application in the pharmaceutical and food industries (30). Muller and Loeffer estimated that 100,000-200,000 separate species had been recorded up to 1971 (31). No fungi capable of direct enzymic attack on minerals seem to have been reported. Two other activities, the synthesis of organic acids and absorption, have been identified as causes of mineral leaching by fungi.

Mineral leaching by fungi producing organic acids. Many fungi produce organic acids (33). Reports on mineral leaching by fungi indicate that the most aggressive lixivants are simpler carboxylic acids like acetic, oxalic, and citric acids (34). Evidence provided by commercial processes to produce carboxylic acids indicates that species of the genus Aspergillus are the most efficient known producers of acids in this category. Indeed most larger volume fermentations are limited to one species, Aspergillus niger van Tieghem (A.niger) (30). A patent by Miles Laboratories (35) indicated citric acid yields in the region of 90% which appears to be a general limit for the industrial citric acid processes using A.niger. Other factors influencing the choice of A.niger are the diversity of byproducts, its competetive behaviour with regard the growth of other organisms, and the low toxicity of the

fungus and its products.

A number of workers have demonstrated the mineral leaching ability of Aspergilli and other acidophilic fungi. Individual cases are considered in detail in Section 1.2.9. A.niger has been shown to leach iron and copper from various ores (36,37). Silicate minerals including biotite and leucite are also susceptable to attack (38,39). Species of Penicillium appear to be equally aggressive and have been shown to leach titanium from granitic rocks (40), and copper from various ores (41). Indian workers showed Paecilomyces variotii to be effective in leaching zinc from an oxidised ore (37).

Mineral leaching due to metal absorption by fungi. In their reviews of biodegradation of silicates both Le Roux et al. (34) and Silverman (7) noted that fungi can accumulate large amounts of potassium, and act as ion sinks in the presence of potassium bearing minerals. Fungi can also accumulate metals by adsorption (42-44). This is considered in greater detail in Section 1.2

1.1.3. Mineral degradation by other microorganisms.

Algae are simple plants ranging in size from single-celled organisms less than 1 μm across to giant multi-celled Pacific sea weeds that can grow to 180 m. They contain chlorophyll and therefore require sunlight and carbon dioxide in order to grow (45). The potential value of algae in mineral benefication lies in their ability to concentrate metals. Madwick and Ralph (46) noted that Hormidium fluitans could concentrate titanium, silver, and

vanadium by factors of 8000, 4000, and 500, respectively when grown on mine waste water. Copper was accumulated such that cell polymers contained approximately 0.2 % copper. Blue-green salt-water algae are very effective accumulators of heavy metals (47-49), and a water treatment process employing micro-algae has been described (50).

Lichens are dual plants formed by a fungus and a member of the alga group. The organisms coexist forming a true symbiotic relationship. Alga cells (phycobionts) contain green chlorophyll and manufacture sugars by fixation of carbon dioxide, they also provide the fungus with valuable nutrients (51). The fungus (mycobiont) provides inorganic nutrients and vitamins to promote photosynthesis and serves as a shelter for the alga cells to prevent drying out (51).

Lichens exude lichenic acids. These are complex molecules containing many functional groups suitable for chelation (34). Jenkins and Davis (52) indicated that mineral leaching by lichens is insignificant except in the case of rocks that weather rapidly. Other workers have shown that lichenic acids (including physodic, lobaric, squamatic acids) can leach iron from granite, greensand marl, muscovite and sandstone, but less efficiently than simpler carboxylic acids (53-55).

1.1.4. Aims of the project.

As mentioned, fungi such as Aspergillus niger can promote mineral leaching but relevant studies have been few and industrial applications nil. The present project is a new study of fungal leaching. It has the following general aims:

(1) to provide an introduction to mycology and review of the literature on acid production under the conditions envisaged in mineral leaching applications, and mineral leaching by fungi,

(2) to examine conditions for fungal leaching of silicates, particularly nepheline, and

(3) to design and test semi-continuous laboratory equipment for fungal leaching.

1.2 Literature Survey.

Fungi can be classified into three groups: macrofungi which produce large fruiting bodies (agarics); microfungi whose fruiting bodies are visible under the microscope (including those producing filamentous growth); and budding fungi commonly known as yeasts (Saccharomycetales). Individual species within groups can be split further according to character, into strains. Strains are categorised in terms of cell shape and size, growth rate, product formation, pigmentation, etc. (27). This work is concerned only with micro or filamentous fungi, particularly A.niger, and only this group will be considered in detail.

An understanding of the biology of fungi is a prerequisite to any authoritative study of bioleaching. In this context the following will be considered: the structure, development, and growth kinetics of fungi; aspects of metabolism related to acid biosynthesis; and the growth of fungi to produce acids. The ultimate goal here in elucidating the properties of fungal cells is to determine to what extent metals released during mineral leaching interfere with biochemical activities and, in particular, acid biosynthesis.

1.2.1. Growth and development.

Spore production. Fungi produce large numbers of spores, each representing a potential offspring, which secure their long term survival (56). Spores of each species are unique

and can be used for the purpose of identification (27). Spore production is normally triggered in response to a change in the environment which threatens the survival of the fungus (57). Spore producing apparatus grows as illustrated in Fig. 1.4, reproduced from Thom and Raper (27). Special branches, conidiophores, develop (A-B) and swell out at their apices to form vesicles (C-D). From the vesicles sprout protrusions called sterigmata (E-F) and these produce chains of conidiospores (spores) at their apices (G). All spores show a high degree of dormancy. This can be endogenous (having to be broken by heat shock, prolonged ageing, or certain chemicals) or constitutive (whereby germination begins once nutrients and water are present). Spores of A.niger are constitutive and require temperatures between 20 and 35°C, pH levels between 4.0 and 6.5, a relative humidity between 80 and 95%, and an adequate supply of nutrients before germination commences (57). Spores of certain species of Aspergillus can cause lung disease (endocarditis and aspergilloma) if inhaled (58). However the incidence of disease in man is very low.

Vegetative growth. The vegetative state of filamentous fungi called mycelium consists of microscopic strands called hyphae. Hyphae of most fungi are between 5 and 10 µm in diameter but can be as small as 1-2 µm and as large as 25 µm (59). Hyphae grow longitudinally by formation of new cell wall material at their tips. Branching occurs at frequent intervals enabling the fungus to grow at an exponential rate under favourable conditions (59,60).

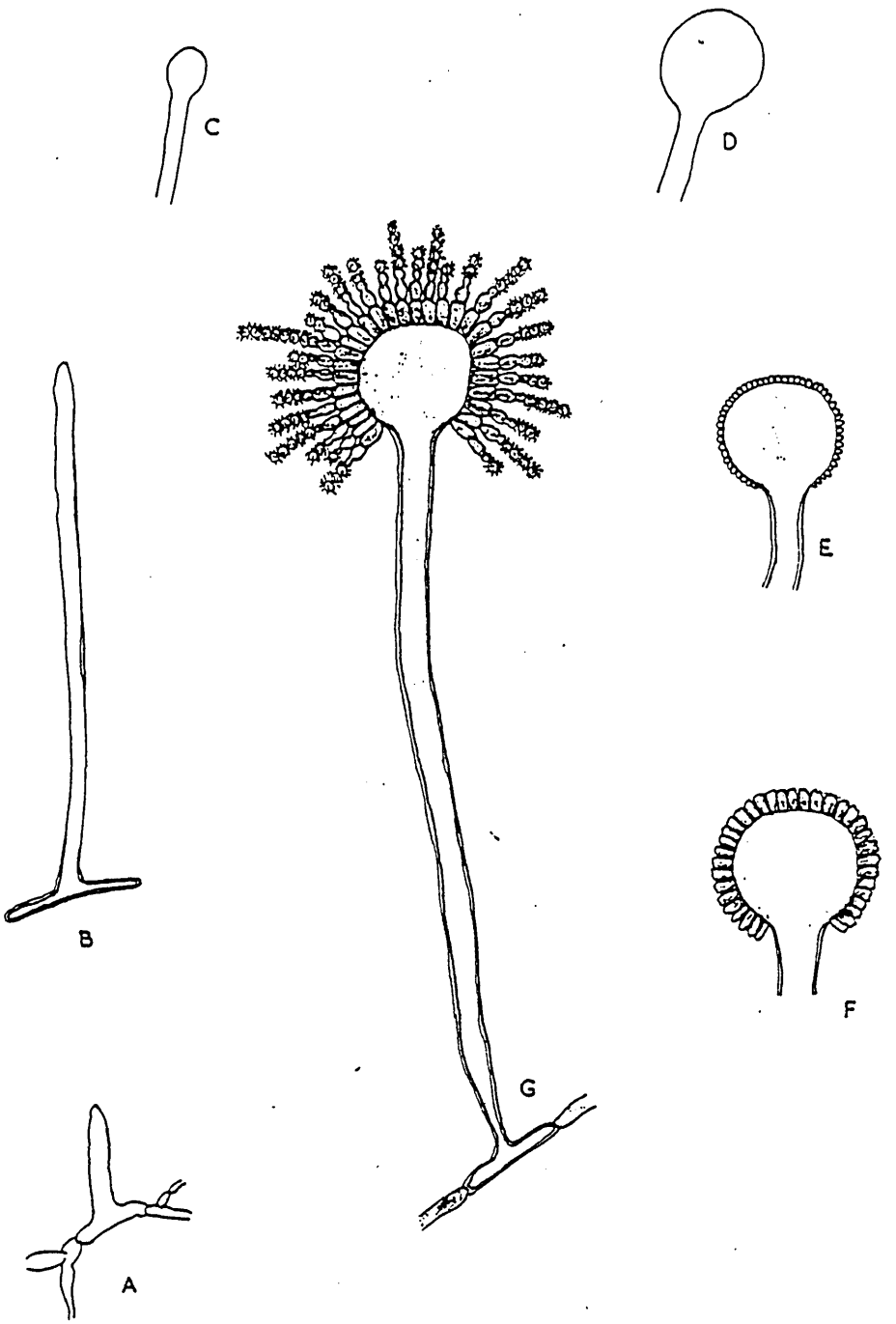


Fig 1.4 Stages in the development of spore bearing apparatus.

Protoplasm (the semifluid cell contents) continually moves forward to occupy newly formed areas and leaves behind an empty outer casing (61).

1.2.2. Structure of hyphae.

With the aid of electron microscopy it has been shown that the cell wall is composed of fibers within an amorphous matrix (62-64). The fibrous material provides a skeletal framework and is composed of interwoven microfibrils of chitin (65). Fibers have a high enough degree of crystallinity to be distinguished using X-ray powder diffraction techniques (66). The amorphous 'cementing ' matrix makes up 80-90% of the cell wall and is composed of polysaccharides (mannans, galactans, glucans, and heteropolysaccharides), proteins, lipids, and mineral constituents (65-68). Frey-Wyssling and Muhlethaler (62) produced evidence of laminations in the cell wall. Electron microscope pictures showed fibers to be orientated in different directions forming a laminate. Aronson and Preston (63) observed similar laminations in cell walls of Allomyces. All fungi are coencytic: the protoplasm is continuous throughout hyphae. In certain species hyphae are interrupted by crosswalls dividing hyphae into cells. In nearly all cases septa are incomplete (allowing protoplasmic continuity throughout hyphae) and probably only exist to strengthen the cell wall (30).

Besides having a protective function the cell wall acts to regulate uptake and release of substances to and from the cell. A membrane on the inside of the structure

controls this second function (69). Although the membrane and bulk structures are contiguous and difficult to distinguish they have been photographed by electron microscopy (70).

The cell wall/membrane is not an inert structure but rather a region of diverse enzyme activity (71). Enzymes play a significant role in the synthesis of new cell wall, intra- and extra-cellular breakdown of nutrients into fragments suitable for use by the organism, and the transport of inorganic nutrients both in and out of the cell (72-78).

Four different major transport processes are known to be active in the cell wall. Three are based on diffusion (79-80). In the other transport of substrate across the membrane occurs concomitantly with, and as a consequence of, chemical transformation of the substrate (80). It is not proposed to enter into this field of discussion.

1.2.3. Sites of action of inhibitors.

Intracellular. Many commercial fungicides operate inside the cell by disruption of vital processes. Access to the cell is gained by dissolving in the lipoid compounds which make up the cell membrane. Intracellular inhibitors are characterised by lipid solubility and include compounds like captan (81).

Cell surface. Polikarpov (82) noted that radioactive compounds are readily accumulated by microorganisms living

in sea water. Living and dead cells are equally effective. This was substantiated by Chiu (42) working with a fungal culture obtained from sewage sludge. Tsezos and Volesky (43), working with uranium and thorium, compared biosorption isotherms of cell wall preparations of six microorganisms with corresponding adsorption isotherms of a commercial ion exchange resin (IRA 400) and activated charcoal. Cell wall material from Rhizopus arrhizus was able to accumulate in excess of 180 mg metal/g fungus at pH 4.0, and at an equilibrium uranium concentration of 30 mg/l it removed approximately 2.5 to 3.0 times more uranium than IRA 400 and activated charcoal respectively. Horikoshi et al. (44) studied the uranium biosorption of forty two microorganisms. They indicated that biosorption capacity was affected by pH and the carbonate ion concentration but not by temperature or metabolic inhibitors. Uranium could be washed off cell wall material by aqueous ethylenediamine tetraacetic acid (EDTA) suggesting that the accumulation was a physiochemical adsorption rather than a biological reaction. The uptake of uranium accurately fitted Freudlich's adsorption model (83). The high ion exchange capacity of natural polysaccharides similar to those making up the amorphous matrix of cell walls is well known (84). Bivalent metal ions can exchange with counter ions of the polysaccharide as indicated below for alginic acid.

$$2NaAlg + M^{2+} = MAlg_2 + 2Na^{+} . \qquad (1.10)$$

Excessive adsorption of heavy metal ions (including

silver, molybdenum and cadmium) usually inhibits fungal growth. Somers (85) suggests that the toxicity of metal ions, of low lipid solubility, is a result of accumulation in cell wall material where important receptor sites or enzymes are deactivated.

According to Brown and Silzer (86) the toxicity of surface active agents (e.g., n-dodecylguanidine acetate) is a result of blockage of vital anionic sites at the cell surface.

Extracellular. Fungi can excrete enzymes into the environment to break down nutrients into a form suitable for absorption into the cell. Amylase is secreted by Aspergilli in order to break down disaccharides (starch) into monosaccharides (maltose) (87). Many fungi including A.niger synthesize the enzyme cellulase (88). This is used to split the cellulose molecule into glucose units. Both enzymes are deactivated by metals such as silver, copper, mercury and iron (89).

1.2.4. Other factors affecting chemical inhibition.

pH. The effect of pH on the toxicity of inhibitors was discussed at length by Albert (90). He concluded that, in general, undissociated molecules were more toxic than hydrated ions at low pH. However other workers have shown that the toxicity of copper sulphate and mercuric chloride decrease with decreasing pH (81).

Temperature. Under normal circumstances the rates of enzymically controlled reactions increase with temperature up to the point at which enzymes suffer from thermal

deactivation. For the majority of enzymes this temperature lies between 60-90 °C (91). Many chemical inhibitors cause premature deactivation. Kitos et al. (92) demonstrated that inhibition of citric acid biosynthesis by copper, zinc, manganese and iron in A.niger increases with temperature. The conversion efficiency of sucrose to citrate decreased from 75% to 45% upon raising the temperature from 25 to 35 °C using metal loadings optimised for acid production at 25 °C. This is to be expected since both the rate of adsorption of metal ions onto the cell wall and the rate of enzyme deactivation would be expected to increase with temperature.

1.2.5. Growth kinetics of fungi.

The growth cycle of fungi can be split into six distinct stages as indicated on Fig. 1.5, reproduced from Trinci (93): the lag, acceleration, unrestricted growth, deceleration, stationary and declining phases. Depending on the growth conditions some can be small or absent.

Lag/acceleration phases. The rate of growth can be equal or close to zero either if spores are at the germination stage, or the environment of a system containing mature cells is substantially altered (56). In each case the lag is a result of spores or mature cells adapting growth apparatus to meet the requirements imposed by the new environment. After germination, and under favourable conditions, the cell mass increases rapidly.

Unrestricted growth phase. Kinetics to describe the (third) stage differ according to the morphology of the

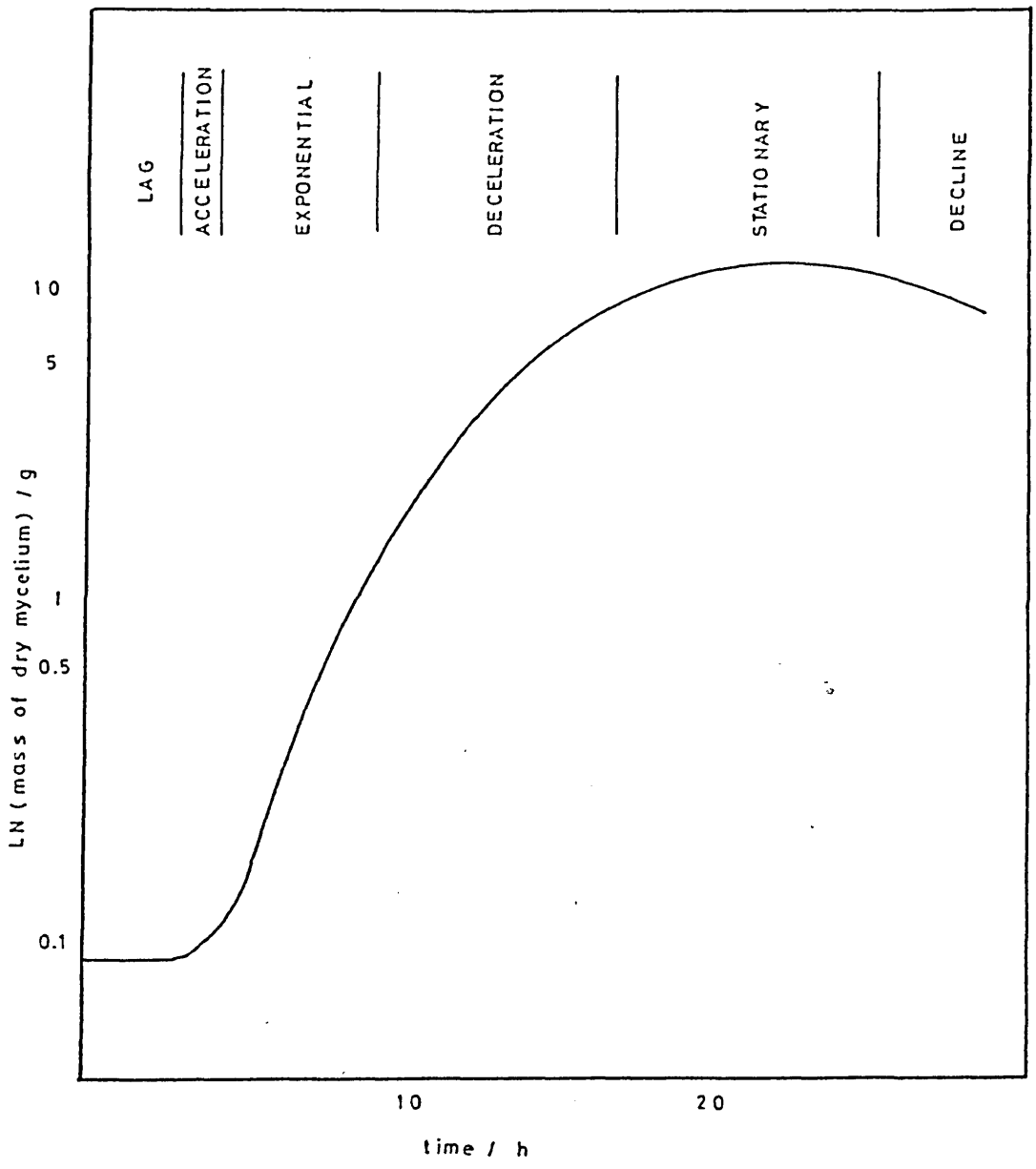


Figure 1.5. Graph of logarithm of mycelium dry weight as a function of time to show stages in the growth cycle of fungi.

cells produced. Three types of cell have been described for A.niger (94). They are: discrete cells that closely resemble a yeast; compact or floccose pellets; and true filamentous forms composed entirely of discrete long, branched, strands of cells. Autocatalytic growth will occur so long as there is no restriction to the flow of nutrients to cells. Optimum cell performance is obtained with a 'balanced' medium, that is one affording the maximum growth rate. Such a medium has been described by Steinberg (95) for A.niger. The medium he formulated was so well balanced that a decrease in the concentration of any single nutrient resulted in diminished growth.

Compact pellets of fungi are less permeable than discrete cells or filaments. The difference in accessibility of nutrients gives rise to two distinct kinetic growth models according to whether fungi are predominant as dispersed filaments or pellets.

(a) Dispersed filament model. Unrestricted growth of a fungus in its filamentous form, in the absence of growth inhibitors and in the presence of excess nutrients, is normally exponential (59,93,96). Growth can be represented by

$$dx/dt = ux \qquad (1.11)$$

where the specific growth rate, μ, is a constant characteristic of the strain and growth conditions used, x is the cell mass and t represents time. Eqn (1.11) can be integrated to give the mass of cells, x(t), at any time t:

$$x(t) = x(0)e^{\mu t} \quad (1.12)$$

$$\text{and} \quad \text{Ln } x(t) = \mu t + \text{Ln } x(0) , \quad (1.13)$$

where x(0) and x(t) represent the total cell masses at times 0 and t, respectively. A logarithmic relationship is convenient for graphical representation. Exponential or autocatalytic growth is indicated when a linear relationship exists between Lnx and time as shown on Fig. 1.5.

(2) Pellet growth. Pirt (97) suggested that when fungi are grown as discrete or floccose pellets, nutrients would not diffuse inwards fast enough to maintain exponential growth throughout the whole pellet. Yano et al. (98) considered that the diffusion of oxygen into the pellets was the rate limiting step controlling fungal growth and indicated that this could lead to a cube root model. Righelato (99) noted that this is likely to occur because the pellet mass is proportional to the cube of its radius whereas the surface area is proportional to the square of its radius. He suggested that pellets comprise a dead core surrounded by a peripheral shell which is growing exponentially and whose thickness depends upon the availability of nutrients. Hence

$$dx/dt = \mu xp \quad (1.14)$$

where xp is the mass of the peripheral growth zone of the pellet, and

$$dr/dt = \mu w ,$$

$$\text{or} \quad r = \mu w t + r(0) . \qquad (1.15)$$

In Eqns. (1.15) and (1.16) r and r(0) represent overall pellet radii at times 0 and t, respectively, and w is the thickness of the peripheral growth zone. Substituting the mass x for pellet radius r gives

$$x^{1/3} = \mu w t (3/(4\pi D))^{-1/3} + x(0)^{1/3} . \qquad (1.16)$$

Thus the growth of a single pellet, of uniform size, is predicted to follow a cube root growth pattern once r is greater than w. While r is smaller than w exponential growth would occur.

Restricted growth phase. It is clear that cells do not continue with exponential or cubic growth as the theoretical yield of cells for one week's growth (assuming x(0)=1 mg and a doubling time of 3h) would amount to several million tonnes. Deceleration in the growth rate occurs in response to the exhaustion of nutrients and the build up of toxic products. Kinetics governing the deceleration stage have been studied by many workers using principles derived for bacterial and yeast cultures (100-103).

Monod (100) considered growth deceleration in response to exhaustion of substrate. The Monod equation can be written as (352)

$$dx/dt = x[\mu(max)(S/(k_s+S))] . \qquad (1.17)$$

In this equation $\mu(max)$ is the maximum specific growth rate and is a constant. The square brackets represent μ in Eqn. (1.11), k_s is defined as the saturation constant for uptake of the growth limiting substrate, and S is the concentration of the growth limiting substrate. During unrestricted growth $S \gg k_s$ and μ tends to $\mu(max)$. Once S approaches k_s the specific growth rate declines rapidly and eventually tends to $\mu(max)/k_s$.

Contois (103) extended Monod's work indicating that there is a linear relationship between uptake of a growth limiting nutrient and production of cells up to the start of the deceleration phase. He showed the relationship was valid for carbon, nitrogen, sulphur, and phosphorus as limiting nutrients in the growth of the bacterium Aerobacter aerogenes. Other workers (113,114) have inferred the relationship to be equally valid for filamentous fungi.

Some data have been fitted to a logistic law of the form

$$dx/dt = \mu x(1-cx) \quad , \qquad (1.18)$$

where c is a constant (107). This allows for a decrease in the growth rate as the organism mass increases but is of limited value as it cannot be used to assess the cause of the diminishing growth rate.

Stationary/declining phases. Eventually a stage is reached when the bulk cell mass becomes constant and then slowly decreases due to lysis (Fig. 1.5). During this stage the fungus breaks down byproducts and dead cell material until the energy obtained from any further break down is

insufficient to support the organism (106). Sinclair and Topiwala (107) added a term to take account of decay in cell growth.

$$dx/dt = x\mu(max)[S/(k_s+S)] + \gamma x \qquad (1.19)$$

where γ is a cell death constant. This model was also used by Chiu et al. (108).

Kinetic models taking account of differentiation along hyphae. According to Zalokar(59) there is differentiation along hyphae. He indicated that the tip is active in synthesis of cell wall material, the median portion of the filament has most other processes and the posterior portion is empty of functioning protoplasm. Thus models describing unrestricted, restricted and stationary growth phases are interrelated.

Kjeldgaard et al. (109) indicated that in Penicillium chrysogenum the ribonucleic acid (RNA) concentration and growth rate are closely interrelated. Fencl (110) studied RNA synthesis at different stages in the growth of A.niger. The RNA concentration did not decrease gradually from newer to older cell material but occurred at random along filaments, in disagreement with the findings of Kjeldgaard et al. Machek and Fencl (111) suggested that differentiation of cells along filaments must be taken into account when modelling the growth kinetics of fungi. Working with A.niger, using a batch fermentation and nitrogen limitation, they distinguished unrestricted,

restricted, and stationary phases of growth. They noted that during the unrestricted or 'growth' phase there were no significant differences between the biochemical activities of different cells whereas, during the restricted phase, differences were considerable. They also noted that hyphae could elongate according to either linear or exponential rules, but that there were many transient, intermediate, types of growth. Megee et al. (112) developed a kinetic model which took account of differentiation along hyphae. Although their model may have some theoretical basis it is too complicated for simple application. It contained fourteen Michaelis-Menten constants, nineteen rate constants, and ten stoichiometric constants.

Kinetic models of the complete growth cycle. In a number of studies attempts have been made to model the whole growth cycle taking account of transitions between different growth phases. Khan and Ghose (113) used an equation of the form

$$dx/dt = k\emptyset x \quad . \qquad (1.20)$$

In this equation k is a constant and $\emptyset$ is a growth coefficient which varies according to the growth phase. A value of $\emptyset=0$ corresponds to the lag phase, $0<\emptyset<1$ corresponds to a transient phase and $\emptyset=1$ corresponds to the exponential phase. The deceleration phase corresponds to

$$\emptyset = xc(xm-x)/x(xm-xc) \quad , \qquad (1.21)$$

where xm is the maximum theoretical cell concentration and xc is the concentration at the beginning of the stationary phase.

Kristiansen (114) distinguised between cells oriented to growth, of mass xb, cells oriented to production of citric acid, of mass xc, and cells deactivated with regard acid production, of mass xd. He used simple mathematical relationships to describe each phase and included a term to account for the transition from one phase to another. The models correspond closely with Eqns (1.11) and (1.17) for unrestricted and restricted growth. For continuous fermentation his equations take the form:

$$dxb/dt = \mu bxb - Dxb - ktxb - kxb \quad (1.22)$$

$$dxc/dt = \mu xc + ktxb - Dxc - kcxc - kdxc \quad (1.23)$$

$$dxd/dt = kdxc - Dxd \quad . \quad (1.24)$$

The terms kt and kd are coefficients related to the transition from cells oriented to growth, xb, to cells oriented to acid production, xc; and from xc to inactivated cells, xd, respectively. Terms k and kc are respiration coefficients associated with growth and acid production respectively, accounting for carbon dioxide losses. The dilution rate, D, is defined as the flow rate divided by the fermenter volume. For batch leaching terms containing D should be neglected.

Product formation. In view of the fact that the mechanisms for the accumulation of extracellular products are not fully understood any attempt to mathematically

model the complex metabolic processes leading to acid synthesis would be difficult. Simple models all follow the same relationship, which was first described by Luedking and Piret (115). These workers studied the production of lactic acid by the bacterium Lactobacillus delbrueckii and showed that the instantaneous rate of acid production dP/dt, could be related to the instantaneous rate of bacterial growth dx/dt, and the cell mass x. The following relationship was proposed,

$$dP/dt = \alpha dx/dt + \beta x \qquad (1.25)$$

where α and β are constants. By manipulating values of α and β the equations can account for growth associated products, non-growth associated products and intermediary product formation. The same model was used by Kono and Asai (116), and by Khan and Ghose (113) to describe the formation of citric acid by A.niger.

Eqn (1.25) does not account for product loss, either by consumption as a substrate or break down by enzymes. Constanides et al. (117) included a break down term to account for product loss:

$$dP/dt = \alpha dx/dt + \beta x + \gamma P \quad , \qquad (1.26)$$

where γ is a product loss constant. Shu (118) derived a relationship in terms of cell age assuming constant environmental conditions. The relationship took the form,

$$dP/d\emptyset = \sum_{i=1}^{n} Aie^{-ki\emptyset} \qquad (1.27)$$

where $\emptyset$ is the cell age and Ai and Ki are constants. He suggested that Luedking and Piret's model was merely a special case of his own with i=2:

$$dP/d\emptyset = A1e^{-k1\emptyset} + A2e^{-k2\emptyset} \quad . \qquad (1.28)$$

1.2.6. Metabolism in fungi.

An essential element in fungal growth is the break down of foodstuffs to provide energy. This energy can be liberated as heat, used for mechanical work or stored for use in making materials required by the cell (119). Energy is stored in the pyrophosphate bonds of adenosine triphosphate (ATP) which is present in all lifeforms known to man (120). Sequences of biochemical reactions which enable fungi to activate pyrophosphate bonds in ATP at the expense of free energy liberated during the degradation of foodstuffs; and convert nutrient foodstuffs to complex molecules which constitute the fungal cell, are termed metabolic pathways and take place within the cell.

The break down of nutrients can be split into three stages (Fig. 1.6) (121). The first two liberate approximately 1/3 of the energy available to the cell and provide the chemical precursors for the third, where the remaining 2/3 is liberated. The thermodynamic efficiency is high and of the order of 70% (119). Stage three is

responsible for the accumulation of carboxylic acids.

For simplicity fungal metabolism is usually considered in two parts termed primary and secondary biosynthetic pathways. These represent the sequences of reactions, and their interrelationships with one another, which are functioning during optimum and sub-optimum cell biosynthesis, respectively.

Primary pathways. Primary pathways operate when the fungus is cultured under optimum chemical and physical conditions for cell biosynthesis. The optimum growth rate (corresponding to a maximum value of μ), which as indicated in Section 1.2.5 can be exponential, is achieved when the growth rate is restricted by genetic characteristics of the organism since nutrients and enzymes are usually present in excess (122).

Secondary pathways. Biosynthetic reactions continually self-regulate to suit the cell's needs according to the concentrations of nutrients available. Secondary pathways become operational when a nutrient necessary for cell synthesis becomes exhausted and can be considered as adaptations of primary pathways regulated to make use of any alterntive nutrient or mineral (123). It is considered that secondary metabolism is largely enzyme limited (i.e. reactions making up secondary metabolic pathways become operational when enzymes necessary for primary reactions are largely exhausted), although there is surprisingly little direct experimental evidence for this generalisation (353). Owing to the large number of contributory reactions and difficulties associated with

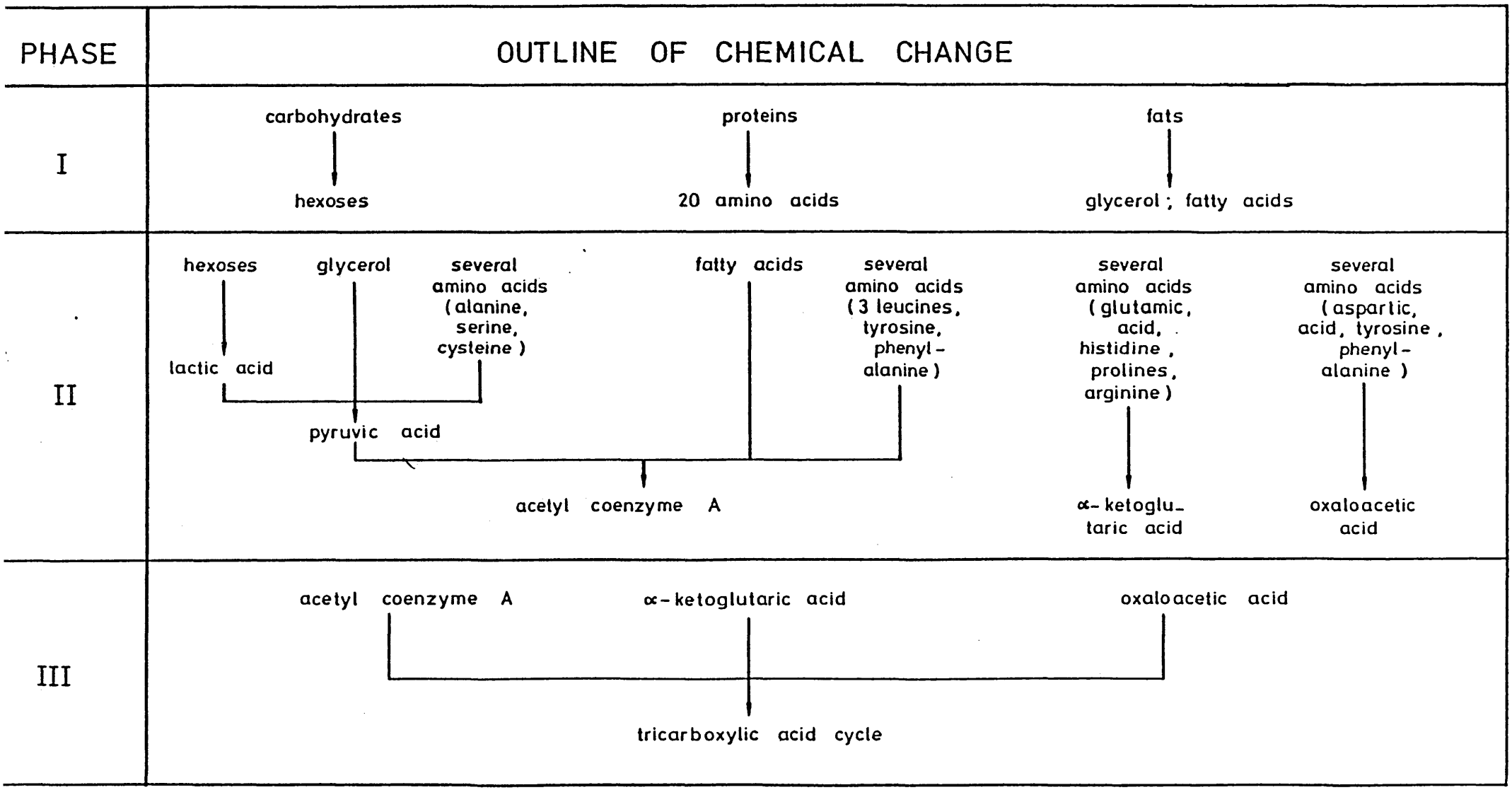


Fig. 1.6: The three main phases of energy production from foodstuffs.

enzyme limited reactions, the quantitative/regulatory aspects of secondary biosynthetic pathways are not as well understood as for primary pathways.

It is generally considered, although not proven (see pages 33-34), that organic acid production in A.niger is a secondary metabolic function. Currie (124) noted the stepwise break down of sucrose to carbon dioxide by A.niger. The first step resulted in the appearance of citric acid . This was re-absorbed and oxalic acid appeared in its place. Finally oxalic acid disappeared and carbon dioxide was produced.

Currie suggested that each step resulted in the fungus recovering chemical energy, based on the stepwise reduction of Gibbs free energy of the products. For this reason citric acid is often referred to as an energy storage product (125).

Energy production. Stage three of the break down of foodstuffs to energy (referred to in the introduction to this section), takes place in discrete compartments called mitochondria (126). In stage three, three major precursors of stage two (acetyl coenzyme A, ketoglutaric acid and oxaloacetic acid) are oxidised to carbon dioxide and water (127). During this process a series of di and tri carboxylic acids appear as intermediates (Fig 1.7)(127). In the cycle, commonly known as the Krebs or Tricarboxylic acid cycle (TCA cycle), during one complete turn one acetate equivalent is completely oxidised to carbon dioxide and water (127). There is continual tapping off of intermediate acids to serve as precursors for cell

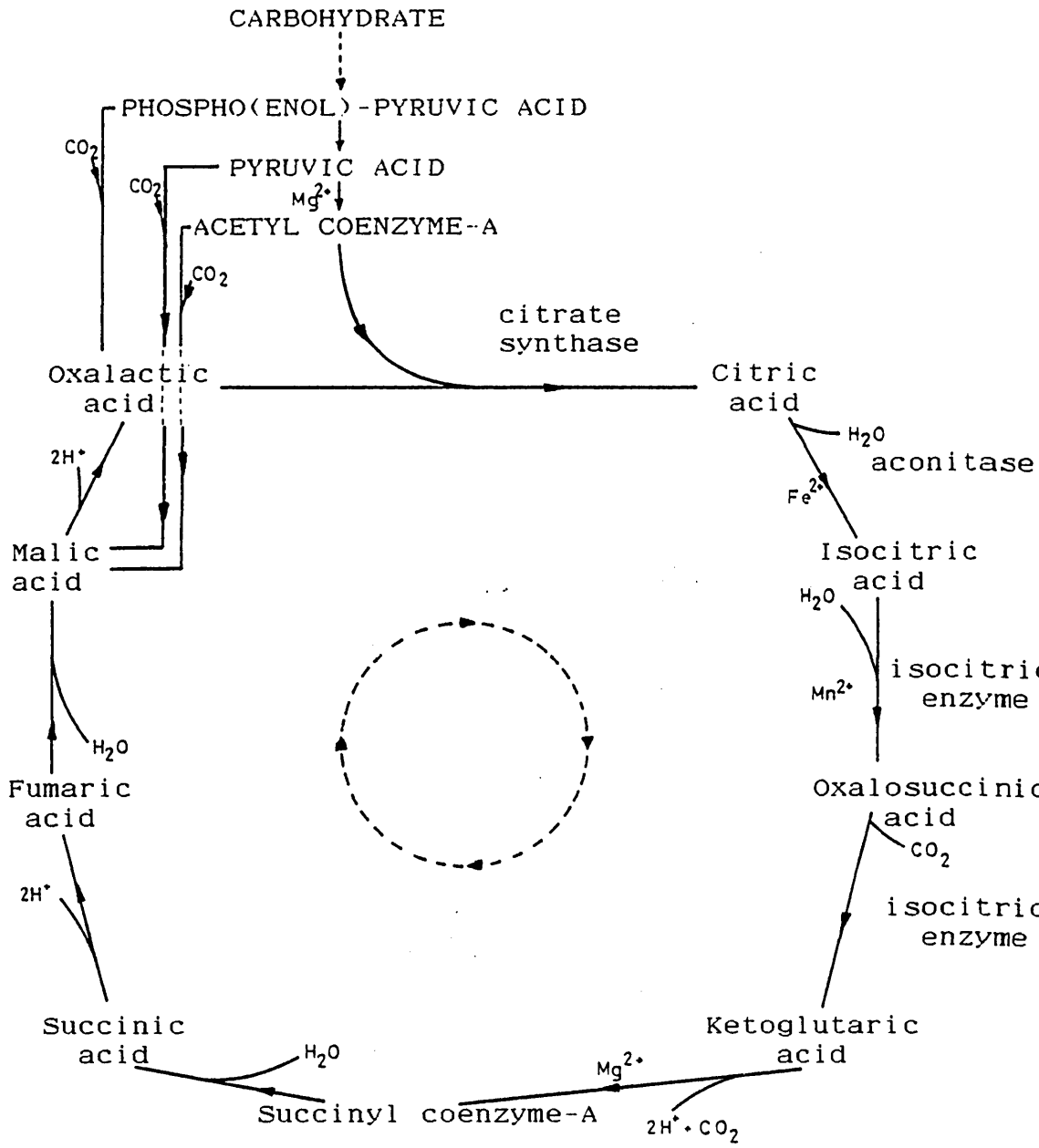


Fig 1.7 Simplified Tricarboxylic Acid Cycle (TCA cycle) with ancillary CO_2 fixation reactions.

biosynthesis reactions which complicates the overall picture (128). The resulting deficit of intermediary acids must be replenished in order to balance the cycle. Besides increasing the flow of the three main precursors to the cycle, three other ancillary pathways have been reported which inject acid intermediates into the cycle (128). These involve carbon dioxide fixation. They are included in Fig 1.7 for completeness but are not discussed any further.

Little has been said about the enzymes which regulate the equilibria between the different acids around the cycle. These enzymes are only present in mitochondria (129). They often require the presence of specific metal ions to be active but are rapidly deactivated by the wrong metals (130). The activation and/or deactivation of specific enzymes has been proposed as the cause of accumulation of specific acids via the TCA cycle. This is discussed below.

Mechanism of acid production by A.niger. There have been numerous reports concerning the mechanism of acid biosynthesis by Aspergilli. Cleland and Johnson (131) showed that accumulated citric acid was not broken down as part of the TCA cycle and all the acid came from the condensation of a two carbon (acetyl) with a four carbon (oxaloacetic) compound. Shu et al. (132) showed that 40% of citric acid was formed via recycled dicarboxylic acid and indicated that the TCA cycle was fully operational. Bloomstein and Johnson (133) also found that the cycle was operational during acid production. This was supported by La Nauze (134) and later by Ahmed (135).

Ahmed et al. (136) presented evidence that the activity

of TCA cycle enzymes was as high during the growth stage as during the acid production stage. These results support those of La Nauze (134) but disprove the theory of Ramakrishnan et al. (137) that over production of citrate occurred because of a flow restriction in the TCA cycle caused by the disappearance of aconitase and isocitrate dehydrogenase (Fig. 1.7). In the work of Ahmed et al. it is interesting that the activity of citrate synthase, responsible for the appearance of citrate, was significantly higher than all other enzymes during fermentation.

A different approach concerning the mechanism of acid synthesis was used by Verhoft and Spradlin (138). They applied mass and energy balances to a citric acid fermentation and derived a metabolic scheme to explain citrate accumulation from the results. The scheme is set out in Fig. 1.8. It assumes a total breakdown of the TCA cycle, in disagreement with both La Nauze and Ahmed.

Metals have a critical influence on acid biosynthesis, particularly on the accumulation of citrate (134). Mechanisms involved are not understood, particularly since metals involved are taken up into fungal cells very slowly (139). The observed effects of different metals and other compounds on fungi are discussed in detail in the next section.

In conclusion, although it is generally accepted that an intermediate reaction in the biosynthesis of citrate is the condensation of acetyl-coenzyme A with oxalacetate there is no direct evidence that the TCA cycle is involved and no

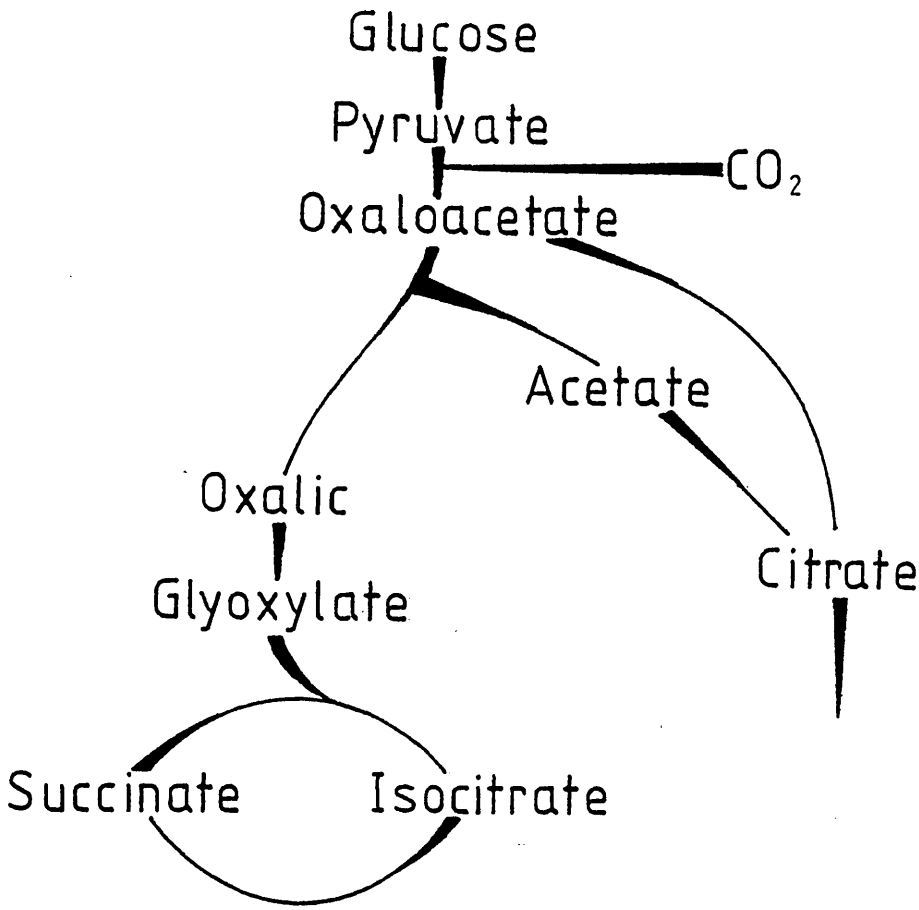


Figure 1.8 Metabolic scheme of Verhoff and Spradlin to describe synthesis of citric acid.

one has been able to explain how metals disrupt acid biosynthesis.

1.2.7. Cultivation of filamentous fungi to produce organic acids.

In 1923 Chas. Pfizer and Co.Ltd. commenced production of citric acid from sucrose using A.niger (140). Other filamentous fungi have since been used to produce other carboxylic acids on a large scale and many others identified as producers of carboxylic acids (Table 1.1) (141). A brief account is given below of the current state of the art of commercial acid production.

Fungi used in commercial acid fermentations.

Aspergillus niger. A.niger is used on a large scale to produce citric and gluconic acids from sucrose and glucose respectively (142,143). Oxalic acid can also be produced (144).

Early processes were based on 'surface' fermentation where the fungus floats as a mat on liquid growth medium in shallow aluminium pans. A full description of the process was given by Mallea (145). According to Schierholt (146) surface fermentation is most economic for small scale operation (<5tonnes/year) using low grade molasses. However, it is still practiced on a large scale by Pfizer and other major producer (147). Submerged processes based on fungus pellets are also used (142). Although considerably more expensive in terms of capital costs, much higher product formation rates are possible than with

TABLE 1.1 IMPORTANT ACID PRODUCTS PRODUCED BY FUNGI.

Acid	Fungi and CMI strain number(s)
citric	Aspergillus carbonarius(41873), A.foetidus (15594), A.niger(27809, 41874, 51433, 75353, 84304).
fulvic	Penicillium grieseofulvum (75832).
fumaric	Aspergillus terreus (89356), A. fumaricus (16141), Penicilluim grieseofulvum (75832).
gluconic	Aspergillus carbonarius(41873), A.niger (41876), A.wentii(23010), Caldariomyces fumago(89362).
itaconic	Aspergillus terreus(44243,89357,126254), Penicillium fellutanum(40232).
lactic	Rhizopus oryzae(40564).
malic	Cochliobolus specifer(91972).
oxalic	Aspergillus terreus(89355,89356), A.niger (243400).
succinic	Aspergillus terreus(17294,89356), Caldariomyces fumago(89362), Cochliobolus spicifer(91972).

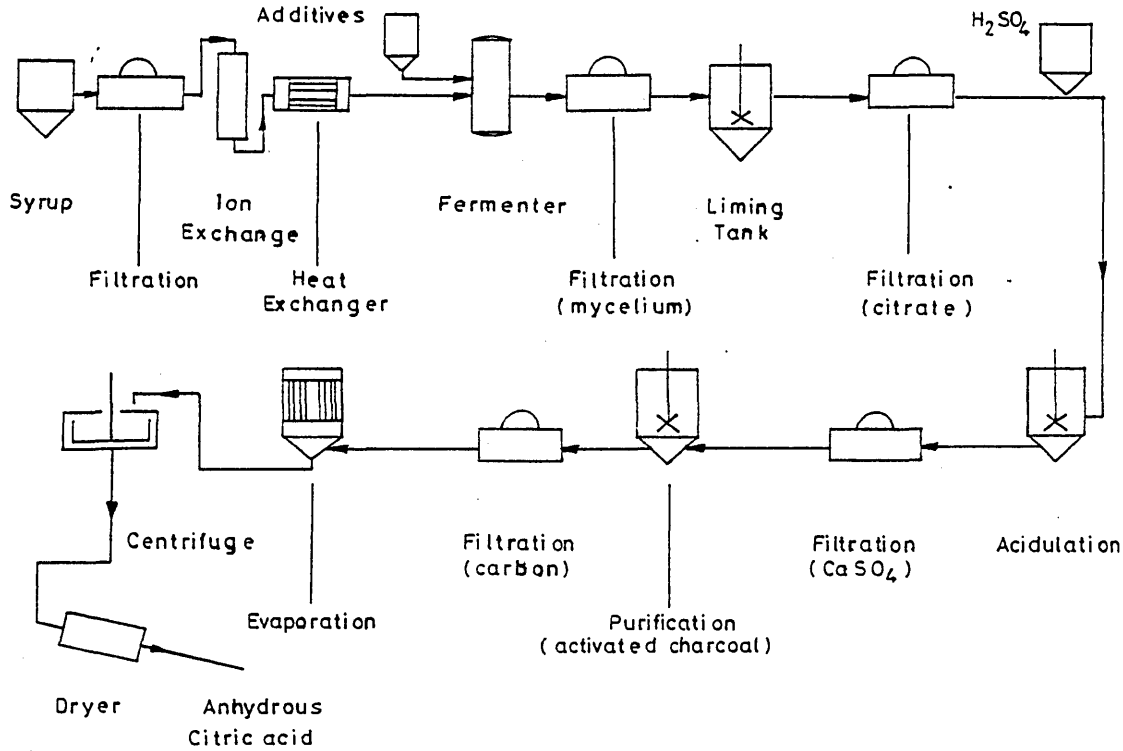


Fig 1.9 Schematic representation of a typical submerged citric acid fermentation process.

equivalent surface processes. For this reason Schierholt indicated that submerged fermentations are better suited to large scale high throughput operation (>5tonnes/year). A typical flowsheet for the manufacture of citric acid is set out in Fig. 1.9 (149).

Other Aspergillus species. A.clavatus, A.wentii and A.luchuensis have all been used by Miles Laboratories (35) to produce citric acid with varying degrees of success. A.itaconicus and A.terreus have both been used to produce itaconic acid from inexpensive carbohydrates (150).

Penicillia. May and Herrick (151,152) used P.luteum-purpurogenum to produce gluconic acid as early as 1928. A few years later the process was abandoned in favour of that using A.niger. P.citrinum and P.luteum have been tested by Miles Laboratories (35) to establish their citric acid producing abilities.

Rhizopus. Prior to 1970 R.oryzae was used to produce both fumaric and lactic acids for use in the food and pharmaceutical industries (153). The fermentation process became redundant in the early 1970's when it became cheaper to produce fumaric acid from crude oil.

Other fungi. Botrytis cinerea, Mucor piriformis and Trichoderma viride have been shown to produce large amounts of citric acid (142), and others shown to produce different acids in significant quantities (Table 1.1). A process to produce citric acid from cellulose waste using Trichoderma viride has been patented (154).

1.2.8. Chemical and physical conditions affecting growth and acid production.

Fungal metabolism is closely related to the chemical and physical environment around growing cells. Most industrial uses of fungi involve the manipulation and control of the growth environment in order to stimulate production of a specific product. Literature concerning the chemical and physical environments are considered separately and in greater detail below.

Chemical environment.

The nutrient requirements of fungi have been reviewed by a number of authors (57,71,155,156). Essential elements include carbon, oxygen, nitrogen, sulphur, phosphorus, potassium, hydrogen and magnesium. With the exception of oxygen, which is always supplied as a gas, nutrients are best assimilated by fungi in the form of soluble salts in aqueous solution. Frequently trace elements, present in nutrients, have a significant effect on metabolism. Clark et al.(157) showed that separate additions of 1 mg Mn/l, 0.5 mg Al/l, 5.0 mg Zn/l, 100.0 mg Fe/l, 3.0 mg Cu/l, and 0.1 mg Co/l to fermentations employing A.niger gave citric acid yields of 1.5, 7.3, 7.5, 7.5, 8.6 g/l, respectively, compared to 8.8 g/l for the control without metals.

What follows is an account of the effects of metals, non metals and organic compounds on growth and acid biosynthesis. Most emphasis is placed on Aspergilli, although some other microorganisms are considered.

Alkali metals. Potassium is required by all fungi. Under

normal conditions 0.001-0.004 M is adequate (158-160). When A.niger is grown on potassium deficient media oxalic acid can accumulate (161-163).

Alkali metals stimulate sporulation in the order Li>Na>K>Rb and potassium has a marked growth promoting effect which the others do not equal (164,165). In yeasts it has been shown that potassium can be accumulated rapidly such that the concentration ratio inside to outside cells in vitro is >=5000:1 (166). This uptake is counterbalanced by a stoichiometric expulsion of protons (167).

Both Rothstein (168,169) and Conway and Duggan (166) showed that potassium is transported via specific receptor sites on the cell membrane. Other ions can compete for the receptor sites and thereby reduce the flow of potassium into the cell. The relative affinity of receptors for alkali metal cations in yeast cells is K>Rb>Cs>Na>Li in the ratio 1:3:15:20:30. Magnesium can also be transported by the same receptor sites but its affinity is low.

In citric acid fermentations it has been reported that the ratio of alkali metals to phosphate is critical (170). Rothstein (171) postulated that, as only the species $H_2PO_4^-$ can be transported into the cell, during phosphate uptake the medium becomes slightly alkaline and the cell more acid. Therefore the acidification of the cell associated with phosphate uptake is counterbalanced by alkalisation associated with potassium uptake. Thus, cells which have previously taken up potassium can subsequently take up larger amounts of phosphate and if potassium and phosphate are presented to the cell together a much greater

quantity of both are absorbed. Burnett (172) stated that this mechanism applied to filamentous fungi and that uptake of alkali was related to the hydrogen ion and dissolved oxygen concentrations of the growth medium employed.

Aluminium. Bertrand (173) reported that aluminium was necessary for growth of A.niger. He showed that additions of 5,10,20,50 and 100 µg Al/l increased the dry cell weight of A.niger above that of controls. Matsuda et al. (174) indicated that aluminium concentrations above 25 ppm were toxic to all bacteria and species of Penicillium tested but not to A.niger. Sulochana (175) showed that fungal growth was increased threefold by the addition of 200 ppm aluminium. However, growth was increased to a greater degree by lithium, manganese, cobalt and boron.

Arsenic. Chughtai and Walker (176) reported that alkali metal arsenites stimulate production of citric acid by A.niger. Stimulation may result from the inhibitory effect of arsenic on enzymes in the TCA cycle (130). Arsenic inhibits the oxidation of ketoglutaric acid which reduces flow around the cycle. It also inhibits the formation of acetyl coenzyme-A which is a major precursor in the TCA cycle (Fig 1.7) (177).

Rothstein (178) noted that arsenate is transported into yeast cells by the same carrier system that accounts for phosphate. In the process the carrier system is slowly deactivated.

Barium. Cochrane (57) reported that barium is only toxic to A.niger if sulphur is supplied in the form of sulphate suggesting that its toxicity can be attributed to the

removal of nutrient sulphur as insoluble barium sulphate.

Boron. Borax is reported to be toxic to A.niger above a concentration of 1.3 g/l (179).

Calcium. Calcium appears to have very little effect on A.niger except when other essential nutrients are missing (165). In other fungi between 0.5 and 20 ppm Ca^{2+} has been shown to stimulate growth.

Cobalt. Cobalt is accumulated by Neurospora crassa by a factor of up to 23 times depending upon the surrounding concentration (180). Up to 40% is bound up with protein. Ballantine (181) noted that cobalt accumulation in N.crassa was affected by the local iron concentration. This was confirmed by Hunter (182) who indicated that cobalt stimulated production of an iron binding agent in Neurospora. He also noted that cobalt uptake was inhibited by magnesium ions. Nicholas (183) indicated that A.niger synthesised vitamin B when grown on cobalt rich media and, like Neurospora, cobalt uptake was affected by magnesium ions.

Copper. Fungi require between 0.01 and 0.1 ppm copper for normal growth (158,184-185). Some species can grow on a saturated solution of copper sulphate (186). Together with iron and zinc, copper has a marked effect on citric acid fermentations employing A.niger. Shu and Johnson (187) showed that on its own copper had little effect but together with zinc yields of citric acid were increased. Schweiger (188) noted that copper was antagonistic towards iron, and two patents have been issued concerned with the addition of copper to impure substrates to counter

inhibition by iron (189-190). The addition of copper offers the additional advantage that it selectively inhibits the growth of contaminating Penicillium purpurogenum (191).

There is considerable variation in metal concentrations (Fe, Cu, Zn) identified by different workers for optimum acid production. Narroquin (192) suggested that this was due to variation in the trace element requirements of different strains of A.niger.

Halogens. Fluoroacetate is readily converted into fluoroacetyl coenzyme in place of acetyl coenzyme in the TCA cycle (130). But fluorocitrate inhibits aconitase and might be expected to result in the appearance of citric acid. It is of interest that certain poisonous plants, which contain monofluoroacetic acid, have been used as rodenticides. When the plant material is ingested by amimals large quantities of citric acid accumulate which causes poisoning. LaNauze (134) investigated whether monofluoroacetic acid caused similar poisoning in fungi. In the case of A.niger no increase in citric acid production was observed.

Heavy metals. Horsfall (81) summarized the relative toxicities of heavy metals for the majority of fungi as follows, in order of decreasing toxicity Ag>Hg>Cu>Cd>Cr>Ni >Pb>Co>Zn>Fe.

Zlochevskaya and Rabofnova (193) found that a concentration of 296 mg/l lead ions only slightly effected growth of A.niger, and had no effect on sporulation. McCallan and Miller (194) showed that the toxicity of silver and mercury towards A.niger doubled for every threefold increase in concentration exposure time.

Rothstein (171) showed that mercury caused excessive leakage of small molecules from yeast cells. However Ashworth and Amin (195) noted that A.niger could tolerate relatively high concentrations of mercury and organomercury compounds. Uranyl ions bind reversibly with phosphoryl and carboxyl groups in the cell walls of yeasts (171). This process inhibits uptake of glucose but can be reversed by adding chelating agents or other cations which displace uranyl ions from their binding sites. Talbert and Johnson (196) reported that although rare earth elements inhibit growth of A.niger they are readily detoxified as insoluble oxalates. It has been noted that microorganisms readily concentrate silver and cesium against a concentration gradient (197).

Iron. Fungi require between 0.1 and 0.3 ppm iron for normal growth (158,184,185,198). A.niger can utilise either ferrous or ferric iron (183). In citric acid fermentations the concentration of iron has to be controlled in order to ensure high yields of acid (199). The iron requirement varies from strain to strain (192) and also upon the concentration of copper and zinc (200).

Neilands (201) noted that A.niger released into the growth medium relatively large amounts of a substance or substances, not citrate, which bind ferric iron.

Magnesium. Nicholas and Fielding (202) found that the dry cell weight of A.niger to be proportional to the magnesium content of the growth medium, maximum yields required 20 mg magnesium per litre. Nowosielski (203) used these results to measure the magnesium content of soils and

found the results to be in good agreement with similar results determined by flame photometry. Zodrow et al. (204) indicated that this colinearity held until a threshhold point is reached at approximately 0.1% magnesium. Kauffman-Costa and Tudor (205) showed that at higher concentrations above 0.306 % Mg the medium becomes toxic to A.niger.

Laborey and Lavollay (206) indicated a triple interaction between magnesium, zinc and cadmium, the former acting as an antagonist to the toxic effects of the other two. Magnesium shows similar antagonistic behaviour with other metals like aluminium, copper, and mercury (207-209). MacLeod and Snell (210) explained this behaviour suggesting that the metals bind competitively onto important receptor sites and that the resulting metal-enzyme complex is either inactive or less active than the natural magnesium-enzyme complex.

Manganese. The role of manganese in the activation of TCA cycle enzymes is well known (130) and its concentration must be controlled in citric acid fermentations (200). It is essential in the formation of glucose dehydrogenase in gluconic acid fermentations employing A.niger (211). Sulochana and Lakmanan (211) tested five different strains of A.niger for response to manganese. Above 0.006 mg/ml there was no further increase in mycelium dry weight.

Molybdenum. Nicholas and Fielding (202) found that A.niger could be used to detect extremely low concentrations of molybdenum. The addition of 0.1 ppb of Mo^{2+} to 50 ml of purified medium resulted in an

increase of 57 mg in the dry cell weight. Mulder (212) showed that A.niger responds to as little as 0.02 ppb of the metal. Ryman et al. (213) found that between 0.2 and 1 mg/ml molybdate inhibited growth of A.niger, but also that methionine prevented inhibition by and uptake of molybdenum ions.

The importance of molybdenum in nitrogen metabolism was highlighted by Steinberg (214,215). He noted that A.niger required more molybdenum when cultured on a medium containing nitrate nitrogen than on a medium containing ammonium nitrogen. Nicholas et al.(216) showed that this was due to the requirement of molybdenum for the formation and activation of nitrate reductase which is essential for the uptake of nitrate, and is common to all fungi and many other organisms.

Strontium. Lewin et al.(217) noted that strontium is taken up and firmly bound by mycelium of Rhizopus sp.

Vanadium. Vanadium can be adsorbed by fleshy fungi from soils (218).

Zinc. Zinc is required by nearly all fungi for normal growth (220). Between 0.5 and 1.0 ppm has been quoted as the optimum range (184,185). Many workers have indicated the importance of zinc in controlling citric acid fermentations (184). Wold and Suzuki(220) reported that the onset of the acid production phase is controlled by the concentration of zinc. At low concentrations (below 1 µg/l) growth is inhibited and the rate of acid production high. If zinc is added during the acid production phase (up to 2 µMole/l) normal growth is resumed. Shu and Johnson (148)

indicated that there is a relationship between zinc and iron, this was also shown by Trumphy amd Millis (221) using a different strain of fungus.

Nitrogen. Nitrogen is usually supplied either as nitrate or ammonium salts. Under conditions of nitrogen starvation A.niger can utilise other diverse organics including the cyanide radical(222). There is evidence that the ammonium ion is preferred to the nitrate ion, but utilisation depends upon the pH (223).

Currie (144) noted that nitrogen sources suitable for selective production of oxalic acid by A.niger are limited to those which give rise to physiological alkalinity. Included in this category are $Ca(NO_3)_2$, $(NH_4)_2HPO_4$, KNO_3 , $NaNO_3$, NH_4NO_3, and peptone. He noted that salts like NH_4Cl and $(NH_4)_2SO_4$ never give rise to high concentrations of oxalate. Ammonium carbonate is preferred in commercial submerged citric acid fermentations as it suppresses formation of pigments and slime, and oxalic acid (224). Both Shepherd (225) and Chmiel (226) demonstrated that addition of nitrogen salts during the acid production stage increased the overall yield of citric acid.

Gerhardt et al.(227) described a procedure for removing undesirable metals from beet molasses prior to fermentation by the addition of potassium ferrocyanide. In a later report they indicated that this pretreatment increased citric acid yields from 20% to 45-50% after ten days 'surface' fermentation at pH 7.0. Acid accumulated between pH 5.0 and 8.0. Below pH 4.0 no growth occurred.

Chughtai and Walker (176) investigated the influence of

sodium cyanide on A.niger. They suggested that preformed mycelial mats of A.niger treated with cyanide at concentrations ranging from 0.006 to 0.04 M utilised more sugar, and synthesised more acid in a given time than the controls. They also indicated that cyanide inhibited the break down of citric acid.

Phosphorus. Accumulation of citric acid is favoured by low levels of mono or dibasic phosphate (<0.02%) (224). In some fungi orthophosphates can be replaced by other inorganic phosphates (229) or casein (230) but not be phosphites or hypophosphites (229).

Shu and Johnson (187) noted that low levels of phosphate were only necessary in citric acid fermentations if iron and zinc were present in excess. Martain and Steel (231) studied the effect of adding phosphate during the acid producing stage. They showed that the addition of phosphate shortened the fermentation, did not effect the yield of citric acid, and suppressed the formation of oxalic acid. A later report by Steel et al.(232) showed similar effects except that the acid yield fell sharply.

Sulphur. Sulphur is normally supplied to citric acid fermentations as magnesium sulphate at concentrations ranging from 0.1 to 0.25 g/l (188). Persulphate, sulphite, bisulphite, hyposulphite, thiosulphate, sulphide, and disulphide can also be utilised by A.niger (233). Steinberg(233) noted that A.niger grows better on weathered than on fresh sulphides and disulphides. Other fungi have been reported which can reduce sulphite (234), enzymically reduce sulphur to hydrogen sulphide (197,235,236) and

reduce selenites to selenium (237). Penicillium luteum has been shown to oxidise elemental sulphur (238).

The ability of fungi to volatilise sulphur compounds by methylation is widely recognised and has been summarised by Challenger and Charlton (239). They noted many other similar reactions involving disulphide, selenate, tellurite, and arsenic compounds.

Silicon. Engel et al. (240) cultured A.niger on a medium ccontaining 280-330 mg SiO_2/l (as silica gel). The surface mycelium accumulated up to 2% and submerged mycelium up to 9% silica.

Low molecular weight alcohols. Sakaguchi and Baba (241) were first to observe that low molecular weight alcohols affect growth of A.niger. Moyer (242) studied acid production by A.niger in the presence of methanol, ethanol and propan-2-ol. Each alcohol stimulated acid production, reduced sugar consumed in production of mycelium, and greatly increased tolerance of the fungus to trace metals. In one test 1.04 g citric acid was produced from 1 g sucrose (92.8% of the theoretical yield). He noted that methanol was not consumed by the fungus. This is in agreement with Mosbach et al. (243) who studied the role of carbon dioxide, formic acid, and methanol in the biosynthesis of citric acid by A.niger, but not with Baba (244) who showed that A.niger could grow on methanol as the sole carbon source. Qadeer et al. (245) indicated that the most effective methanol concentration was 3%, in agreement with Moyer. Propan-2-ol was found to have a similar, but less marked effect than methanol at an optimum

concentration of 2% (245).

Carbohydrates. Mono-, di-, and polysaccharides can all be used as primary sources of carbon by A.niger (246). Disaccharides and polysaccharides are usually broken down by hydrolytic enzymes such as amylases and cellulases which are either secreted into the surrounding medium or are fixed to the cell wall (Section 1.2.3). These enzymes cannot tolerate high concentrations of heavy metals.

There is evidence to show that mixed carbohydrates are better than single pure carbohydrates (247-249). The reason for this is not known.

Storage products have already been mentioned with regard to the accumulation of citric acid (Section 1.2.6). Species of Aspergillus produce other storage products including polysaccharides (polyols, glucosanes) which may escape into the medium and alter its characteristics (250).

Citric acid fermentations are usually carried out using inexpensive carbon sources like beet molasses or corn starch at concentrations up to 16% (251). A medium containing 50% glucose has been cited as being toxic to A.niger (252). Other processes have been described which use cellulose as a carbon source (253) but are not considered to be economic in comparison to those using sugars (254).

Lipids. Millis et al. (255) found that unsaturated fatty acids inhibited the growth of A.niger but increased citric acid yields. A patent based on these findings was filed by Gold and Kieber (256) who noted that 0.05-0.1 % non-ionic lipid based detergents encouraged filamentous

growth. Tween 20 (polyoxyethylene(20)-sorbitan monolaurate) was an exception. It promoted pellet growth and improved acid yields. A major disadvantage of antifoam and detergent compounds is their effect of reducing the oxygen gas-liquid mass transfer coefficient in submerged fermenters (258,259).

The insolubility of natural lipids does not exclude their use by fungi as sources of carbon (260). Zobel (261) indicated that numerous fungi and yeasts could grow on crude oil and other purified hydrocarbons.

Carboxylic acids. The breakdown of carboxylic acids and their salts by fungi is of obvious interest in mineral leaching applications.

Citric acid is broken down by A.niger into acetone dicarboxylic acid and malonic acid (262). Based on Currie's findings these acids are broken down further to oxalic acid (124). Other acids including tartaric, formic, lactic, glycolic, glycoxylic, and acetic are also broken down to oxalic acid (263). Break down is accelerated in the presence of the ammonium ion (264). Citrate salts at neutral pH's are readily broken down by natural populations of microorganisms (251). Oxalate salts including oxalic acid are not as susceptable to breakdown (124).

Physical environment

Aeration. All known filamentous fungi are essentially aerobic (265). Oxygen requirements vary from species to species. According to Blain (266) mycelium of A.niger had an oxygen uptake rate of 0.2-0.5 $\mu l O_2$/mg/min. Other workers

have indicated that the specific oxygen demand for A.niger is of the order of 3.0 mM O_2/g cells/hr (267). Unlike other essential nutrients, gaseous oxygen is not readily soluble in fermentation media through which it must pass in order to be accessible to fungi in submerged culture. Oxygen is commonly supplied to submerged fermentations by bubbling air through the liquid. Andrew (268) reviewed the theory and practice concerning the transfer of oxygen to submerged cultures using bubble spargers. In its simplest form the rate of transfer of oxygen into the liquid phase is equal to the gas-liquid mass transfer coefficient, k_1, multiplied by the gas-liquid interfacial area, a, multiplied by the gas concentration gradient across the transfer interface. Assuming constant physical conditions the rate of transfer of gas can be increased by: reducing the bubble size, which increases a; increasing agitation which increases both a and k_1; or by designing the fermenter such that the gas-liquid contact time is increased. Andrew noted that in large fermenters the value of k_1a is virtually constant at a given gas-holdup. Hence the gas transfer rate must be controlled by increasing the gas-liquid contact time. In the case of high viscosity media high speed agitators are employed to decrease the bubble size such that bubbles have a low rise velocity. Conversely low viscosity media require low speed multiblade agitators which rely on gas drag-down for increased gas-liquid contact time. Andrew suggested that for oxygen absorption into cultures having viscosities close to that of water a value of 0.4 s^{-1} should be taken for k_1a/ε, where ε is equal to the gas-hold up per unit

mixture volume at 20 °C, and a value of 0.4 $\mu^{-0.5}s^{-1}$ for viscous cultures at 20°C, where μ is the liquid viscosity. The value of k_1 should be increased by a factor of 1.025 for every kelvin rise in temperature.

Agitation is an equally important factor in the diffusion of oxygen and other nutrients into mycelium. In the case of rigid pellets Pirt (97) calculated that if oxygen entered by simple diffusion growth would be restricted to a peripheral zone 77 µm wide. This was substantiated by Philips (269) using Penicillium chrysogenum. Haung and Bungay (270) indicated that in slow moving media (28.3 cm/min) oxygen penetrated no further into pellets of A.niger than 135µm. The oxygen diffusivity coefficient within pellets was calculated to be $2.9x10^{-6}cm^2/sec$. Under agitated conditions Miura (271) showed that this was increased to approximately $10^{-4}cm^2/sec$ (greater than that for stagnant conditions by an order of magnitude).

It is well known that mass transfer of oxygen into solution decreases with increasing mycelium content in submerged cultures (272). This is probably as a result of increased viscosity due to fungal byproducts (polysaccharides, acids), and/or increased coalescence of small bubbles by filaments of fungus reducing both the surface area, a, and the gas-liquid contact time. Chmiel(273) indicated that the limitation on the specific rate of production of acid was related to the decrease in dissolved oxygen at high mycelium densities. Rose (274) noted that in citric acid fermentations employing A.niger

oxygen consumption was significantly greater during acid production than during growth.

Kovats and Gackowska (275) reported that cells of A.niger actively producing acid are sensitive to oxygen deficiency. If the supply of oxygen was stopped during the acid production phase, product formation was limited or ceased altogether, even if aeration was resumed.

pH. Most fungi grow in the pH range 3 < pH < 8 (276). Moyer (242)indicated that the initial pH had no effect on the yield of citric acid obtained using A.niger. This was disputed by Choudhary and Pirt (277) who suggested that low initial pH values (<2.0) would favour acid production. Khan and Ghose (113) indicated that a higher pH (4.0-5.0) was preferred.

Although different workers have disputed the significance of initial pH on acid biosynthesis, the control of pH is important in optimising the fermentation time and fungus morphology best suited to processing equipment used to recover products. Chmiel (273) showed that there is a relationship between the cell mass and the acid production rate. The relationship was linear up to 4 g cells/l (0.7 g acid/l/hr) and peaked around 12 g cells/l (1 g acid/l/hr) before declining. Therefore, in order to optimise the rate of production of acid it is necessary to produce approximately 12 g cells/l before the end of the acid production phase. Low pH values cause a divergence from exponential growth as a result of abnormally short malformed hyphae (224), but is generally considered best for acid production. Chmiel used a two

stage process in which the pH was maintained around 4.0 in order to produce the optimum cell concentration. This was followed by a reduction in pH to inhibit growth and encourage acid biosynthesis.

Galbraith and Smith (278) indicated that pH was a major factor in the control of cell morphology. They showed that in order to produce pellets, which are superior to filaments from a product recovery viewpoint, the initial pH should be approximately 5.0. It was suggested that pH values between 3 and 5 promoted agglutination and flocculation of spores into clumps before and during fermentation and hence reduced the number of discrete growth centers in the medium.

Temperature. Most fungi make some growth between 25 and 30°C (279). Nielsen and Presden (280) noted that the Q10 value (Q10 is defined as the ratio of the respiration rate at a given temperature to that at a temperature 10 °C lower), for carbon dioxide evolution from growing mycelium of A.niger decreased rapidly as the temperature was increased (from 312 over the range 7-17°C to only 1.7 over the range 27-37°C). The optimum temperature for citric acid biosynthesis lies between 28 and 32°C (113,281). As the temperature is increased beyond this level the growth rate increases and large amounts of sugar are oxidised to carbon dioxide and oxalic acid (234).

Moyer (242) noted that there was a relationship between the incubation temperature and the supply of nutrients to the cell. He also noted that more nitrogen was required to maintain a fast fermentation at 27°C than at 32°C.

Agitation. The purpose of providing an agitator in a fermenter is to obtain mixing and to achieve heat and mass transfer.

The mixing time, Tmix, defined as the time in seconds for a pulsed input to a system to be smoothed, varies with vessel volume, v, according to the empirical formula $Tmix=kv^{0.3}$ (282). The constant of proportionality, k, is related to the vessel size and configuration (283), and also to the degree of turbulence in the system, which is a function of the number and type of impellars (284). Hence as the viscosity rises,due to increases in cell concentration and/or lengthened hyphae, the more difficult it becomes to provide adequate mixing (268).

1.2.9. Mineral degradation by fungi.

The colonisation of exposed rocks by fungi is well known and it has been suggested by a number of independent workers that continued growth of fungi on mineral surfaces can cause mineral alteration (4,7,34,285). Although many workers have proposed mechanisms to explain observed degradation, few if any have studied alteration and leaching reactions in detail (286).

This section considers important contributions to the subject. It is split into four parts. The first three deal with cases of mineral alteration due to absorption, silicate leaching, and non-silicate leaching by fungi. The final part considers mechanisms proposed to explain the biodegradation of silicate minerals.

Mineral alteration due to metal absorption by fungi. Eno

and Reuszer (287) reported that A.niger could accumulate potassium in mycelium during growth in the presence of biotite, muscovite, greensand and microline. Muller and Forster (288) reported a similar uptake of potassium by mycelium of A.niger when the latter was incubated on orthoclase and oligoclase felspars. Based on the findings of Section 1.2.8 (pp 39-40), it is likely that other alkali metals (and possibly magnesium) are absorbed from minerals in a similar manner, thereby causing alteration.

Silicate leaching. Grovdev and Grenchev (286), prompted by the successful application of bacterial leaching, considered the bioleaching of aluminium from clays as a potential source of the metal. The leaching ability of twenty eight fungi and eight strains of Bacillus circulans (a silicate bacterium) were compared. All produced significant leaching (10-30% removal of aluminium after 30 days). The most aggressive was a strain of A.niger. Although acid products were detected in spent media (carboxylic and amino acids), there were no clear relationships between acids produced and leaching rates observed.

Rossi (39) studied the bioleaching of potassium from leucite. He noted that leaching produced by fungi was comparable with that produced by a mixture of 0.1 M oxalic and 0.1 M citric acids. In both cases the reaction products gelified. Between 20% and 30% of available potassium was leached over a period of 150 days. Volkova et al. (289) studied the decomposition of nepheline (compositionally similar to leucite) by organic acids of microbial origin.

They indicated that dilute acids (0.01 M ascorbic, tartaric, citric, and malic acids) dissolved 2-4% SiO_2 and 4-5% Al_2O_3 from nepheline. Reaction products gelified in a similar manner to leucite.

Silverman and Munoz (40) investigated fungal degradation of sixteen different rocks and minerals using a species of Penicillium. They compared the degradation produced by spent medium (which was acidic) with fresh medium to which was added an equivalent amount of citric acid, and spent medium which was neutralised with sodium hydroxide. Whereas similar rates of degradation were observed for the first two media, that produced by the third was negligible. They concluded that degradation was a result of organic acids and not extracellular enzymes produced by fungi.

Boyle et al.(38) compared the degradation of biotite using oxalic, citric, and hydrochloric acids. Iron, aluminium, and magnesium were extracted more rapidly using organic acids than with hydrochloric acid. They attributed this difference to the chelating ability of the organic acids.

Leaching of non-silicates by fungi. Arrieta and Grez(36) studied the iron leaching ability of nine fungi including species of Aspergillus, Penicillium, Mucor, Fusarium, and Cephalosporium. Strains of Aspergillus were the most aggressive although others, notably species of Penicillium and Fusarium, produced significant leaching. There was a degree of selectivity in the minerals different fungi would leach. The leaching action was suggested to be related to the chemical and physical structure of the mineral and the

concentration and character of metabolic products produced by the fungi.

Dave and Natarajan (37) investigated the leaching of oxidised copper and zinc ores by fungi. Two fungi (A.niger and Paecilomyces varioti) which were screened from mine waste water had good mineral leaching ability. The former was best suited to leaching copper (up to 65% recovered based on metal available), and the latter was most suited to zinc ores (up to 31% recovered based on metal available). They attributed the leaching ability of A.niger to the production of citric and oxalic acids. Weinberg et al.(41) reported that Penicillium species were able to leach copper from chalcocite and native copper concentrates. They attributed leaching to acetic acid which was detected in the fermentation media.

As compared with bacteria there are very few reports concerning the direct oxidation/reduction of minerals by fungi. Steinberg (233) and other workers (235-237) noted that A.niger could degrade sulphide minerals, probably as a result of direct enzymic attack. Schweisfurth (293) summarised many cases of manganese oxidation by fungi which he suggested were probably a result of direct fungal action.

Mechanism of silicate leaching. The reports discussed previously highlight two properties of fungi which can contribute to or cause mineral alteration: fungal adsorption/absorption of mineral weathering products, and the production of organic acids. Both types of alteration can be explained with reference to current concepts of

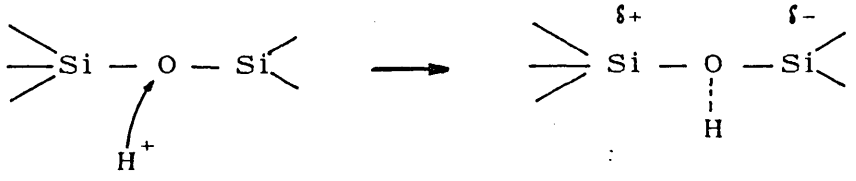
chemical (abiological) weathering.

Loughnan (290) indicated that silicates can be leached directly by hydration in a the manner described by

$$M^{+}[MINERAL]^{-} + H^{+}OH^{-} = H^{+}[MINERAL]^{-} + M^{+}OH^{-}, \qquad (1.29)$$

where $M^{+}[MINERAL]^{-}$ represents the unweathered mineral, $H^{+}[MINERAL]^{-}$ the residual weathered mineral, and M^{+} is a cation. Cations susceptable to hydration will pass into solution at a rate dependent upon the hydrogen ion concentration in the aqueous phase. In the case of Eqn (1.29) for pure water, this concentration is very low and alteration should only be noticeable over a geological time scale. However, if the pH$<<$7.0 the equilibrium will tend further to the right in Eqn (1.29). Under these conditions, if $M^{+}OH^{-}$ is removed from the system, such as by adsorption onto fungi, and sufficient hydrogen ions are available, then more mineral will dissolve to satisfy the equilibrium.

Matveeva (291) suggested a second mode of attack whereby hydrogen ions in solution can attack the mineral lattice directly. The favoured mechanism being hydrogen ion attack of the oxygen link in the aluminosilicate framework. The proton redistributes charge along the bond making aluminium susceptable to attack by OH ions.



(1.30)

As before, the rate of reaction should be expected to increase with decreasing pH.

Fungi can increase the concentration of hydrogen ions, and hence the rate of reactions in Eqns (1.29) and (1.30), by producing organic acids. Organic acids may also be important as chelating agents. Silverman (6) noted that the removal of weathering products (M^+OH^- and $H^+[MINERAL]^-$) by chelation is likely to aid the rate of leaching. Evidence for direct chelation of metals from silicate mineral lattices independent of hydrogen ions is sparse. Schalscha et al.(292) reported that the sodium salts of citric and salicylic acids removed some iron and aluminium from augite, epidote, biotite and granodiorite in the pH range 6.8 to 7.7, but leaching was very slow.

CHAPTER 2 ANALYTICAL, MINERALOGICAL, AND BIOCHEMICAL METHODS.

This chapter describes the principle analytical techniques employed for the determination of metal ions and organic compounds. The selection and preliminary appraisal of mineral and fungal systems are discussed. All reagents were of Analar grade unless otherwise stated.

2.1 Analytical Methods.

Atomic absorption/emission spectrometry was used routinely for the determination of metal ions in aqueous solution. Classical wet chemical techniques were used to determine sucrose, glucose, oxalic acid and citric acid. Information on minor organic phases produced during fermentation were obtained from gas-liquid chromatography. Special phase analyses were carried out by scanning electron microscopy, electron microprobe scans, and x-ray diffraction. Spore concentrations were measured by image analysis.

2.1.1. Atomic absorption/emission spectrometry.

Baird Alpha-1 and Alpha-3 machines were employed in the emission mode for the elements sodium, potassium, strontium and barium, and in the absorption mode for aluminium, silicon, magnesium, calcium, titanium, manganese, iron, lanthanum, copper and zinc. An air-acetylene flame was used

for all elements except aluminium and silicon, which required nitrous oxide-acetylene (294). In the case of silicon the response was increased by the addition of 25%v/v methanol to samples and standards. This decreased the solution viscosity and increased the rate of nebulization.

All samples and standards were prepared in a similar manner as aliquots taken from a known total volume. Visible solids were removed by centrifuging at 2000 rpm for 5 mins. The clear liquid was split into N 0.5 ml samples using a digital autopipette, where N was the number of elements to be analysed. Each sample was diluted with 0.5 ml distilled deionised water (DDW), and, where required, 1 ml ionisation suppressor. The ionisation suppressor was 1 g/l sodium chloride (K,La), or 1 g/l potassium chloride (Na, Ba, Sr, Al, Mg, Ca, Ti). A suppressor was not required for the elements Fe, Cu, Zn, Mn, and Si. Solutions were diluted as necessary and measured according to the standard procedures (294).

Standard solutions were prepared by diluting Spectroscopic grade atomic absorption reagents containing 0.005 mg metal/ml (B.D.H. Chemicals Ltd) so as to be in the same range of concentration as the samples. A 0.5 ml sample of each dilution was added to 0.5 ml ionisation suppressor (where required), and 0.5 ml of DDW. Standard absorbance data were fitted to polynomial equations of the form $y=a+bx+cx^2+dx^3$ + ,where y represents metal concentration, and x represents absorbance. Sample metal concentrations were calculated by substituting sample absorbance data into

the above equations.

Analytical errors were calculated for each element by measuring the concentration of a known solution (0.5 g/l), n times. The relative errors, shown in Table 2.1, represented the minimum instrumental and sample preparation errors likely to be incurred. Values of variance (Table 2.1) gave a measure of the variability of the n samples tested with respect to the true concentration (0.5 g/l), which provided a means of identifying 'rogue' points. The relative errors of aluminium and silicon were high, probably as a result of the rapid buildup of ash on the burner jet. Wherever possible solutions containing these metals were diluted to <0.05 g/l, which reduced relative errors to 1.5-2.3% for aluminium and 2.5% for silicon.

Glucose and sucrose had no significant effect on the absorbances of sodium, potassium, aluminium, and silicon. Oxalic and citric acids at concentrations >8 g/l suppressed the absorbances of nearly all the elements tested. Where this phenomena significantly affected absorbance values, standards were prepared containing similar concentrations of acids as sample solutions.

2.1.2. Gas-liquid chromatography.

A Perkin Elmer F30 gas chromatograph was used to provide qualitative analyses of mixed organic acids resulting from fermentation procedures. In order to achieve adequate volatility, the acids were converted to their methyl esters by reaction with acidified methanol. Methylation was carried out as follows (295). A 1.0 ml

TABLE 2.1 ANALYTICAL ERRORS IN THE DETERMINATION OF METALS BY ATOMIC ABSORPTION SPECTROMETRY.

Metal	Number of analyses/ n	Average/ gl^{-1}	Error/ %	Variance/ 10^{-4}
Na	10	0.500	-	-
K	10	0.500	-	-
Ba	10	0.502	0.4	2.6
Sr	10	0.502	0.4	2.5
Mg	10	0.502	0.4	2.7
Ca	10	0.502	0.4	2.8
Ti	6	0.504	0.6	3.1
Al	10	0.520	4.0	3.7
Si	10	0.528	5.6	3.8
Mn	10	0.508	1.2	2.9
Fe	10	0.508	1.2	2.5
La	16	0.500	-	-
Cu	10	0.506	0.9	2.5
Zn	10	0.508	1.2	2.6

sample was heated with 2.0 ml methanol and 0.4 ml 50% sulphuric acid at 55°C for 30 minutes. The sample was diluted with 1.0 ml water and 0.5 ml chloroform, mixed thoroughly, and centrifuged to separate the emulsified layers. A 14.0 µl sample of the chloroform layer was removed using a Hamilton series 7000 microsyringe and analysed using a two metre, 4 mm i.d., glass column packed with 10% SP1200/1% phosphoric acid on 80/100 mesh Chromosorb WAW (obtained from Supelco Ltd). The column was held at 155°C and then programmed to rise to 180°C in 30 minutes. The inlet and detector were held at 150° C. The helium gas flow rate was 70 ml/min. The column was reconditioned after every twenty samples by injecting 14.0 µl methanol.

Chromatographic peaks were identified by comparison with those produced from a standard non-volatile acid mixture containing pyruvic, lactic, oxalactic, methyl-malonic, malonic, fumaric and succinic acids (obtained from Supelco Ltd). A typical chromatogram from A.niger grown on sucrose (Section 2.3) is illustrated on Fig. 2.1. Retention times of derivatised acids accurate to ±10 sec are recorded on Table 2.2.

2.1.3. Electron microprobe analysis (EMA) and scanning electron microscopy (SEM).

These techniques were valuable tools for the examination of mineral and fungal surfaces, revealing information on mineral composition (EMA), mineral-fungus interaction (SEM), and fungus characteristics such as spore shape and

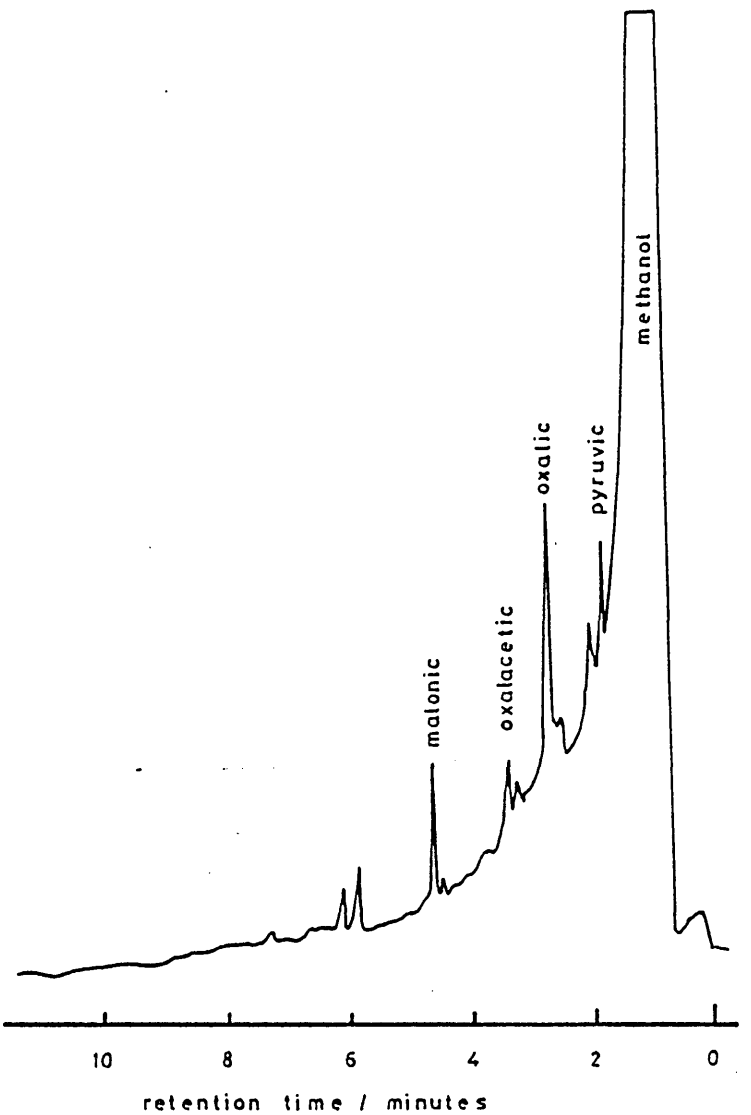


Fig 2.1 A typical chromatogram showing acids (all converted to methyl esters), produced by A.niger grown on sucrose.

TABLE 2.2 RETENTION TIMES OF METHYL DERIVATIVES OF FUNGALLY PRODUCED CARBOXYLIC ACIDS.

Methyl derivative	Retention time/ minutes
Dimethyl pyruvate	1.85
Dimethyl oxalate	3.30
Dimethyl oxalacetate	4.50
Dimethyl malonate	5.37
Dimethyl fumarate	9.10
Dimethyl succinate	9.75
Trimethyl citrate	28.50

size (SEM). All visual information was stored in the form of photomicrographs.

Four machines were used as follows; CAMEBAX-MICRO, and JOEL 733 for EMA; and JOEL SEM 35, CAMEBAX-MICRO, and Cambridge SPECTRSCAN 600 for SEM.

Typical mineral samples to be analysed by EMA were prepared as follows. The crushed sample (Section 2.2) was set in Araldite containing 9 parts resin containing 10% sample to 1 part hardener. The Araldite resin was modified to increase its electrical properties by adding 10% graphite and 18% di-n-butyl phthalate (the carbon was ground into the mixture using a pestle and mortar). The required masses of resin, hardener and mineral were added together and the mixture thoroughly agitated to ensure even distribution of minerals throughout the plastic. The mixture was heat cured in a cylindrical die. The resulting disc was cut to expose a cross-section of mineral grains and polished to a flatness of 1 μm on a diamond lap. Finally the polished surface was coated with carbon in a coating chamber.

For optimum results by SEM fungi must be fixed and dehydrated. In the process of fixation as applied to fungi their structures are chemically altered so that they can be dehydrated without distortion from their original form. The removal of volatile liquids from fungi is essential to avert the destruction of samples which would result from the rapid depressurisation during the coating process, mentioned below, and in the specimen chamber of the SEM.

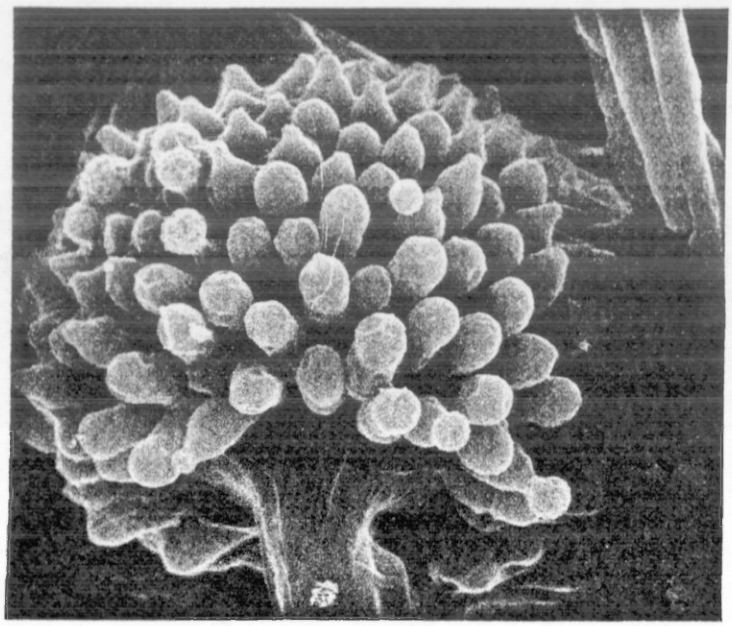


Fig 2.2 Conidiophore at an early stage of growth showing progressive stages in spore development ×7700.

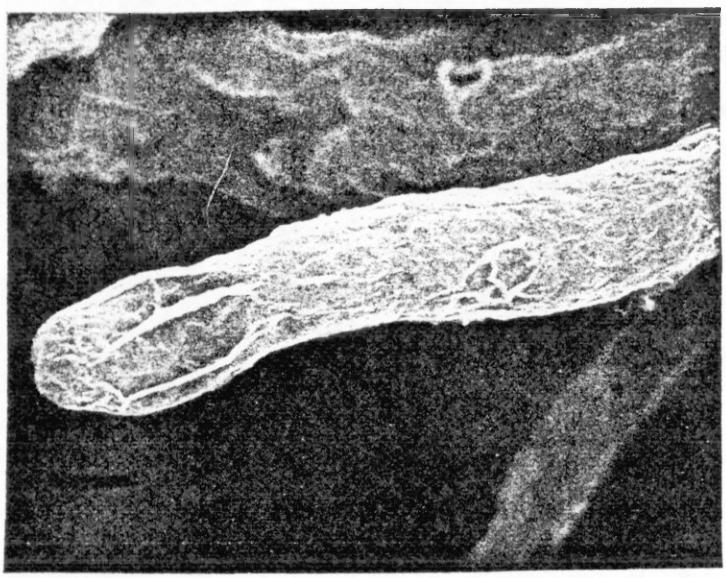


Fig 2.3 Typical hyphae filament ×11000.

Fungus and fungus-mineral samples to be photographed by SEM were prepared as follows. Samples were fixed by placing them in a desiccator with a petri dish containing 5 ml 1% osmium tetroxide solution at room temperature for 144 hrs. They were then dehydrated in a separate desiccator for 48hrs, and coated with gold in a sputter chamber. A current of 10 mA(at an accelerating voltage of 25 kV) was passed for 2 minutes. This was sufficient to stop the fungus gaining an electrostatic charge when excited by the SEM electron beam.

Equipment operating procedures are set out in manufacturer's manuals. The analytical technique employed for EMA elemental analyses is described in Section 2.2. Certain operating conditions are given here. Thus, for EMA an accelerating voltage of 15 kV was used for all analyses. The following minerals of known composition, supplied by the equipment manufacturer's, were used as elemental standards: albite feldspar (Na,Al,Si); microline feldspar (K); sphene (Ti,Ca); magnetite (Fe); and magnesite (Mg). For SEM an accelerating voltage of 8-12kV was employed routinely. Higher voltages up to 30 kV were used for increased definition at higher magnifications. However voltages above 25 kV rapidly distorted samples and could not be used continuously.

Typical SEM photographs of A.niger are illustrated on Figs 2.2-2.3. These show a typical conidiophore at an early stage of development (Fig 2.2) and a typical hyphae filament (Fig 2.3).

2.1.4. Omnicon image analysis.

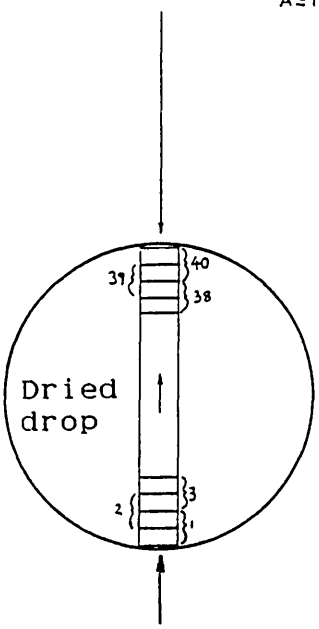
Spore concentrations were measured using an Omnicon image analyser. Liquid containing spores to be counted (Section 2.3) was violently agitated using a reciprocating shaker for 15 minutes in order to suspend spores. A 0.05 ml sample of this liquid was quickly removed, before settling occurred, and discharged onto a glass slide so as to form a round drop approximately 1 cm in diameter. The liquid was slowly evaporated at 30°C with a cover to exclude dust and other particles. When dry the sample was set up on the video microscope (part of analyser),to produce sufficient contrast between the black spores and the white background. The spore counting procedure employed is illustrated and described on Fig. 2.4.

Spores tended to deposit in concentric bands from the circumference to the drop center. These probably resulted from surface tension effects as the drop dried out. Hence it was necessary to scan across the dried drop diameter. If the concentration of spores was too high, spores at the outer rim could be many layers thick. In such cases the initial sample was diluted such that spores were deposited as a monolayer. In some samples clumping of spores occurred. This was overcome by diluting with an equal volume of 5% silicone antifoam in 1.0 M sulphuric acid.

Errors in estimations of spore concentrations were determined statistically by using a single drop to provide a number of estimates of the same concentration. The accuracy was assumed to be related to the number of diameters used to calculate the average number of spores

For this diameter,

$$(S_A/F_A)_{ave} = \sum_{A=1}^{40} (S_A/F_A)/40.$$



Movement of analyser across drop diameter half a frame at a time.



View of part of a frame. Plant hairs - such as can be seen in the photograph - must be removed before commencing counting.

Counting procedure.

(1) The average cross-sectional area of a single spore, $(S_A)_{ave}$, is measured.
(2) The drop is scanned across several diameters, half a frame at a time, measuring the area of each whole frame covered by spores. Areas corresponding to successive frames across each diameter are averaged to give the average frame area covered by spores across each diameter of the drop, $(S_A/F_A)_{ave}$.
(3) The average number of spores per frame area, $(S/F_A)_{ave}$, is calculated from $(S_A/F_A)_{ave}/(S_A)_{dve}$.
(4) The number of spores per drop, and therefore the concentration of spores in the sample, is calculated from, spores/drop=(drop area/frame area) $(S/F_A)_{ave}$.

Fig 2.4 Procedure used to estimate spore concentrations.

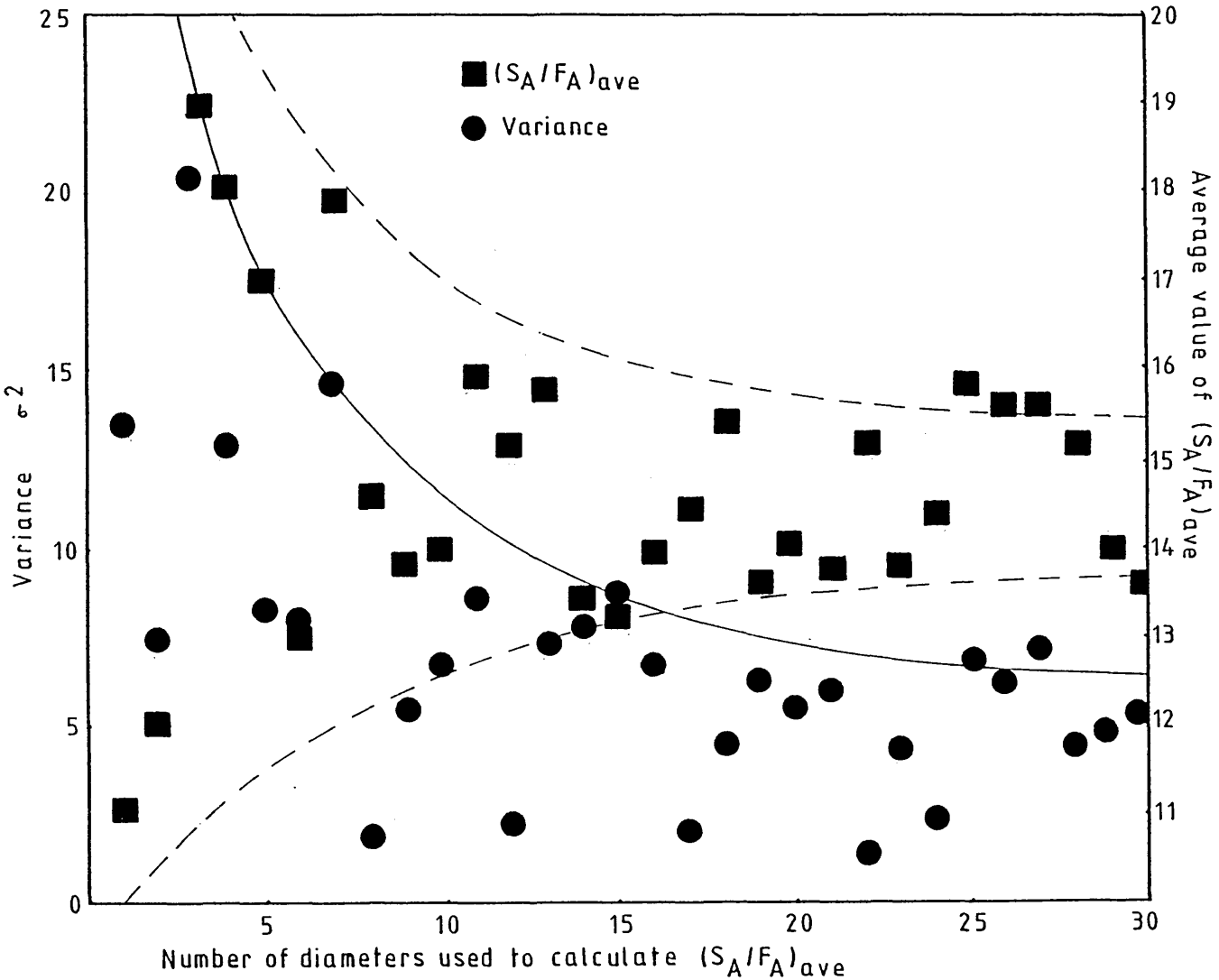


Fig 2.5 Variance of $(S_A/F_A)_{ave}$ and average values of $(S_A/F_A)_{ave}$ as a function of the number of drop diameters used to calculate $(S_A/F_A)_{ave}$.

per frame (S/F). Fig. 2.5 which is a plot of the variance of S/F about the sample mean as a function of the number of diameters used to calculate S/F. The figure shows that S/F gradually converges, but if more than twenty five diameters are used to estimate S/F the corresponding decrease in the error in S/F becomes insignificant. The minimum error obtainable using this technique was of the order of 10%.

Once the inoculum spore concentration had been estimated it was diluted or concentrated to contain 50.0×10^6 spores/ml and stored at $<4^{\circ}C$ until required.

2.1.5. X-ray diffraction.

Qualitative mineralogical analyses of altered and unaltered mineral samples were carried out by X-ray diffraction using a Philips PW 1310 X-ray generator (fitted with a copper target), PW 1050/35 wide angle goniometer with a graphite monochromator and PW 1352 scintillation counter/scaler unit.

The basic principles of X-ray powder diffraction have been adequately described in standard texts (296,297) and will not be described here. Samples to be analysed were prepared and analysed as follows. A 1 g sample was powdered in an agate pestle and mortar to -300 mesh, compressed into a 'Philips' aluminium powder mount, which was placed in line with the X-ray source. The X-ray generator was operated at 40 kV and 30 mA. Spectra were recorded on a chart recorder and peaks were identified using data from the Powder Diffraction File (PDF) of the American Society for Testing Materials (ASTM) (298).

2.1.6. Classical wet-chemical analysis of saccharides

Titrimetric analysis of sucrose and glucose. Sucrose, after conversion to invert sugar(see below), and glucose were determined by Lane and Eynon's(299) method. In this method a measured quantity of the sample containing the sugar is used to reduce a known quantity of hot copper tartrate solution to red cuprous oxide. The procedure adopted was modified from the published technique as set out below.

Solutions A, B and C were prepared as follows. A contained 34.639 g copper sulphate pentahydrate dissolved in 500 mls of DDW at 25° C; B contained 173 g sodium-potassium tartrate plus 50.0 g carbonate free sodium hydroxide in 500 ml DDW at 25°C; and solution C was a 1% solution of methylene blue. Carbonate free sodium hydroxide was prepared by adding a solution containing 1.5728 g barium hydroxide dissolved in 50 ml DDW to a solution containing 50.3248 g sodium hydroxide (containing 1% sodium carbonate), dissolved in 450 mls DDW. The solution was thoroughly mixed and left to stand for one week in order to allow the precipitate of barium carbonate to settle out. Samples of this reagent were removed as required taking care not to disturb the carbonate sediment.

An equal volume of A and B were mixed and diluted with an equal volume of DDW. Once A and B were mixed the resulting product was subject to aging and was used within a day of preparation. A 10 ml sample of this mixture was

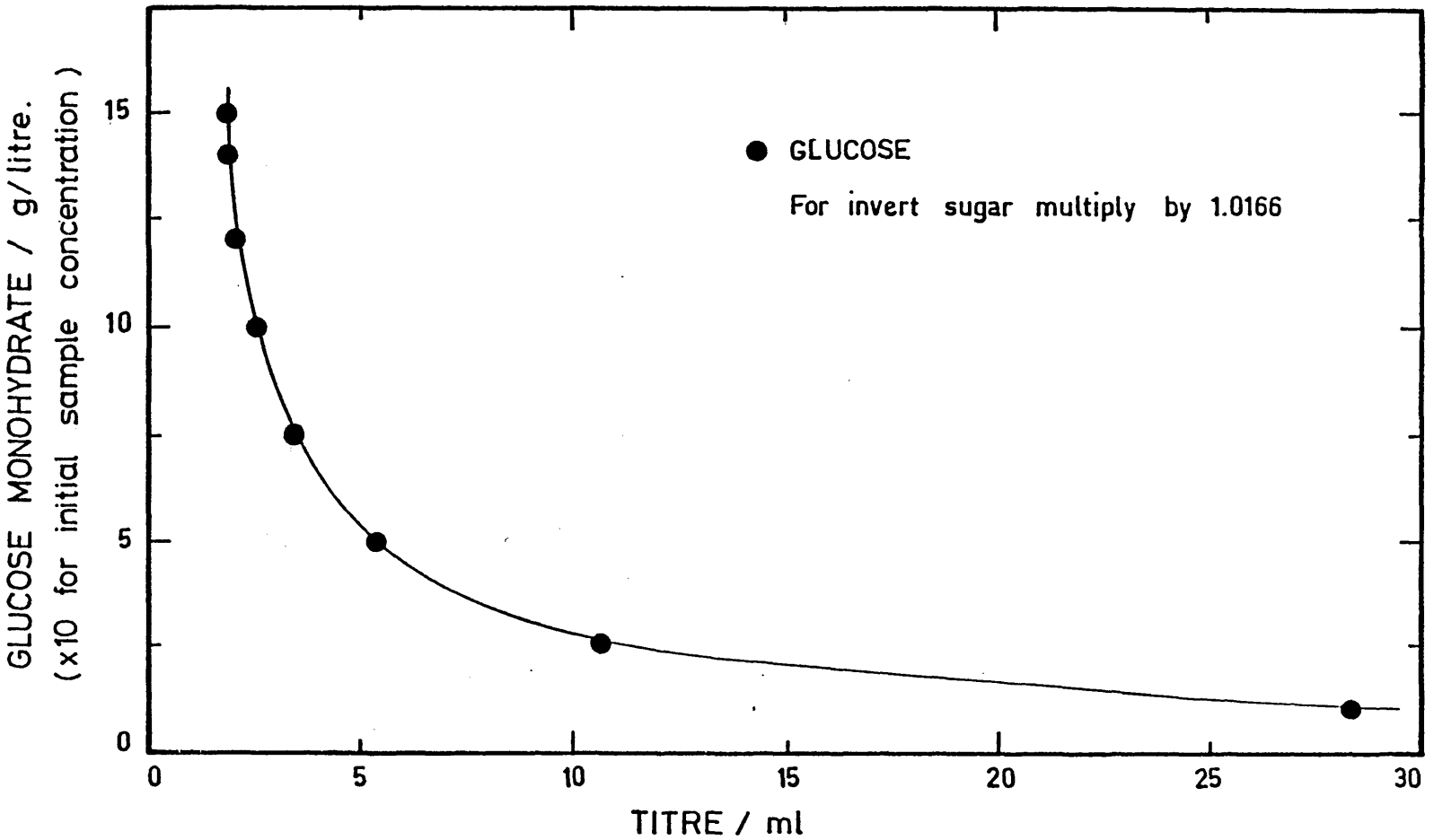


Fig. 2.6: Calibration curve for the analysis of inducing sugars using Lane and Eynons method.

placed in a 40 ml beaker. The unknown glucose or invert sugar sample was diluted by a factor of ten and placed in a 50 ml burette. Almost all the sugar solution required for the reduction was added to the cold reagent (quantity determined by trial and error). The resulting mixture was heated to boiling point and maintained at moderate ebullition for two minutes. Without removing from the flame five drops of solution C were added and the titration completed by adding more sugar solution dropwise until the blue colour had disappeared, leaving bright red cuprous oxide. The titration was completed within 3 minutes. It was necessary to carry out a minimum of three consecutive tests in order to obtain a titre reproduceable to ±0.01 ml. Calibration curves were prepared (Fig 2.6), relating glucose and invert sugar concentrations to titre values. These were used to calculate unknown glucose and invert sugar concentrations.

The technique could be used to detect sugar concentrations over the range 20-160 g/l. For samples containing less than 20 g/l total reducing sugars, the initial solution was diluted by a factor less than ten such that it contained between 0.02-0.16 g/l total reducing sugar.

The errors associated with the measurment of sucrose and glucose samples were estmated by analysing ten known samples of each saccharide. After sufficient practice glucose analyses were on average accurate to 0.4% using a microburette or 1.7% using a standard 50ml burette with 50 ml divisions. Similarly sucrose could be determined to

1.0% or 2.0%, respectively.

Sucrose hydrolysis. Sucrose is not a reducing sugar and must be hydrolysed to invert sugar (equimolar mixture of glucose and fructose) for analysis by Lane and Eynon's method. Sucrose was hydrolysed using the enzyme invertase (Eqn 2.1).

$$\underset{\text{sucrose}}{C_{12}H_{22}O_{11}} + H_2O = \underset{\text{glucose}}{C_6H_{12}O_6} + \underset{\text{fructose}}{C_6H_{12}O_6} \qquad (2.1)$$

Concentrated yeast invertase extract was obtained from B.D.H. Ltd. The manufacturer suggested that 1ml enzyme hydrolyses 4 g sucrose (in 20 ml 0.1 M potassium dihydrogen phosphate) within 30 minutes at 20°C. Further information concerning invertase is given in the Enzyme Biotechnology Handbook (89). The optimum pH for the reaction (Eqn 2.1) is 4.5, and the optimum temperature is between 50 and 60°C. The enzyme is inhibited reversibly by heavy metals and the rate of hydrolysis is slowly reduced above 8% w/w sucrose until at 70% sucrose only a quarter of the highest activity is obtained.

Samples to be analysed contained no more that 130 g/l sucrose and were treated in an identical manner. To 10 ml carboxylic acid-free sample (see under carboxylic acid analysis) was added 9.0 ml 0.2 M potassium dihydrogen phosphate (to buffer the solution to pH 4.0) and 1 ml invertase concentrate. The whole mixture was warmed at 40°C in a water bath for 30 minutes and then irradiated in a microwave oven (λ=5 cm, 0.5 Kw, 2450 MHz) for two minutes.

The irradiation step was found to be necessary after preliminary analyses indicated that free invertase interfered with Lane and Eynon's method (causing an increase in titre values). Two minutes of microwave radiation was sufficient to destroy free invertase leaving sugars unaffected. The resulting mixture was analysed as set out earlier.

2.1.7. Gravimetric determination of citric acid.

Citric acid was determined gravimetrically as penta-bromoacetone (300). Alkali permanganate converts citric acid to acetone dicarboxylic acid.

$$\begin{array}{l} CH_2COOH \\ | \\ HOOC\text{-}C\text{-}OH \\ | \\ CH_2COOH \end{array} + [O] = \begin{array}{l} CH_2COOH \\ | \\ C{=}O \\ | \\ CH_2COOH \end{array} + CO_2 + H_2O \qquad (2.2)$$

In the presence of bromine colourless penta-bromoacetone (PBA) precipitates.

$$\begin{array}{l} CH_2COOH \\ | \\ C{=}O \\ | \\ CH_2COOH \end{array} + 5Br_2 = \begin{array}{l} CHBr_2 \\ | \\ C{=}O \\ | \\ CHBr_3 \end{array} + 2CO_2 + 5HBr \qquad (2.3)$$

Wohlk (300) indicated that oxalic, tartaric, malic, and succinic acids, and their salts, do not interfere. Other compounds which precipitate with bromine must be removed.

In each test a 20 ml sample was centrifuged at 2000 rpm for 10 minutes to remove suspended matter. The upper 10 ml was carefully removed and added to 20 ml 0.01 M potassium permanganate, saturated with bromine. The whole mixture was

warmed at 60°C in a water bath for 30 minutes. It was then cooled below 6 °C and the excess bromine/permanganate destroyed with sulphosalicylic acid. The resulting suspension of PBA was centrifuged and excess liquid decanted. The residual slurry was filtered onto a composite Whatman 542/Millipore (0.42µm) retention filter paper and washed with 5 ml DDW. The PBA precipitate was dried at 20°C (mpt 79-80°C) by desiccation. The weight of citric acid in the original sample was calculated on an anhydrous basis as the weight of PBA multiplied by a conversion factor equal to 0.5642.

The accuracy of this technique, as measured by the analysis of ten consecutive known samples, varied between 2 and 8%. The error increased as the citrate concentration decreased. Below 3 g/l citrate the error was >8%, and an alternative technique was employed. This technique involved the reaction of PBA with sodium sulphide and measurement at 450 nm using a Perkin Elmer photometer. The technique is fully described by Perlman et al. (301). It was infrequently used in the present work.

2.1.8. Determination of oxalic acid.

Oxalic acid was analysed by the precipitation and AA analysis of its lanthanum salt. Lanthanum oxalate is sparingly soluble in inorganic acids below pH 1.0 but is otherwise insoluble (8×10^{-5} g/100 ml DDW at 25 °C). The precipitate produced by adding 3 ml 20% lanthanum chloride to a 0.5 ml sample was filtered on a 0.45 µm retention millipore filter paper, washed thoroughly and then

dissolved in 0.1 M hydrochloric acid. This solution was analysed for lanthanum (Section 2.1.1). The result was used to calculate the original concentration of oxalic acid, assuming the formula $La_2(C_2O_4)_2.9H_2O$.

The analytical error was calculated by analysis of ten standard solutions ranging in concentration from 0.1 to 50 g/l oxalic acid (all diluted by a factor of 100), and ranged from 1.8 to 5.5%.

2.1.9. Other analytical methods.

All nitrogen analyses were carried out by the Analytical Services Laboratory using Kjeldahl's and Nessler's methods (302). Values of pH were measured using a Philips PW9410 meter with a Pye Unicam combination Ag/AgCl electrode. The probes were washed thoroughly with DDW after each measurement and stored in DDW after use.

2.2. Selection and Appraisal of Nepheline Bearing Samples.

Nepheline is named from the Greek, nephele, meaning a cloud and referring to the cloudy appearance developed on immersing the mineral in strong acid. Another name, elaeolite, is also from the Greek, elaion, meaning oil and refers to the characteristic greasy lustre of nepheline. Nepheline is a member of the feldspathoid group of aluminosilicate minerals (303). It crystallizes in the hexagonal system and has a structure based on a three dimensional framework of linked SiO_4 and AlO_4 tetrahedra. The framework is fairly open and resembles the structure of tridymite, a high temperature polymorph of silica. Electrcal neutrality is maintained by sodium and potassium cations in the ratio 3:1. This ratio is governed by the nepheline structure in which sites available for alkali metal ions are of two different sizes and have similar distribution ratios in the unit cell. As a consequence of this open structure and the relatively high Al:Si ratio (>1:1) in the framework, nepheline is structurally weak and is readily degraded by acids. Silica is often a product of degradation and clouds the transparent surface of the mineral.

Rocks containing nepheline are formed during the cooling of magmatic fluids deficient in silica. If crystallization occurs at depth the rate of cooling is slow (as a result of the earth's low thermal conductivity) and the pressure is high. Rock formed under these conditions are coarse



Fig 2.7 Open cast nepheline syenite quarry at Nephton, Ontario.

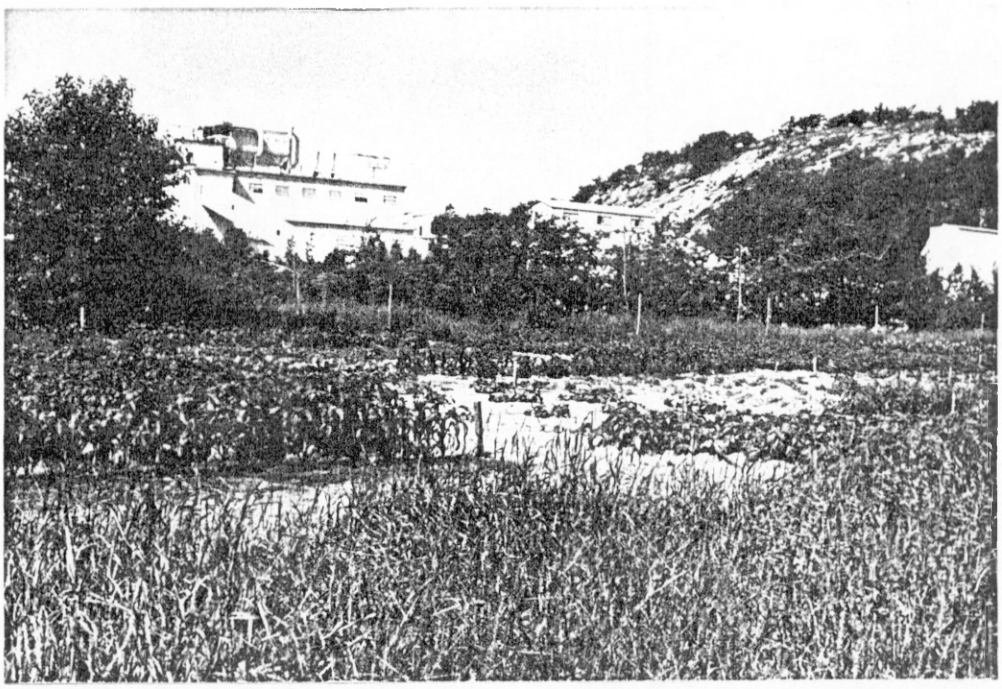


Fig 2.8 Crop trials on potassium rich gangue from the processing plant (background).

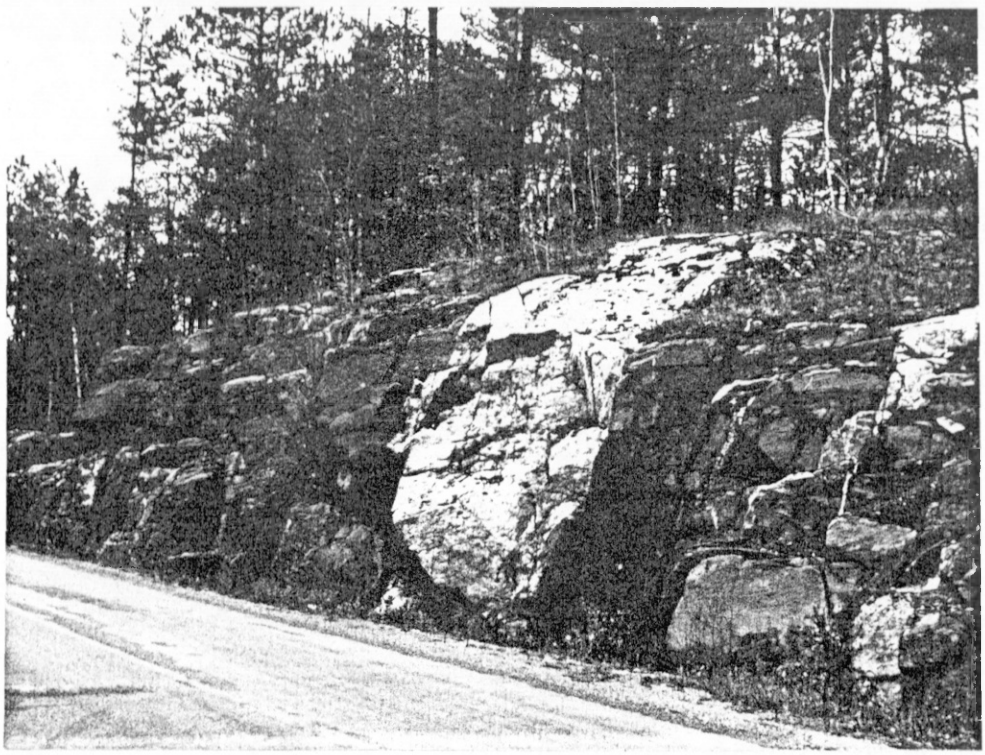


Fig 2.9 Typical intruded pegmatite dyke in the Bancroft district.

grained, ranging from pegmatites (which contain large crystals up to several meters in length with in a matrix of smaller crystals), to syenites in which all crystals in the matrix are about 3-6 mm in length. If silica-deficient magmatic material rises to the surface, the rate of cooling is rapid and a relatively fine-grained rock is formed (phonolite).

All of these nepheline bearing rocks should be susceptable to attack by acidophilic fungi. Fungi are therefore of potential value in the recovery of alumina and potash from them. The leaching characteristics of each rock will be different and it is necessary to test samples of all three to establish the one most suitable for detailed study.

An outstanding example of nepheline pegmatite can be found in the Haliburton-Bancroft district of Ontario where crystals of nepheline and albite (feldspar) are up to 2 m in linear dimension. These rocks have been investigated as a source of corundum (304), a frequent accessory mineral in amounts up to 5%. So far no other uses have been proposed for the rocks. The author visited this area, and the Nephton district of Ontario, to collect mineral samples and view open cast mining operations of nepheline syenite carried out by Industmin Ltd (Figs 2.7-2.8). A 6 Kg sample of near-pure nepheline, taken from inside large nepheline crystals from a pegmatite dyke close to a disused quarry outside Bancroft (Fig 2.9), was brought back for testwork.

Large deposits of nepheline syenite having a low iron content find extensive use in the glass/ceramics industries

(305), as fillers in paints and other products (306), for the production of alumina and cement (USSR only), and more recently as a glassing agent for radioactive wastes. Outside the USSR there are two producing countries (Canada and Norway). The Canadian deposits are situated at Nephton and account for over 0.5 million tonnes/year or 63% of Western production, the majority of which is used by the glass/ceranics industries. The Norwegian deposit at Stjernoya Island, accounts for the remaining 37% of Western production (0.3 million tonnes/year). As a glass/ceramic flux, the product must be low in iron to reduce colouration and have a precise composition/size range for precise melting characteristics. After the rock has been mined it is crushed and magnetic minerals are removed by magnetic separators. The resulting material, which contains <0.1% iron, is then screened to provide two size fractions (32 mesh (glass flux) and 325 mesh (ceramic flux)). A typical flow diagram for nepheline syenite beneficiation is given in Fig 2.10.

With regard to aluminium production in the USSR, estimates by the US Bureau Of Mines indicated that almost 1 million tonnes of nepheline concentrates were produced in 1966 (307). By 1983 this had increased to 6 million tonnes from which were produced 0.5 million tonnes aluminium, 6 million tonnes Portland cement, and 0.2 million tonnes of soda and potash (308). This dramatic rise originated from the lack of high grade bauxite behind the iron curtain. At present nepheline accounts for 16% of aluminium produced in the USSR (308).

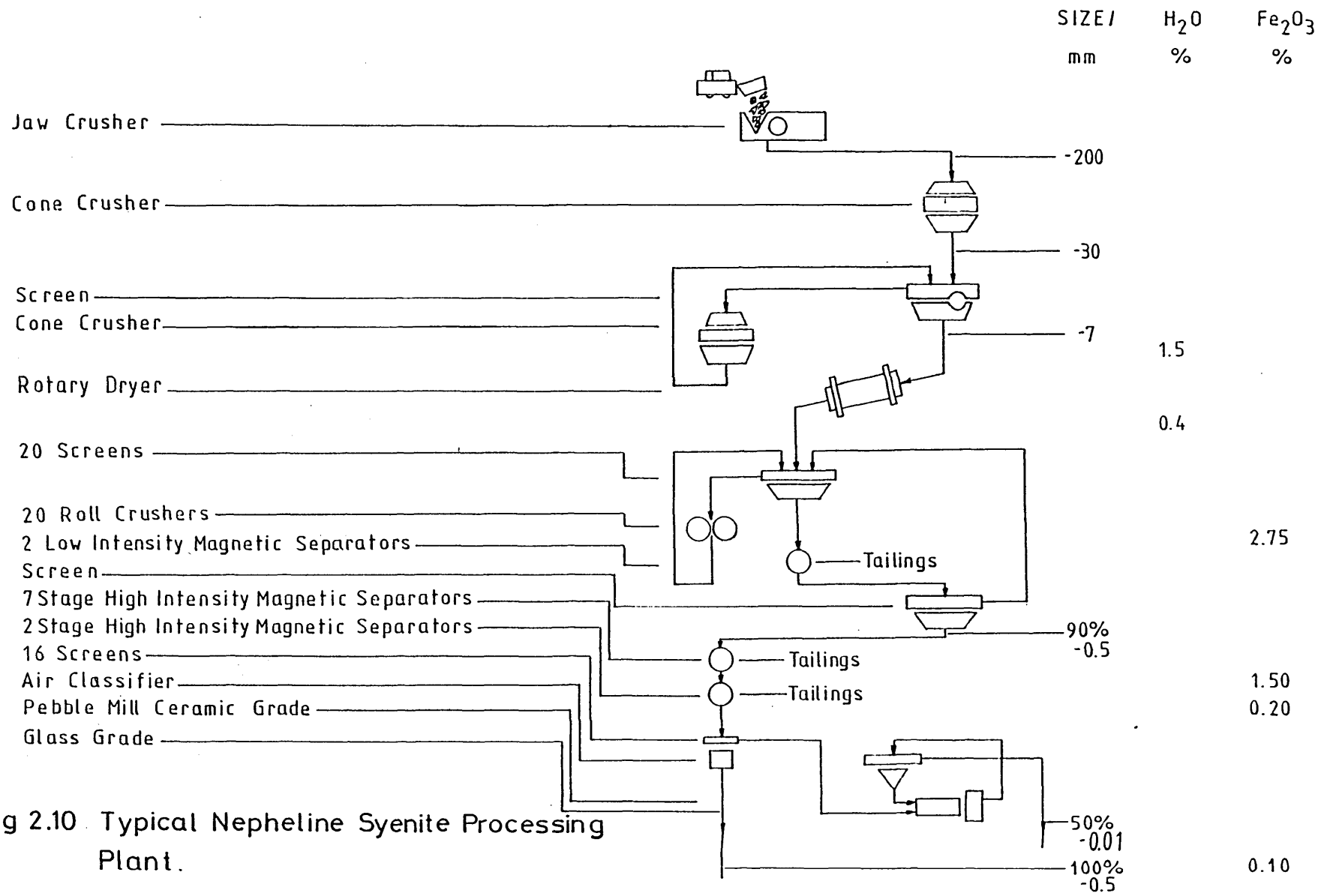


Fig 2.10 Typical Nepheline Syenite Processing Plant.

For testwork purposes nepheline syenite as samples of -0.5 cm untreated run of mine ore, and -32 mesh glass grade product (in total 100 Kg) were obtained from Stjernoya Island by sea to the UK agents (Nornef Minerals Ltd at Runcorn docks, Cheshire). Samples were collected from Runcorn by car.

Phonolites are mined in Germany and Czechslovakia as raw materials for the manufacture of low grade (dark green) bottle glass(306). Another use is as a hard-wearing roadstone. Quarries for this product are found in Scotland and France.

Although phonolite was readily available in Scotland, rock from this deposit had a relatively low nepheline content (4%)(306). A 600 g sample was purchased from Gregory Bottley and LLoyd Ltd. This came from the deposit currently mined in the Ceske Stredahon Mountains, Czechslovakia.

The aim of this section was to determine representative elemental and mineralogical compositions of the nepheline bearing samples: Bancroft nepheline, Norwegian syenite, and Czech phonolite. A preliminary assessment was carried out in order to identify major mineral phases present in each case and also to determine the approximate liberation sizes of nepheline and iron-bearing mineral grains. This information was used in a detailed elemental and mineralogical analysis.

2.2.1 Preliminary mineral appraisal.

The major mineral phases in each sample were identified

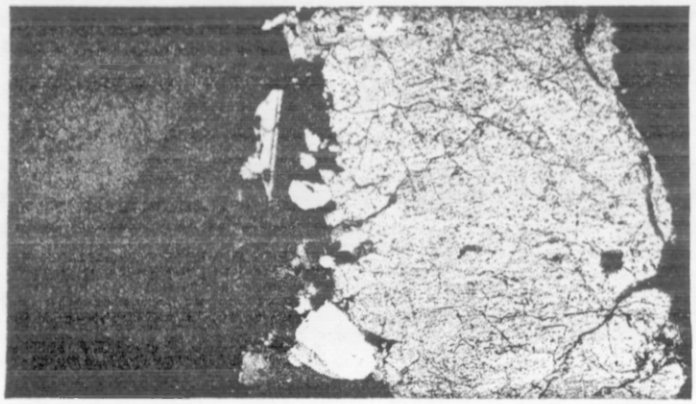


Fig 2.11 Optical photomicrograph of Bancroft nepheline in thin section 30×.

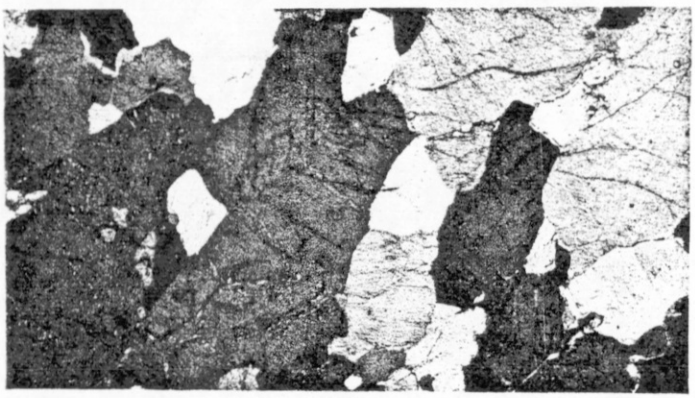


Fig 2.12 Optical photomicrograph of Sterjnoya syenite in thin section 10×.

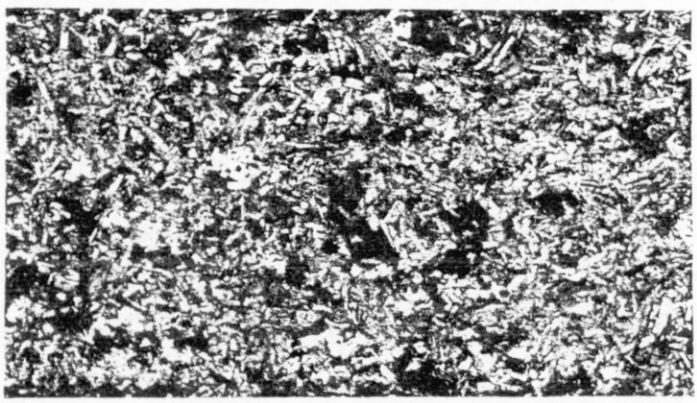


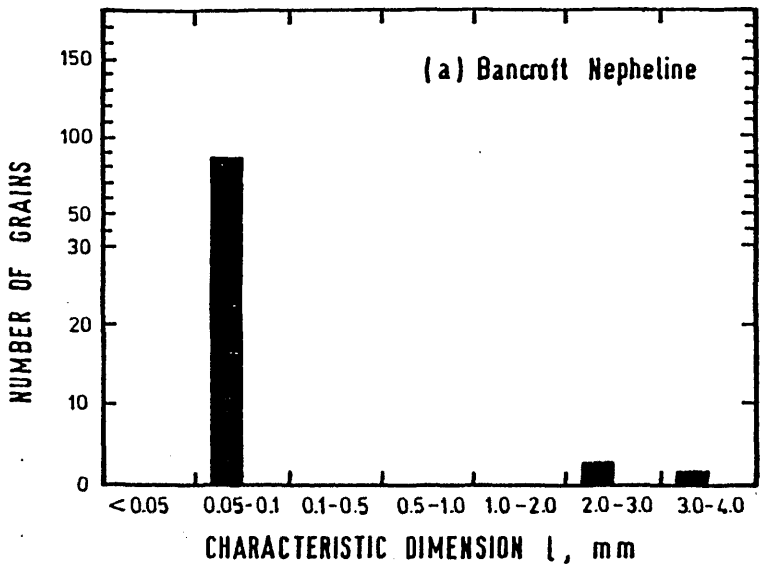
Fig 2.13 Optical photomicrograph of Czech phonolite in thin section 30×.

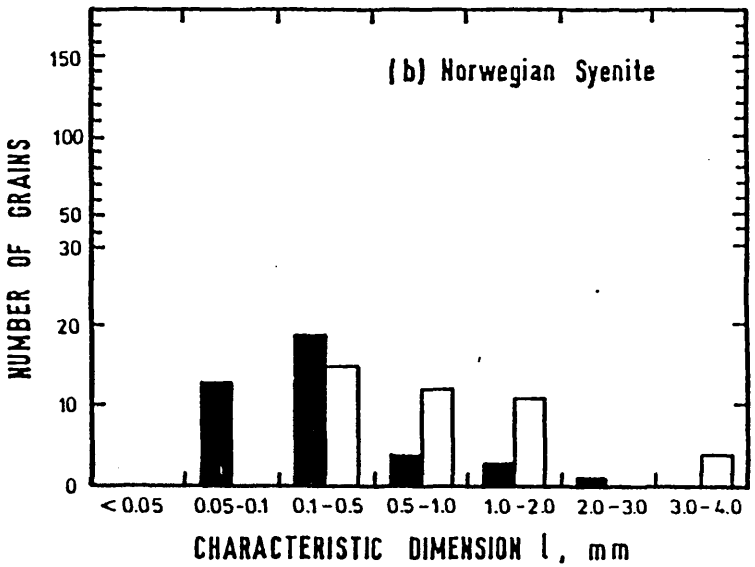
(as thin sections, Figs 2.11-2.13) with the aid of standard texts(303,309).

Minerals in Bancroft nepheline (Fig 2.11) included feldspar (light grey in photograph); sodalite (readily identified from its blue colour in the bulk sample); magnetite (which occurred as small octahedra, opaque in Fig 2.11); and biotite mica (not in the figure but visible in the bulk sample as large flakes). The sample of Norwegian syenite (Fig 2.12) included nepheline, feldspar, magnetite, and sphene. Sphene was identified from its spheroidal cross-section, high birefringence and large dispersion. Four other phases were found but could not be positively be identified. The photograph of the phonolite sample (Fig 2.13) was overexposed to increase the contrast between iron bearing minerals and feldspar/feldspathoid minerals. The dark grains (black in Fig 2.13) were strongly pleochroic with high extinction angles, indicating that they could be intermediates of augite. The regular blade-like crystals making up a major proportion of the rock were identified as a type of feldspar. Three other minerals were found but could not be positively identified.

2.2.2 Estimate of liberation sizes.

A liberation analysis was carried out on polished, stained, specimens of rock to estimate the crystal size distribution and hence the liberation sizes of feldspathoid and iron bearing minerals in each sample. This information was to establish the size to which samples need to be crushed in order to remove iron-bearing minerals by





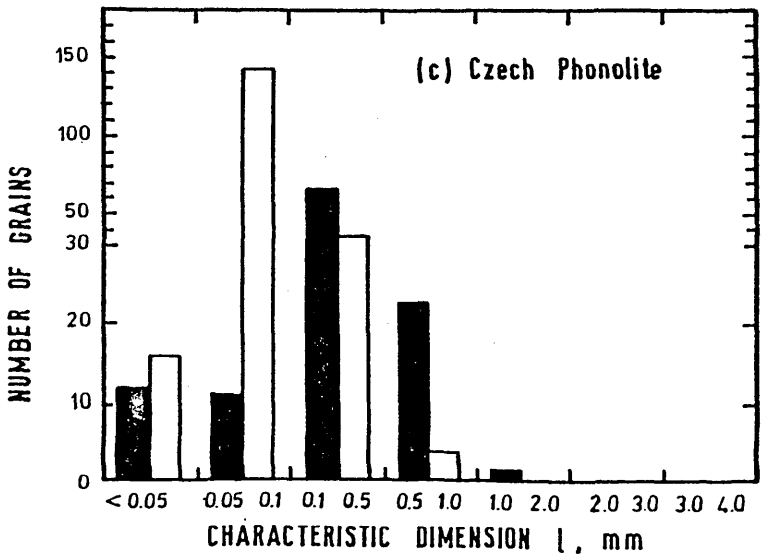




Fig. 2.14: Histograms of number of grains as a function of characteristic dimension l for Bancroft nepheline, Norwegian syenite and Czech phonolite.

magnetic separation and leach feldspathoids efficiently with acid (Section 2.2.6). Four discs of each sample (which were assumed to be representative with respect to crystal size) were polished, and selectively stained to highlight feldspar, feldspathoid, and iron bearing crystals (310). Using this technique potassium feldspar was stained yellow, feldspathoids greenish-blue, plagioclase feldspar was unchanged and iron-bearing minerals remained dark.

Data were obtained by measuring, with reference to a diffraction grating, all relevant crystals (major and minor axes) within an area of 8 cm^2 (4x2cm^2 samples) using a 'Swift' petrological microscope.

The results (Fig 2.14 a-c) were illustrated as hystograms of the number of crystals observed as a function of size (where l is the average of major and minor grain dimensions). In Bancroft nepheline (Fig 2.14-a) two separate distributions can be seen for iron-bearing grains. The large peak at the lower size range (0.05-0.1 mm) represented magnetite octahedra, and the other biotite flakes (2-4 mm). This indicated liberation sizes of 2 mm (biotite) and 50 μm (magnetite).

From Fig 2.14-b (nepheline syenite) it can be seen that the major proportion of nepheline was in the form of large crystals (3-4 mm), although substantial numbers of smaller grains (0.1-2 mm) were also present. The liberation size of iron-bearing minerals was similar to that of Bancroft nepheline (50 μm).

In the Czech phonolite (Fig 2.14-c), unlike the other samples , the overall size-range of iron-bearing crystals

was larger than that of the feldspathoid minerals. There was a large proportion of -50 μm crystals. Hence it would be necessary to grind the phonolite substantially below 50 μm in order to liberate the minerals.

Conventional magnetic separators were not suitable for the removal of iron-bearing grains sized at or below 50 μm. A superconducting magnet was employed for this purpose. Several passes were required to remove all visible magnetic minerals and to clean up the magnetic fraction of light minerals.

2.2.3 Scheme of elemental and mineralogical analysis.

Detailed elemental and mineralogical analyses were carried out for each sample based on the results of Section 2.2.1 and 2.2.2 and the procedure set out in Fig 2.15, for Bancroft nepheline.

In this procedure 200 g of Bancroft sample (1 inch lumps), Norwegian syenite (0.5 inch lumps), or Czech phonolite (0.5 inch lumps), was crushed and screened to provide approximately 25 g each of the size fractions -1700+850, -850+300, -300+75, and -75 μm, which were stored for later use. The +1700 μm fraction (about 82 g) was ground to -30 μm in an agate mill.

Cumulative sampling errors, denoted by e, and calculated using Gy's nomogram (311),are included for each stage. Final cumulative sampling errors for Norwegian syenite and Czech phonolite were 3.5 and 6.0 repectively. The major errors occurred upon taking the first 200 g sample. These errors were significant but acceptable. They could have

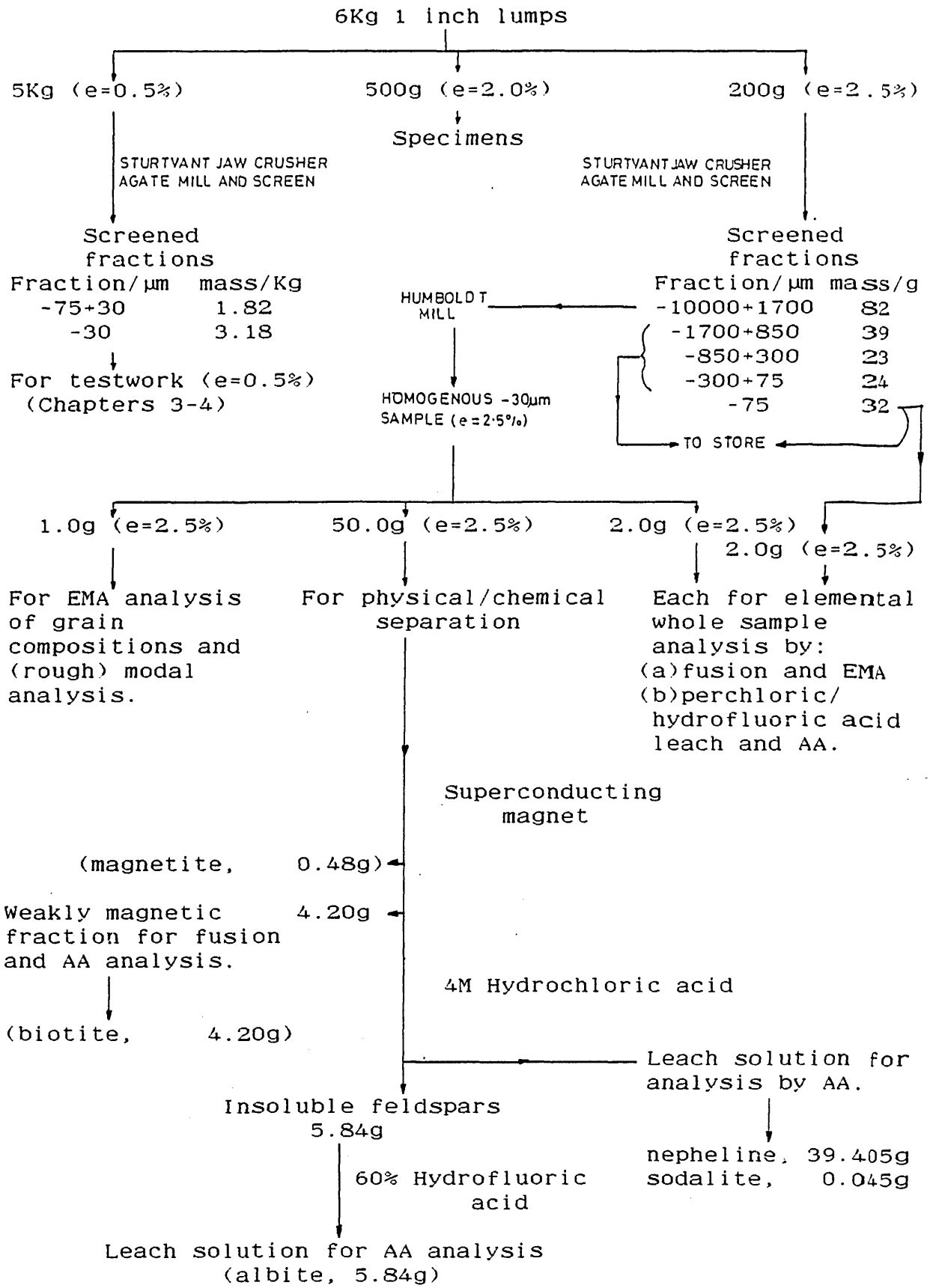


Fig 2.15 Scheme of sample preparation and analysis for Bancroft nepheline.

been reduced only by dealing with samples of considerably larger mass.

Elemental analyses were carried out using two different methods. In the first a sample was leached with hydrofluoric/perchloric acids and the resulting solution analysed by AA. Although silicon was lost by this technique its concentration could be deduced from a mass balance. To substantiate the results, a second technique was employed. This entailed fusion of a sample with lithium metaborate followed by analysis of the bead by electron microprobe techniques (Section 2.1.3).

Replicate elemental analyses were carried out using 1 g samples of -75+53 μm material in order to establish whether this sample was sufficiently representative of the bulk phase. This information was required for testwork described in Chapter 3.

A rough modal analysis of mineral phases present in each sample, and an accurate elemental analysis of each mineral phase was obtained using EMA. A more precise quantitative mineralogical analysis was carried out using a physical/chemical separation technique. In this technique, magnetics were removed by low and high intensity magnetic separators. As magnetite only occurred as isolated octahedra it could be readily separated from other magnetic minerals of lower susceptibility. The relative proportions of magnetics in the mixture recovered by high intensity magnetic separator were determined by fusing the mixture with lithium metaborate. The bead was then dissolved in nitric acid or citric acid (the latter giving less silica

precipitation), and the resulting solution analysed by AA to determine the concentrations of elements unique to each mineral phase as determined from EMA analyses.

Non-magnetics were separated into those soluble in dilute hydrochloric acid (feldspathoids) and those practically insoluble in hydrochloric but soluble in hydrofluoric acid (feldspars). In each case the concentration of individual mineral phases were determined in a similar manner to magnetic mixtures.

2.2.4. Elemental analysis by fusion/EMA and by acid leach/AA.

For fusion/EMA a 1.0000 g sample was added to 5.0000 g Spectrosol grade lithium metaborate in a 5:95 gold:platinum crucible (with lid). The mixture was fused for precisely 15 minutes in a preheated oven at 1000°C. Upon removal from the oven the crucible was tilted to allow the fused mixture to collect together and then rapidly quenched, with the lid on, to separate the bead from the crucible. Two beads for each sample (one blank) were analysed by EMA using similarly prepared standards containing metal oxides. titanium, barium, and strontium were not analysed by this technique reducing the number of standards required to eight, which is all that could fit into the equipment at any time.

For acid leach/AA a 1.0000 g sample was leached with 50 ml of a 50/50 mixture of perchloric/hydrofluoric acids in a 100 ml Teflon beaker. The mixture was heated to dryness on a hotplate and replenished with fresh acid (and

TABLE 2.3 ELEMENTAL ANALYSES OF BANCROFT NEPHELINE, NORWEGIAN SYENITE, AND CZECH PHONOLITE.

	Nepheline		Syenite		Phonolite	
	leach	fusion	leach	fusion	leach	fusion
	%	%	%	%	%	%
SiO_2	44.5	43.6	53.8	53.2	55.2	54.8
TiO_2	0.2	-	0.5	-	-	-
Al_2O_3	30.0	29.3	23.2	22.8	23.5	23.7
Fe_2O_3	2.9	2.1	2.4	1.8	3.2	3.6
MnO	-	-	-	0.1	0.3	0.1
MgO	0.6	1.2	0.2	0.9	0.6	0.9
BaO	-	-	0.3	-	-	-
SrO	-	-	0.2	-	-	-
CaO	0.6	0.7	2.5	3.8	3.2	3.8
Na_2O	13.3	13.2	8.2	8.5	6.4	6.3
K_2O	7.3	7.3	8.3	8.7	6.2	6.6
Totals	99.40	97.40	99.60	99.80	98.72	99.80

reheated) twice to dissolve all dark minerals. After boiling dry a third time the residues were dissolved in 5 M hydrochloric acid. This solution was analysed by AA for sodium, potassium, aluminium, iron, manganese, calcium, magnesium, titanium, barium, and strontium. Silicon, which is volatilised during the acid leach was deduced from a mass balance assuming undetected elements were insignificant and that iron had a valency of 3+.

The results are compared in Table 2.3. With the exception of magnesium for which the probe estimate is approximately double that of the AA for all samples, results of both techniques are closely comparable. The reason for the discrepency in magnesium analyses was not determined and was not considered of great importance because of its relatively low concentration.

2.2.5. Mineralogical analyses by electron microprobe.

The aim was to analyse a number of grains, Xn, for elements likely to be present in the contained mineral phase(s). This should allow the mineral phase(s) in these grains to be identified and counted. For large values of Xn counts of the different phases represent the modal composition of the whole sample. However, the number of grains necessary (for Bancroft nepheline) was of the order of 8000 to achieve a 1% error at the 95% confidence level (assuming the sample is representative and constituent minerals are normally distributed). Limited availability precluded such a large number of analyses. The actual number of grains analysed for Bancroft nepheline, nepheline

TABLE 2.4 ELECTRON MICROPROBE ANALYSIS OF BANCROFT NEPHELINE.

MINERAL - %	AVERAGE ELEMENTAL COMPOSITION %									
	Si	Na	Al	K	Fe	Ca	Mg	Ti	O	TOTAL
Nepheline 56	20.59	12.17	17.21	6.92	-	-	-	-	43.01	99.90
" 2	21.54	9.57	13.18	6.89	-	-	-	-	48.74	99.92
" 22	20.42	12.00	17.95	6.30	-	-	-	-	43.26	99.93
" 4	17.37	10.88	16.87	7.06	-	-	-	-	47.75	99.93
Albite 6	31.95	8.08	12.01	0.95	-	-	-	-	46.58	99.57
Sodalite 4	18.61	16.92	16.00	-	0.41	-	-	-	42.07	94.01
Biotite 4	16.51	6.66	9.57	0.03	17.88	0.27	0.91	1.61	36.25	89.69
Magnetite 2	0.01	-	-	-	69.56	-	-	-	29.93	99.50

TABLE 2.5 ELECTRON MICROPROBE ANALYSIS OF NORWEGIAN SYENITE.

MINERAL - %	AVERAGE ELEMENTAL COMPOSITION %									
	Si	Na	Al	K	Fe	Ca	Mg	Ti	O	TOTAL
Feldspar - Na 48	27.56	6.96	11.45	0.13	0.02	1.52	-	0.04	44.64	92.29
Feldspar - K 45	18.87	11.74	17.14	4.98	0.14	0.35	-	0.02	42.02	95.21
Nepheline 35	26.47	11.87	19.87	10.51	0.05	0.04	-	-	42.31	92.96
Calcite 4.0	0.06	0.12	0.01	-	0.20	38.17	0.05	-	15.47	54.08
Ilmenite 0.8	0.005	6.03	0.02	-	28.63	0.01	0.36	-	12.58	41.98
Sphene 3.2	11.76	0.04	0.84	0.02	0.59	18.75	-	-	21.96	54.10
Magnetite 2.4	0.02	0.03	0.63	-	68.07	0.01	0.01	2.43	29.86	98.63
Pyroxene 2.4	21.26	8.08	9.28	0.09	4.01	1.02	-	1.80	39.06	85.24
Hornblende 2.4	16.96	2.49	7.14	1.71	13.00	6.76	4.2	-	37.10	88.14

TABLE 2.6 ELECTRON MICROPROBE ANALYSIS OF CZECH PHONOLITE.

MINERAL - %		AVERAGE ELEMENTAL COMPOSITION/%									
		Si	Na	Al	K	Fe	Ca	Mg	Ti	O	TOTAL
Sanidine	40	28.7	3.97	11.12	8.03	0.83	0.25	0.03	0.41	46.32	99.69
Nepheline	25	21.59	9.57	13.31	6.69	-	-	-	-	48.73	99.89
Sodalite	10	18.15	17.26	16.02	-	0.59	0.13	-	-	41.51	93.64
Hauyne	2.5	15.91	7.71	14.96	4.51	-	6.79	-	-	37.76	87.64
Aegirine-Augite	20	26.86	1.38	1.03	0.06	7.44	3.82	2.11	0.15	42.83	84.65
Sphene	2.5	14.89	-	-	-	0.10	19.4	-	24.06	40.72	99.15

syenite and phonolite were 50, 124 and 40 respectively. The ratios 50/125/40 were approximately proportional to the relative numbers of different mineral phases in each sample. Modal analyses were therefore semi-quantitative and comparable.

A 1.0000 g sample of each rock was encapsulated in resin as described in Section 2.1.3 and analysed for aluminium, silicon, sodium, potassium, titanium, calcium, and magnesium. In a number of cases minerals only present at trace level, found in preliminary thin section analyses, could not be immediately found by the probe. In such cases it was necessary to prepare a specimen known to have exposed on its surface the phase(s) in question which could then be found and analysed.

Tables 2.4-2.6 give the grain compositions and rough modal analyses for each sample. Each table includes the identity of the mineral in question (column 1); the approximate proportion of each mineral phase (column 2); and the average elemental analyses (columns 3-12). In all cases oxygen was calculated from the metal valencies applicable to the mineral phase in question (iron was assumed to have a valency of 3+). It will be noticed that for a number of minerals the totals (column 12) are substantially less than 100% (calcite and ilmenite in the sample of nepheline syenite). In each case this can be traced to a missing element or elements. In the case of calcite carbon is not included in the mass balance, and in the case of ilmenite, titanium was not determined for this particular run.

2.2.6. Physical/chemical separations.

In this technique use was made of the relatively high magnetic susceptibility of magnetite, biotite, etc., the higher solubility of feldspathoids, and the inertness of feldspars to achieve separations (and therefore) modal proportions.

Samples of each rock were first treated by super-conducting magnet (Oxford Instruments field strength 2.7 tesla) to remove magnetic minerals. The resulting magnetic fraction was then treated using a Rapid Magnetic type LOG 1-4 separator to separate magnetite from the other minerals. Methods employed were as described in standard texts (312,313). The magnetite-free fraction was fused with lithium metaborate and dissolved in nitric/citric acid (as in Section 2.2.3). The resulting solution was analysed by AA (as in Section 2.1.1) for magnesium and sodium. In the magnetite-free fraction obtained from nepheline syenite (sphene, hornblende, pyroxene, Table 2.5), only hornblende contains magnesium and pyroxene contains approximately 99.5% of the sodium contained in pyroxene and sphene. Hence the relative proportions of each mineral could be calculated. Similarly in the magnetite-free fraction from the phonolite sample, sphene does not contain any magnesium or sodium (Table 2.6), and the proportion of aeginine-augite could be calculated.

The non-magnetic fraction of Bancroft nepheline was leached with dilute hydrochloric acid to separate feldspathoid and feldspar minerals. Feldspars leached very

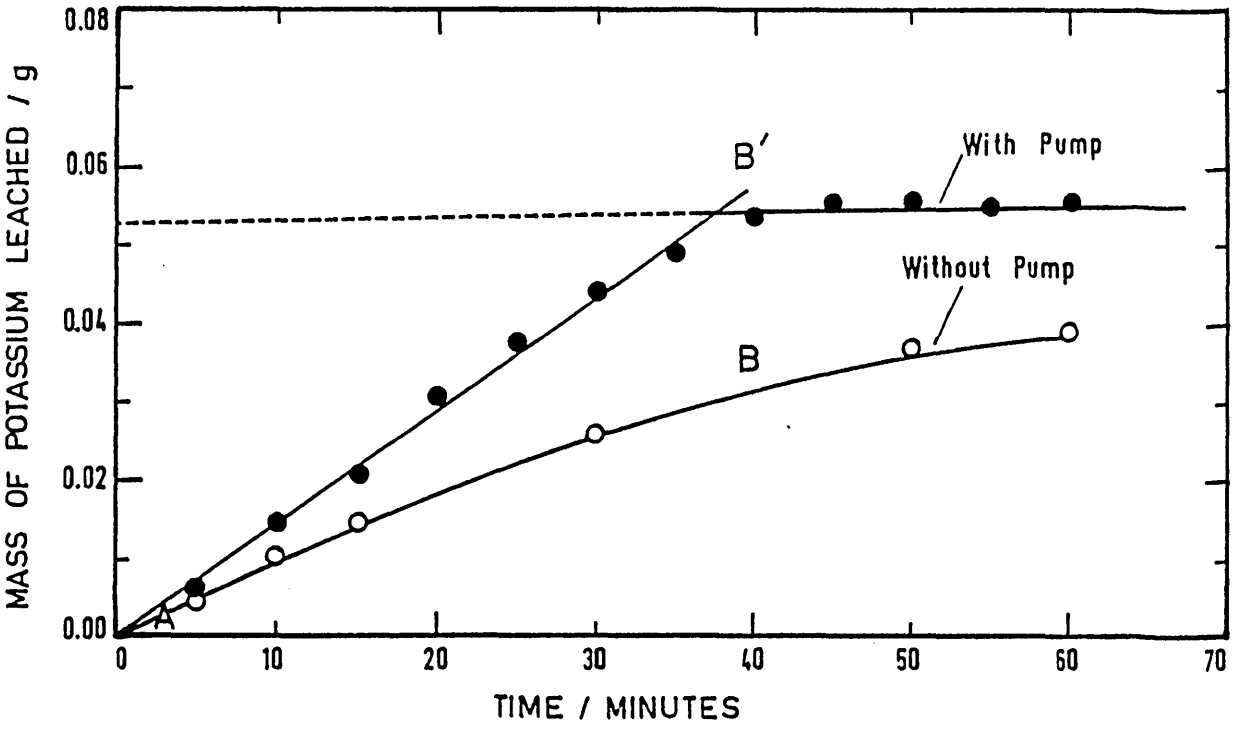


Fig. 2.16: Potassium leached out of the non-magnetic fraction of the Bancroft nepheline sample as a function of time.

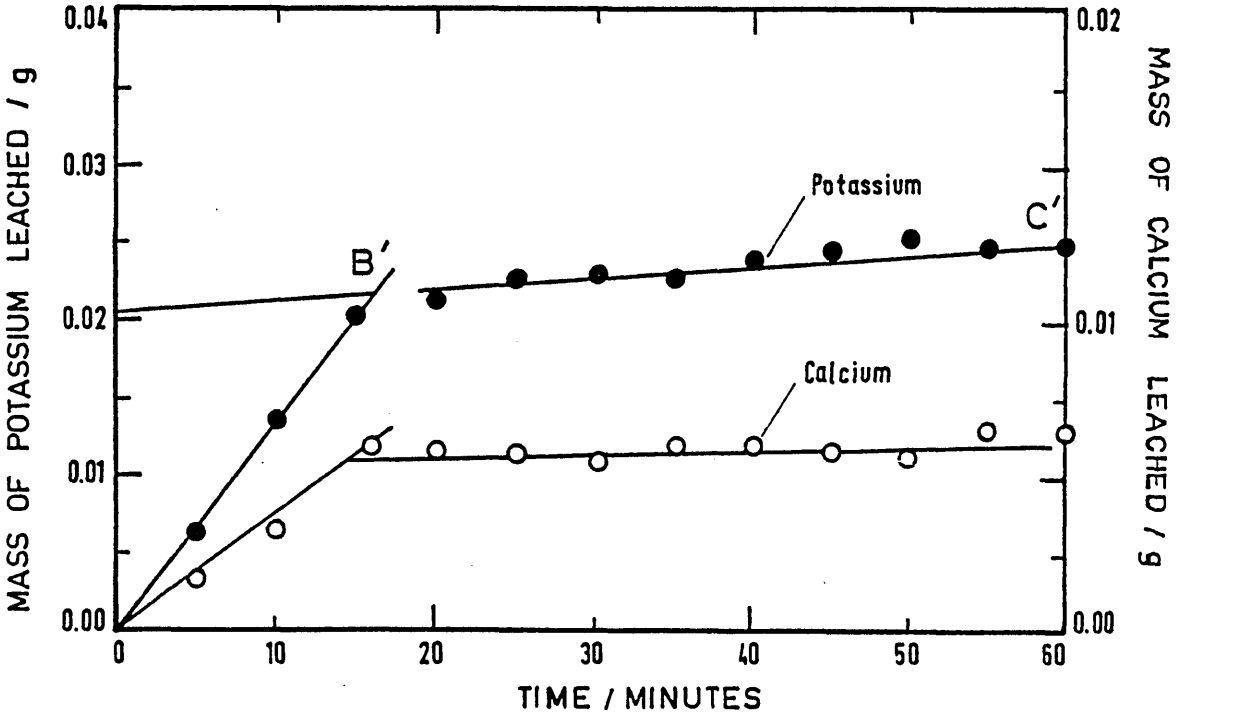


Fig. 2.18: Potassium and calcium leached out of the non-magnetic fraction of the Norwegian syenite sample as a function of time.

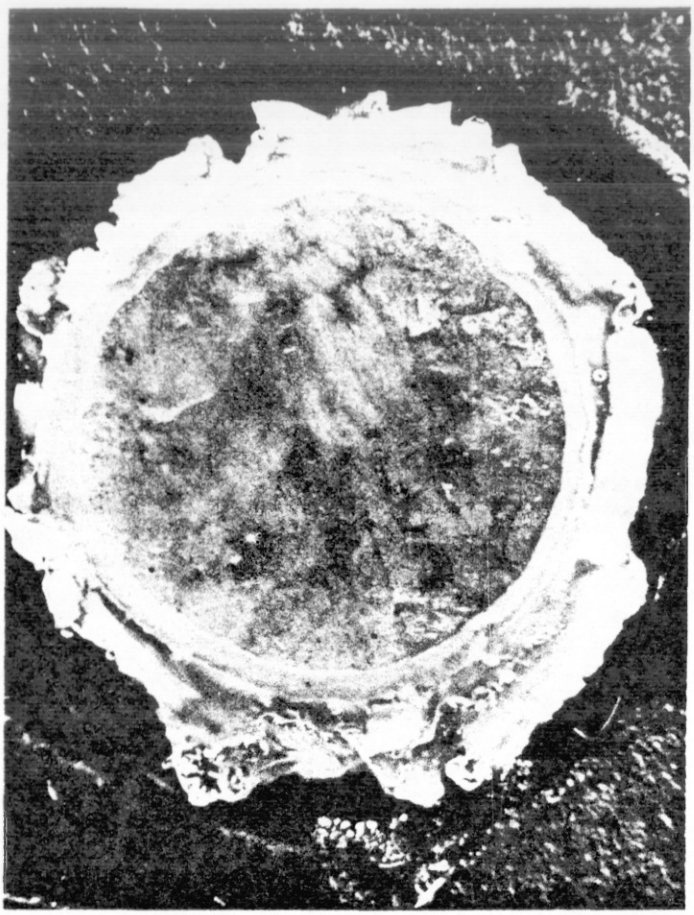


Fig 2.17 Silica gel product layers coating a reacted grain of nepheline (in cross-section) 8×.

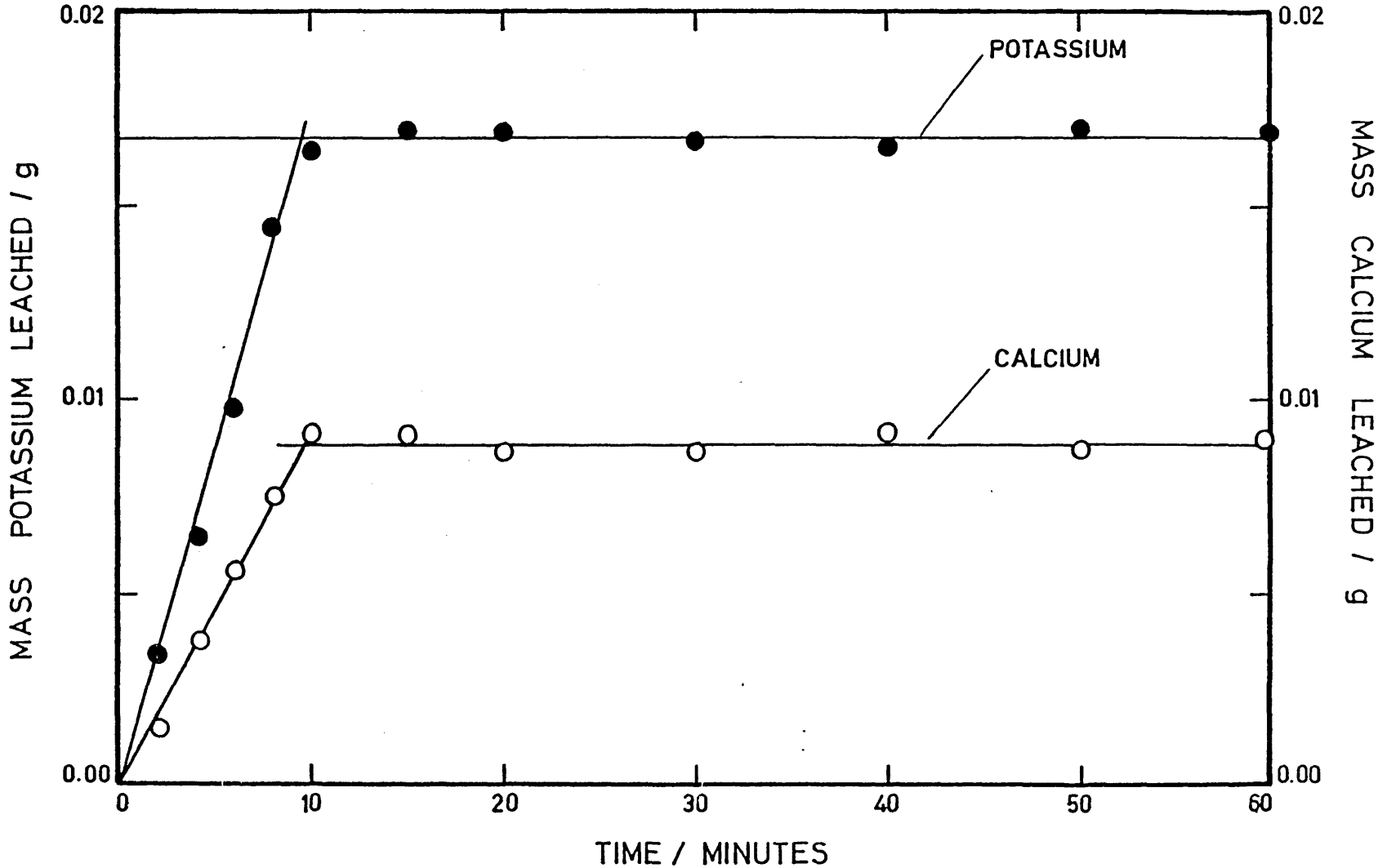


Fig. 2.19 : Potassium and calcium leached out of the non-magnetic fraction of Phonolite as a function of time.

slowly in comparison to the other minerals. This is illustrated on Fig 2.16 which is a graph of the mass of potassium leached as a function of time. Between points A and B all readily soluble minerals (nepheline and sodalite) are dissolved leaving insoluble feldspars. It will be noted from the curve AB that solubles are not leached in a linear manner without special leaching conditions. This is due to the build-up of a gel reaction layer around grains which rapidly slows down the rate of reaction. This is illustrated on Fig 2.17. More uniform leaching rates, noted by the straighter curve AB' were obtained by recycling the rock-acid mixture through a gear pump during the leach. The gear pump rapidly removed the gel layer surrounding reacting grains by its mild grinding action and enabled a more accurate estimate of the soluble mineral content (noted by the point at which the slope changes) to be calculated.

The proportions of soluble minerals in the non-magnetic fractions were calculated from Figs 2.16, 2.18 and 2.19, as follows. The liquid containing 'solubles' was analysed for sodium, potassium and calcium by AA. Only nepheline and sodalite are completely dissolved from the Bancroft nepheline sample. The proportions of each were readily calculated, from Fig 2.18 as only nepheline contains potassium (Table 2.4). In the sample of nepheline syenite only nepheline and calcite are completely dissolved. Their proportions can be calculated as only calcite contains calcium (Table 2.5). In the phonolite sample the proportion of hauyne can be calculated as only this mineral contains

calcium (Table 2.6). Nepheline can be determined in a similar manner from the concentration of potassium taking account of potassium in hauyne and noting that there is no potassium in sodalite. Sodalite represents what is left from a mass balance of all non-magnetic minerals soluble in hydrochloric acid.

The sample of nepheline syenite contained two insoluble feldspar phases. Their concentrations were determined by dissolving the mixture in hydrofluoric acid, and analysing the resulting solution for sodium and potassium by AA. As the ratio of Na/K for each phase is known (Table 2.3) their proportions could be calculated.

The experimental procedure was as follows. Samples of each rock (50 g of -30 μm) were treated to remove magnetic minerals as set out above. A sample of the non-magnetic fractions (0.5 g) were then leached with 200 ml of 4 M hydrochloric acid in a 500 ml conical flask on a reciprocating shaker. The temperature was maintained at 20° C using an air blower. The rock acid mixture was pumped at 1 l/min through a modified (steel bearings sealed with silicone vacuum grease) nylon headed gear pump (model SEIL 11/07-83/4). Samples of liquid (0.5 ml) were removed after five minute intervals for 1 hour using a syringe with filter adapter. All filter papers were saved and weighed to determine the weight of attached solids. Liquid samples were diluted and analysed by AA (as in Section 2.1.1) for sodium, potassium and calcium taking account of solid and liquid sampling losses. Mineral proportions were calculated as set out above.

TABLE 2.7 COMPARISON OF MINERALOGICAL ANALYSES OF NEPHELINE BEARING SAMPLES AS DETERMINED BY CHEMICAL AND MICROPROBE TECHNIQUES.

Mineral	Composition/ wt%			
	Chemical		Microprobe	
	%	±	%	±
Bancroft nepheline				
nepheline	78.81	0.6	84.0	8.5
albite	11.68	0.2	6.0	5.5
sodalite	0.09	0.001	4.0	4.5
biotite	8.40	0.08	4.0	4.5
magnetite	0.97	0.01	2.0	3.0
Norwegian syenite				
feldspar (K)	55.31	1.1	45.0	18.0
feldspar (Na)	0.73	0.01	5.0	8.0
nepheline	38.85	0.3	35.0	18.0
hornblende	0.82	0.1	2.5	5.5
calcite	2.07	0.1	4.0	7.0
ilmenite	0.32	0.003	1.0	3.0
sphene	0.73	0.007	3.0	6.5
magnetite	0.57	0.005	2.5	5.5
pyroxene	0.60	0.015	2.5	5.5
Czech phonolite				
sanidine	59.32	0.7	40.0	10.0
nepheline	14.75	0.1	25.0	9.0
sodalite	10.36	0.1	10.0	6.0
hauyne	1.08	0.07	2.5	3.0
aegirine-augite	13.70	0.3	20.0	8.5
sphene	0.79	0.008	2.5	3.0

In Table 2.7 the results of EMA and physical/chemical analyses are compared. Included in the table is the estimated error in the proportion of each phase. For EMA analyses this was calculated using the formula $Error=z*(x(1-x)/n)^{0.5}$,where z is to 1.63 for Gaussian distributions for 95% certainty, x is the calculated mineral proportion, and n is the size of the sample population. The errors for the physical/chemical analyses represent those relevant to the AA analysis as this step had the greatest error.

2.3 Selection and Appraisal of Fungal Systems.

Five freeze dried cultures (Table 2.8) of Aspergilli and Penicillia were purchased from the Commonwealth Mycological Institute (CMI) culture collection in Kew Gardens. Each was selected on known ability to produce organic acids, preference being given to non-toxic metal ion tolerant fungi (32). In addition, seven other fungi were isolated from decaying organic matter and available mineral samples. These were identified by the CMI and are also given in Table 2.8. All fungi were screened comparatively to identify that most suitable for a detailed study of nepheline biodegradation.

The main criteria for the choice were: the efficiency of organic acid synthesis; the efficiency of mineral biodegradation; and the lack of toxicity. Six carbon sources were tested: sucrose, glucose, whey, molasses, starch, and microcrystalline cellulose. These were pinpointed as major fermentable constituents found in waste or byproducts of the agricultural and food industries (Table 2.9). All carbon sources, excluding whey and molasses, were Analar grade chemicals. Whey was obtained from United Dairies Ltd., and molasses from a stockist, sold as agricultural grade. Composition data are given in Table 2.9.

This section describes typical procedures employed for culture and fermentation, together with their application in screening the microorganisms in Table 2.8. Details of

TABLE 2.8 FUNGI USED FOR SCREENING.

FUNGUS	C.M.I. IDENTIFICATION NUMBER	SOURCE	MYCELIUM COLOUR	OTHER DATA
Aspergillus niger	31821	Historic	White/yellow	Used commercially for the production of citric acid.
Aspergillus niger	243400	Rocks in Scotland 1972	White	Reported by C.M.I. to produce oxalic acid.
Aspergillus terreus	89356	Historic	White	Reported by C.M.I. to produce oxalic acid.
Penicillium janthinellum	136529	Soil covering oil shale	Grey	-
Penicillium purpurogenum	90178	Historic	Orange/yellow	Once used commercially to produce gluconic acid.
Trichodoma viride		Decaying Organic matter	Cream	-
Aspergillus fumigatus		Sample of tantalite from Nigeria	White	Better known as 'fowl pest' produces succinic acid.
Rhizopus oryzae		Dust from mineral ore store	Cream	-
Penicillium rubr'um		"	Pink	-
Pencillium mirabilis		Stjernoya nepheline syenite	Brown	-
Pencillium grieso-fulvum		"	Apple Green	-
Alternatia alternata		"	Dark Green	-

TABLE 2.9 SPECIFICATIONS OF AGRICULTURAL, FOOD AND WOOD PROCESSING WASTES.

WASTE	SOURCE	ANALYSIS - SPECIFICATION
Molasses	Sugar refining	Water 20 %, organics 72.5 %, Total Sugar (saccharides 36.5 %, invert 23.5 %), Nitrogen (Total) 0.6 %, crude protein 0.2 %, mineral salts 6.5 % (314).
Sulphite pulp liquor	Wood Processing	325 kg carbohydrate/tonne dry fibre (varies according to season and type of wood) (315).
Whey, whey permeate	Dairy processing	Whey - Lactose 69 %. Moisture 4 %. Protein 12.5 %, Fat 1.25 %, Mineral Salts 9.5 %, Sodium chloride 3.5 %, Titre' acidity 0.2 %, pH of a 10 % solution 5.5, calorific value 90 cal/oz (316).
Citrus, olive, tomato pulps	Various	-
Canning, freezing, drying waste waters.	Various	-
Oat, wheat, rice bran, straw, paper.	Various	Di - polysaccharides, cellulose diluted with inert lignin.

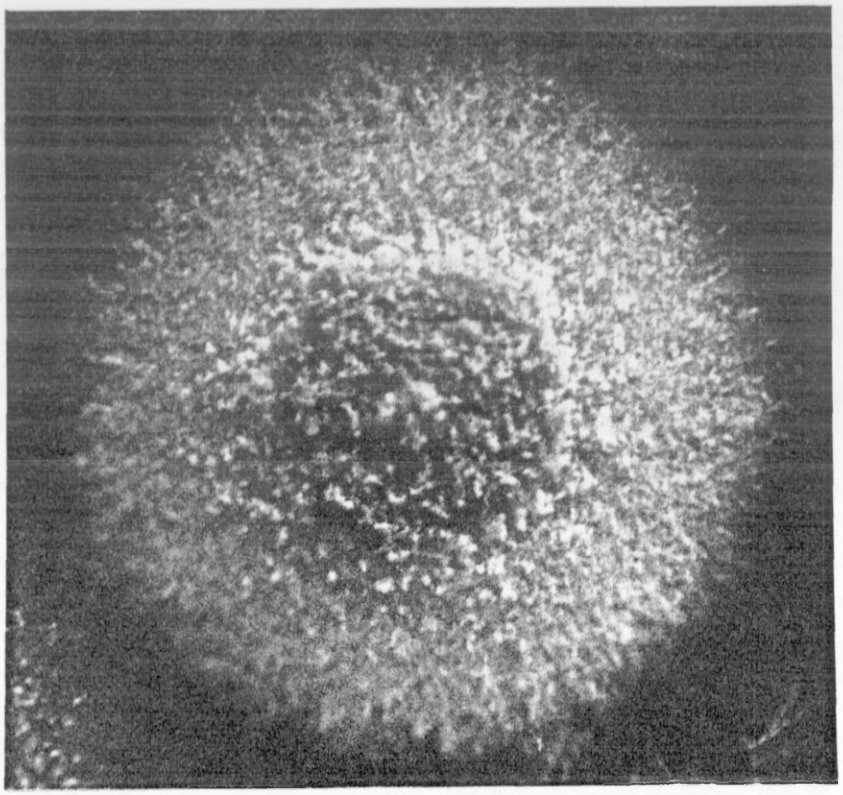
comparative tests are given for the two most efficient acid producers (strains of A.niger) in which the fungi were encouraged to grow on and react with nepheline surfaces. For the most aggressive strain (CMI 31821) three optimised growth media were developed, one for citric and two for oxalic acid production. Consideration was given to the use of additives, including methanol, ferrocyanide, arsenite, and copper ions which are reported to suppress the toxic effects of metal ions (Section 1.2.8).

The overall aim was to identify the preferred fungal-mineral system for efficient nepheline degradation.

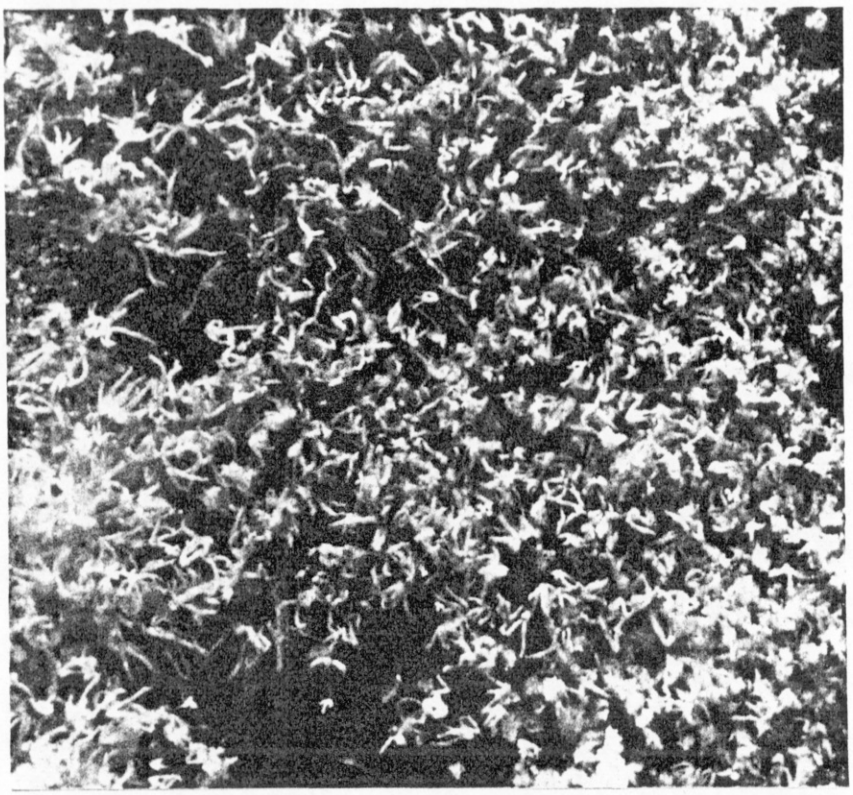
2.3.1 Preparation of cultures and inoculum.

Fungi (CMI freeze dried spores) were revived as suggested by CMI, using the solid sporulation medium described by Steel et al. (232), for the purposes of this work called SM1. This medium contained 300 g/l molasses, 0.5 g/l potassium dihydrogen phosphate and 20 g/l agar (as a gelling agent). Wild fungi were removed from mineral/soil samples by wiping a cotton-wool swab over the contaminated materials, and then over sterile SM1 set in a petri dish. Dishes were incubated at 28° C. Once colonies became visible, samples of each fungus were separated and grown individually, again on SM1. By this means all fungi present on the original samples, which could grow on SM1 were isolated. Typical cultures are illustrated in Figs 2.20 a-h.

Doelger and Prescott (317) indicated that the acid yield obtained from sucrose using A.niger increased as the fungus

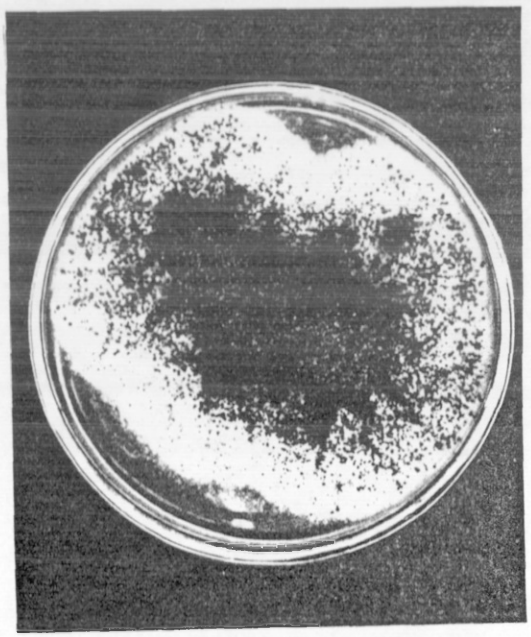


(a) P.janthinellum ×25.

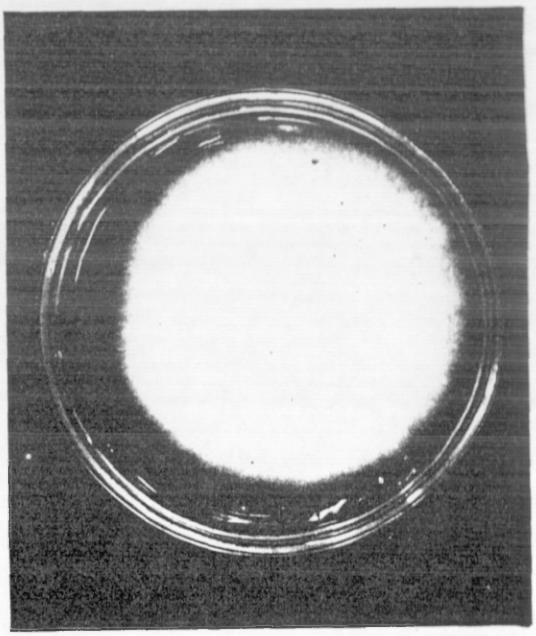


(b) P.mirabilis ×40.

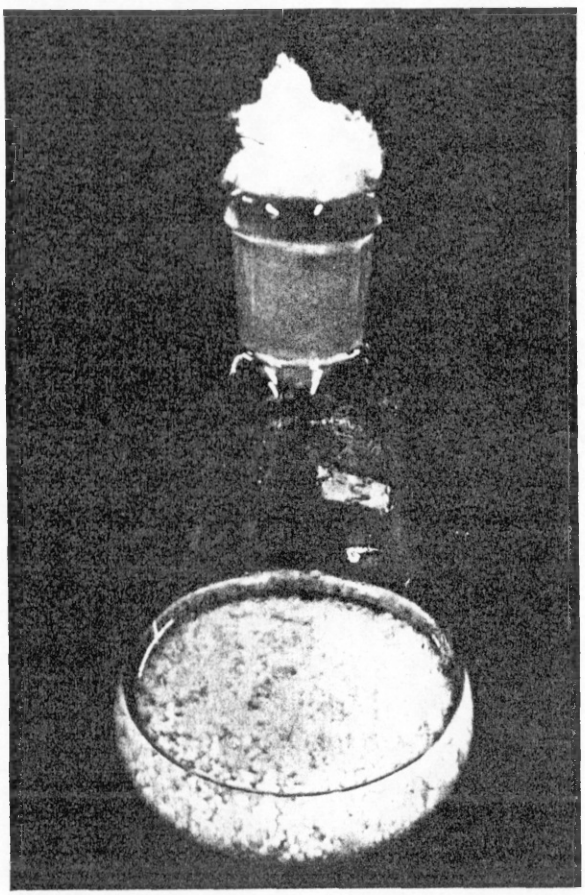
Fig. 2.20 (a)-(h) Photographs showing typical fungal cultures.



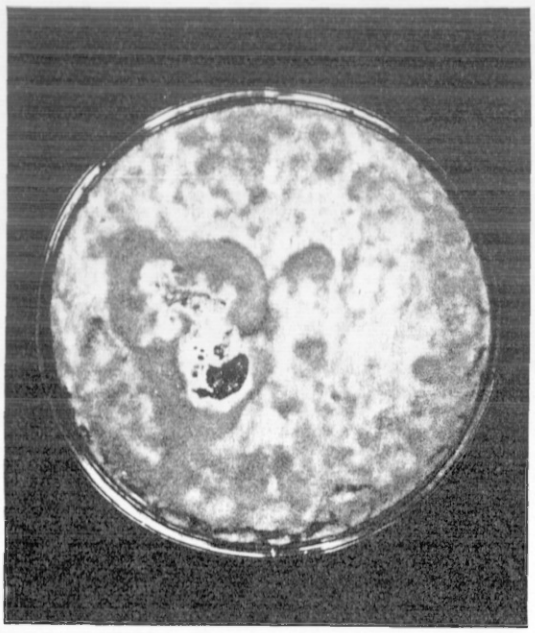
(c) A.niger 31821.



(d) A.niger 243400.



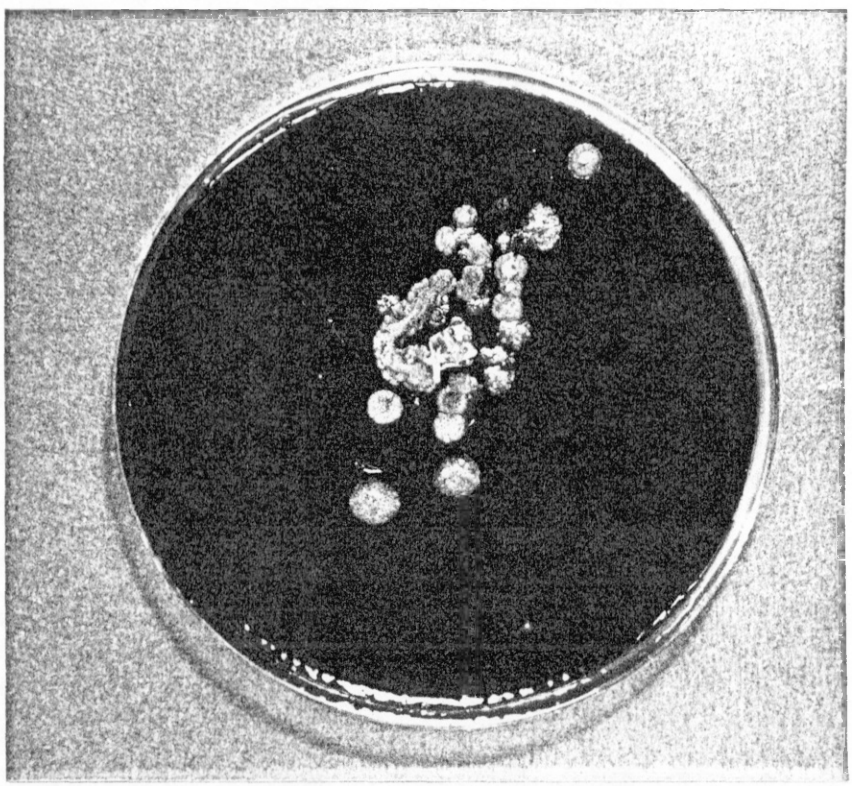
(e) A.niger 31821 in pellet form.



(f) A.terreus.



(g) A.alternata.



(h) T.viride.

became more acclimatised to its growth environment. Thus, spores used for the preparation of inoculum (see below) were grown on solid media of similar composition to that to be used for subsequent fermentations. Spore inoculum used to start liquid based fermentations was prepared by washing spores from mature plates of solid growth medium, as described above with DDW to which had been added 1 drop Tween 20 surfactant/l DDW (see Lipids, Section 1.2.8).

2.3.2 Typical fermentation procedure.

Liquid-based fungal screening and appraisal tests were carried out in 500 ml conical flasks plugged with cotton wool, agitated on a A500 orbital shaker. The flasks typically contained 100 ml growth medium. Under these conditions the gas-liquid interfacial area per unit volume of fermentation media (0.63 cm^2 /ml) was sufficient to maintain an adequate supply of oxygen without having to force gas into the system.

All liquid media, mineral samples and equipment having any contact with fungus were presterilized at 122°C for 45 minutes, in a pressure cooker or a laboratory autoclave, to ensure that data obtained were relevant to the required fungus, and not a contaminant.

Fermentations were started by inoculating liquid media with spores of the required fungus. Where filamentous growth was required sufficient inoculum was added to give a spore concentration of $>1 \times 10^6$ spores /ml, and where pellet growth was required the concentration was similarly

$<1\times10^5$ spores /ml (Section 1.2.8).

Preliminary fermentations with A.niger (CMI 31821) indicated that, for filamentous growth, acid and cell yields were only reproducible if the spore concentration in liquid media were similar at the outset of the fermentation. Hence it was necessary routinely to measure and adjust the inoculum spore concentration (Section 2.1).

The rate of fungus development varied according to the incubation temperature used. For the majority of tests carried out at 26°C, germination started after 1.5-3 days. Fungal growth continued for 18-24 days depending upon the medium employed. After fermentation the volume in each flask was measured with the aid of a measuring cylinder, and the contents centrifuged for five minutes at 3000 rpm in a MSE laboratory centrifuge. The clear liquid was decanted taking care not to lose any sediment, and analysed for carboxylic acids and residual carbohydrate. In tests discussed in Chapter 3 nitrogen and metal ions were also analysed as in Section 2.1. The solids were resuspended in DDW, centrifuged as before, and the liquid decanted. The washed residual slurry was filtered under vacuum through a composite Whatman 542/ Millipore 0.45 µm retention filter paper. The papers were recovered taking care to remove all adhering mycelium, dried with clean papers (used as a control) at 65°C for 24 hours, and desiccated over silica gel to constant dry weight. All loaded and clean papers were weighed on a five figure Stanton beam balance to give dry masses of mycelium to 0.1 mg.

2.3.3 Comparative fermentations producing carboxylic acids.

Each fungus (Table 2.8) was grown in six media (Tables 2.10-2.11) differing only with respect to the carbon source used and based on a patent specification (224). The tables give nutrient compositions and carbon sources (LM1-LM6) employed. Each fermentation was carried out as above at 28°C for 168 hours. The spent media were analysed to determine residual carbohydrate excluding starch, whey and cellulose (which were difficult to analyse); oxalic, citric and gluconic acids; and the cell yield excluding fermentations employing cellulose (where the separation of cellulose from cells was difficult). Cell colours and mycelial form were also recorded. The results are set out on Table 2.12. As aids to the selection of the best acid producer two other ratio's have been calculated. The ratio of the total acid produced to carbohydrate consumed (AC) is a measure of the carbohydate to acid conversion efficiency and should be as high as possible. The second ratio of the cell to acid yield (CA), which should be as low as possible, in conjunction with AC gives an indication of the acid producing efficiency taking account of residual carbohydrate and respiration losses (carbon lost as CO_2). The number obtained by dividing the second by the first ratio, AC/CA (Table 2.12, last column), gives a measure of fermentation efficiency (with respect to acid produced). In theory AC/CA tend to infinity, i.e. CA tends to zero. In practice cells must be present for acid to be produced so CA>0, and commercial data indicate that AC/CA always tends

TABLE 2.10 CARBON SOURCES USED IN COMPARATIVE FERMENTATIONS.

Lable	Carbon source
LM1	Sucrose
LM2	Glucose
LM3	Potato starch
LM4	Molasses
LM5	Whey powder
LM6	Microcrystalline cellulose powder

TABLE 2.11 COMPOSITION OF NUTRIENT MEDIUM EMPLOYED FOR LM1-LM6.

Nutrient	Concentration/ g/l
Carbon source	10.0
$(NH_4)_2CO_3$	1.5
KH_2PO_4	0.1
$MgSO_4 7H\ O$	0.8
H^+ (pH)	6.5
Cu^{2+}	0.01 mg/l
Zn^{2+}	0.01 mg/l
Fe^{2+}	0.01 mg/l

TABLE 2.12 RESULTS OF COMPARATIVE FERMENTATIONS.

FUNGUS	CARBON SOURCE	:: CELL		ACID YIELDS					RESIDUAL CARBOHYDRATE g	A TOTAL ACID/ CARBOHYDRATE CONSUMED	B CELL YIELD/ ACID YIELD	A/B
		FORM	COLOUR	YIELD/g	CITRIC/g	OXALIC/g	GLUCONIC/g	TOTAL/g				
A. niger 31821		P	White	0.35	3.1	0.3		3.4	2.92	48	0.1	480
		P	White	0.32	1.8	0.1	1.7	3.6	2.65	49	0.08	612
		P	White	0.32	2.4	0.8		3.2			0.1	
		P	Yellow	0.38	3.2	0.7	1.3	5.2	1.87	64	0.06	1066
		P	White	0.37		0.3		0.3			1.23	
		P	White		0.07		0.1	0.17				
A. niger 243400		P	White	0.13	1.7	0.6		2.3	3.03	33	0.13	253
		P	White	0.32	1.1	0.1	0.7	1.9	3.45	29	0.16	181
		P	White	0.31	1.4	0.2	0.1	1.9			0.18	
		P	White	0.38	2.0	0.8	1.1	3.9	0.72	42	0.09	466
		P	White	0.36		0.3		0.3			1.2	
		P	White			0.03	0.07	0.1				
A. terrus		F	White	0.21	0.3	0.6		0.9	4.37	16	0.23	69
		F	White	0.28	0.1	0.1	0.5	0.7	6.11	18	0.4	45
		F	White	0.27	0.3	0.4		0.7			0.38	
		F	White	0.37	0.6	0.6	0.3	1.5	3.75	24	0.24	100
		F	White	0.20								
		F	White									
A. fumigatus		P	White	0.32	0.2	1.2	0.2	1.6	1.57	19	0.2	95
		P	White	0.32	0.1	0.6	0.1	0.8	3.84	13	0.4	32
		P	White	0.34	0.3	0.3	0.4	1.0			0.34	
		P	White	0.39	0.1	1.8	0.6	2.5	1.93	31	0.15	206
		P	White	0.20	0.1			0.1			2.0	
		P	White			0.07	0.07	0.14				
P. janthinellum		F	Green	0.25	0.3	0.5		0.8	2.72		0.31	35
		F	Green	0.33	0.2	0.1	0.3	0.6	5.02	12	0.55	21
		F	Green	0.31	0.2	0.6		0.8			0.38	
		F	Yellow	0.41	0.1	0.8		0.9	1.82	11	0.45	24
		F	Yellow	0.28	0.3	0.1		0.3			0.93	
		F	Green		0.02	0.05		0.07				

CONT

FUNGUS	CARBON SOURCE	CELL		ACID YIELDS					RESIDUAL CARBOHYDRATE g	A TOTAL ACID/ CARBOHYDRATE CONSUMED	B CELL YIELD/ ACID YIELD	A/B
		FORM	COLOUR	YIELD/g	CITRIC/g	OXALIC/g	GLUCONIC/g	TOTAL/g				
P. purpurogenum		P	Green	0.38	0.8	0.5	0.3	1.6	3.0	23	0.23	100
		P	Green	0.4	0.9	0.2	1.7	2.8	2.0	35	0.14	250
		B	Green	0.37	0.2		0.4	0.6			0.61	
		P	Orange	0.48	1.3	0.3	1.2	2.5	2.42	33	0.19	173
		P	Orange									
		P	Yellow									
R. oryzae		F	White	0.41	0.1	1.3	0.3	1.7	2.27	22	0.24	91
		F	White	0.38	0.5	0.2	0.8	1.5	2.85	21	0.25	84
		F	White	0.36	0.4	0.6		1.0			0.36	
		F	White	0.48	0.6	1.8	0.1	3.6	1.82	44	0.13	338
		F	White	0.59	0.1	0.2		0.3			1.96	
		F	White		0.1			0.1				
T. viride		F	Olive	0.51	0.3	0.1		0.4	4.2	7	1.27	5.5
		F	Olive	0.43	0.2	0.7		0.9	3.07	13	0.47	27.6
		F	Olive	0.82		0.2		0.2			4.1	
		F	Olive	0.77	0.8	0.1		0.9	2.5	12	0.85	14.11
		F	Olive	0.11								
		F	Olive		0.1	0.2		0.3				

F = filamentous growth. P = pellet growth.

to 1600 (AC=95, CA=0.06).

As can be seen in Table 2.12 A.niger CMI 31821 was the most efficient acid producer overall (AC/CA=1066) giving the highest and equal highest yields of citric and gluconic acids, respectively. The second most efficient acid producer (AC/CA=466) was A.niger CMI 243400. P.purpurogenum and R.oryzae produced high yields of gluconic and oxalic acids respectively. P.rubrium, P.mirabilis, P.griesofulvum and Alternaria alternata only produced traces of the three acid sought and are not included in the table. It is significant that small but measurable amounts of acid were produced from microcrystalline cellulose using Aspergilli and T.viride. There are obvious economic advantages in using cheap cellulose based materials in place of more expensive sugars for acid production.

2.3.4 Fermentation of A.niger CMI 31821 and A.niger CMI 243400 on nepheline discs.

Preliminary tests (similar to those described below) with R.oryzae showed that the mycelium growth was significantly increased at the expense of acid produced in the presence of nepheline bearing rock samples. The mass of mineral degraded by this organism was insignificant in comparison to the strains of A.niger. P.purpurogenum was found to be parasitic to A.niger, was difficult to eradicate once established, and was inhibited by aluminium. Hence of the four acid producing strains of fungi mentioned above only strains of A.niger were considered in detail.

Eleven discs of each rock/mineral (Section 2.2) 1.0 cm

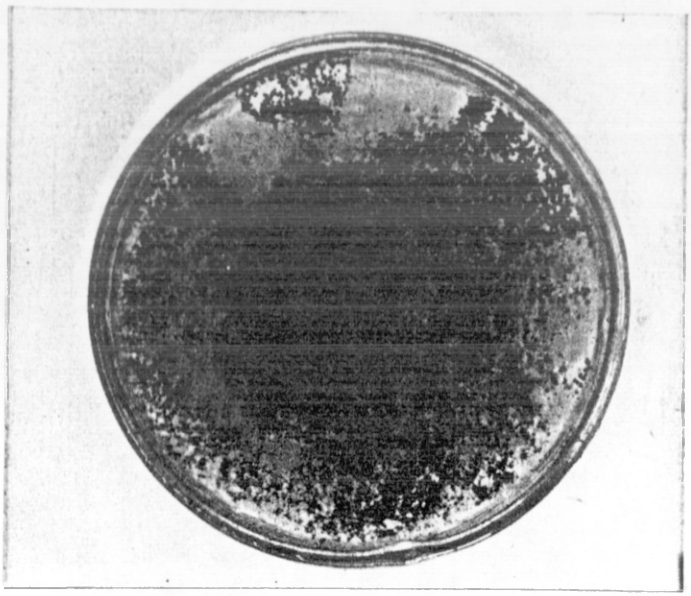


Fig 2.21 Sporulation on fungus grown in contact with a nepheline disc.

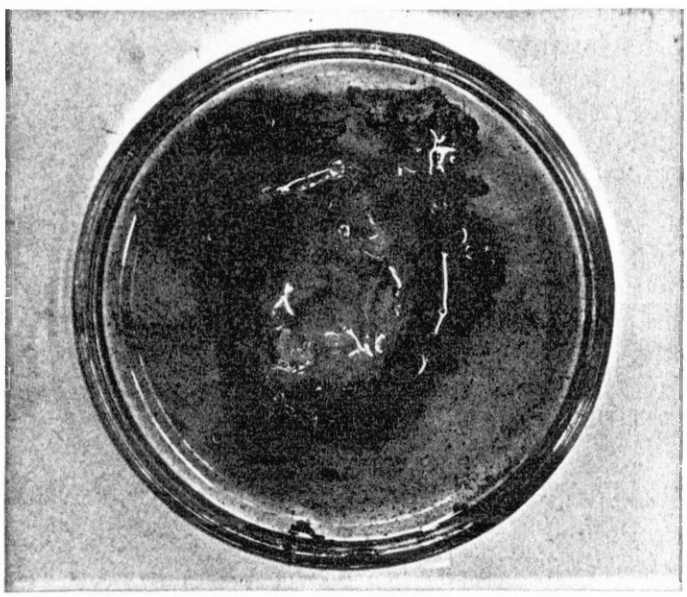


Fig 2.22 Underside of the above mat showing yellow pigmentation where fungus was directly in contact with mineral.



'Fig 2.23 Optical photomicrograph showing hyphae 'rooted' into silica gel coating a disc of nepheline ×180.

in diameter and 4 mm thick were cut with a diamond tipped borer, shaped with a diamond arbor, and polished on one face on a lap using 600 mesh carborundum paper. All surfaces other than the polished face were sealed with an inert silicone sealant (containing polyfluoralkylsiloxane). Once the sealant had dried each disc was sterilised by flaming briefly in burning methanol, and placed in a sterile petri dish, which was filled with liquid medium LM1 (sucrose) just sufficient to wet the upper polished surface of the rock. Five discs of each rock were inoculated with one pregrown fungus pellet 3.0-4.0 mm in diameter, for both strains of Aspergillus (a total of 30 inoculated discs), and fermented with frequent topping up with fresh medium (to account for evaporation). The eleventh disc of each rock was used as a blank without fungus. During fermentation the fungus grew rapidly as a mat over the rock and evenly over the liquid surface. The upper surface of the mat rapidly became covered with spores (Fig 2.21). On the underside of the mat, mycelium was yellow-coloured where it had been in direct contact with nepheline (Fig 2.22). If the liquid level was allowed to decrease the fungus became firmly attached to the rock, with hyphae rooted into the gel layer up to the unaltered disc surface (Fig 2.23). These findings are discussed in greater detail in Chapter 4.

One disc of each rock was removed for analysis (leaving mycelium intact) after 1, 2, 4, 6 and 8 weeks of growth. Pitting depths were measured using a micrometer divider, making sure that the divider point touching the reaction

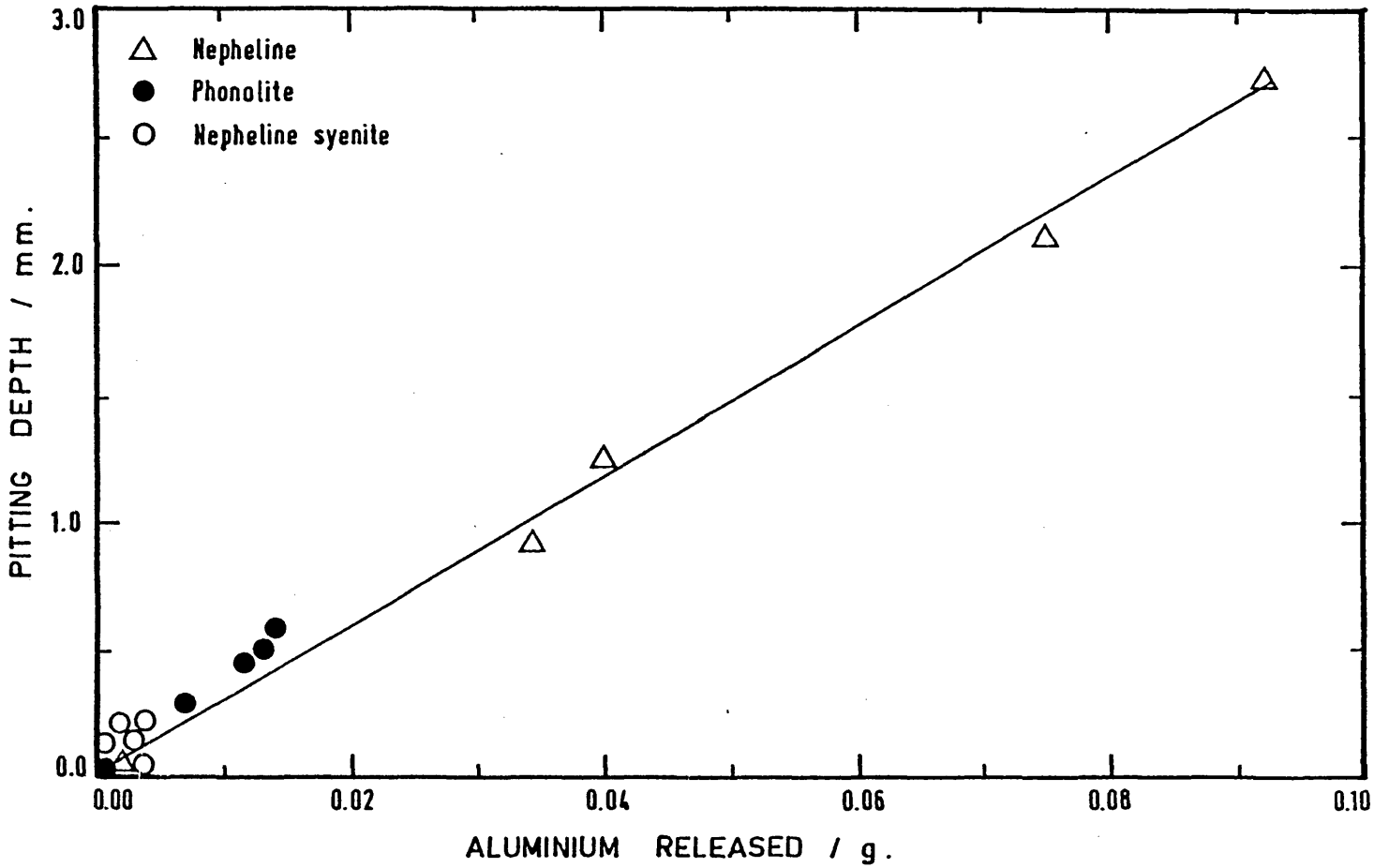


Fig. 2.24: Pitting depth as a function of aluminium released for each sample leached by A. niger CMI 31821.

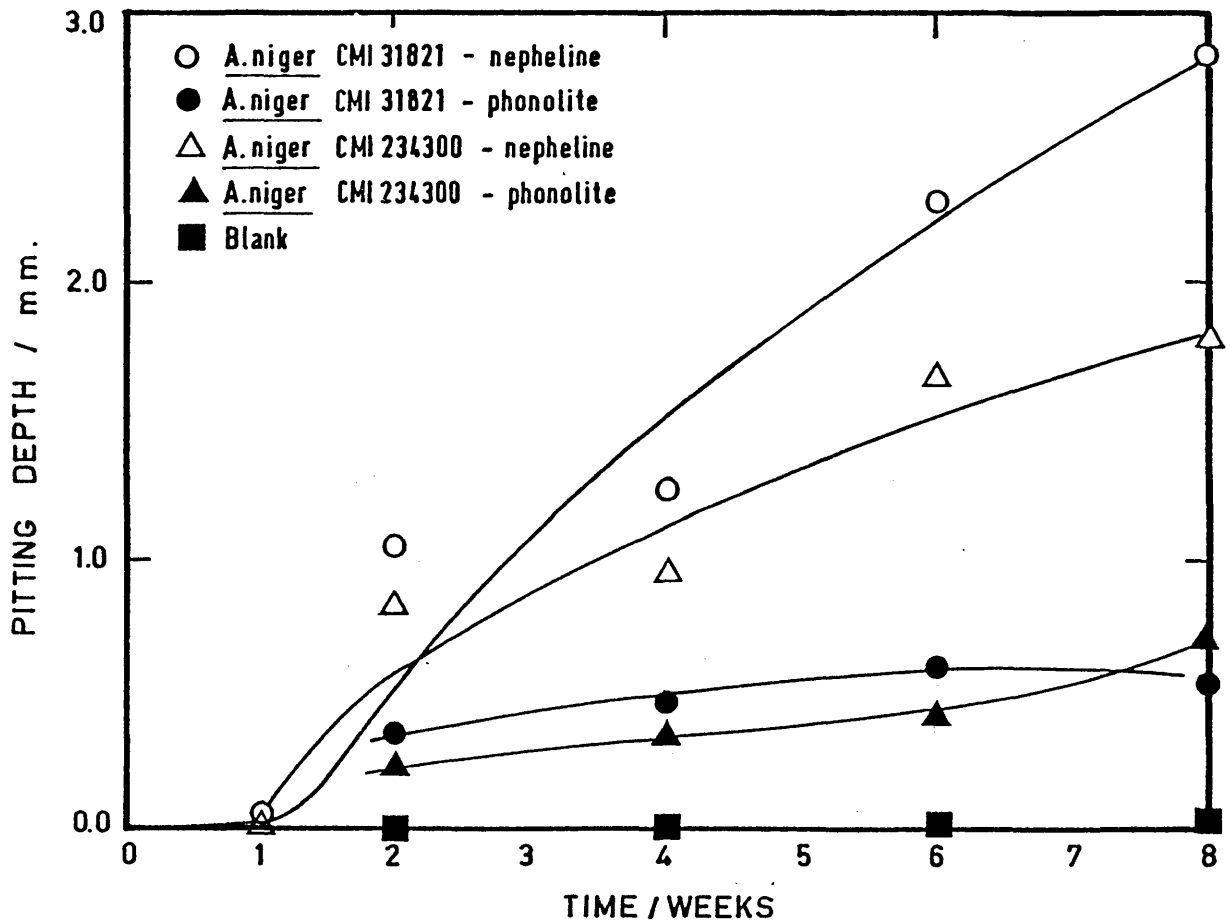


Fig. 2.25: Pitting depth as a function of time for strains of A.niger on Bancroft nepheline and Czech phonolite.

surface pierced the silica gel layer to unreacted mineral. The discs were dried and stored at 4°C. In three series of tests (one for each rock/mineral sample), after filtration to remove solids, samples of residual culture liquid were analysed for aluminium.

The results are illustrated in Figs 2.24-2.25. The first figure is a graph of pitting depth as a function of aluminium released into solution for each type of rock/mineral sample. It can be seen that there is a good linear relationship between the two variables for Bancroft nepheline and Czech phonolite. This was expected for the Bancroft sample which was primarily composed of one reactive mineral phase. In the case of the phonolite, the ratio of the volume of soluble mineral to average mineral grain size was sufficiently high to allow the rock to degrade uniformly both across and into the exposed disc. This was not the case for nepheline syenite, for which no correlation was found. Observations of leached surfaces of nepheline syenite indicated that nepheline crystals were larger and not interconnected in the matrix, so that the lixivant could not penetrate beyond the first layer of exposed grains (Fig 2.26).

Fig 2.25 is a plot of pitting depth as a function of time for the two strains of A.niger on Bancroft nepheline and Czech phonolite, CMI 31821 was the most aggressive. The figure also shows that, after 8 weeks leaching with CMI 31821, six times more Bancroft nepheline degraded than with phonolite. This was probably a result of the difference in the surface area of exposed reactive mineral and also by

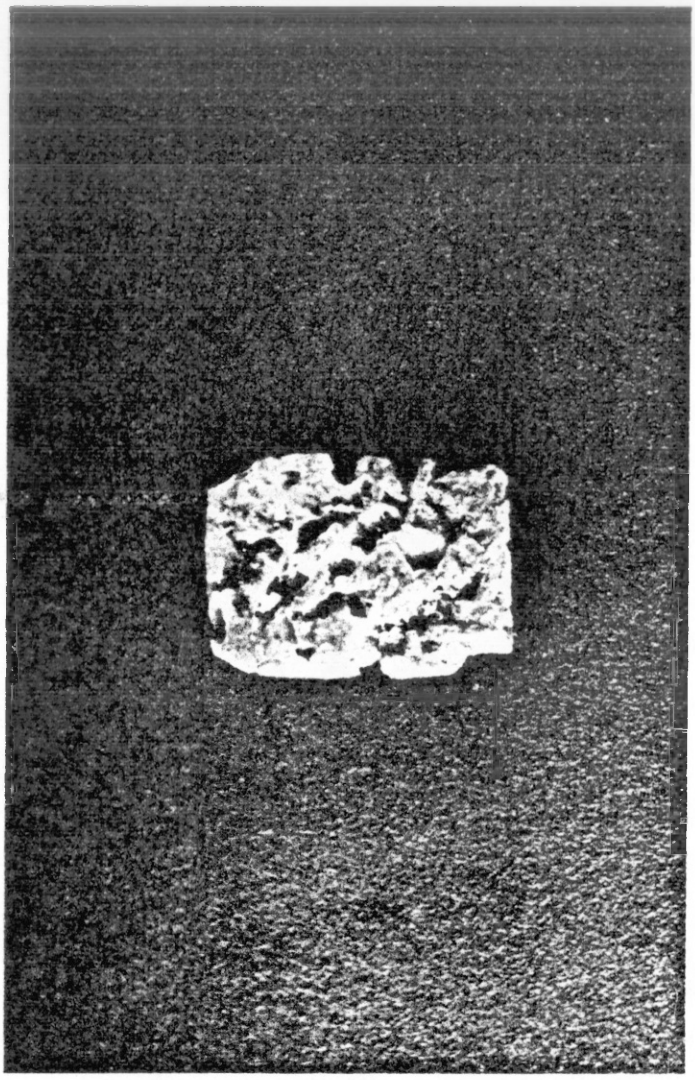


Fig 2.26 Piece of Norwegian syenite showing relative degradation of nepheline and feldspar crystals.

the inhibitory effect of the metals released into solution by the lower grade phonolite. Hence it was decided to work with Bancroft nepheline and A.niger CMI 31821.

2.3.5 Optimisation of growth media for acid biosynthesis by A.niger 31821.

Growth media were optimised to maximise the yield of oxalic or citric acid. As the carbon/acid conversion efficiency increases so does the potential mass and rate of mineral leached.

Three growth media were considered. The first was initially the same as LM1 and was optimised for citric acid production. The second was chosen from literature (263) specifically for oxalic acid production. The third was the same as the first but optimised for oxalic acid production.

Five preliminary fermentations were carried out , at 15, 20, 25, 30, and 35°C, to establish how temperature affected acid yields using medium LM1. These tests (illustrated in Table 2.13) showed that both the rate of acid production and the degree of oxidation (indicated by the proportion of oxalic acid), increased with temperature. Below 20°C growth and acid production rates were prohibitively slow. The fermentation temperature chosen corresponds to the average of the lowest acceptable temperature for acid biosynthesis (20° C) and the optimum for citric acid production (32°C). It was also a convenient temperature for laboratory work (and probably any industrial leaching process).

The optimisation was conducted by means of a factorial analysis. Separate fermentations were carried out in which

TABLE 2.13 THE EFFECT OF TEMPERATURE ON THE PRODUCTION OF CITRIC AND OXALIC ACIDS BY A.NIGER 31821.

Temp ^{o}C	15	20	25	30	35
Total Acidity/g/lit	4.3	28.6	87.2	101.3	71.5
Oxalic/g/lit	0	0.3	0.5	5.3	6.2
Yield (Overall)	3.3.	22.0	66.9	77.9	70.4
Yield (Sucrose consumed)	27.4	33.2	92.0	88.5	74.3
Temp ^{o}C	15	20	25	30	35
Total Acidity/g/lit	2.7	15.3	61.4	66.4	69,3
Citric/g/lit	0	0	0	0	0
Yield (Overall)	3.3	19.1	76.6	83.0	86.6
Yield (Acetate consumed)	17.2	20.5	69.0	71.2	73.2

TABLE 2.14 OPTIMISATION OF SUCROSE BASED GROWTH MEDIUM FOR THE PRODUCTION OF CITRIC ACID BY A.NIGER 31821.

COMPONENT	INITIAL CONCENTRATION g/Lit	g/Lit							
Sucrose	100	130	130	130	130	130	130	130	130
$(NH_4)_2CO_3$	1.5	1.5	1.8	1.8	1.8	1.8	1.8	1.8	1.8
KH_2PO_4	0.1	0.1	0.1	0.25	0.25	0.25	0.25	0.25	0.25
$MgSO_4 7H_2O$	0.8	0.8	0.8	0.8	1.2	1.2	1.2	1.2	1.2
H^+ (pH)	6.5	6.5	6.5	6.5	6.5	4.3	4.3	4.3	4.3
Cu mg/Lit	0.01	0.01	0.01	0.01	0.01	0.01	1.6	1.6	1.6
Fe mg/Lit	0.01	0.01	0.01	0.01	0.01	0.01	0.01	0.08	0.08
Zn mg/Lit	0.01	0.01	0.01	0.01	0.01	0.01	0.01	0.01	10.0
Total Acidity	-	42.3	44.4	47.9	50.5	50.8	67.9	73.5	87.4
Oxalic Acid	-	1.8	1.6	1.9	1.8	0.5	2.3	1.2	0.8
Yield (Overall)	-	32.5	34.2	36.8	38.8	39.1	52.2	56.5	67.2
Yield (Sucrose Consumed)	-	83.0	82.1	93.4	96.3	94.0	92.2	93.5	91.5

TABLE 2.15 OPTIMISATION OF SUCROSE BASED GROWTH MEDIUM FOR THE PRODUCTION OF OXALIC ACID BY A.NIGER 31821.

COMPONENT	INITIAL CONCENTRATION g/Lit	g/Lit						
Sucrose	50	30	30	30	30	30	30	30
$NaNO_3$	3.0	3.0	2.5	2.5	2.5	2.5	2.5	2.5
KH_2PO_4	1.0	1.0	1.0	1.3	1.3	1.3	1.3	1.3
$MgSO_4 7H.O$	0.05	0.05	0.05	0.08	0.08	0.08	0.08	0.08
KCl	0.2	0.2	0.2	0.2	0.2	0.05	0.05	0.05
$FeSO_4 7H_2O$	0.1	0.1	0.1	0.1	0.1	0.1	0.8	0.8
H^+ (pH)	7.5	7.5	7.5	7.5	7.5	7.5	7.5	9.0
Total Acidity	-	4.8	5.5	5.4	5.7	6.0	9.2	12.1
Citric Acid	-	1.7	1.2	0.9	0.7	0.3	0.5	0.0
Yield(Overall)	-	16.0	17.6	18.0	19.0	20.0	30.6	40.3
Yield (Sucrose Consumed)	-	43.5	45.2	46.2	47.3	47.8	52.3	59.7

TABLE 2.16 OPTIMISATION OF ACETATE BASED GROWTH MEDIUM FOR THE PRODUCTION OF OXALIC ACID BY A.NIGER 31821.

COMPONENT	INITIAL CONCENTRATION g/Lit	g/L						
Sodium Acetate	50	80	80	80	80	80	80	80
$NaNO_3$	3.0	3.0	2.5	2.5	2.5	2.5	2.5	2.5
kH_2PO_4	1.0	1.0	1.0	0.8	0.8	0.8	0.8	0.8
$MgSO_4 7H_2O$	0.05	0.05	0.05	0.05	0.1	0.1	0.1	0.1
KCl	0.2	0.2	0.2	0.2	0.2	0.05	0.05	0.05
$FeSO_4 7H_2O$	0.1	0.1	0.1	0.1	0.1	0.1	0.8	0.8
H^+ (pH)	7.5	7.5	7.5	7.5	7.5	7.5	7.5	8.5
Total Acidity	-	38.0	41.3	43.2	43.9	44.2	48.2	61.5
Citric Acid	-	0.6	0.8	0.4	0.5	0.4	0.0	0.0
Yield (Overall)	-	47.5	51.6	54.0	54.8	55.2	60.2	66.8
Yield (Acetate Consumed)	-	59.8	59.1	59.2	60.5	63.4	68.2	69.5

the concentration of a nutrient N1 was varied about its initial value to find the concentration corresponding to maximum acid production holding all other nutrients at their initial concentrations. Once the optimum concentration of the first nutrient was found similar fermentations were carried out for nutrient N2 holding N1 at its optimum concentration and other nutrients at their initial values. By this means the optimum concentrations of each nutrient were determined in turn in the order carbon, nitrogen, phosphorus, magnesium, sulphur, hydrogen ions, and trace elements (Fe, Cu, Zn). The result was a growth medium optimised for maximum acid production.

Each fermentation (of volume 100 ml) was inoculated with 1×10^6 spores/ml and was carried out at 26° C for fourteen days using the procedure set out in Section 2.3.2.

The results are in Tables 2.14-2.16. The yield of citric acid based on carbohydrate consumed (90%, Table 2.14) was similar to reported commercial yields (Chapter 1). However, owing to the low fermentation temperature employed, overall yields of citric and oxalic acids were low compared to commercial processes. The overall yield of oxalic acid using sodium acetate as the sole carbon source was significantly higher than that with sucrose. The reason for this is not known.

2.3.6 Effect of chemical additives on acid biosynthesis by A.niger 31821.

Chemical additives (sodium arsenite, sodium ferrocyanide, methanol and copper ions) have been shown to

increase citric acid yields in growth media containing sub-optimal metal concentrations. Ferrocyanides or cupric ions are frequently added to commercial citric acid fermentations where raw molasses is the carbon source (Chapter 1). Unlike citric acid, oxalic acid fermentations are apparently relatively insensitive to additives and in the literature there is little data for oxalic acid production. Therefore the emphasis here is on additives cited for citric acid fermentations.

Fermentations were carried out to determine the effect of each additive on the citric and oxalic acid yields obtained from media containing a sub-optimal concentration of iron (which is readily released from Bancroft nepheline). In the case of copper a theory, derived from experimental results, was proposed to explain the antagonistic behaviour of copper and iron (antagonistic in this context refers to the suppression by copper of iron's inhibitory effect on acid biosynthesis).

Tests with methanol, sodium arsenite and sodium ferrocyanide. Standard fermentation tests (Section 2.3.2) were carried out with the optimised from of LM1 containing either zero or 10 g/l ferric iron and a range of concentrations of each additive (copper is considered separately later). After seven days, each fermentation was stopped and analysed for citric and oxalic acids as in Section 2.1.

The results are set out in Table 2.17. It can be seen that methanol desensitized mycelium against iron and completely prevented the biosynthesis of oxalic acid. As

TABLE 2.17 THE EFFECT OF METHANOL, SODIUM FERROCYANIDE AND SODIUM ARSENITE ON ACID BIOSYNTHESIS BY A. NIGER 31821.

IRON CONCENTRATION/ g/L	METHANOL ADDED/g/L							
	0		10		20		30	
	CITRIC g/L	OXALIC g/L	CITRIC g/L	OXALIC g/L	CITRIC g/L	OXALIC g/L	CITRIC g/L	OXALIC g/L
0	10.4	0.6	10.1	0	4.7	0	10.6	0
10	6.8	1.8	10.5	0	10.5	0	11.7	0
	SODIUM FERROCYANIDE ADDED/g/L							
	0		1		5		20	
	CITRIC g/L	OXALIC g/L	CITRIC g/L	OXALIC g/L	CITRIC g/L	OXALIC g/L	CITRIC g/L	OXALIC g/L
0	10.1	0.4	8.3	0.2	7.6	0	2.1	0
10	6.8	1.2	8.2	0	6.7	0	4.8	0
	SODIUM ARSENITE ADDED/g/L							
	0		1		5		20	
	CITRIC g/L	OXALIC g/L	CITRIC g/L	OXALIC g/L	CITRIC g/L	OXALIC g/L	CITRIC g/L	OXALIC g/L
0	10.3	0.5	9.7	0.7	8.6	0.5	0.7	0
10	6.6	1.6	8.2	0.3	-	-	-	-

TABLE 2.18 THE EFFECT OF IRON AND COPPER ON THE BIOSYNTHESIS OF CARBOXYLIC ACIDS BY A.NIGER 31821.

Fe:Cu ratio mass basis	Mass of Fe^{3+} at pH 6.0/mg/ml						Mass of Fe^{3+} at pH 4.0/mg/ml					
	0.001		0.1		10.0		0.001		0.1		1.0	
	CITRIC g/L	OXALIC g/L	CITRIC g/L	OXALIC g/L	CITRIC g/L	OXALIC g/L	CITRIC g/L	OXALIC g/L	CITRIC g/L	OXALIC g/L	CITRIC g/L	OXALIC g/L
1:1	8.3	0.1	6.9	0.6	2.56	2.6	10.2	0	8.2	0.2	4.2	1.7
1:2	8.5	0.2	7.2	0.7	3.78	2.7	10.2	0	8.4	0.09	3.9	1.3
1:3	8.8	0.1	7.8	0.5	3.96	2.2	10.1	0	8.4	0	4.2	0.3

the concentration of methanol increased, mycelium turned yellow and the growth rate decreased. Both sodium arsenite and ferrocyanide were toxic towards A.niger at concentrations exceeding 1 g/l, and acid yields were reduced significantly. In the presence of 5 g/l Na_3ASO_3 and 10 gFe^{3+}/l the fungus did not germinate.

Tests with copper. Fermentation tests (as for the other additives) were carried out with the addition of copper and iron. Three Fe:Cu ratios were tested (1:1,1:2,1:3), over a range of iron concentrations (0.001, 0.1, 10.0 gFe^{3+}/l), with an initial pH of 6.0. All tests were repeated with an initial pH of 4.0.

The results are set out in Table 2.18. It can be seen that, as the iron loading increased, both the ratio of citric to oxalic acids and the total acid yield decreased. In fermentations with an initial pH of 4.0 acid yields did not vary significantly as the Fe:Cu ratio increased. However, in those with an initial pH of 6.0 acid yields decreased as the Fe:Cu ratio increased.

No firm explanation has been given in the literature for the antagonistic behaviour of copper and iron. However, MacLeod and Snell (210) hypothesised that the antagonistic behaviour of zinc, cadmium and magnesium was due to the metals binding competitively with important enzymes attached to the cell wall which also act as precursors for the transport of ions into the cell. This hypothesis would explain the observation that the addition of copper to media containing sub-optimal levels of iron increase the citric acid yield. Iron is known to disrupt the TCA cycle,

probably by inhibition of citrate synthase, which is responsible for the synthesis of citrate. If copper binds selectively with precursors responsible for the transport of iron into the cell then the flow of iron will be reduced and acid production will continue irrespective of the concentration of iron in the media surrounding the cell. Other workers have indicated that metals bind predominantly with organophosphorus compounds in the cell wall and very little metal enters the cell (171,318). The metal binding capacity should therefore be related to the phosphorus content of the cell wall.

These hypotheses (that the antagonistic behaviour of copper and iron is due to competetive binding on the cell wall, and that binding capacity is a function of the cell wall phosphorus content) were tested by measuring the adsorption isotherms of copper in tha presence of iron and copper alone on two types of mycelium (low and high phosphorus content), and two pH values (3 and 6).

Production of mycelium. As indicated in Section 1.2.8 potassium and phosphorus are taken up together by cells: phosphorus ($H_2PO_4^-$) is normally only absorbed into the cell if a potassium ion is absorbed at the same time. Other alkali metal ions can substitute for potassium and arsenite can substitute for phosphorus. Hence the phosphorus content of mycelium can be increased by raising the concentration of potassium dihydrogen phosphate in the medium. Low phosphorus mycelium was produced using LM1 and high phosphorus mycelium was produced by using optimised LM1 together with 15 g/l KH_2PO_4.

Both fermentations were split into two stages. During the first stage spores were germinated and grown on the relevant growth medium for three days. Small pellets were then transferred to fresh medium which contained no copper, iron or zinc. The fermentation was continued for a further fourteen days after which the mycelium was separated and washed as in Section 2.3.2, killed in liquid nitrogen, and dried by desiccation. The two stage fermentations were necessary to stop mycelium becoming contaminated with metals (in LM1 required for germination) prior to the adsorption tests.

Preparation of adsorption standards. Adsorption standards were prepared containing (100 mgCu + 100 mgFe)/l; (20 mgCu + 20 mgFe)/l; (2 mgCu + 2 mgFe)/l; 100 mgCu/l; 40 mgCu/l; 20 mgCu/l; 10 mgCu/l; 100 mgFe/l; 40 mgFe/l; 20 mgFe/l; and 10 mgFe/l from Spectrosol grade atomic absorption reagents. The solutions containing (2 mgCu + 2 mgFe)/l, 10 mgCu/l and 10 mgFe/l were analysed by AA in order to establish the preparation errors. From AA analyses the first mixture analysed contained (2.08 mgCu + 2.09 mgFe)/l, the second 10.4 mgCu/l and the third 10.7 mgFe/l (all values are 2%, AA errors). Metal concentrations in adsorption standards were therefore assumed to be 6%.

Adsorption tests. Adsorption isotherms were determined for copper in the presence of iron at two pH's (3 and 6), and copper and iron alone at pH 6. A typical test is described below for low phosphorus mycelium at ph 6.

To a 50 ml sample of each standard adsorption reagent

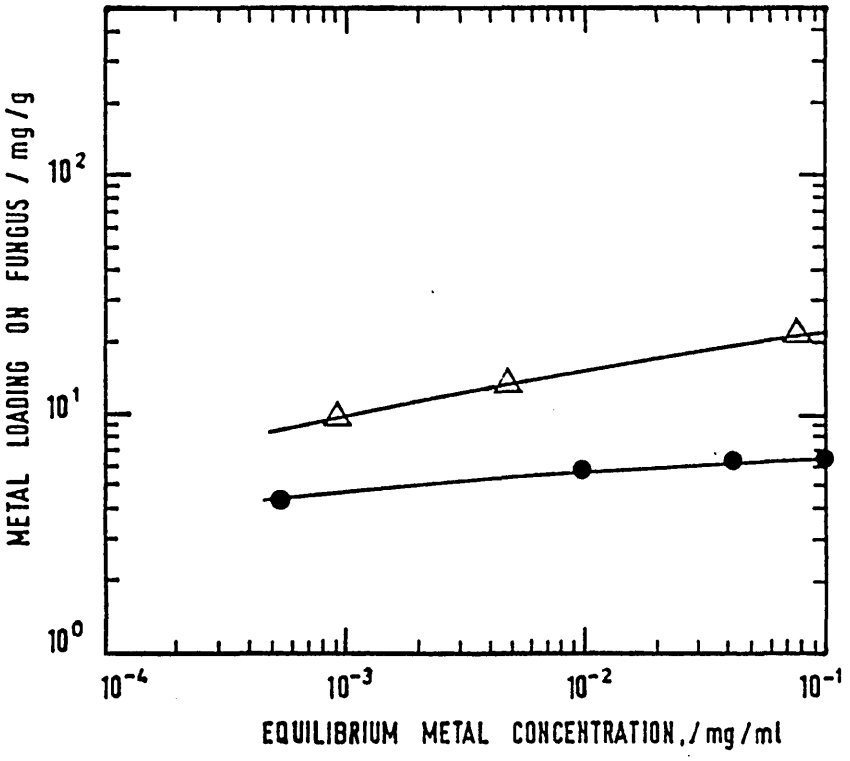


Fig. 2.27: Adsorption isotherms for copper in the presence of iron onto mycelium of A.niger at pH 6.0 .

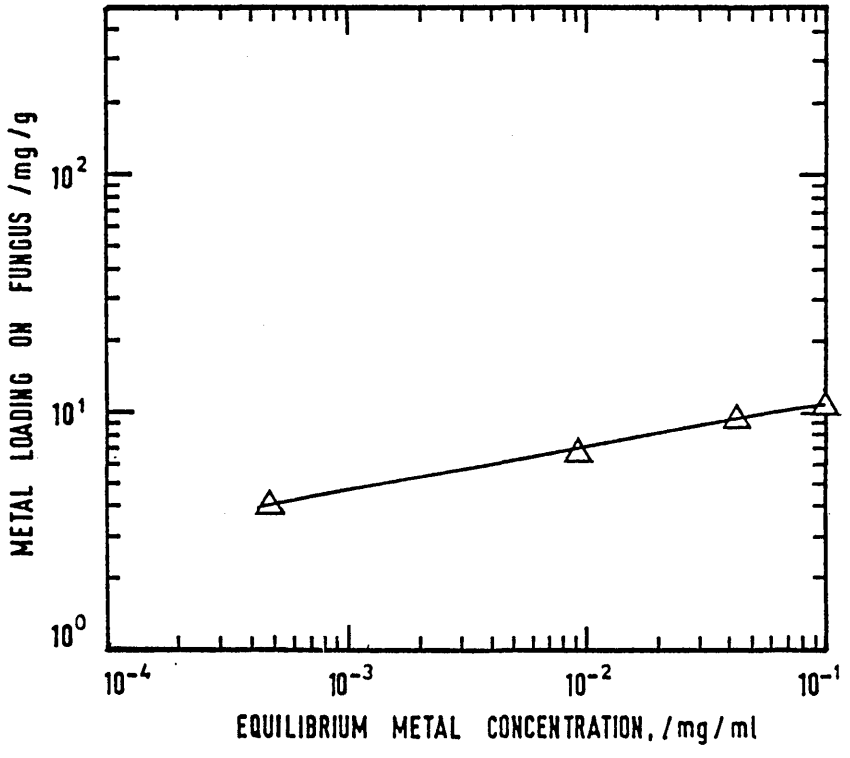


Fig. 2.28: Adsorption isotherms for copper in the presence of iron onto mycelium of A.niger at pH 3.0 .

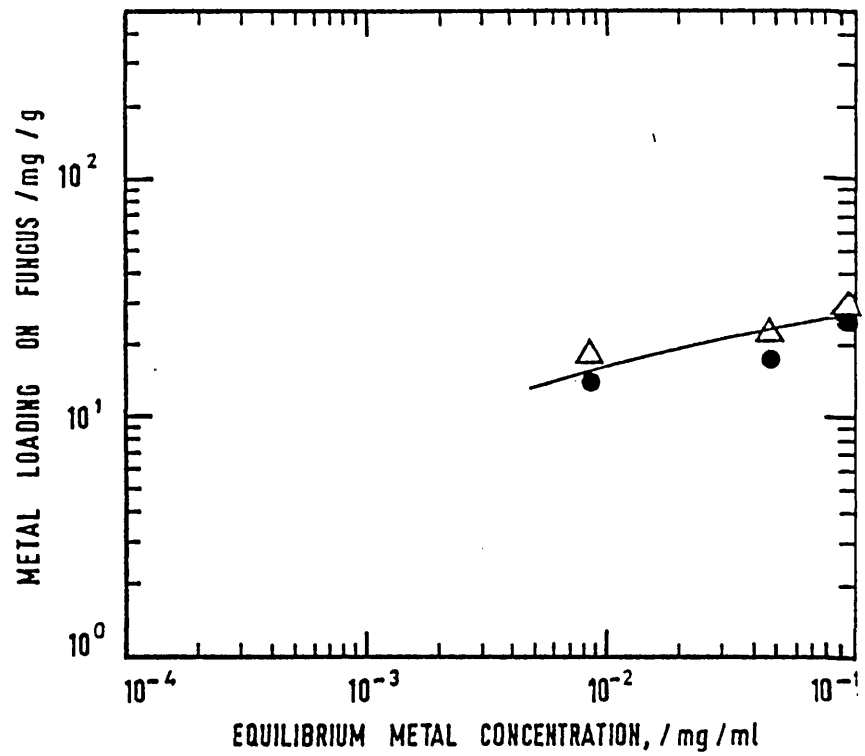


Fig. 2.29: Adsorption isotherms of copper and iron separately onto mycelium of A.niger at pH 6.0 .

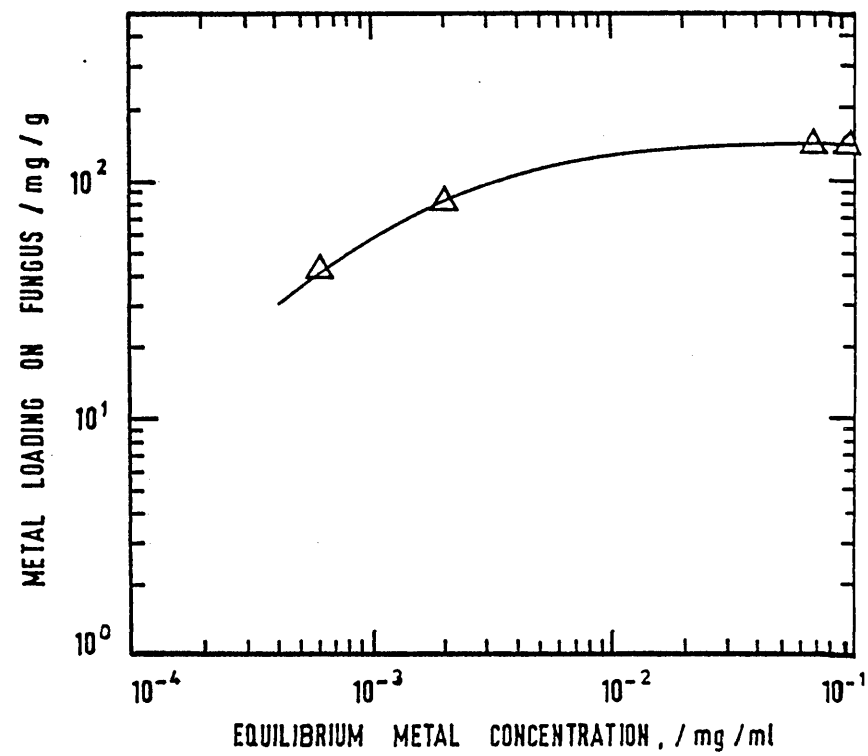


Fig. 2.30 : Adsorption isotherms of copper onto mycelium of phosphate rich A.niger at pH 6.0 .

was added a 10±0.1 mg sample of low phosphorus mycelium and 40 ml DDW. The mixtures were shaken on a shaker for 24 hours at room temperature. After this time the pH was adjusted to 6 and the volume made up to 100 ml with DDW (the initial standards were adjusted by a factor of two). The flasks and contents were replaced on the shaker for a further 24 hours. After the total time of 48 hours a sample of mycelium-free liquid was removed from each flask with a syringe and filter adaptor. These samples were analysed for iron and copper by AA as in Section 2.1. This procedure was repeated for low phosphorus mycelium at pH 3 and then high phosphorus mycelium at pH 6 for copper alone. Finally all tests were rerun to establish isotherm reproducibility.

The results are shown as Freudlich isotherms (83) (see below) in Figs 2.27-2.30. These isotherms can be represented as

$$C(*) = K(V(C(0)-C(*)))^{n} , \qquad (2.4)$$

$$\text{or } \mathrm{Ln}C(*) = \mathrm{Ln}K + n\mathrm{Ln}(V(C(0)-C(*))) , \qquad (2.5)$$

where C(0) is the initial concentration, C(*) is the equilibrium metal concentration, V is the volume of solvent divided by the mass of adsorbent, and K and n are constants. Hence there should be a linear relationship between LnC(*) and Ln(V(C(0)-C(*)). Figures 2.27 and 2.28 show that this relationship holds up to a point at which adsorption sites become saturated. Comparing Figs 2.27 and 2.28 it can be seen that between pH 6 and 3 for copper in the presence of iron the saturation point decreases with pH

(very little iron was adsorbed by mycelium at pH 3). From Figs 2.27 and 2.29 it is evident that copper ions are able to bind onto a wider range of cell wall sites and also bind competitively with respect to iron. It is interesting that the saturation point for copper is increased markedly for phosphorus rich mycelium (Fig 2.30). However after five similar consecutive tests, Fig 2.30 could not be reproduced. Consecutive isotherms were not related and were of a lesser magnitude than that represented in Fig 2.30. All other isotherms were reproducable to within K ±15% and n ±8% of the values in Figs 2.27-2.29.

Returning to the results in Table 2.18 it is evident that, in the fermentation with an initial pH of 6, sufficient iron adsorbed, and hence had access to the cell during the growth phase (during which time the pH only decreased slowly), to effect the citric acid biosynthesis during the acid producing stage (when the pH dropped rapidly to 2-3). Conversely in the test where the initial pH was 4, less iron could adsorb (particularly in the presence of copper ions which effectively blocked sites of adsorption), resulting in higher citric acid yields, thus supporting the origional hypothesis.

2.4 General Conclusions.

The work in this chapter indicates that Bancroft nepheline-A.niger 31821 provided a suitable system for a detailed study of the biodegradation of nepheline. Of the three nepheline bearing samples tested, that from Bancroft was selected on the following basis.

(1) It had the highest nepheline content.

(2) The concentration of iron bearing minerals was relatively small.

(3) It was degraded rapidly by fungi.

The appraisal carried out showed the following characteristics. A 6 Kg sample was available for testwork (later a further 12 Kg was obtained from the same locality). Provided each sub-sample was >1 g at 30 μm, and analytical errors were as recommended, overall sampling and analytical errors should be expected to be routinely of the order of 3%.

Of the microorganisms tested A.niger CMI 31821 was selected.

(1) It had a wide substrate specificity.

(2) It produced high yields of citric and oxalic acids from sucrose.

(3) Mineral leaching rates were the highest of any fungi tested.

(4) It was insensitive to metals in the presence of methanol.

(5) It was non toxic under the envisaged growth conditions.

The medium for the selective production of citric acid was chosen for a detailed study because the yields obtained were significantly higher than for oxalic acid (90% compared to 60%). Small but measureable yields of acids were obtained using microcrystalline cellulose. There are obvious economic advantages in using cellulose based carbon sources (wood pulp, bagasse, etc.) in place of expensive sugars. However the benefit of lower substrate cost must be balanced against the disadvantages which include lower acid yields and much longer fermentation times.

Using the recommended analytical techniques for the determination of sucrose, citric and oxalic acids measurement errors should be expected to be routinely 1.0%, 3.0% and 3.5%, respectively.

CHAPTER 3. MECHANISM OF NEPHELINE BIODEGRADATION WITH A.NIGER 31821.

This chapter describes a study of factors influencing the rate of biodegradation of Bancroft nepheline. The main aims were to:

(1) measure the rate of reaction of nepheline with purified citric, oxalic and hydrochloric acids under various conditions and fit the results to appropriate kinetic equations,

(2) measure the rate of citric and oxalic acid biosynthesis by A.niger CMI 31821 in nutrient medium LM1 at constant hydrogen, aluminium, potassium, sodium and silicon ion concentrations (simulating a leach solution) and fit the results to appropriate kinetic equations,

(3) combine the results of (1) and (2) (by means of a computer program) in a model to optimise the fermentation conditions for simultaneous maximum rates of acid production and mineral leaching, and

(4) show that the computer predictions are consistent with physical reality.

As will be seen the integrated system was complex and therefore could not be studied experimentally in full detail. The computer model (3) was a practical way of studying the fermentation system in the time available,

3.1 Rate of Reaction of Nepheline with Citric, Oxalic and Hydrochloric Acids.

This section deals with citric and oxalic acid leaching. Hydrochloric acid is included for the purpose of comparison. The reaction rates of inorganic acids, including hydrochloric acid, with nepheline had been studied previously by South African workers (318). There are no reports of similar studies with fungal acids but these might have some advantages.

An indication was given earlier (Section 2.2.1) of the main factors controlling the rate of leaching of nepheline by acids; e.g., acid concentration and build up of a gel layer. The gel layer surrounding reacting grains (Fig 2.17) increases in thickness as the reaction proceeds and increasingly inhibits the flow of acid to the reaction interface. A number of models might adequately describe this behaviour (319-321).

Valensi (321) reported a 'shrinking core" model for a reacting sphere, taking account of volume changes during the reaction and assuming Fick's diffusion law (322) to hold. The Valensi equation for the fraction reacted, R, is given by

$$z+2(1-z)M_rDCt/\alpha\rho_r r_0^2 = (1+(z-1)R)^{2/3}+(z-1)(1-R)^{2/3}, \quad (3.1)$$

where M_r is the molecular weight of the reactant, D is the unknown diffusivity of the reagent through the product layer, C is the initial reagent concentration, ρ_r is the reactant density, r_0 is the reactant radius (assuming a

spherical particle), α is a stoichiometric factor equal to the reciprocal of the number of moles of acid to degrade one mole of reactant, t is the time from the outset of the reaction, and z is $v_p/v_r\alpha$ (v_p and v_r being the specific volumes of the product and reactant, respectively). The term $2(1-z)M_rDC/\alpha\rho_r r_0^2$ has the dimensions of time and represents the rate constant, K, for the reaction.

If the nepheline/acid reaction is diffusion controlled there will be a linear relationship between the right hand side of Eqn (3.1) and t, with a slope of K and intercept z. Values of R can be readily calculated from concentrations of soluble products (sodium, potassium and aluminium) at different times. However, v_p, the specific volume of silica gel around reacting grains, is difficult to measure precisely. Crank (320) and other workers (319) assumed that the particle diameter remained constant during the reaction leading to a much simplified derivation of the rate equation. A simplified equation based on Crank's findings was given by Habashi (351) and this is reproduced as Eqn (3.2)

$$2M_rDCt/\alpha\rho_r r_0^2 = 1 - 2R/3 - (1-R)^{2/3}. \qquad (3.2)$$

Carter (323) showed this relationship to hold for a significant degree of the reaction of metal spheres of 75 μm diameter undergoing oxidation. Thus, during the early stages of the reaction of nepheline it was assumed that K could be measured with adequate precision using Eqn (3.2).

3.1.1. Preliminary experimental work.

In Section 1.2.9 it was noted that the stoichiometry of reaction of aluminosilicates with acids is predominantly

governed by the concentration of hydrogen ions in solution. Preliminary work showed that Eqn(3.2) held only at constant pH. Thus, in the main work described below the pH was kept constant. The rate of agitation also had an effect. As the rate was increased the outer layer of gel became detached and the kinetics deviated from Eqn(3.2). At the outer edge of the grain weakly held flakes were visible and the gel rigidity increased towards the reaction interface.

Three tests were carried out at constant molarity, one each employing citric (1M), oxalic (1M), and hydrochloric acid (1M), the reaction was carried out to completion in order to investigate the mass balance of the reactions. Solid products were analysed by XRD, and AA (after digestion in hydrofluoric acid) as in Section 2.1; and the liquid by AA as in Section 2.1.

Two tests using the typical procedure, below, were carried out using +53 -75 μm and +75 -150 μm fractions. They were shown to be consistent with Eqn (3.2) (i.e. $K \propto 1/r_0^2$). More detailed work is described below.

3.1.2 Typical experimental procedure.

Leaching tests were carried out with each acid at four constant pH levels of 1.83, 2.31, 3.15 and 3.75. The citric acid concentration corresponding to pH 1.83 is 0.25 M or 48.03 g/l. This corresponds to that which could reasonably be obtained by fermentation of sucrose using A.niger. Values of pH of 2.31, 3.15 and 3.75 correspond to 0.025, 0.001 and 0.0001 M citric acid solutions, respectively. The molarities of the other acids corresponding to these pH's

are; for oxalic 1.83 (0.073 M), 2.31 (0.013 M), 3.15 (0.004 M), 3.75 (0.0008 M); and hydrochloric, 1.83 (0.014 M), 2.31 (0.0049 M), 3.15 (0.0007 M), and 3.75 (0.00017 M).

Typically 1.2688 g samples (containing 1 g of nepheline) of +37 -53 μm Bancroft nepheline (Table 2.4) were reacted with 100 ml of each acid at the specified pH in a Teflon beaker for 120 minutes. The temperature was 26±2°C, and the mixtures were agitated with a turbine mixer (Citenco 0.1 h.p.) rotating at approximately 60 r.p.m. Appropriate quantities of acid were added from a burette to maintain constant pH (measured by a pH probe). After the designated reaction time a 10-20 ml sample was rapidly removed using a syringe with filter adapter. This was analysed by AA as in Section 2.1.

To reduce systematic errors, data for each time interval were collected from separate tests. Thus, for seven points corresponding to 5, 10, 15, 30, 45, 75, and 120 minutes, seven separate tests were required.

Typical tests for citric acid were repeated with 50, 100 and 150 g/l sucrose to establish if the carbon source had any effect on the relationship between pH and K. Other chemicals present in the fermentation media, being at relatively low concentrations, were considered insignificant.

3.1.3 Results and discussion.

Stoichiometry. Fig 3.1 shows XRD spectra of the solids at various stages during leaching. There is a gradual decrease in the proportion of nepheline, noted by the

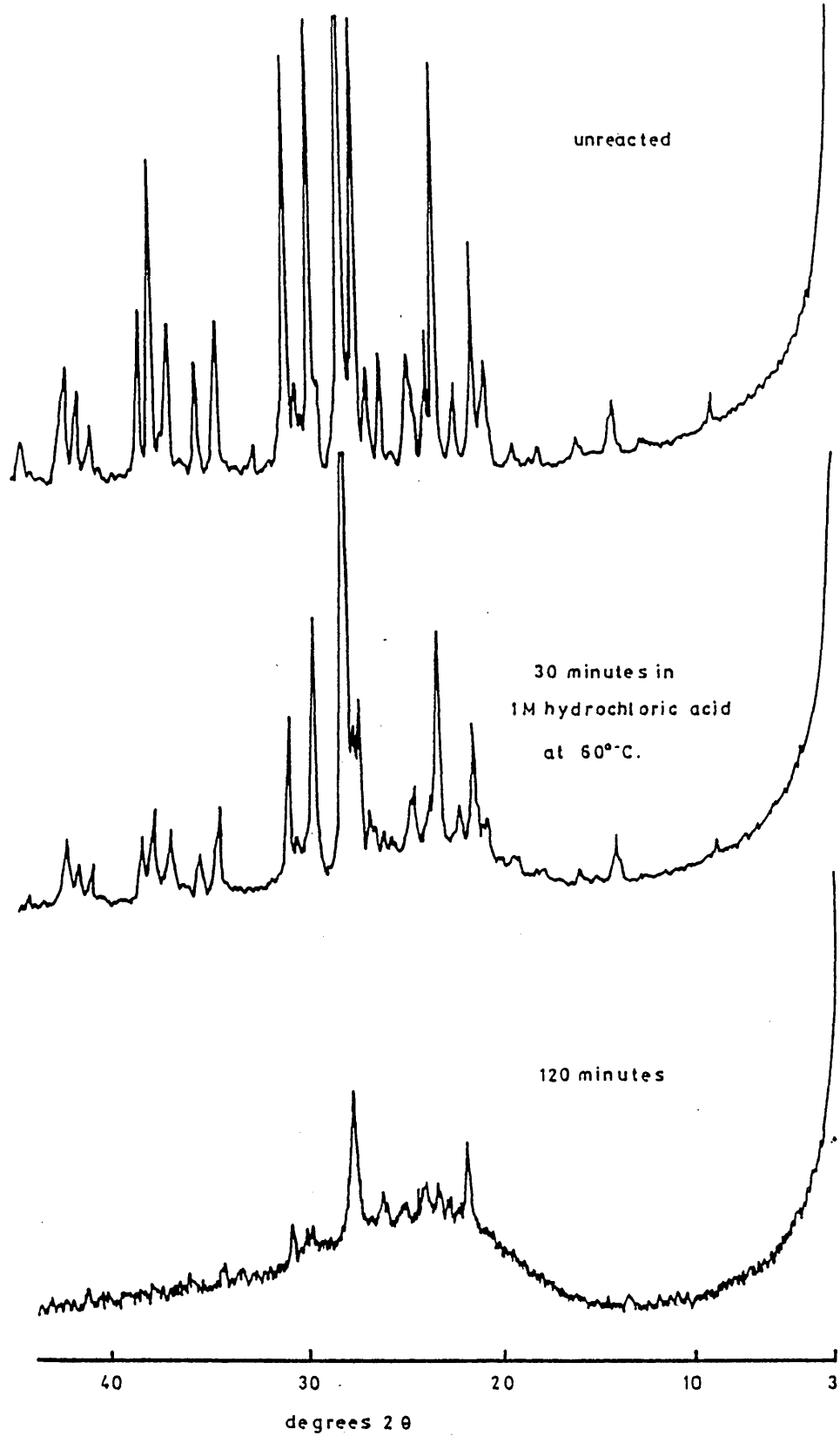


Fig 3.1 XRD spectra of solids at various stages of leaching in hydrochloric acid.

reduction in major peaks. On the basis of the peak at 28°2Ø, the feldspar remains essentially unchanged. The transition from crystalline to amorphous material (seen as the gradual appearance of a broad hump at 24°2Ø) becomes essentially complete. Analysis of the solid remaining after reaction indicates that the amorphous material was predominantly silica gel (>90%) and the crystalline material was unaltered feldspar together with partially altered ferromagnesian minerals.

The silica was in two forms: compact and dispersed. A large proportion of the solid could be separated by filtration (compact). The second form was not removed by filtration and could be measured by AA (dispersed silica).

On the basis of the analyses carried out, stoichiometric equations for the reaction of Bancroft nepheline with each type of acid are given by,

$$Na_{3.02}KAl_{3.71}Si_{4.20}O_{15.78} + 15HCl =$$
$$0.57SiO_2(col) + 3.73SiO_2(s) + 3.68Al^{3+}(aq) + 3.0Na^{+}(aq) +$$
$$0.97K^{+}(aq) + 7.37H_2O(l) + 0.26H^{+}(aq) + 15Cl^{-}(aq) \qquad (3.3)$$

$$Na_{3.02}KAl_{3.71}Si_{4.20}O_{15.78} + 6.66H_3CIT =$$
$$0.67SiO_2(col) + 3.53SiO_2(s) + 3.65AlCIT(aq) + 2.97Na^{+}(aq) +$$
$$0.98K^{+}(aq) + 7.36H_2O(l) + 0.26H_3CIT(aq) + 2.75CIT^{3-}(aq) \qquad (3.4)$$

$$Na_{3.02}KAl_{3.71}Si_{4.20}O_{15.78} + 15HOx^{-} =$$
$$0.58SiO_2(col) + 3.62SiO_2(s) + 3.69AlOx_2^{-}(aq) + 3.01Na^{+}(aq) +$$
$$0.97K^{+}(aq) + 7.37H_2O(l) + 0.26HOx^{-}(aq) + 7.36Ox^{2-}(aq) \; . \qquad (3.5)$$

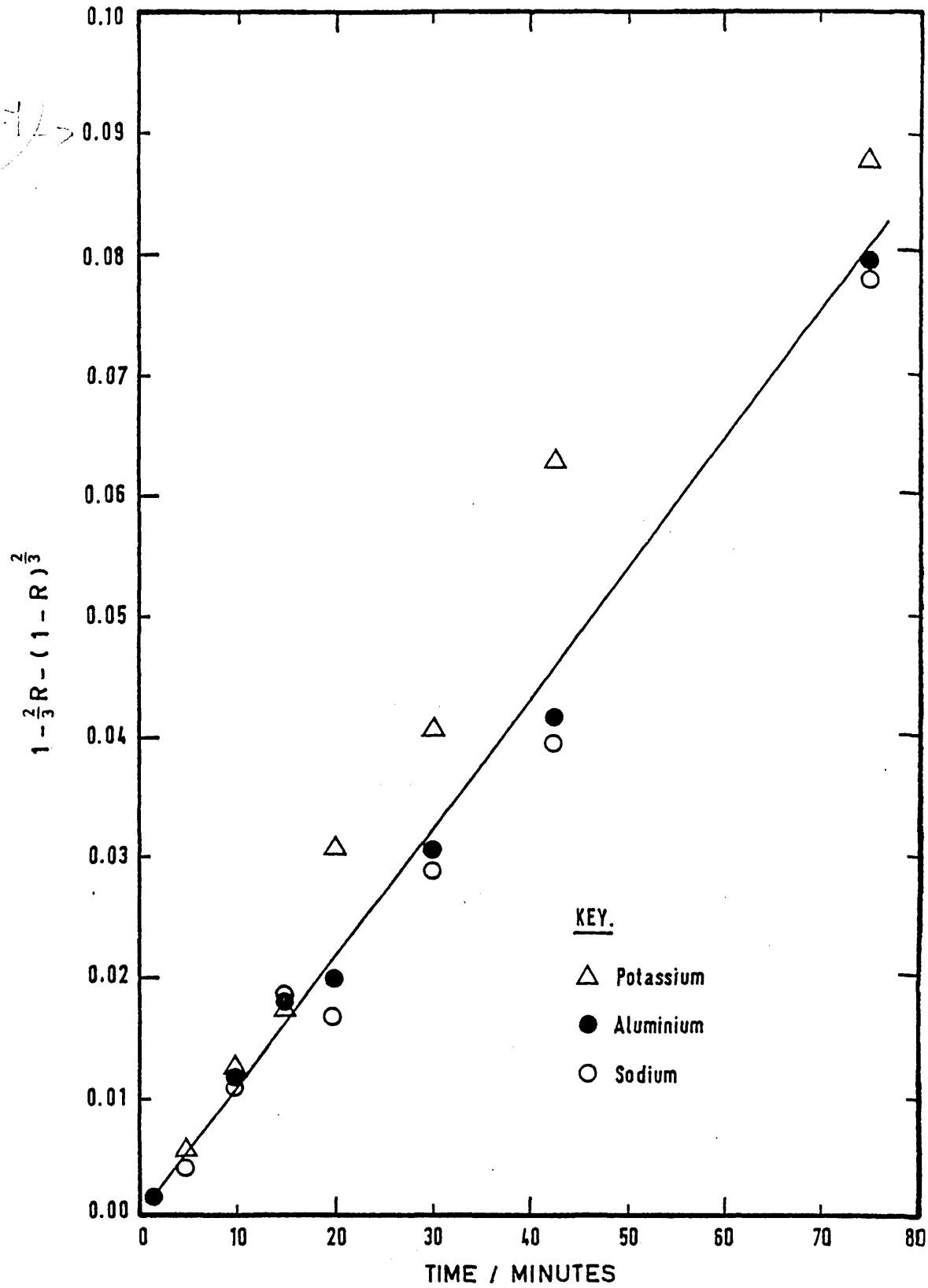


Fig. 3.2: Graphs of $(1-\frac{2}{3}R-(1-R)^{\frac{2}{3}})$ as a function of time for aluminium, sodium and potassium leached from Bancroft nepheline by citric acid at pH 2.31.

In deriving these equations it was assumed that, in the acidic solutions employed (1.83<pH<4.00), citric and oxalic acids are present predominantly as H_3 CIT and HOx^-, respectively (324), and in the presence of aluminium the AlCIT and $AlOx_2^-$ ions are predominant in solution (325).

From the stoichiometric equations (3.3-3.5) it is evident that the ratio of compact to dispersed silica is similar for each acid tested. There were no other readily observable differences in the stoichiometry.

The fact that no intermediate reaction products were indicated on the XRD charts or in the analyses of silica gel products suggests that elements were leached in a congruent manner.

Calculation of rate constants. Fig 3.2 shows plots of $1-2R/3-(1-R)^{2/3}$ versus time for citric acid leaching of potassium, sodium and aluminium ions at pH 2.31. For the initial stages of reaction (up to 20 minutes) it is evident that the elements are leached congruently and the plots are approximately linear. As the reaction proceeds further significant deviations occur, and these are discussed under 'Reaction mechanism' below.

Similar plots for each combination of element, pH and acid tested were prepared. Figs 3.3-3.5 give typical results. Values of K (the slope of the plots) were calculated as follows.

(1) The slope of each line together with its correlation coefficient were determined. Lines producing coefficients <0.97 were discarded. Table 3.1 shows the results.

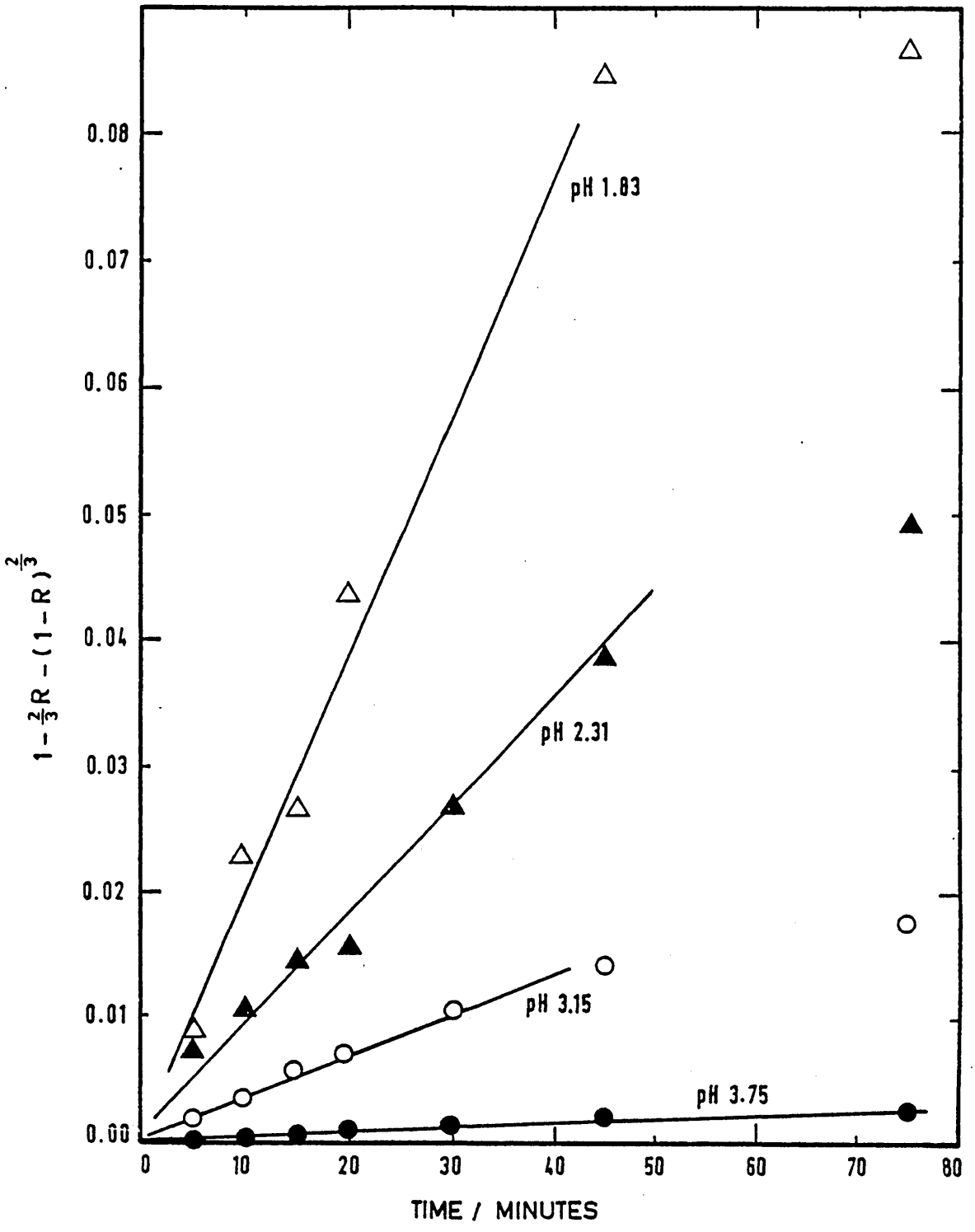


Fig. 3.3: Graphs of $[1-\frac{2}{3}R-(1-R)^{\frac{2}{3}}]$ as a function of time for aluminium leached from Bancroft nepheline by oxalic acid at pH's 1.83, 2.31, 3.15 and 3.75.

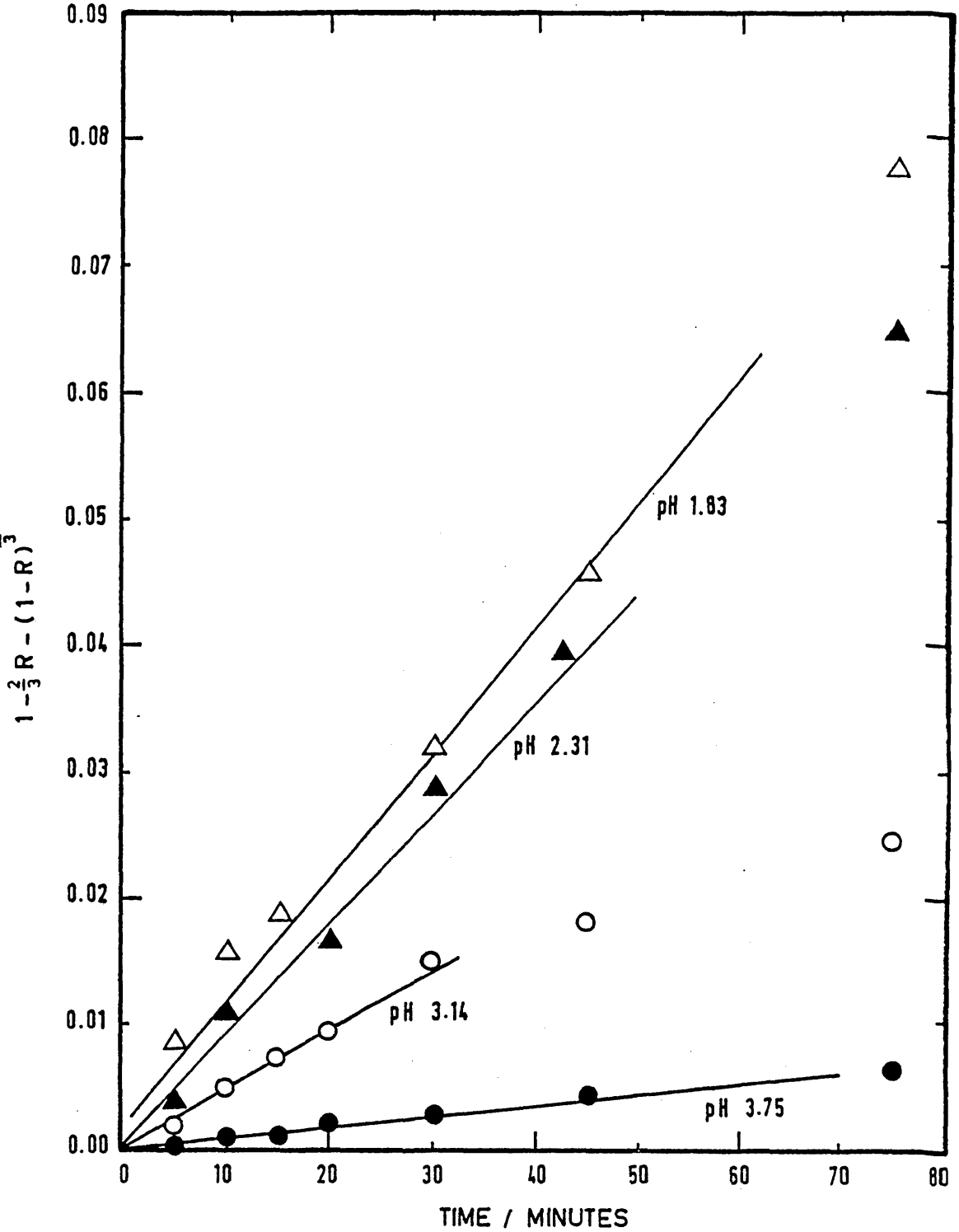


Fig. 3.4: Graphs of $[1-\frac{2}{3}R-(1-R)^{\frac{2}{3}}]$ as a function of time for sodium leached from Bancroft nepheline by citric acid at pH's 1.83, 2.31, 3.15 and 3.75.

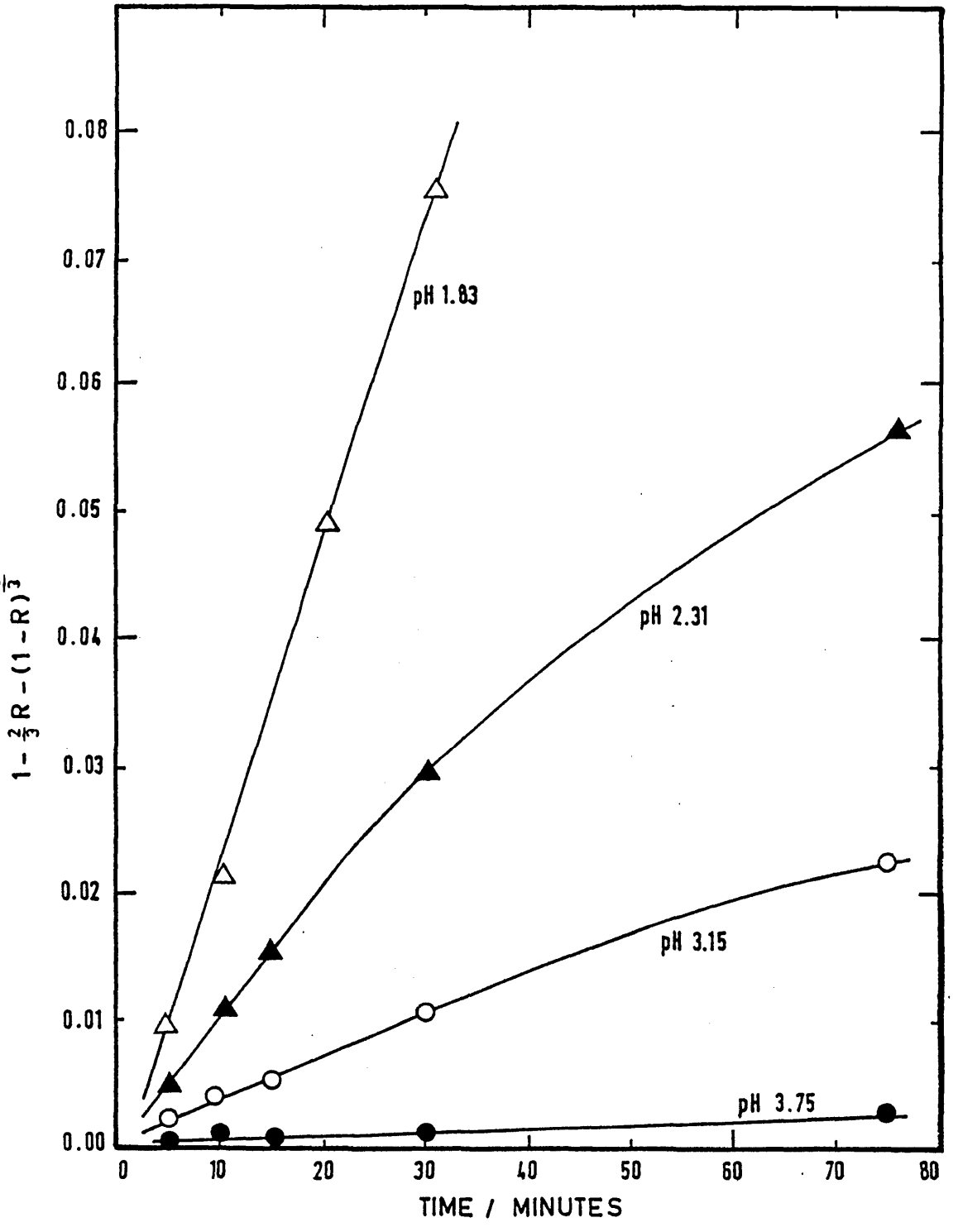


Fig. 3.5: Graphs of $[1-\frac{2}{3}R-(1-R)^{\frac{2}{3}}$ as a function of time for Aluminium leached from Bancroft nepheline by hydrochloric acid at pH's 1.83, 2.31, 3.15 and 3.75.

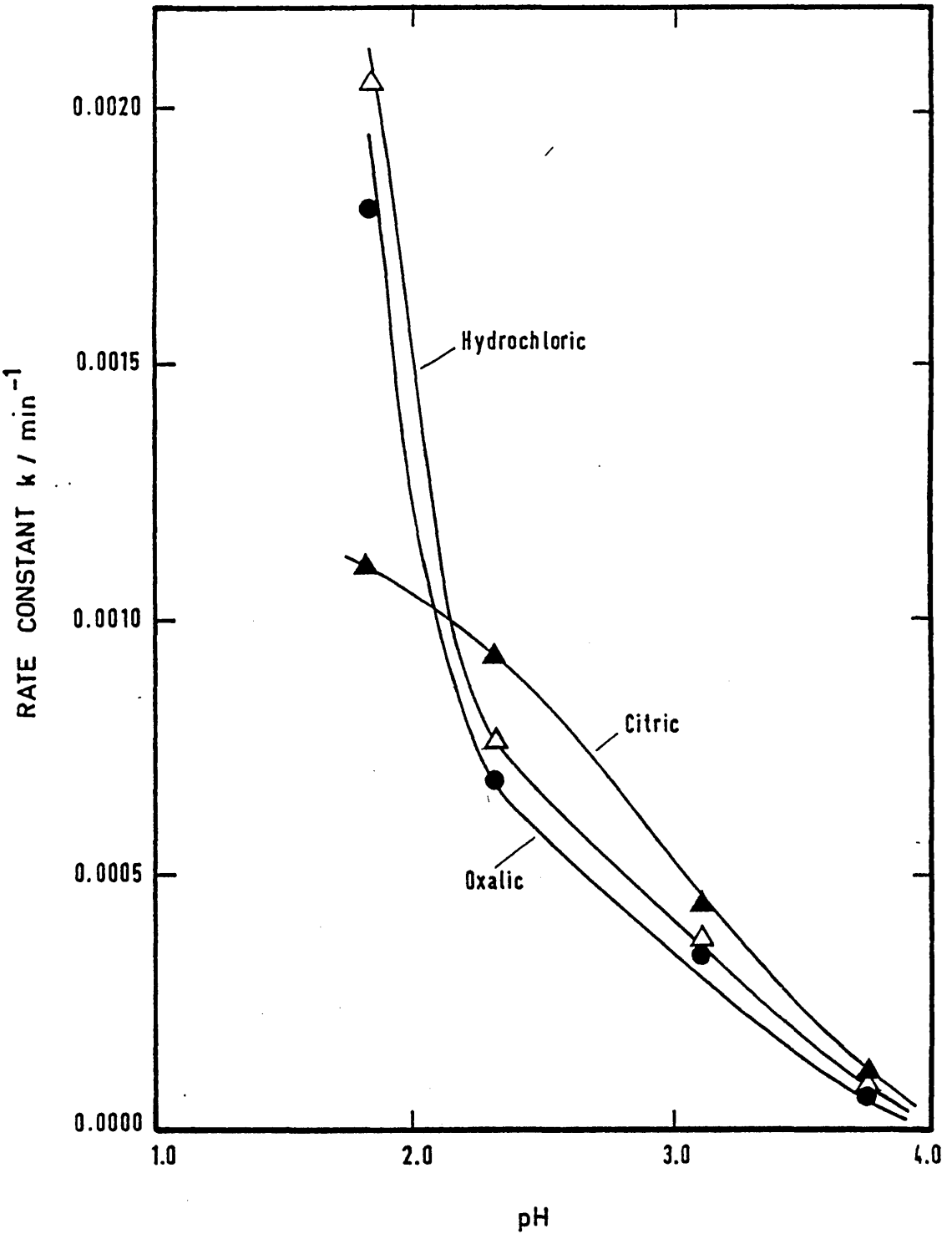


Fig. 3.6 : Plots of pH as a function of rate constant for the reaction between nepheline and oxalic, citric and hydrochloric acids.

(2) For all combinations of pH and acid tested, each group of three Crank rate constants (corresponding values of K for sodium, potassium and aluminium) were averaged. These averages are also shown in Table 3.1.

(3) Average values of K were plotted as a function of pH (Fig 3.6) and fitted to polynomials for the pH range 2.3-4.0 for citric, oxalic and hydrochloric acids, respectively, as in Eqns (3.6-3.8).

$$10^5K = -3.945 + 176.93pH - 78.38pH^2 + 8.592pH^3 \quad (3.6)$$

$$10^4K = 223.56 - 215.32pH + 70.29pH^2 - 7.657pH^3 \quad (3.7)$$

$$10^4K = 257.8 - 248.64pH + 81.137pH^2 - 8.8286pH^3 \quad (3.8)$$

Equations (3.6-3.8) are considered again in Section 3.3. It is evident from Fig 3.6 that, between pH 2.3 and 4.0, the curves for each acid are similar. Above pH 4.0 the reaction rate becomes insignificant. Below pH 2.3, K increases more rapidly for oxalic and hydrochloric acids than for citric acid, presumably because of increases in viscosity for the latter (at pH 1.83 the concentration of citric acid is 48 g/l, oxalic acid 6.5 g/l and hydrochloric acid 0.5 g/l).

Effect of sucrose on the reaction rate constant. The effect of sucrose on the relationship between pH and K for citric acid is illustrated in Fig 3.7. The addition of 50 g/l had little effect. Further additions resulted in significant displacement of the curves towards lower reaction rates, once again probably as a result of changes in viscosity.

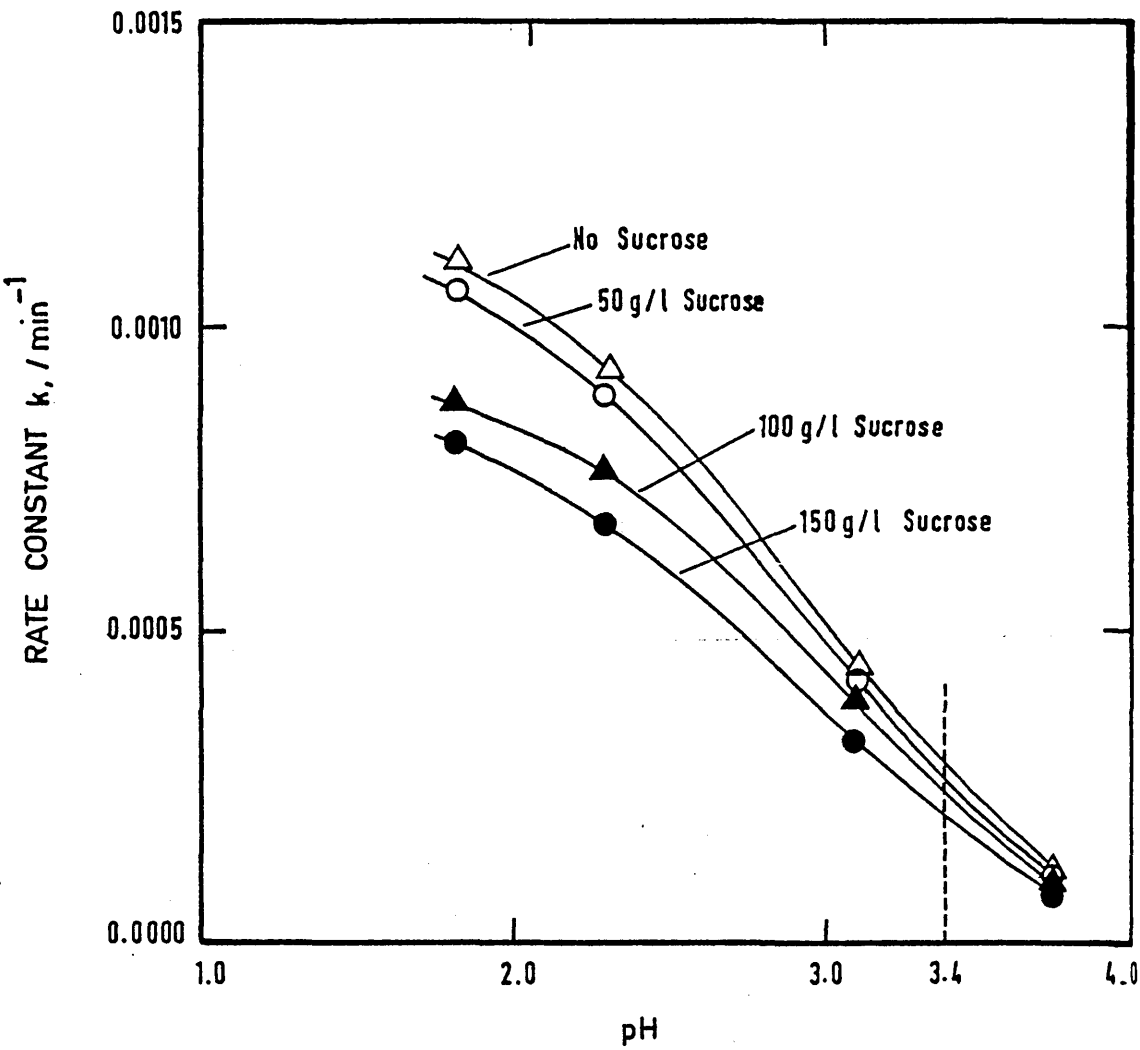


Fig. 3.7 : Graph illustrating the effect of Sucrose on the relationship between pH and k.

TABLE 3.1 RATE CONSTANTS (SLOPES) FOR EACH ELEMENT/ACID/pH COMBINATION TESTED.

pH		OXALIC ACID				CITRIC ACID				HYDROCHLORIC ACID			
		Na	K	Al	AVE	Na	K	Al	AVE	Na	K	Al	AVE
1.83	Slope	.0012	.0023	.0018	.0018	.0009	.0013	.0010	.0011	.00202	.0020	.0020	.0020
	Corr Coef	.992	.998	.993		.997	.999	.998		.987	.999		
2.31	Slope	.0004	.0009	.0006	.0006	.0008	.0010	.0009	.00092	.000768	.00078	.00073	.00076
	Corr Coef	.984	.991	.986		.982	.995	.994		.992	.987	.989	
3.15	Slope	.00033	.00034	.00035	.00034	.0004	.0005	.0003	.0004	.00044	.000399	.00022	.0003
	Corr Coef	.983	.927	.997		.981	.989	.988		.992	.989	.994	
3.75	Slope	.00049	.00008	.00009	.00007	.00008	.00014	.00008	.000104	.000085	.000089	.000034	.000087
	Corr Coef	.968	.998	.999		.986	.978	.991		.982	.987	.960	

units of slope h^{-1}

The effect of sucrose in real fermentations, where the initial concentration is 130 g/l, is likely to be small, because,

(1) at low pH values, where the curves in Fig 3.7 diverge, most of the sugar would have been converted to acid, and

(2) at high pH values, where the sugar concentration is high, differences between the curves are insignificant.

Comparison of experimental and computer predicted curves of fraction of nepheline reacted with time for citric acid leaching. Computer predictions were carried out,

(1) as the basis of more complicated predictions later, and

(2) to assess the internal consistency of the Crank leaching model.

By differentiation of Eqn (3.2) over a finite time element Δt the following is obtained.

$$K(ave)\Delta t = (2/3(1-R)^{1/3}) - 2/3 \quad . \qquad (3.9)$$

Note that the rate constant changes with pH (Eqns 3.6-3.8) and K is therefore replaced with an average value (K(ave)), which is assumed to be constant over the time element in question. Hence over the time element Δt, the fraction reacted, R, can be measured providing K(ave) is known. The value of K(ave) can be estimated from measurements of pH over Δt from Eqn (3.6).

In practice experimental values of pH were fitted to a

polynomial of the form, $pH=a+bt+ct^2+dt^3$, etc. Hence K(ave) could be calculated using Eqn (3.6) as a function of t. The procedure for predicting the curve of R as a function of time was as follows.

(a) A time increment Δt was chosen (typically 0.25 sec - 1 hour) depending on the rate of reaction.

(b) An algorithm suitable for computer use defined as,

$$K(ave)\underbrace{(t(n+1)-t(n))}_{\Delta t} = \underbrace{(f(R(n+1))-f(R(n)))}_{\Delta R}, \qquad (3.10)$$

where n is a counter, K(ave) is taken as $(K(n+1)+K(n))/2$, $(t(n+1)-t(n))$ is Δt, $f(R(n+1))$ is $1-(2R(n+1)/3)-(1-R(n+1))^{2/3}$, $f(R(n))$ is $1-(2R(n)/3)-(1-R(n))^{2/3}$, and $(f(R(n+1))-f(R(n)))$ is ΔR, was solved using the Newton Raphson technique (326) for R(1) (t=0,n=0, R(n)=0).

(c) The counter, n, was increased by 1, R(1) was substituted into Eqn (3.10), and the latter was solved as before for R(2).

(d) The procedure was repeated until the required degree of reaction (normally complete reaction) had been achieved. Values of T and R corresponding to $\Sigma\Delta t$ and $\Sigma\Delta R$, respectively, were stored.

Steps (a) to (d) were repeated for different values of Δt. As Δt decreased the predicted curves were expected to converge closer on the line represented by the model as described by the complete derivative of Eqn (3.2). A listing of the computer program is given in the Appendix.

The program was tested for the reaction of nepheline

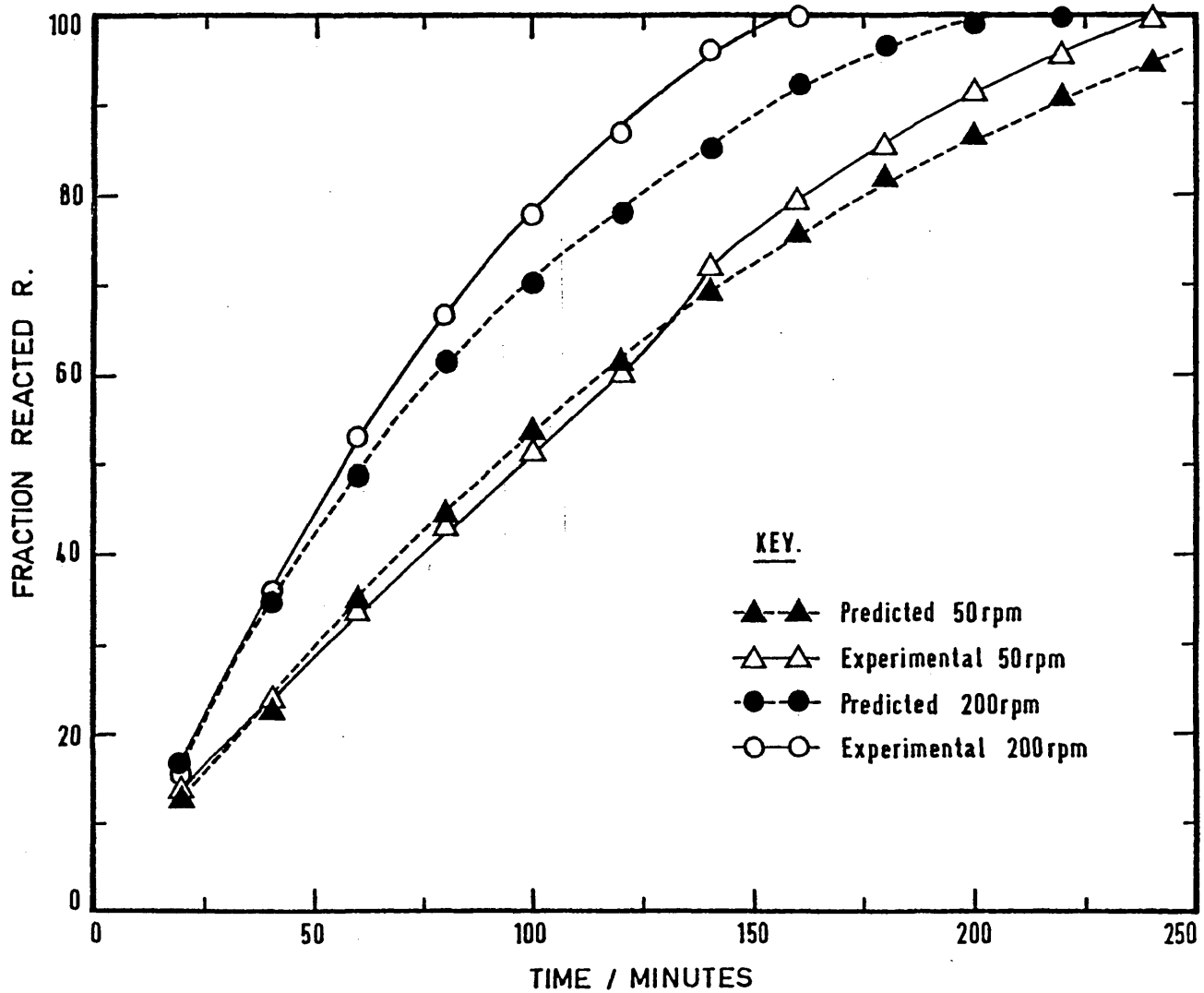


Fig. 3.8: Comparison of reaction paths, predicted by computer from pH measurements and measured experimentally.

(-50μm) with fungally-produced citric acid as follows. A solution (0.25 M) of citric acid was produced by fermentation as in Section 2.3 . This acid was reacted with nepheline at two different agitation rates (50,200 rpm) as in Section 3.1.2, but without pH control, to yield aluminium released with time. Predicted curves of R versus t (calculated as above from pH measurements) were compared with corresponding experimental curves (calculated from measurements of aluminium released) and these are given in Fig 3.8.

As can be seen there is a close correlation between predicted and experimental curves over the first 40-50 minutes. This close fit continues throughout the leach for the test carried out at 30 rpm. In the other test (at 200 rpm) there is increasing divergence with time. This is attributed to the progressive breakdown of the gel layer surrounding reacting grains at the higher stirring rate.

Reaction mechanism. Mechanisms for the reaction of aluminosilicate minerals with acids were reviewed in Chapter 1. Although little or no information was available for nepheline, a variety of geological and soil science studies were reported on other aluminosilicates.

Matveeva (291) suggested that the degradation of aluminosilicates could be split into two main stages. First, cations which are susceptable to hydration pass into solution. This was supported by Eno and Reuszer (287) who showed that metabolites of A.niger removed potassium from biotite, muscovite, microline and minerals in greensand, by an ion exchange process involving the transfer of hydrogen

ions to the mineral structures. Secondly, Matveeva suggested that hydrogen ions are liable to attack mineral at the oxygen link in the aluminosilicate framework. This causes a redistribution of charge along the Al-O-Si bond making the aluminium susceptable to attack by OH^- ions. Bearing in mind the low concentration of OH^- ions in acid solutions, it is more probable that other species in solution (such as the citrate and oxalate ligands) react with the aluminium causing it to go into solution.

The first step in the degradation of nepheline appears to be as proposed by Matveeva: i.e., ion exchange of hydrogen ions for interstitial alkali metal ions (Eqn 3.10). This process should occur more readily in nepheline because of its open framework in which interstitial ions are only weakly held (Section 2.2). This step should result in the formation of a metastable surface layer corresponding to the intermediate, $HAlSiO_4^-$,

$$NaAlSiO_4 + H^+ = HAl^+SiO_4^- + Na^+ \quad (3.10)$$

On the basis of experimental results in Fig 3.6; Eqn (3.10) is rate controlling. Thus, the relationships between pH and K are similar for citric, oxalic and hydrochloric acids despite large differences in the nature and concentration of ligands. A similar layer ($HAlSi_3O_8$) has been proposed for the reaction of feldspars with hydrogen ions (327). However, in this case the altered mineral surface is much more stable (because of the higher ratio of silica to aluminium and tighter feldspar lattice),

and any further reaction must be rate controlling.

Steps following Eqn (3.10) in the reaction sequence of nepheline are less certain because they are relatively rapid and therefore less applicable to detailed study. However it is likely that further sequential protonation (Eqns 3.11-3.13) takes precedence over ligand attack (Eqns 3.17-3.18) because of the sheer bulk of the organic ligands and the fact that only citrate (as H_3 CIT) has sufficient hydrogen to complete the reaction.

$$HAlSiO_4 + H^+ = HAlSi(OH)O_3^+ , \quad (3.11)$$

$$H_2AlSiO_4^+ + H^+ = H\,AlSi(OH)_2O_2^{2+} , \quad (3.12)$$

$$H_3AlSiO_4^{2+} + H^+ = Al^{3+} + Si(OH)_4 . \quad (3.13)$$

The reactions would then be completed by rapid complexing (Eqns 3.14-3.16).

$$Al^{3+} + H_3CIT = AlCIT + 3H^+ \quad k = 10^7 \quad (3.14)$$

$$Al^{3+} + 2HOx^- = AlOx_2^- + 2H^+ \quad k = 6x10^6 \quad (3.15)$$

$$Al^{3+} + Cl^- = AlCl^{2+} \quad (3.16)$$

$$HAlSiO_4 + H_3CIT = AlCIT + Si(OH)_4 \quad (3.17)$$

$$HAlSiO_4 + 2HOx^- = AlOx_2^- + Si(OH)_3O^- \quad (3.18)$$

When a silica gel layer is present it will obviously slow the reaction and may be rate-determining overall. The ratio v_p / v_r (Eqn 3.1), where v_p is for orthosilicic acid ($Si(OH)_4$, v_p=0.63) and v_r is for nepheline (v_r=0.39), is of the order of 1.6. Hence, during reaction the system increases in size. This is illustrated in Fig 2.17, which

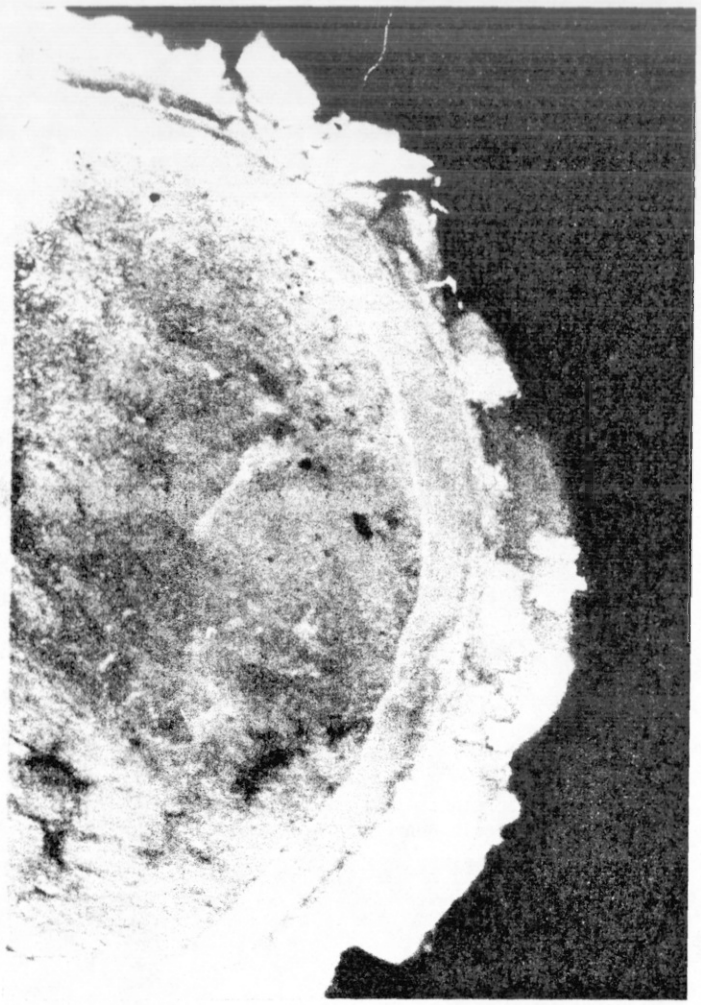


Fig 3.9 Magnified segment of Fig 2.17 showing distinct silica gel layers around a reacting semi-sphere of Bancroft nepheline ×18.

also indicates that the orthosilicic acid becomes hydrated as $v_p/v_r \sim 1.6$ overall (i.e., 3.0). At the reaction interface the gel will be under compression. This causes it to flow outwards. At a certain distance from the reaction zone compression will be replaced by tension and cracks may develop. Such cracks are observed in practice (Fig 2.17) and allow liquid to penetrate into the outer crack zone probably increasing the rate of hydration. This increased hydration apparently causes the outer crack zone to expand more rapidly than the underlying compact zone, thus causing it to break away. The distance from the reaction interface to the start of the crack zone will be related to the rate of flow of gel outwards, and the rate of formation of gel (which is a function of the reaction area and the reagent concentration at the reaction zone). For a spherical particle the reaction area decreases as the reaction proceeds. Consequently the rate of flow of gel also decreases and the thickness of the compact zone increases. Hence the particle diameter (measured as unreacted plus compact silica layers) may only decrease slowly during reaction. This was observed in practice.

Fig 3.9 is a segment of Fig 2.17, magnified, showing a partially reacted grain of nepheline in cross-section. The grain was initially a hemisphere 1 cm in diameter, polished on the sectional face and Araldited to a glass coverslip. It was reacted with concentrated hydrochloric acid without agitation at room temperature for 10 minutes; and carefully washed and dried. The silica gel in Fig 3.9 is white, while the dark band is Araldite and represents the

original diameter of the particle. As can be seen the outer floccose layer is highly cracked and has in places split cleanly away from the underlying compact silica zone. It can also be seen that the diameter of the unreacted mineral together with the layer of compact silica is approximately the same as the unreacted sphere. The kinetics should deviate rapidly from the Crank model if the floccose silica gel is taken into account. However, as the floccose layer is broken away (particularly under mild conditions of agitation) uncovering the compact silica, the model was actually a reasonable fit, at least during the early stages of the reaction. At high agitation rates, such as those described in Section 2.2.6 (in which the acid/nepheline mixture was recirculated through a gear pump) both the compact and floccose layers were removed by attrition. This resulted in a relationship between aluminium released and time.

In conclusion, for the leaching of nepheline over pH, temperature and agitation ranges relevant to fermentation there appears to be little or no advantage in using citric or oxalic acids in place of hydrochloric acid. Reaction rates are similar and the ratio of compact to dispersed silica is the same for each acid under the same conditions.

The reaction mechanism can be split into three basic stages: the transfer of reagents (hydrogen ions and ligand species) through the silica gel to the reaction zone; the breakup of the nepheline structure at the surface, by one of the routes previously described (to form silica gel and

dissolved species of aluminium, potassium and sodium at a rate directly proportional to the hydrogen ion concentration in situ); and diffusion of the products through the gel layer.

An indication has been given of the most likely reactions taking place at the reaction interface and a possible mechanism to explain why the reaction roughly fits Crank's model even though $v_p / v_r > 1$. Considerable further experimental work would need to be done in order to prove these results beyond reasonable doubt. In particular, it is important to establish whether the heat of reaction had any effect on the mechanisms discribed above. There was insufficient time to study this in full detail.

3.2 The Effect of Aluminium, Sodium, Potassium, Silicon and Hydrogen Ions on the Biosynthesis of Citric Acid by A.niger.

In Chapter 1 a range of inorganic and organic species - for instance copper ions and methanol - were reported to significantly affect fungal metabolism, and in Chapter 2 an indication was given of the ways in which fungi accumulate metal ions by ion-exchange. It must be expected that the rate of fungal acid synthesis, dP/dt, (and therefore the rate of nepheline leaching) will depend upon the build up of leaching products. The purpose of this section is to derive from experimental data (mainly measurements of changes in total cell mass and total acid concentration with time at set pH values) the dependence of the rate constants K1 and K2 (Eqn 3.23) on pH in the range 2-4 and on added metals in the range zero - 6.150 g/l. These concentrations have the same elemental ratios expected from congruent nepheline leaching (Na/K/Al/Si:3.0/1/3.7/4.2).

For simplicity and practicality the equations of Monod (Eqn 1.18), Kristiansen (Eqn's 1.24-1.26) and Luedking and Piret (Eqn 1.27) are employed in the modified form (Eqns 3.19-3.23) appropriate to present experimental conditions. As the acid producing cells (x2) cannot be determined directly from the total cell concentration (xT), fairly lengthy procedures requiring these, and other, derived equations are needed.

$$dx1/dt = \mu 1_{max} x1(S/k+S)) \qquad (3.19)$$

$$dx1/dt = \mu 1x1 - kt1x1 \qquad (3.20)$$

$$dx2/dt = \mu 2x2 + kt1x1 - kt2x2 \qquad (3.21)$$

$$dx3/dt = kt2x2 \qquad (3.22)$$

$$dP/dt = K1(dx2/dt) + K2x2 \quad . \qquad (3.23)$$

In these equations x1 and $\mu 1_{max}$ in Eqn (3.19) replace x and μ(max) in Eqn (1.17); x1, x2, x3, μ1, μ2, kt1 and kt2 in Eqns (3.19-3.22) replace xb, xc, xd, μb, μc, kt and kd, respectively in Eqns (1.22-1.24); and x2, K1 and K2 in Eqn (3.23) replace x, α and β in Eqn (1.25), respectively.

3.2.1 Theoretical basis of calculation of K1 and K2.

As indicated in Section 1.5 the growth of fungus can be described in terms of three progressive physiological stages oriented to growth (x1), acid production (x2) and deactivation (x3). The sum of x1,x2 and x3 is xT (the total cell mass per unit fermentation volume). Note, however, that the individual concentrations x1, x2, x3 are hypothetical or 'practical' in nature because cells may have more than one function at any particular time. Fig 3.10 gives an example of the results of experimental measurements and calculations (to be explained later) showing how these concentrations vary with time. The curves in the figure relate to a particular set of experimental conditions but always follow the same general form. While xT conforms to the sequence: induction period, exponential growth, nutrient limitation; x1 is seen to increase to a sharp maximum (after 30 hours in Fig 3.10), giving way (from 25 to 55 hours) to x2 which also increases to a sharp

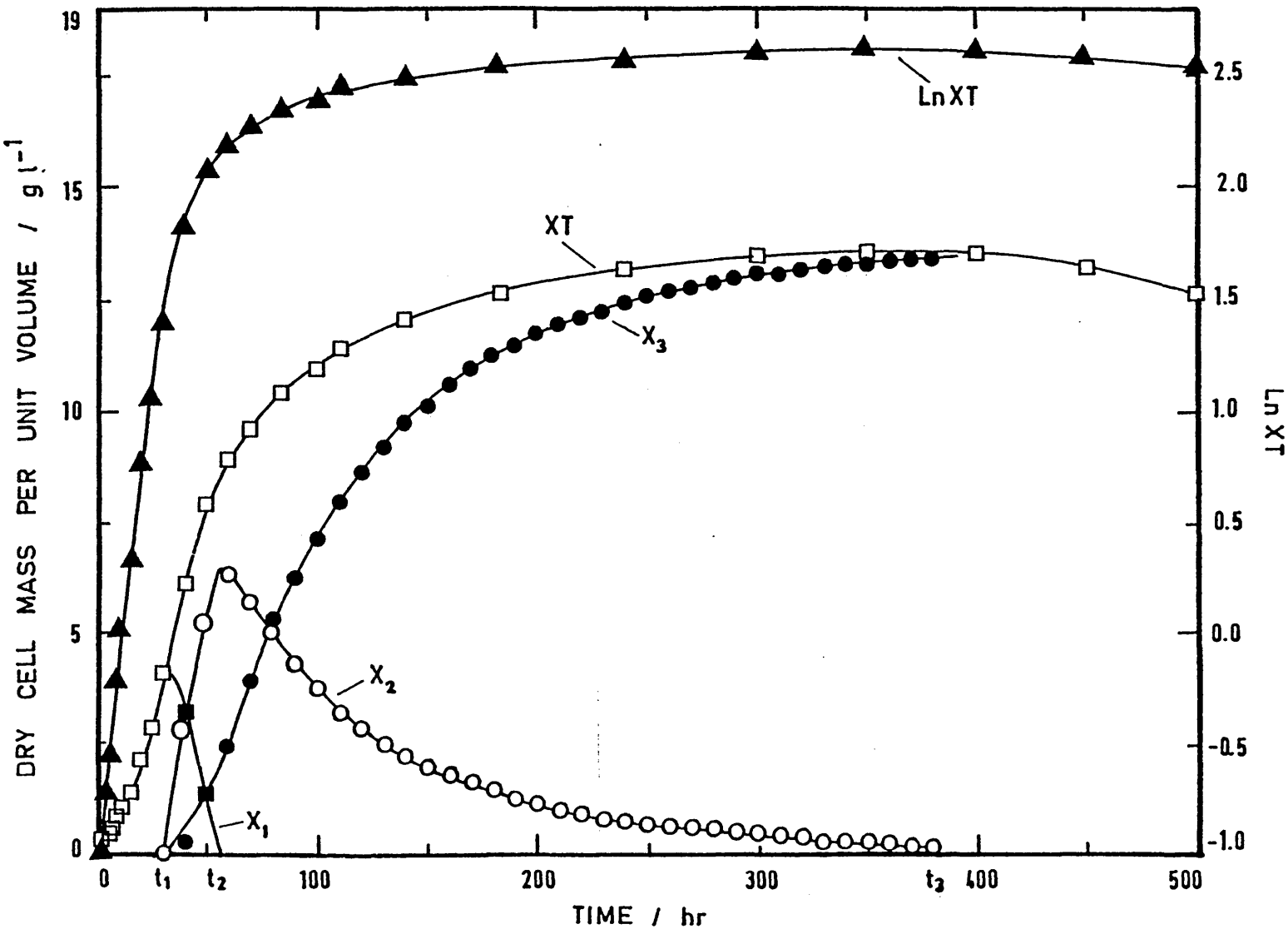


Fig. 3.10 : Relationships between XT, X_1, X_2, X_3, and LnXT, with time for A.niger 31821 at pH 3.3 without added

peak (after 55 hours), but declines slowly giving way to x3. Deactivated cells are noticeable once x2 appears (after 30 hours) and increase exponentially to the value xT (after 380 hours). These curves of x1, x2 and x3 are assumed to be described mathematically by Eqns (3.19-3.23).

Two cell transitions are defined. The first, Ø1, refers to the change from growth cells to acid cells and goes from t1 to t2 (Fig 3.10). The second, Ø2, refers to the transition from acid cells to deactivated cells and goes from t1 to t3. To determine the curves (particularly for x2) in the figure for different sets of conditions, it is first necessary to estimate the starting time (t1) of Ø1 and Ø2, and the finishing times (t2 and t3) of Ø1 and Ø2, respectively. Values of u1 are also required together with a knowledge of points at which particular terms in Eqns (3.20-3.22) become predominant. Variations of x2 with time can be calculated and used in Eqn (3.23) to determine the required constants K1 and K2.

Theory of determination of μ1 and t1. During the growth stage, when all essential nutrients are abundant, the total cell concentration is assumed to increase exponentially ((Eqn 3.20) without the right hand term). The transition term kt1x1 (which represents the change from primary to secondary metabolic pathways when any major nutrient becomes limiting) will be negligible. Any respiration is also assumed negligible. Under these conditions Eqn (3.20) can be integrated to give,

$$Lnx1 = \mu 1t + Lnx1_0 . \qquad (3.24)$$

In this equation $x1_0$ represents the concentration of growth cells at t=0. Up to t1, xT is equal to x1 and the value of $\mu 1$ is obtained as the slope of a plot of LnxT versus t (Fig 3.10). In this case $\mu 1$ approximates closely to $\mu 1_{max}$ in Eqn (3.19). More generally, $\mu 1$ varies as a function of hypha branching frequency and is related to the physical and chemical environment around growing cells (Section 1.8). Under essentially constant conditions of temperature and viscosity, $\mu 1$ can be defined approximately by the Monod equation (Eqn 1.17) relating cell growth rate to x and the concentration of a growth limiting nutrient. In the case of nitrogen as the limiting nutrient, for x1 this becomes (cf. Eqn 3.19 with N in place of S):

$$dx1/dt = \mu 1_{max} x1(N/(kn+N)) , \qquad (3.25)$$

where N is the concentration of nitrogen, $\mu 1_{max}$ is the (constant) maximum specific growth rate, and kn is another constant. According to Pirt (328), kn is approximately 10^{-4}g/l for A.niger citric acid fermentations.

Kristiansen (104) indicated that there was a linear relationship between the uptake of nitrogen and the production of cells during the growth stage of A.niger. Hence a empirical relationship could be assumed in the present work between the nitrogen concentration, N, and x1:

$$N = kx1 + N(0) . \qquad (3.26)$$

In this equation, k is a (negative) constant and N(0) is

the initial nitrogen concentration. It is convenient from a practical point of view to define a term $x1^*$ as the concentration of growth cells when nitrogen becomes limiting ($N=10^{-4}$g/l). The time, t1, corresponds to $N=10^{-4}$ g/l (as $kn=10^{-4}$g/l). At this point the concentration of growth cells is close to the maximum ($x1_{max}=N(0)/kx1^*$). A practical form of Eqn (3.26) is given in Fig 3.11.

From t1 to t2 all new cells produced are acid cells and old cells gradually revert to acid cells. At t1 the growth term, $\mu 1x1$, becomes negligible because $\mu 1$ is now very small. Deleting this term in Eqn (3.20) the transition of growth to acid cells - which represents the falling part of the x1 curve in Fig 3.10 - is described by

$$dx1/dt = -kt1x1 \quad , \qquad (3.27)$$

where $$kt1 = kt1_{max}(kn/(kn+N)) \quad . \qquad (3.28)$$

As N tends to kn (10^{-4}g/l), kt1 tends to (constant) $kt1_{max}$ and the rate of transition accelerates.

Theory of determination of t2, kt1, and x2 during Ø1.

The specific rate of growth of acid cells ($\mu 2$) can be described with the aid of the Monod equation with the carbon source as the limiting nutrient. For present purposes x becomes x2, μ becomes $\mu 2$ and, as suggested by Contois (103), ks becomes ksx2. Thus, taking $\mu 2=\mu 2_{max}(S/(S+ksx2))$ in Eqn (3.21), x2 becomes:

$$dx2/dt=\mu 2_{max}x2(S/(S+ksx2))+kt1x1-kt2x2. \qquad (3.29)$$

In this equation S is the concentration of the carbon source, ks is a constant, and $\mu 2_{max}$ is the (constant) maximum specific growth rate of acid cells. Assuming the transition Ø1 is essentially complete and the number of deactivated cells remains insignificant (i.e., the terms kt1x1 and kt2x2 are negligible):

$$\dot{x}2 \propto Sx2/(S+ksx2) ,$$
$$1/\dot{x}2 \propto 1/x2 + ks/S , \text{ and}$$
$$S/\dot{x}2 \propto S/x2 + cons . \qquad (3.30)$$

Hence a plot of $1/\dot{x}2$ versus 1/x2 should become linear immediately after the transition from growth to acid cells is complete. At this point the concentration of growth and deactivated cells will be low so the transition should also be represented by a plot of $1/\dot{x}T$ versus 1/xT. This point which corresponds to t2 may be determined with sufficient precision by visual inspection (cf. Fig 3.12).

If Eqn (3.27) is integrated, the result is an exponential relationship between x1 and t:

$$x1 = (x1_{max}+1)-e^{kt1(t2-t1)} . \qquad (3.31)$$

The value of kt1 is equal to $Lnx1^{*}/(t1-t2)$, and x1 can be calculated between t1 and t2.

Theory of determination of t3, kt2, x2 and x3 during Ø2.

The time t3 is defined as that at which organic acid production ceases. This is determined from experimental measurements of citrate plus oxalate concentrations versus

time.

At any time t the total cell growth rate dxT/dt is described by.

$$dxT/dt = dx1/dt + dx2/dt + dx3/dt \quad . \qquad (3.32)$$

Substituting Eqn (3.22) into Eqn (3.32) gives,

$$dxT/dt = dx1/dt + dx2/dt + kt2x2 \ ,$$

$$\text{or} \quad \Delta x2 = \Delta xT - kt2x2\Delta t - \Delta x1 \quad . \qquad (3.33)$$

It is assumed that x2 is limited by the concentration of sugar - by analogy with kt1 (Eqn 3.28) - and kt2 varies as:

$$kt2 = kt2_{max}(ksx2/(ksx2+S)) \quad . \qquad (3.34)$$

Now, Kristiansen (104) noted that ks has a magnitude of the order of 0.9S for citric acid fermentations employing A.niger, and Eqn (3.34) becomes:

$$kt2 = kt2_{max}(0.9/(0.9+(1/x2))) \quad . \qquad (3.35)$$

Substituting this into Eqn (3.33) and noting that x2 (in Eqn (3.35) becomes $x2^*$ (the average acid cell concentration over the time increment), Eqn (3.36) is obtained.

$$x2 = xT-kt2_{max}x2\Delta t(0.9/(0.9+(1/x2^*)))- x1 \quad . \qquad (3.36)$$

At any time, the total cell concentration xT is equal to

the sum of the total growth cell concentration x1 the total acid cell concentration x2 and the total deactivated cell concentration x3, so at time t+Δt:

$$(x2+\Delta x2)=(xT+\Delta xT)-(x3+kt2_{max}x2\Delta t(0.9/(0.9+(1/x2^{*}))))$$
$$-(x1+\Delta x1) \quad . \qquad (3.37)$$

In this equation an increment in total cell concentration, Δ xT, corresponding to Δt can be measured from experimental data, and Δx1 can be calculated from Eqn(3.31). Total concentrations of xT and x1 are given by.

$$xT = \sum_{n=1}^{m} \Delta xT_n \quad . \qquad (3.38)$$

$$x1 = \sum_{n=1}^{m} \Delta x1_n \quad . \qquad (3.39)$$

In which m is the number of time increments and n is a counter. Thus there are two unknowns in Eqn (3.37): Δx2 and $kt2_{max}$. Note that $x2^{*}$ and x2 (at time (n+1) t) are related to Δx2 by:

$$x2^{*} = x2_1 + x2_2 + x2_3 + \ldots + x2_n + x2_{n+1}/2. \qquad (3.40)$$

$$x2 = \sum_{n=1}^{m} \Delta x2_n \quad . \qquad (3.41)$$

Also x3 (at time (n+1)Δt) is given by:

$$x3 = \sum_{n=1}^{m} kt2(0.9/(0.9+(1/x2^{*})))x2\Delta t(n) \quad . \qquad (3.42)$$

Eqn (3.37) can be solved for $kt2_{max}$, x2 and x3, with the aid of a computer program (given in the Appendix), as

follows.

(a) An arbitary value of $kt2_{max}$ (normally 0.001) is chosen.

(b) A convenient time interval Δt=10 hours is chosen and employed in a polynomial fitting the experimental curve of xT versus t to calculate the corresponding values of ΔxT and xT for the time t1 to (t1+10) hours.

(c) Corresponding values of $\Delta x1$ and x1 are calculated (Eqn 3.31).

(d) The values of ΔxT, xT, $\Delta x1$, x1 and kt2 are substituted into Eqn (3.37), noting that $x2^{*}=\Delta x2/2$. Values of $\Delta x2$ and $\Delta x3$ ($=kt2_{max}\ x2\ \Delta t(0.9/(0.9+(1/x2^{*}))))$ are calculated. Values of x2 and x3 are stored.

(e) Operations (b)-(d) are repeated for successive time intervals t=10 hours up to t3, noting that x1 is zero after t2 and xT, x1, x2, x3 and $x2^{*}$ are found from Eqns (3.38, 3.39, 3.41, 3.42 and 3.40), respectively. The cumulative values of xT, x2 and x3 are stored.

(f) The value of $kt2_{max}$ is incremented by 0.002 and (a)-(e) repeated.

(g) Procedures (a)-(f) are repeated until x2 (at t3)$<$0 (same as x3 (at t3)$>$xT).

(h) A plot of $kt2_{max}$ versus x2 (at t3) is drawn by hand to give the best value of $kt2_{max}$ corresponding to the point x2 (at t3) =0.

(i) Steps (b)-(e) are repeated for the best value of $kt2_{max}$ to give final values of x2 and x3 versus time.

Theory of determination of K1 and K2 from dP/dt, dx2/dt and x2. If Eqn (3.23) is divided throughout by x2 the

following is obtained,

$$(dP/dt)/x2 = K1(dx2/dt)/x2 + K2 \qquad (3.43)$$

A plot of (dP/dt)/x2 versus (dx2/dt)/x2 should give a straight line of slope K1 and intercept K2. Values of dP/dt can be obtained from experimental data (such as those shown in Fig 3.13 for pH 3.3 without added metals), and dx2/dt and x2 from the x2 curve (Fig 3.10).

3.2.2 Experimental procedure for the determination of K1 and K2.

Fermentations. Twenty-four fermentations (twelve tests in duplicate) were carried out four at a time in customised Pyrex beakers with lids and stirrers. The beakers typically contained 5 l of optimised LM1 (Section 2.3.5) containing additional metal (Na, K, Al added as chlorides and Si added as SiO_2), and spore concentrations at preset pH values, as below.

All equipment and liquid media were sterilised as in Section 2.3. The contents of the beakers were agitated with Citenco turbine stirrers at a power/volume (Pi/v) factor of 2-6 KW/m^3. Air was admitted at 2-4 l/min (measured by 0-10 l/min Rotameter with aluminium float) from a laboratory ring main via a plastic tube perforated along its length. This flow rate was calculated from preliminary calculations and testwork (Appendix).

Fermentations were started by inoculating the liquid medium with spores of A.niger 31821. For this purpose 3.0 l

of liquid concentrate (calculated to give the required initial concentration of nutrient, metal and hydrogen ion concentrations upon dilution to 5.0 l) was mixed with 1.5-2.0 l stock spore solution (calculated to give $3.0x10^6$ spores/ml upon dilution to 5.0 l (Section 2.1)), and made up to 5.0 l with DDW. At 26± 2 °C , with the agitation and air flow as above, the spores had germinated and growth commenced after 1-1.5 days. Fermentations were continued for 500 hours after germination, with timed pH adjustment, topping-up with DDW and sampling. The pH was adjusted daily to the initial value with sodium hydroxide. The volume was readjusted with DDW to account for evaporation losses immediately before sampling. These operations were typically carried out every two hours during the first 10 hours, and then at convenient greater intervals thereafter up to 500 hours. In each case a 15 ml sample was withdrawn with a plastic syringe while agitating the mixture with nitrogen. The dry cell mass per unit volume, xT, was determined for each sample as in Section 2.3.2. Of the residual liquid, 10,5,1 and 2 ml samples were employed for nitrogen (first 40 hours only), citrate, oxalate, and sucrose (at 500 hours only) analyses respectively, as in Section 2.3.2.

Calculations of K1 and K2. The steps used to calculate K1 and K2 from experimental data (values of xT, P and N with time) are given below. These are based on, and follow the same general order as, the foregoing theory (Section 3.2.1).

(1) The term $\mu 1$ was calculated from experimental values

of LnxT versus time using Eqn (3.24).

(2) Experimental values of xT and N were fitted to a first order relationship (Eqn 3.26). This equation was used to calculate xT ($=x1^{*}=x1_{max}$) at $N=10^{-4}$ g/l.

(3) The quantity $x1^{*}$ was substituted into Eqn (3.24) with $\mu 1$ to determine t1.

(4) The time t2 was determined from a graph of $1/\dot{x}T$ versus 1/xT by dropping a perpendicular from the point where the curve was observed (by eye) to become linear, to the 1/xT axis. The value of 1/xT, where the perpendicular intersects with the axis, was t2.

(5) The transition constant kt1 was obtained by substituting x1=0 and t=t2 into Eqn (3.31). Values of x1 with time during Ø1 were then calculated using the same equation.

(6) The value of t3 was estimated, from a polynomial fitting a graph of P versus t, as the time of the maximum value of P.

(7) The computer program (Section 3.2.1) was used to calculate kt2 and values of x2 and x3 with time.

(8) Experimental measurements of P with time, and values of x2 with time, were fitted to appropriate polynomial equations. These were differentiated to give values of dP/dt and dxT/dt with time.

(9) Values of dP/dt, dx2/dt and x2 were plotted as (dP/dt)/x2 versus (dx2/dt)/x2. The slope (K1), intercept (K2), and correlation coefficients were obtained.

Values of K1 and k2 were determined (as above) for all

permutations of three different pH's (2.3,3.3,4.3) and four metal loadings (0,0.0615,0.615,6.15 g/l total metals) a total of twelve different sets of conditions.

3.2.3 Results and discussion.

A typical set of results is given in Tables 3.2-3.4 and Figs 3.10-3.14, for the fermentation at pH 3.3 without additional metals. Values of K1 and K2 for this and other conditions tested are given in Tables 3.5-3.7. Full tabulations of results are given in the Appendix.

Table 3.2 gives variations of N, xT, LnxT, P, 1/xT, $\dot{x}T$, and $1/\dot{x}T$ with time. Using these data, and the calculation procedures described above, curves of LnxT and xT with time, N versus xT, $1/\dot{x}T$ versus 1/xT, and P with time were plotted (Figs 3.10 to 3.13 respectively). The general form of these curves has already been mentioned (Section 3.2.1). It can be deduced that N decreases to $<10^{-4}$ g/l and acid appeared after 30 hours (t1). More generally the time of this point was between 25 and 35 hours for all conditions tested and was therefore essentially constant. Evidently added metals had no significant effect on nitrogen uptake. The value of t2 at pH 3.3 without metals was 55 hours (Fig 3.10), but increased to 80 hours for tests with the maximum metal loading, giving a range of values for Ø1 at pH 3.3 of 15 to 55 hours. At pH 2.3 and 4.3 the corresponding ranges of Ø1 were 5-10 hours and 27-40 hours, respectively. Thus, there were no clear trends overall between Ø1, pH and metal loading; and perhaps none should be expected in view of the

TABLE 3.2 EXPERIMENTAL RESULTS OF FERMENTATION AT pH 3.3 WITHOUT ADDITIONAL METALS.

TIME/h	(N)/gL^{-1}	DRYCELL WEIGHT PER UNIT VOLUME	Ln x_T	TOTAL ACID P/g L^{-1}	CITRIC ACID gL^{-1}	x_T^{-1}/Lg^{-1}	$,x_T$ GROWTH RATE* $gL^{-1}h^{-1}$	$,1/x_T$ INVERSE GROWTH RATE/Lhg^{-1}
0	0.29							
2	0.263	0.396	-0.926					
4	0.252	0.488	-0.717					
6	0.248	0.576	-0.551					
8	0.226	0.816	-0.203					
10	0.224	1.020	0.019					
15	0.173	1.382	0.323					
20	0.130	2.143	0.762					
25	0.088	2.890	1.061			0.346	0.185	5.386
30	TRACE	4.020	1.391			0.248	0.241	4.149
40		6.123	1.812	3.8		0.163	0.128	7.812
50		7.950	2.073	13.0		0.125	0.093	10.752
60		8.966	2.193	21.7		0.111	0.058	17.241
70		9.604	2.262	30.0		0.104	0.053	18.867
84		10.403	2.343	38.2		0.096	0.046	21.38
100		10.954	2.393	46.0		0.091	0.037	26.66
112		11.402	2.433	50.0				
140		12.005	2.485	58.0	55.6			
183		12.650	2.537	66.4	64.0			
240		13.135	2.575	71.6	67.5			
300		13.450	2.548	74.0	68.3			
350		13.530	2.605	74.5	69.2			
400		13.500	2.602	74.5	68.7			
450		13.210	2.581	74.3	67.4			
500		12.600	2.533	73.7	65.4			

* Values at x_T with time were fitted to a polynomial and the result differentiated to give values of growth rate x_1 with time.

Derived values: t_d = 30 hours $t_{\frac{1}{2}}$ = 55 hours

TABLE 3.3 VALUES OF X1, X2 AND X3 WITH TIME FOR FERMENTATION AT pH 3.3 WITHOUT ADDITIONAL METALS.

TIME/h	ADJUSTED TIME/h	x_T/gL^{-1}	x_1/gL^{-1}	x_3/gL^{-1}	x_2/gL^{-1}
30	0	4.020	4.020	0	0
40	10	6.123	3.127	0.289	2.879
50	20	7.950	1.392	1.21	5.269
55	25	8.500	0	1.90	6.60
60		8.950	0	2.56	6.39
80		10.230	0	3.97	5.72
105	75	11.2227	0	7.74	3.48
155	125	12.2998	0	10.42	1.88
205	175	12.8799	0	11.79	1.08
255	225	13.2500	0	12.60	0.65
305	275	13.4392	0	13.01	0.43
355	325	13.5100	0	13.27	0.24
380		13.5800		13.58	0
405	375	13.5000	0	13.50	0

$kt = 0.064\ hr^{-1}$ $kt = 0.025\ hr^{-1}$

TABLE 3.4 DATA GIVING VALUES OF K1 AND K2 FOR FERMENTATION AT pH 3.3 WITHOUT ADDITIONAL METALS.

TIME/h	$dP/dt/gL^{-1}h^{-1}$	$dx_2/dt/gL^{-1}h^{-1}$	x_2/gL^{-1}	$dP/dt/x_2/h^{-1}$	$dx_2/dt/x_2/h^{-1}$
45	1.26	0.719	4.07	0.31	0.029
80	0.65	-0.063	5.01	0.13	-0.0126
100	0.48	-0.048	3.78	0.128	-0.0128
140	0.20	-0.026	2.23	0.13	-0.0117
220	0.12	-0.010	0.87	0.137	-0.0114
300	0.075	-0.002	0.46	0.163	-0.005
340	0.042	-0.001	0.27	0.156	-0.0065

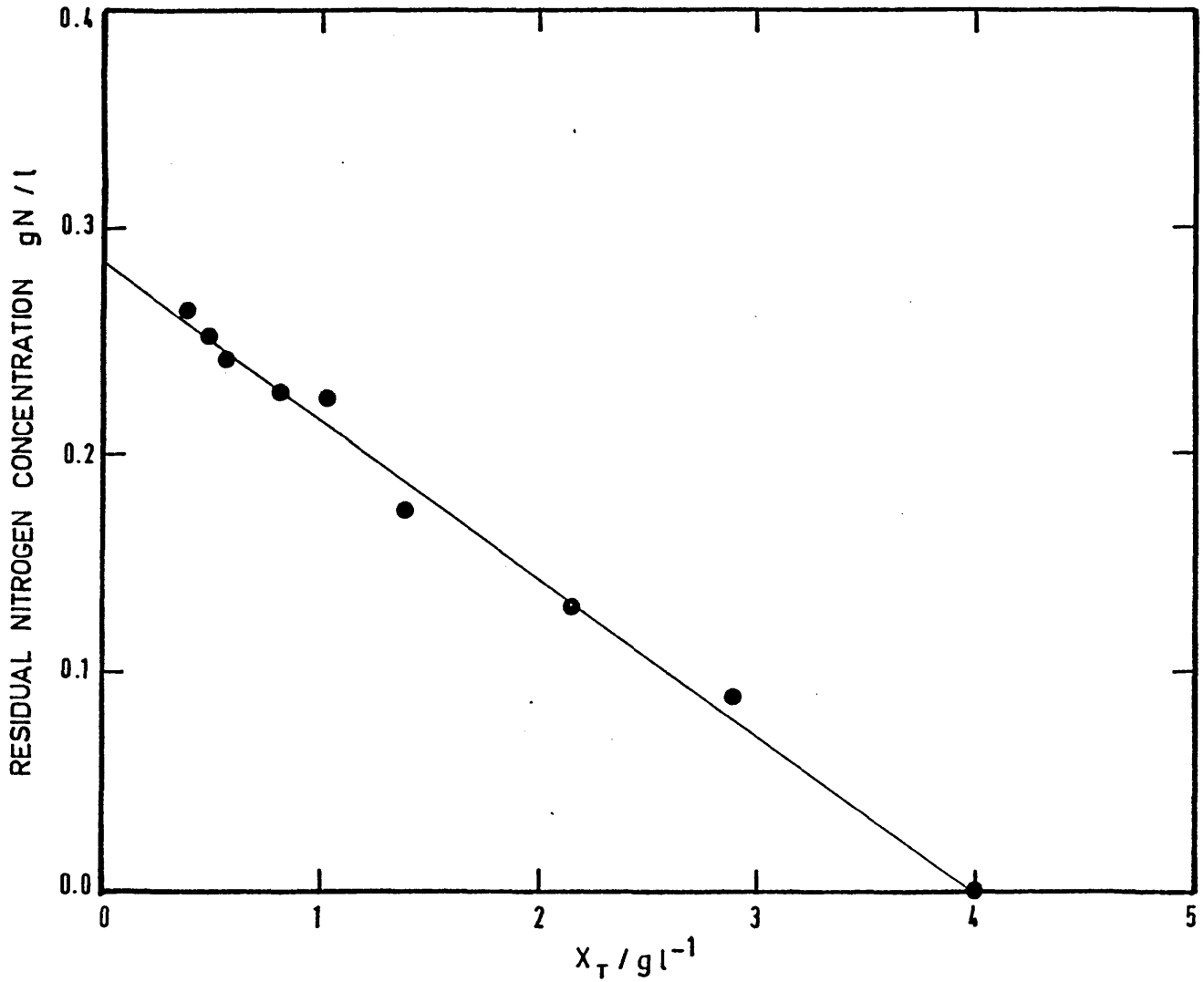


Fig. 3.11: Plot of Equation 3.26 for the conditions in Fig. 3.10.

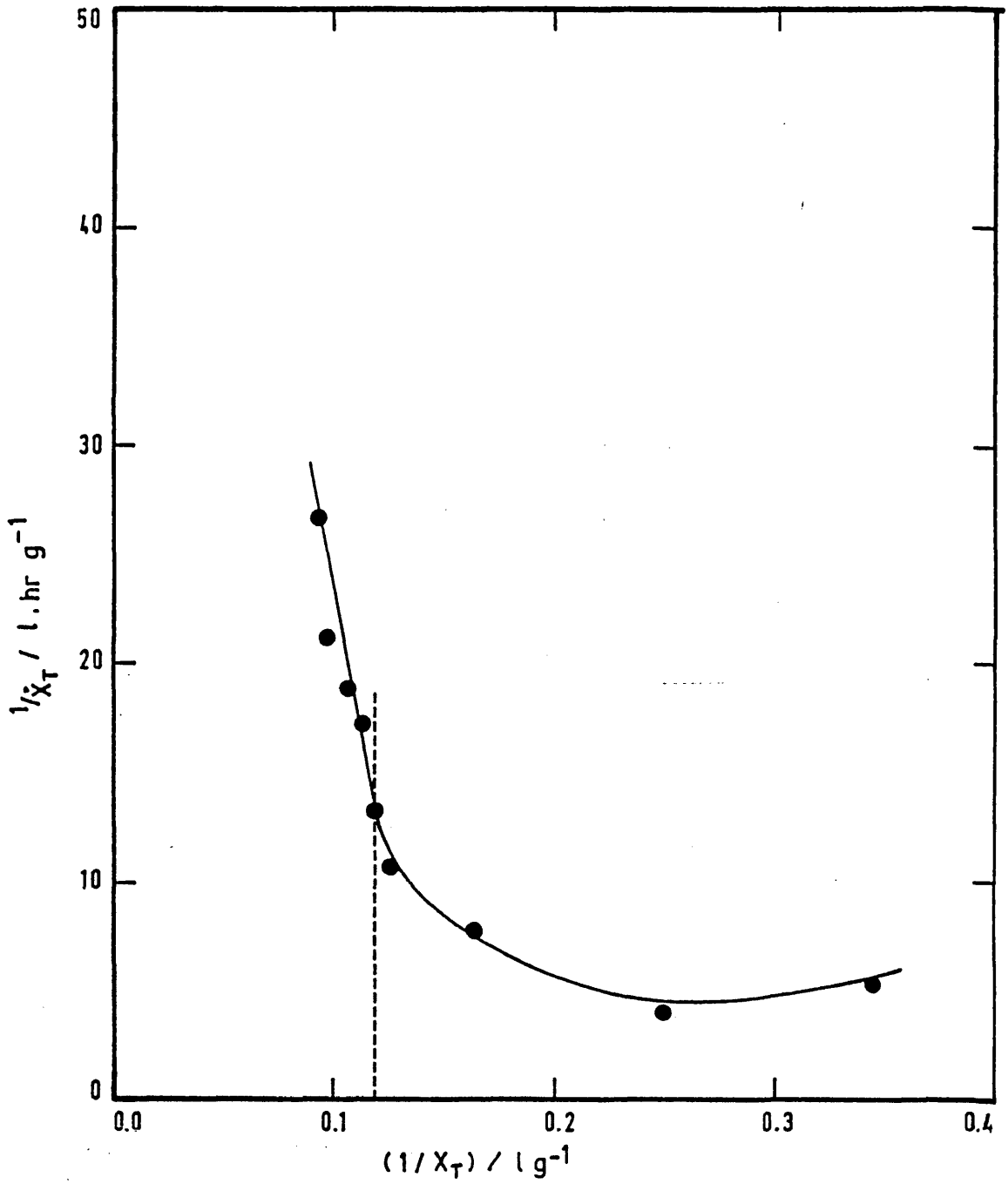


Fig. 3.12: A plot of the inverse rate of growth of total cell concentration versus the inverse of the total cell concentration for the conditions in Fig. 3.10.

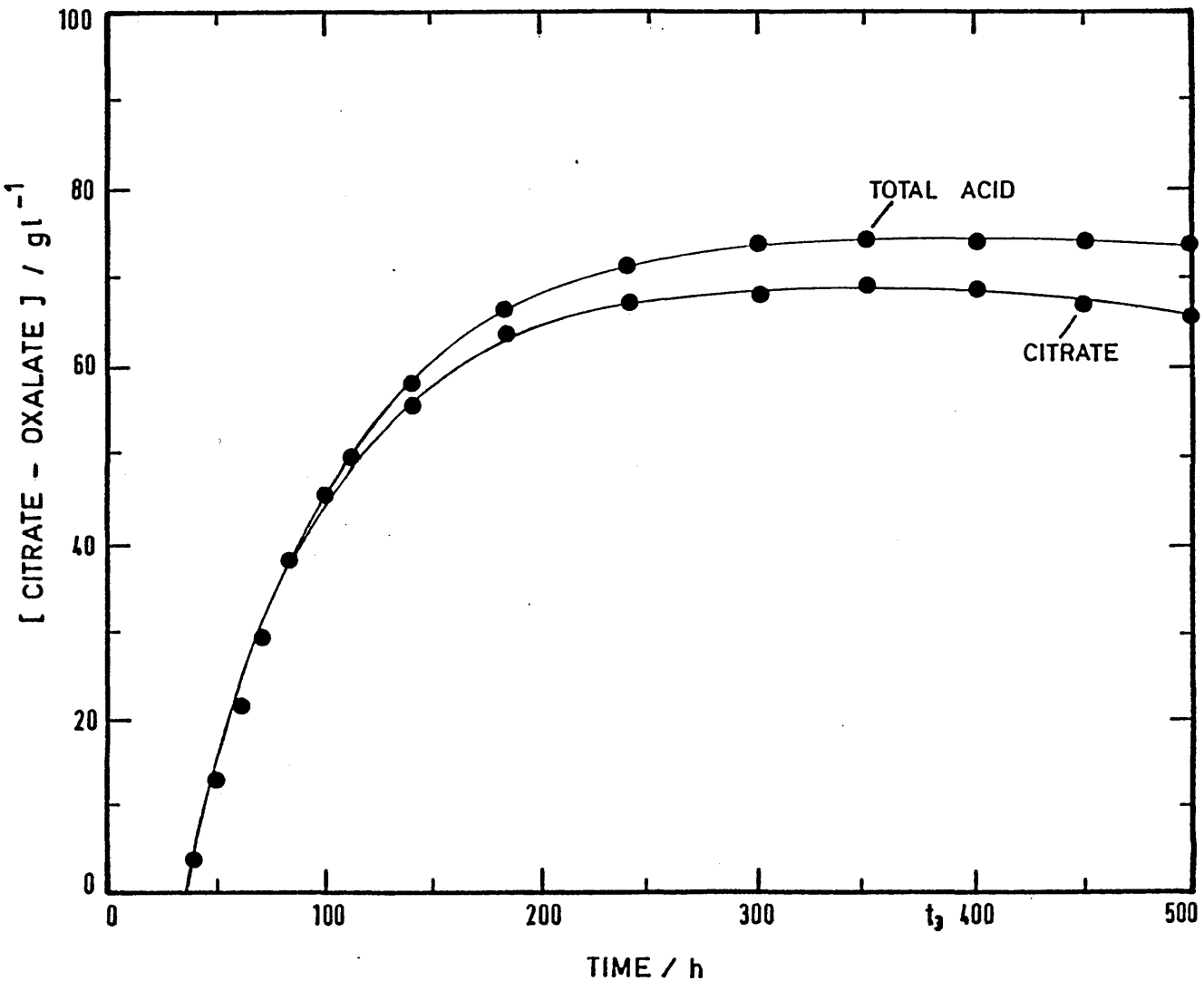


Fig. 3.13: Relationship between total acid and time for conditions in Fig. 3.10.

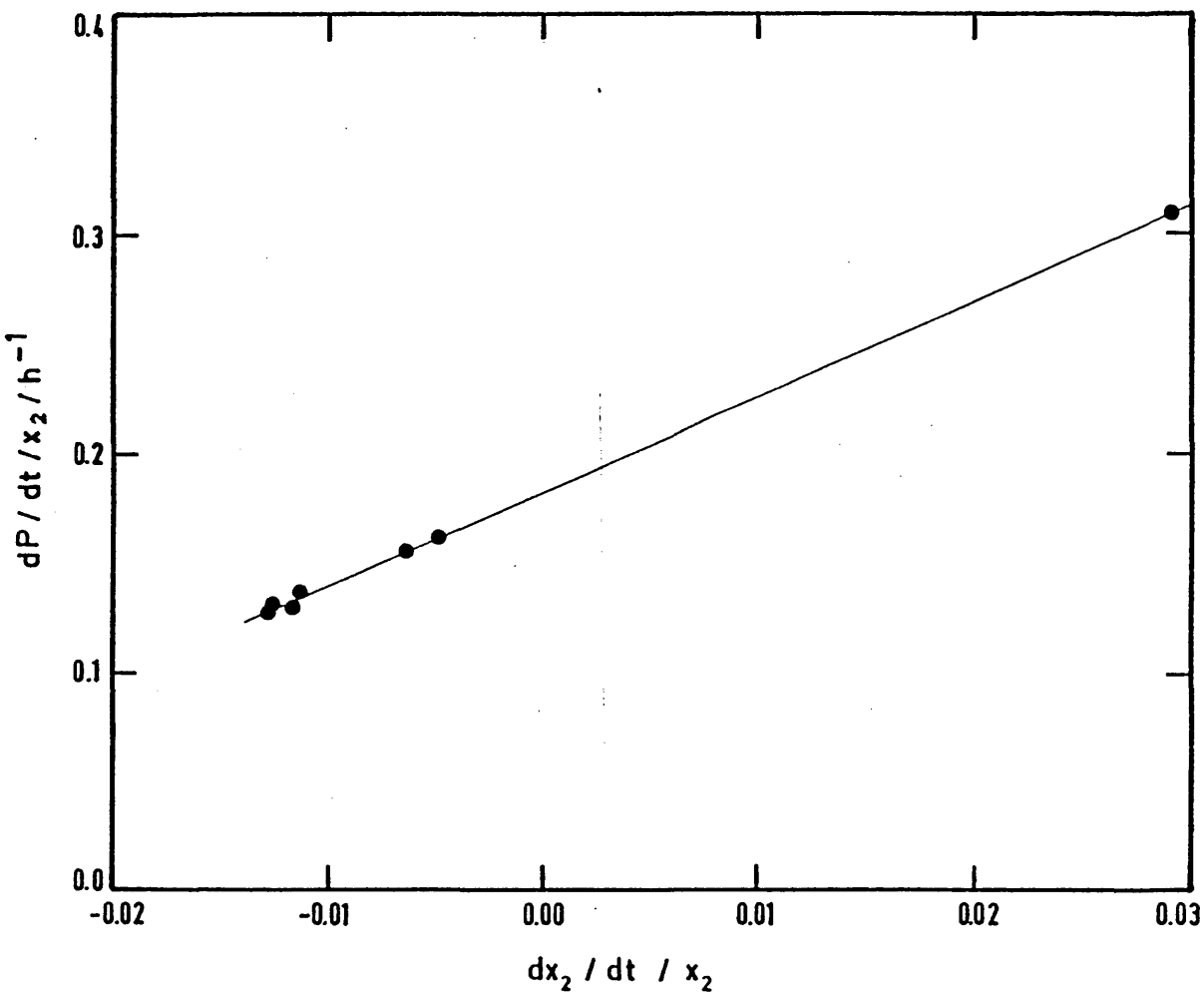


Fig. 3.14 : Relationship between $dP / dt / x_2$ and $dx_2 / dt / x_2$.

sensitivity of biochemical pathways to large variations in the growth environment.

The precision with which the transition time Ø1 could be measured was related to the measurement of t2 (where the largest error was incurred). Using the method described above t2 could be measured to ±5 hours (±20%) which is considered satisfactory for present purposes - because calculations requiring t2 were relatively insensitive to changes in this range (Eqns 3.31 and 3.37).

The value of t3 at pH 3.3 without metals was 380 hours (Fig 3.10) but decreased to 300 hours with the maximum metal loading giving a range of times of Ø2 at pH 3.3 of 275-350 hours. Corresponding ranges of Ø2 for pH 2.3 and 4.3 were 155-275 hours and 290-360 hours, respectively. In general, t3 and t2 decreased with increasing metal and/or hydrogen ion concentration. This is further discussed below.

From Figs 3.10 and 3.13 it can be seen that, as expected, xT and P vary in a similar manner with time - viz. an initial rapid increase coming eventually to a broad maximum. This maximum is at about the same time on the two figures and corresponds to t3. In general, however, the peaks did not coincide, and it is predicted that the time of the maximum cell concentration is less than t3, unlike those in Figs 3.10 and 3.13. Also shown on Fig 3.13 is a curve of citrate concentration versus time. It can be seen that the oxalate concentration (represented by the difference between the curves) is always small in comparison to citrate, but reaches 15% near t3. At shorter

times and lower pH's less oxalate is produced, as expected (Section 1.2.8). This trend probably arises from the conversion of citrate to oxalate as the sugar concentration becomes limiting (when x2 becomes small). The total fungal mass continues to grow slowly after the peak in the concentration of citrate, presumably through metabolism of citrate or other polysaccharides, such as glucans, known to be produced during fermentation. As Eqns (3.19-3.23) apply only to citric acid, partial breakdown of the model might occur towards the end of the fermentation.

Total acid yields ranged from 74% (total) - 67% (carbon consumed) for pH 4.3 with no metals added to 9.7% (total) - 2.2% (carbon consumed) for the fermentation at pH 2.3 with the maximum metal loading. The differences between the maximum yields reported here and those given in Chapter 2, which were of the order of 90% for the same medium, were attributed to the need to maintain a constant pH throughout present fermentations. Acid yields were not apparently related to corresponding curves of x2 with time indicating that the rate of acid production per unit mass of acid cells was not constant. This is in general aggreement with Fencl (110) who noted, from observations of the distribution of RNA concentrations in cell material of A.niger at different stages of growth, that metabolic activities are randomly distributed throughout old and new cell material during the restricted growth stage.

Values of t1, t2 and t3 for the fermentations in the presence of metals released from nepheline have not been reported in the literature and so comparisons cannot be

made. However, this is not the case for $\mu 1$ and the nitrogen yield factor Yn (1/k in Eqn 3.26). Kristiansen (104) indicated a value of $\mu 1$ equal to 0.26 h^{-1} for A.niger at 32° C which compares favourably with those reported here (for 26±2°C) which were between 0.08 and 0.17 h^{-1} (note that $\mu 1$ increases with temperature). The nitrogen yield factor ranged from 10 to 15 which is in general agreement with Kristiansen who indicated a value of 14.

Values of K1 and K2, together with correlation coefficients for their relationships in Eqn (3.43) are presented in Tables 3.5-3.7, respectively. A typical graph is given in Fig 3.14 from which K1 is the slope and K2 the intercept. From Table 3.5 it can be seen that a hundred fold increase in the concentration of metals (from 0.0615 to 6.150 g/l) decreases K1 by approximately 1.8, whereas a hundred fold increase in the hydrogen ion concentration ($5x10^{-5}$ to $5x10^{-3}$ g/l) decreases K1 by approximately 2.2. When the mass differences are taken into account it can be seen that K1 is approximately $1.5x10^{4}$ times more sensitive to hydrogen ions than metal ions. From a similar evaluation of the data in Table 3.6 it can be shown that K2 is about $1.8x10^{3}$ times more sensitive to hydrogen ions than metals. In general K1 is approximately 20 to 30 times greater in magnitude than K2, and x2 30 to 300 times greater than dx2/dt (depending upon the time from the outset of acid production). So K2x2 is approximately equal in magnitude to K1dx2/dt at the start of acid production, but $K2x2 \gg K1dx2/dt$ towards the end of acid production, which is observed in practice.

TABLE 3.5 EXPERIMENTAL VALUES OF K1 AS A FUNCTION OF pH AND METAL LOADING.

pH / Added metals/ g/l	2.3	3.3	4.3
0.0000	3.23	4.28	5.45
0.0615	3.15	3.81	5.72
0.6150	3.18	3.76	4.32
6.1500	2.97	3.51	2.83

TABLE 3.6 EXPERIMENTAL VALUES OF K2/h AS A FUNCTION OF pH AND METAL LOADING.

pH / Added metals/ g/l	2.3	3.3	4.3
0.0000	0.157	0.180	0.201
0.0615	0.140	0.168	0.202
0.6150	0.132	0.108	0.167
6.1500	0.110	0.103	0.110

TABLE 3.7 CORRELATION COEFFICIENTS FOR THE DATA IN TABLES 3.5-3.6.

pH / Added metals/ g/l	2.3	3.3	4.3
0.0000	0.96	0.99	0.99
0.0615	0.99	0.97	0.99
0.6150	0.96	0.80	0.99
6.1500	0.79	0.99	0.99

It can be seen (Fig 3.14) that the relationship between (dP/dt)/x2 and (dx2/dt)/x2 is linear and this should be the case if the model is applicable. In a general way this applied to all conditions tested but there was noticeable scatter in some cases, particularly with high metal loadings. Some of this scatter could be attributed to experimental variations, i.e., 1-2 $^{\circ}$ C changes in temperature. The line shown refers to the time period 50-380 hours (short times positive and long times negative on the (dx2/dt)/x2 scale). For the time period 25-50 hours (early acid production), points are way off the scale to the right and non-linear (and are not included in the calculations to determine K1, K2 and their respective correlation coefficients). This non-linearity at the start of fermentation suggests a breakdown of the model at the peak (initial) rate of acid production. In general there was acceptable correlation during Ø2, giving confidence in the results. The validity of the model will be further checked in Section 3.3 where values of K1 and K2 are employed to predict the results of practical fermentations.

A different model of the cell deactivation was tested in the hope of giving better correlation during early acid production. In this model Eqn (3.22) was replaced by,

$$dx3/dt = kt3x3 , \qquad (3.44)$$

where kt3 is a deactivation constant with the dimensions of time^{-1} . In this equation the rate of deactivation is governed by the concentration of deactivated cells. This

situation might be expected to apply if deactivated cells represent 'diseased' cells (i.e., deactivation propogates via cells carrying the disease). There was no correlation between (dP/dt)/x2 and (dx2/dt)/x2 for this model, indicating that cell deactivation is governed by the concentration of acid cells.

The observed decrease in cell growth, and hence acid production, at high metal loadings probably results mainly from the neutralisation of charged sites on cell surfaces by charged ions or complexes in solution. As has been mentioned (Sections 1.2.3-1.2.8) these sites are important in the transport of nutrients. In nepheline four major charged species are released into solution/suspension. Each is considered below, and shown in a general way to be consistent overall with less acid production at increased metal concentrations.

Deductions from the literature (170) suggest that an excess of alkali metals reduces the citric acid yield (but not the total acid produced). This reduction probably results from the absorption of ions in large amounts into the cell rather than adsorption onto the cell wall sites.

Aluminium forms a 1:1 complex with citric acid below pH 5.5 (325). It can also be complexed by organic species containing phosphorus (cyclic polymers based on $2PO^{3-}$ plus $2Al^{3+}$ units per ring have been produced (329)). The amount adsorbed onto cell wall material will depend upon the concentration of organophosphorus and other anionic exchange groups in the cell wall (Section 2.3.6) and relative stability of Al-citrate, Al-organophosphorus,

etc., complexes in solution and on the cell wall. Based on Rothstein's findings (330), that metal-phosphorus complexing was predominant over metal-carboxylate complexing in the cell walls of yeasts, it might be assumed that aluminium is preferentially adsorbed onto organophosphorus species in the cell wall, and this will obviously increase as the concentration increases, thus increasingly blocking sites required for nutrient transport.

A.niger can accumulate significant amounts of silica (240). The species to which silica bonds in the cell wall are unknown, and not likely to be the same as those for aluminium (because silica gel is a negative colloid under the conditions employed). Consequently silica gel adsorption might be independent of aluminium adsorption. This has not been checked in the present work.

Validity of growth, acid and deactivated cells. Values of x1, x2 and x3 represent relative proportions of the total cell concentration xT with metabolic pathways oriented to unresticted growth, acid production and deactivation, respectively. They are clearly interrelated as are the metabolic pathways.

Bearing in mind the high metabolic rates associated with unrestricted growth (which are a result of the large surface to volume ratios of hyphae and the short path lengths for diffusion of nutrients and products), one might expect the transition between different metabolic pathways to be rapid. However, Kovats and Gackowska (275) noted that if the flow of oxygen to a citric acid fermentation was

stopped during the acid production stage, acid production was slow to recover when oxygenation was resumed. This indicates the transitions are slow processes, thus giving credibility to the values of Ø1 presented here. This is not unexpected as transitions in metabolism (following perturbations in nutrient supply), involve the simultaneous change and regulation of a large number of reactions.

Mitochondria, which are randomly distributed throughout hyphae, are responsible for chemical precursors used for growth and acid production (Section 1.2.6) and are therefore directly related to x1, x2 and x3. The allocation of products for each function probably depends on the location in the hyphae (i.e. mitochondria close to growing hyphal tips are likely to be more active in the synthesis of precursors for new cell wall than for acid production), and on the availability of nutrients. Thus, there are reasonable grounds for distinguishing cell functions in terms of x1, x2 and x3.

3.3 A Computer Model of Nepheline Leaching by A.niger.

A computer model of citric acid fermentation in the presence of nepheline has been designed to make use of the results in Sections 3.1 and 3.2 and predict the values of three parameters giving the maximum average simultaneous rates of acid biosynthesis and nepheline leaching over a specified time. The three parameters are the time from the start of the fermentation (TIME) at which nepheline is introduced to the system, the sugar concentration at TIME (SUG), and the mass of nepheline added per unit volume of fermentation (NEP). TIME limits the proportion of the fermentation during which acid biosynthesis is undisturbed by leaching and leach products, and has an overall effect because of the different rates and mutual interdependence of acid biosynthesis and nepheline leaching. Other variable parameters are not required.

In the computer program the aim was to generate data for the mass of acid produced and nepheline leached with time at different values of SUG, TIME, and NEP in the ranges 5-150 g/l, 40-300 hours, and 0.5-40 g/l, respectively. These ranges were chosen as limits for growth and acid biosynthesis. Conditions predicting optimum (i.e. maximum) rates could then be checked experimentally. Providing the model was satisfactory, the procedure might take the place of some 2-3 years of systematic experimental optimisation.

The model (for which a computer program listing is given in the Appendix) is considered below.

3.3.1 Prediction of acid produced, nepheline leached and pH with time.

An overall outline is given before a description of the sequence of computational steps. Calculations were carried out for some 900 modelled fermentations (one for each set of SUG, TIME and NEP), normally of 150 minutes duration and divided into one-minute time intervals. For a particular set, the value of TIME and Fig 3.13 gives an initial estimate of P (or INACID) for the first minute. From this are calculated pH (Eqn 3.45), leaching rate constant K (Eqn 3.6), fraction of mineral reacted R (Eqn 3.2), acid remaining after 1 minute, REMACID (Eqn 3.48), and concentrations of metals in solution. The values of pH and metal concentration, together with Tables 3.5-3.6, yield interpolated estimates of the citric acid biosynthesis rate constants K1 and K2. The metal concentrations, and experimental curves of acid cell concentration x2 versus time (at set metal concentrations as in Fig 3.15), give interpolated curves and corresponding estimates of x2 (or XX2) and rate of production of acid cells x2 over the first minute. The mass of acid (INCACID) biosynthesised is obtained from K1, K2, XX2 and $\Delta x2$ (Eqn 3.63).

The estimates need adjustment to take account of acid consumed and acid biosynthesised. For this purpose, acid available in the first minute is taken as the average ((INACID+INCACID)+REMACID)/2 (where INACID + INCACID represents acid available at the start of the first minute, and REMACID is that at the end), and used to calculate a new working value of pH (Eqn 3.71). Adjusted values of K,

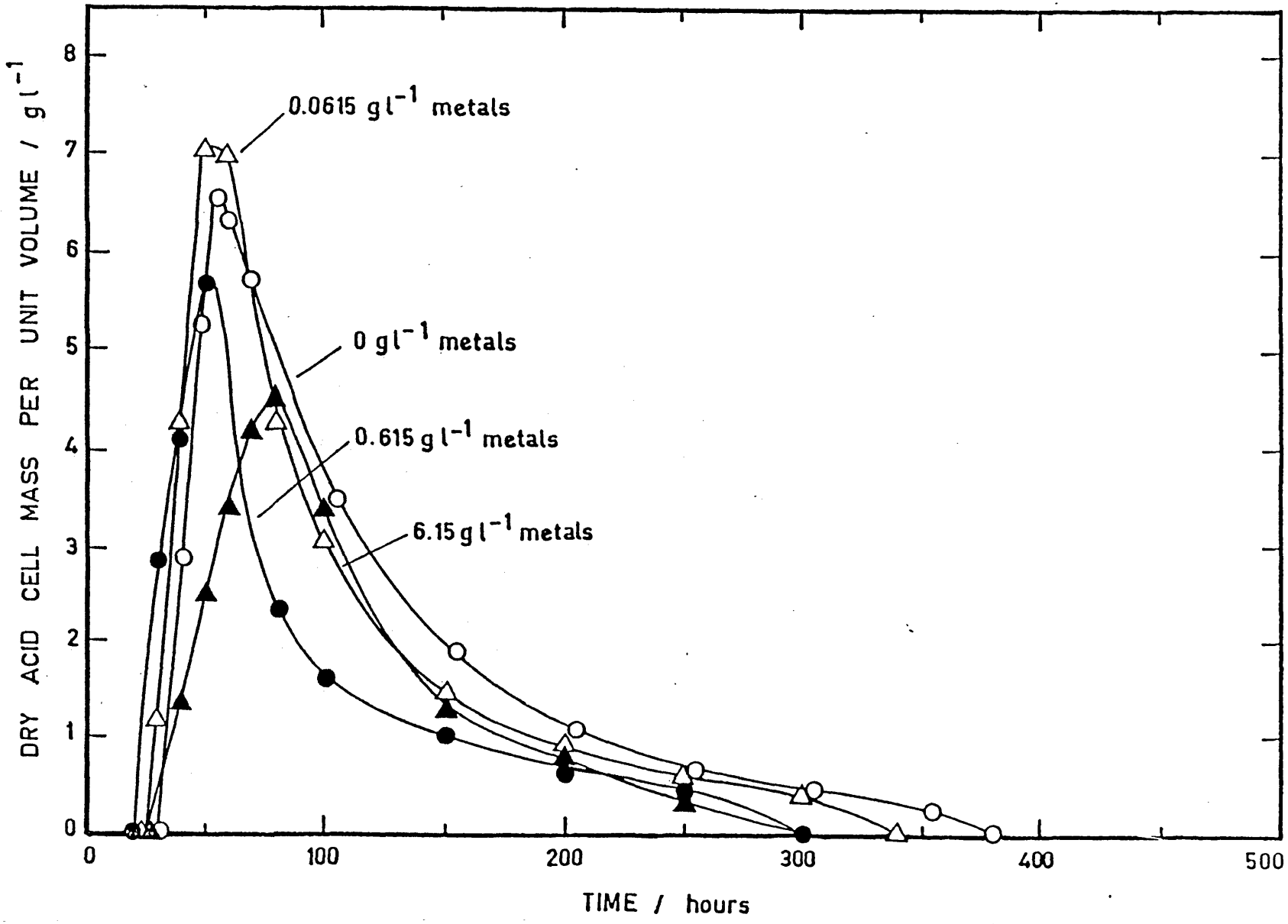


Fig 3.15: Comparison of curves of x_2 with time for 0,0.0615, 0.615 and 6.15 gl^{-1} metals at pH 3.3.

R, REMACID, K1, K2, XX2 and $\Delta x2$ are obtained from this pH and the equations already mentioned. This cycle is repeated (normally ten times) until successive values of REMACID are the same within four places of decimals. Optimised values are thus obtained and stored for later use.

For the second minute the starting pH is based on the optimised REMACID from the first minute (Eqn 3.48). The calculations then proceed as before but with the following refinement: R becomes the total fraction (for minutes 1 and 2) of mineral reacted.

The calculations are repeated for the remaining time increments until all mineral is leached (R=1) or acid biosynthesis ceased and the concentration of free acid becomes zero (in the time limit 150 minutes). The term OF (an optimisation factor) is calculated (see below).

The mass of nepheline leached (NEP ×R) is normally less than the theoretical maximum (0.601923P), and there is a well defined area (AREA) between plots (e.g. Fig 3.16) of metal concentration and theoretical maximum metal concentration with time. The theoretical maximum mass of nepheline which could be leached, based on acid produced over the 150 minutes is defined as $0.601923(P_{max}-INACID)$ or TOT (P_{max} is indicated in Fig 3.16). For a particular set of SUG, TIME and NEP, the AREA is a measure of the average nepheline leaching efficiency (defined as the predicted average rate relative to the maximum average rate) over the 150 minutes and TOT similarly measures the average rate of acid biosynthesis from TIME to the fermentation end. For different sets, AREA and TOT will have different values,

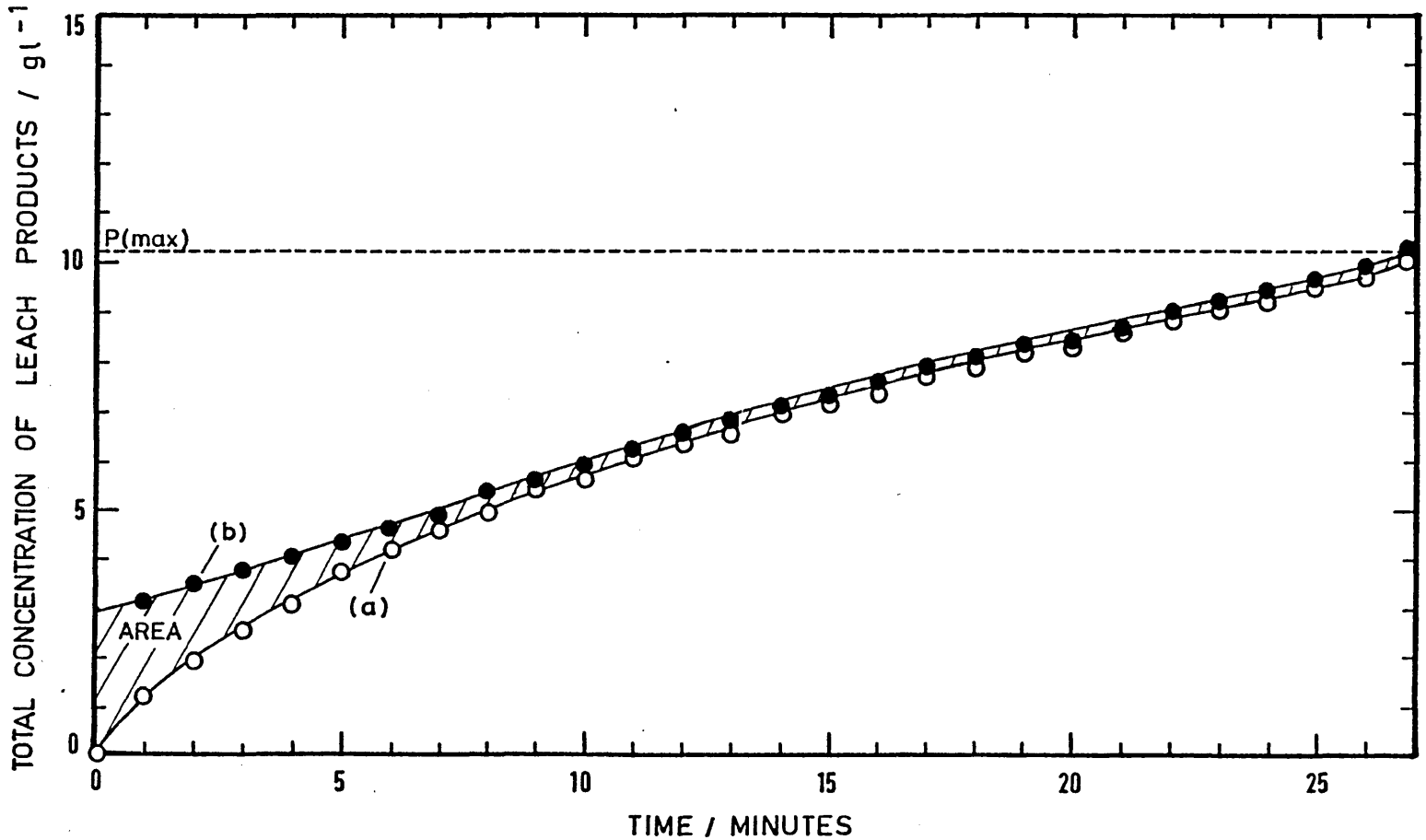


Fig. 3.16: Comparison between computer predicted curves of total concentration of leached products, (a), and the potential concentration of leached products based on acid available, (b), as a function of time, for SUG = 20 g/l and NEP = 10 g/l.

For that set of SUG, TIME and NEP giving maximum average simultaneous rates of acid production and nepheline leaching, TOT/AREA (denoted OF) should be a maximum. Calculations are carried out for all 900 sets of SUG, TIME and NEP, values of the optimisation factor, OF, are retrieved and the conditions giving the maximum value found by inspection.

A detailed account of steps in the program is now given.

(1) The starting values of SUG, TIME and NEP (1, 40 and 0.5 respectively) were set for the time increment (Δt) 0-1 min after TIME.

(2) A value of INACID (P) corresponding to TIME=40 hrs was calculated from the polynomial fitting Fig 3.13 (P versus time) as Eqn (3.45).

$$P = a + b(TIME) + c(TIME)^2 + \ldots\ldots \qquad (3.45)$$

The program used for curve fitting is given in the Appendix.

(3) The 'average' pH over Δt was calculated by Eqn (3.46). For the first minute P replaced (P+REMACID)/2.

$$pH = (5.3763 - Ln(((P+REMACID)/2)/192.12246))/3.829. \qquad (3.46)$$

This equation was derived from experimental data for the purpose of relating pH to citric acid concentration.

(4) An average value of the leaching rate constant, K, was calculated by Eqn (3.6).

$$10^5K = -3.945 + 176.93pH - 78.38(pH)^2 + 8.592(pH)^3 \quad . \qquad (3.6)$$

This was employed in Eqn (3.2), together with the Newton Raphson technique (Section 3.1.3) to determine a value of R, the fraction of mineral reacted, for the first minute.

$$1 - 2R/3 - (1-R)^{2/3} = Kt \qquad (3.2)$$

(5) Free acid remaining at the end of Δt (REMACID) was calculated on the basis of stoichiometry by Eqns (3.47) and (3.48):

$$F1 = P + INCACID \qquad (3.47)$$

$$REMACID = F1 - NEP \times R/0.601923 \quad . \qquad (3.48)$$

In these equations F1 and NEP R/0.601923 were the total free acid available for leaching and the acid used to leach nepheline (NEP×R), respectively. If (R×NEP)/0.601923>F1 it was assumed that all available acid was consumed and REMACID was set to zero.

(6) A value of K1 was obtained by interpolation from Table 3.5 as follows.

Experimental values of K1 as a function of added metals at fixed pH's were fitted to first order linear equations (Eqns 3.49-3.54). Two such equations were required to adequately describe K1 over the range 0<NEP<6.15 g/l for each fixed pH (a total of six equations).

$$K1(1) = 3.23 - (z1 \times 1.300), \text{ for pH 2.3, } z1 < 0.0615 \text{ g/l} \qquad (3.49)$$

$K1(1)=3.21-(z1\times2.002)$, for pH 2.3, $z1>=0.0615$ g/l (3.50)

$K1(2)=4.28-(z1\times7.642)$, for pH 3.3, $z1<0.0615$ g/l (3.51)

$K1(2)=3.80-(z1\times0.0476)$, for pH 3.3, $z1>=0.0615$ g/l (3.52)

$K1(3)=5.34-(z1\times3.505)$, for pH 4.3, $z1<0.0615$ g/l (3.53)

$k1(3)=4.53-(z1\times0.277)$, for pH 4.3, $z1>=0.0615$ g/l (3.54)

In these equations z1 is the concentration of metals in solution (R ×NEP), and the subscripts (1)-(3) indicate working values of K1.

A second series of three equations (3.55-3.57) relating K1 to pH in the ranges $1.8<pH<2.3$, $2.3<pH<3.3$, $3.3<pH<6.5$, were calculated assuming linear relationships between pH and K.

$K1=(pH-1.8)K1(1)/0.5$, for $1.8<pH<2.3$. (3.55)

$K1=(pH-2.3)(K1(2)-K1(1))+K1(1)$, for $2.3<pH<3.3$. (3.56)

$K1=(pH-3.3)(K1(3)-K1(2))+K1(2)$, for $3.3<pH<6.5$. (3.57)

In order to calculate K1, two working values of K1 were calculated by Eqns (3.49-3.54) in the required metal concentration and pH range. For example if $z1>0.25$ and $pH>4.3$, values of K1(2) and K1(3) from equations (3.52) and (3.54) would be used in Eqn (3.57) to calculate K1.

(7) A value of K2 was calculated using the same method as in (6) above but according to the following equations.

$K2(1)=0.1554-(z1\times0.2006)$, for pH 2.3, $z1<0.12$ g/l. (3.58)

$K2(1)=0.1339-(z1\times0.00388)$, for pH 2.3, $z1>=0.12$ g/l. (3.59)

$K2(2)=0.1808-(z1\times0.2254)$, for pH 3.3, $z1<0.32$ g/l. (3.60)

K2(2)=0.1086-(z1×0.000925), for pH 3.3, z1>=0.32 g/l. (3.61)

K2(3)=0.2018-(z1×0.1144), for pH 4.3, z1<0.25 g/l. (3.62)

K2(3)=0.1745-(z1×0.0105), for pH 4.3, z1>=0.25 g/l. (3.63)

K2 =(pH-1.8)K2(1)/0.5, for 1.8<pH<2.3. (3.64)

K2 =(pH-2.3)(K2(2)-K2(1))+K2(1), for 2.3<pH<3.3. (3.65)

K2 =(pH-3.3)(K2(3)-K2(2))+K2(2), for 3.3<pH<6.5. (3.66)

(8) Values of XX2 and Δx2 were calculated representing the average concentration and rate of production of acid cells, respectively over Δt. The calculations of XX2 and Δx2 were based on experimental data of x2 with time for pH 3.3 (plotted in Fig 3.15). For this purpose experimental values of x2 with time for 0 and 0.01 g/l metals at pH 3.3 were fitted to polynomial equations of the form,

$$x2 = a + bTIME + c(TIME^2) + d(TIME^3) + \ldots \quad (3.67)$$

Values of x21(0) , x21(0.06), x22(0) and x22(0.06) (the concentrations of x2 at the start, x21, and end, x22, of Δt, for 0 g/l metals, (0), and 0.0615 g/l metals, (0.06), respectively), were calculated by relevant forms of Eqn (3.67), and used in conjunction with the experimental data in Table 3.8 (from Section 3.2) to calculate values of x21(z1) and x22(z1) by interpolation using the same technique as for K1 and K2. The values of XX2 and Δx2 were calculated as below:

$$XX2 = (x21+x22)/2 \quad (3.68)$$

$$\Delta x2 = ABS(x22-x21) \quad (3.69)$$

TABLE 3.8 EXPERIMENTAL VALUES OF x2 AS A FUNCTION OF TIME AND ADDED METALS.

TIME/hr / added metals/g/l	40	70	280
0.0000	2.88	5.70	0.53
0.0615	4.25	5.70	0.48
0.6150	4.12	3.00	0.34
6.1500	1.35	4.20	0.18

(9) The mass of acid produced, INCACID (incremental acid), over Δt was calculated by Eqn (3.23) in the form:

$$INCACID = K1\Delta x2 + K2x2 \qquad (3.70)$$

(10) The pH was adjusted to account for acid produced over Δt (INCACID) by,

$$pH=(5.3763-Ln((INCACID+INACID+REMACID)/2)/192.1246)/3.829. \qquad (3.71)$$

This pH was used in Eqn (3.46) and steps (4)-(10) were repeated for ten cycles.

(11) Acid produced from the time of introduction of nepheline was compared with the theoretical maximum (0.95SUG, for a sugar to acid conversion efficiency of 95%). If greater than 0.95SUG, INCACID was reduced such that P-INACID was equal to 0.95SUG.

(12) The mass of nepheline leached based on fraction reacted (NEP×R) was compared with the mass leached based on acid consumed (0.601923(P-REMACID), where P is INACID+INCACID. If (R ×NEP) ≠ 0.601923(P-REMACID), R and REMACID were adjusted to account for the discrepancy by Eqns (3.72-3.74). (Typically R ×NEP/0.601923(P-REMACID)= 0.8-0.9).

$$IN = (NEP\times R+0.601923(P-REMACID))/2. \qquad (3.72)$$

$$R = IN/NEP. \qquad (3.73)$$

$$REMACID = P/IN. \qquad (3.74)$$

(13) Values of R, P (INACID+ $\sum_{n=1}^{m}$ INCACID(n)), and pH were stored. The working value of free acid (ACID) was set equal to REMACID, and REMACID then set to zero.

(14) The second time increment after 40 hours was now considered. The value of ACID from (13) was substituted into (3) in place of P noting REMACID was zero, and the cycle repeated for the time increment 1-2 minutes after TIME but with the following refinements: R became the total fraction of mineral reacted, and P in Eqn (3.47) became ACID.

(15) Steps (3)-(14) were repeated for successive time increments either until the acid was exhausted and acid production ceased as represented by the difference in R between this and the last step (i.e. until $R_{m-1} > 0.99R_m$), or until R=1 (all mineral leached).

(16) Data of R×NEP and 0.601923P, from (13) with time (representing real and potential nepheline leached, respectively), were integrated by Simpsons rule (331), Eqn (3.75), for h=TIME to TIME+NΔt where N was the number of cycles required to satisfy (15).

$$\int_a^b f(x)dx = h(f(0)+4f(1)+2f(2)+4f(3)+\ldots+4f(N-1)+f(N)) \qquad (3.75)$$

In Eqn (3.75) f(x) represents the function describing the curve to be integrated between a and b, and f(0), f(1), f(2), etc., represent consecutive values of f(x) at intervals h apart.

The resulting areas U1 and U2, respectively, were used to calculate OF by,

$$OF = 0.601923(P_{max}-INACID)/1+(U1-U2), \qquad (3.76)$$

where $(P_{max}-INACID)$ is the acid produced between TIME and TIME+N Δt and 0.601923 is a stoichiometric factor to convert this into an equivalent mass of nepheline. The area difference U1-U2 in the denominator is increased by 1 in order to reduce the range of OF.

(17) Average values of $d^2 P/dt^2$ and $d^2 (R\times NEP)/dt^2$ were calculated by double differentiation of values of P and R×NEP with time between TIME and TIME+NΔt.

(18) Values of OF, d^2P/dt^2, $d^2(R\times NEP)/dt^2$, were stored.

(19) The next permutations of SUG, TIME, and NEP (5,60,10) were set and steps (2)-(18) repeated.

(20) Once all required permutations of SUG,TIME and NEP were used, stored values of OF, d^2P/dt^2 and $d^2(R\times NEP)/dt^2$ were printed out.

An additional subroutine, which was only used for selected values of SUG, TIME and NEP, allowed data of R, P and pH with time to be printed out. This is included in the Appendix.

3.3.2 Results and discussion.

This is the first integral model of fermentation and leaching although there are models for both separately. The results are unlikely to be better than semi-quantitative owing to the complex nature of the system but are consistent with physical reality and make general

predictions possible.

The aim was to predict a set of values of the parameters NEP, SUG and TIME which give maximum average simultaneous rates of nepheline leaching and acid biosynthesis. An interpretation of the results to determine these optimum values is given below.

Figs 3.17 and 3.18 are three dimensional representations of the relationships between OF, NEP and SUG for TIME=40 hours and 200 hours, respectively. The following observations can be made from these figures. For TIME=40 hours, OF increases with NEP and SUG until a plateau is reached, bounded by the conditions SUG>=35 g/l, NEP>=35 g/l. In this region OF is a constant maximum equal to 17.4. This plateau occurs when the concentration of metals in solution is sufficient to make K1 and K2, and therefore dP/dt, zero. It should be noted that the optimum value of SUG (35 g/l) represents the lower boundary limit for optimum leaching and acid production. This lower limit is well below, and therefore consistent with, the experimentally determined sugar concentration (130 g/l) for optimum citric acid biosynthesis (Chapter 2).

If a slice is taken through the surface (Fig 3.17) parallel to the z-axis (i.e. at constant NEP), a typical curve of the form in Fig 3.19 is obtained. This curve is for NEP=15 g/l. It can be seen that for SUG<20 g/l OF increases linearly with SUG, and above this value OF becomes constant. The value of SUG at the point where OF becomes constant is stoichiometrically equivalent to NEP (i.e. $NEP=0.601923(0.95SUG_{opt}+INACID)$ given that

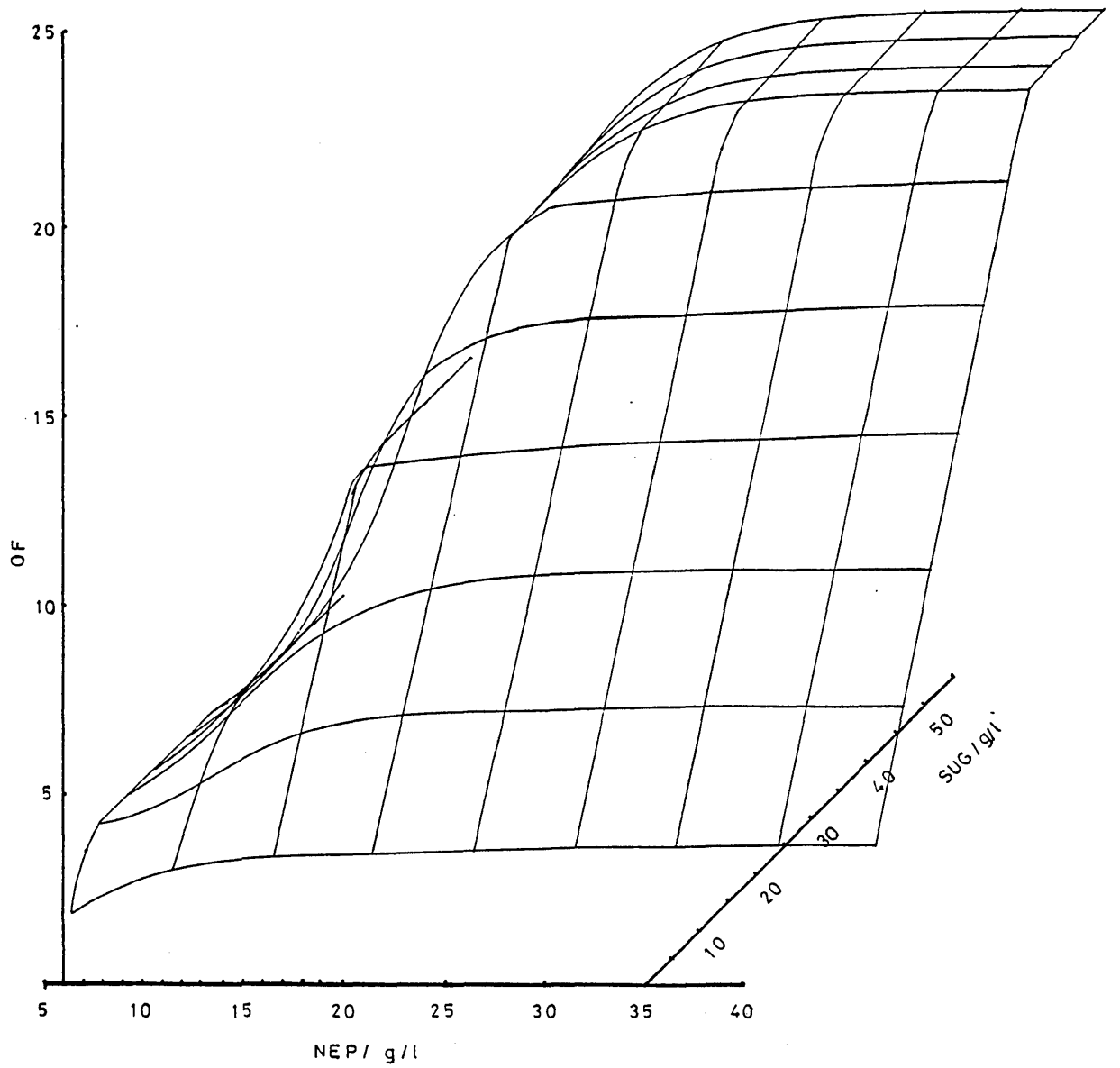


Fig 3.17 Three dimensional representation of the relationship between SUG, NEP and OF for TIME = 40 hrs.

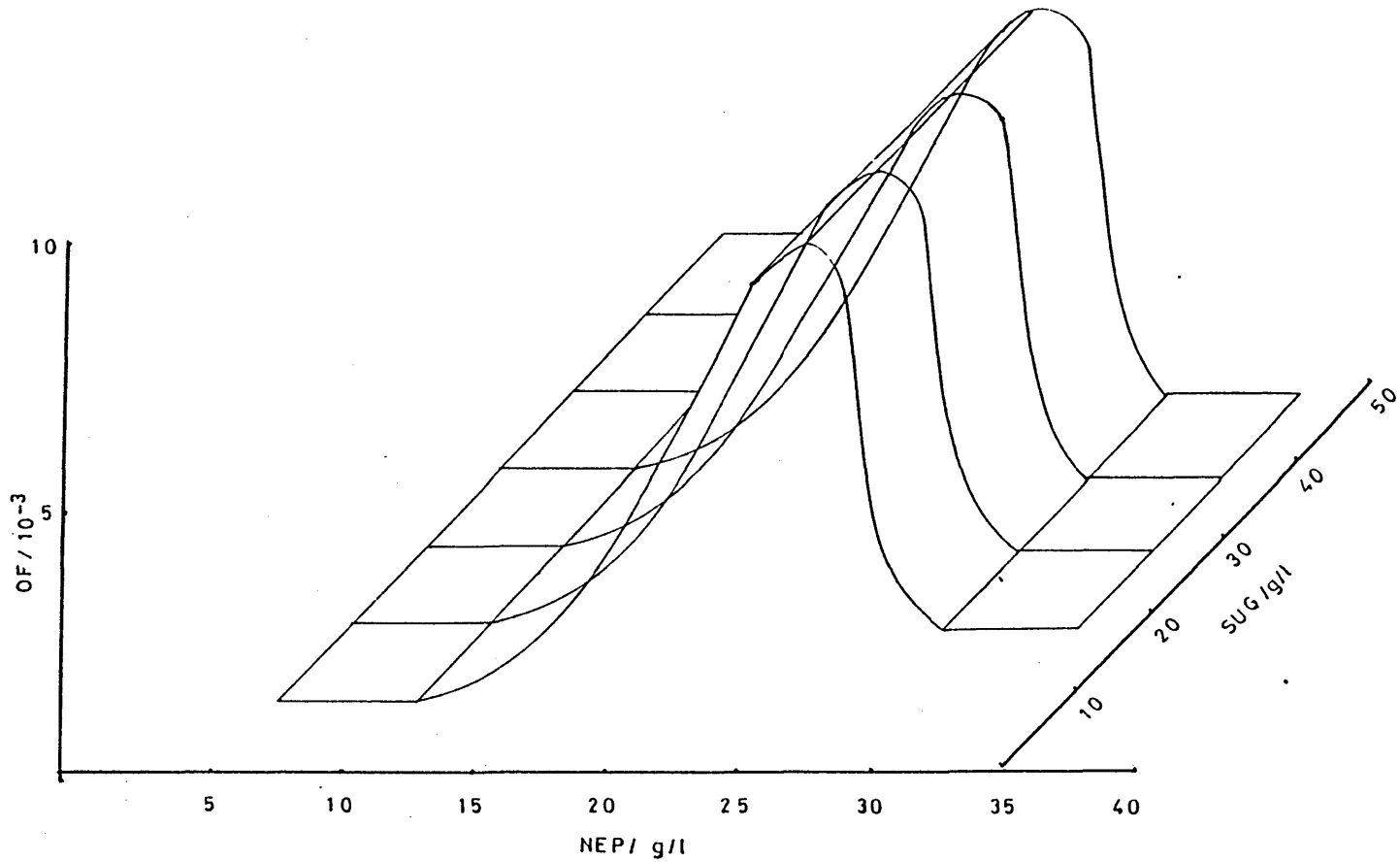


Fig 3.18 Three dimensional representation of the relationships between SUG, NEP and OF for TIME = 200hrs.

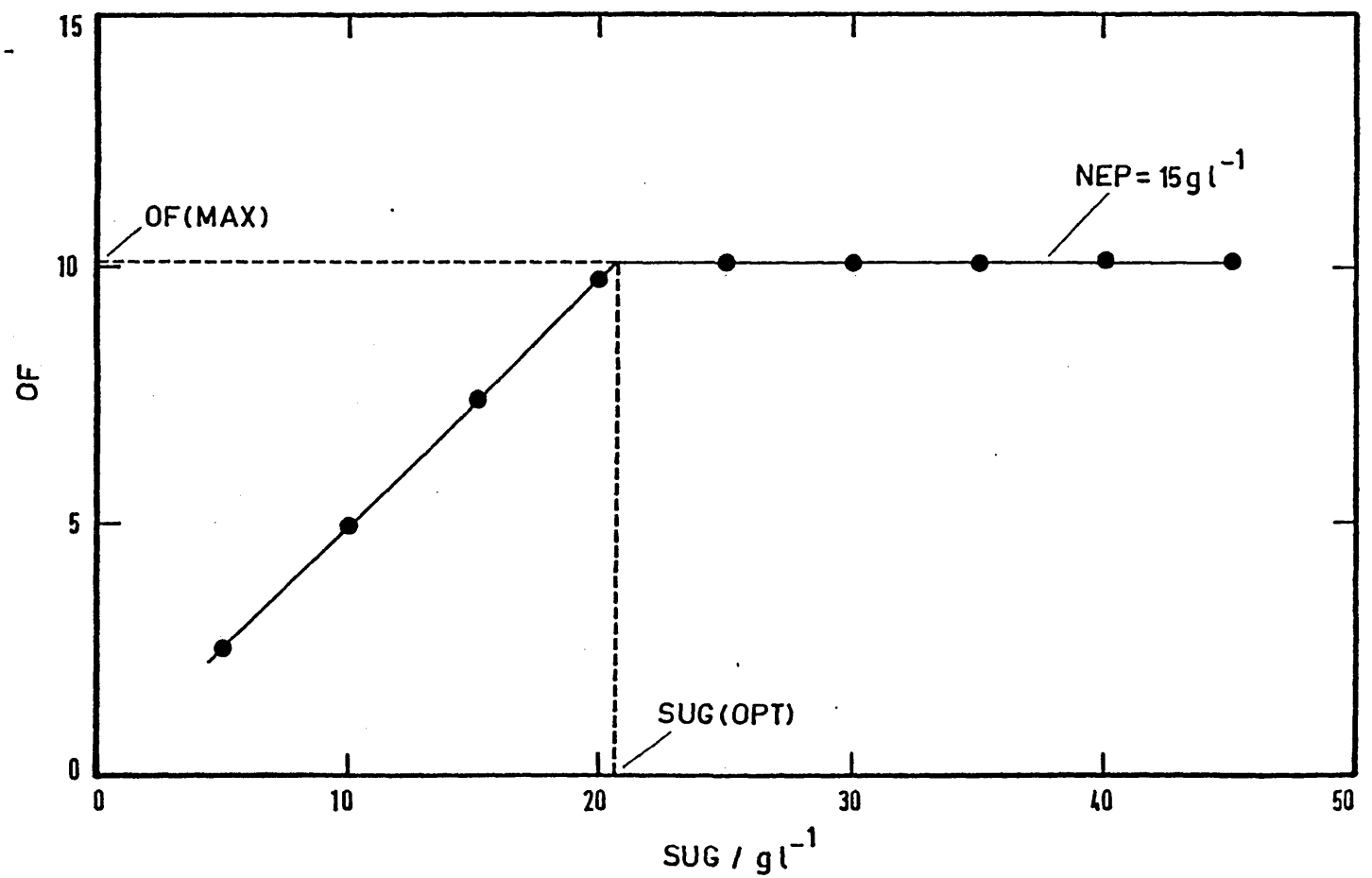


Fig. 3.19: Graph of the optimization factor, OF, versus SUG for NEP = 15 g l^{-1}

INACID=5.3 g/l). It will be noted from step (15) of Section 3.3.1 that OF can be calculated when either acid is exhausted or when R=1. If SUG is below the stoichiometric requirement for NEP (i.e. SUG<20 g/l in Fig 3.19) the fraction reacted, R, cannot equal unity, therefore OF is calculated when acid and sugar are exhausted. Conversely if there is sufficient sugar to meet the stoichiometric requirement (i.e. SUG>20 g/l in Fig 3.19), then OF is calculated when R=1. The transition from SUG<(stoichiometric requirement) to SUG>(stoichiometric requirement) results in the abrupt change in the slope of OF versus SUG at SUG=20 g/l in Fig 3.19.

This is illustrated further in Tables 3.9-3.10 which are of R, P and pH with time for SUG=15 and 25 g/l and NEP=10 g/l, respectively. It will be noted that in Table 3.9, SUG is less than the than the stoichiometric requirement for the complete dissolution of 15 g/l nepheline. Therefore acid (P) is exhausted before R=1 (noted by the increase in pH towards the end of the fermentation). Conversely in Table 3.10, there is an excess of sugar and R reaches unity. It is significant that in both tables the solution is buffered by the nepheline to a pH of approximately 3.1, which is consistent with physical reality.

Turning now to Fig 3.18, and noting that the OF scale is a thousanth of that in Fig 3.17, it can be deduced that OF decreases with TIME. This is not altogether unexpected for the following reasons. From Eqn (3.70) it will be noted that OF is directly proportional to

TABLE 3.9 VALUES OF FRACTION REACTED, R, ACID PRODUCED, P, AND pH WITH TIME FOR SUG=15 g/l, NEP=10 g/l AND TIME=40 h.

Time/ h	R	P/ g/l	pH
40.08	0.19	6.7	2.5
40.16	0.35	9.0	2.9
40.25	0.45	11.3	3.1
40.33	0.53	13.4	3.1
40.41	0.62	15.6	3.1
40.50	0.70	17.7	3.1
40.58	0.75	18.8	3.5
40.66	0.75	18.8	6.5
40.75	0.75	18.8	6.5

TABLE 3.10 VALUES OF FRACTION REACTED, R, ACID PRODUCED, P, AND pH WITH TIME FOR SUG=25 g/l, NEP=10 g/l AND TIME=40 h.

Time/ h	R	P/ g/l	pH
40.08	0.19	6.7	2.5
40.16	0.35	9.0	2.9
40.25	0.45	11.3	3.1
40.33	0.53	13.4	3.1
40.41	0.62	15.6	3.1
40.50	0.70	17.7	3.1
40.58	0.79	19.7	3.1
40.61	0.83	21.7	3.1
40.75	0.93	23.6	2.9
40.83	1.00	25.8	2.8

P_{max}-INACID, and from Eqn (3.45) INACID increases with TIME. However, the initial pH and corresponding acid rate constants, K1 and K2, decrease with increasing INACID, so the difference, P_{max}-INACID, decreases with TIME. It should also be noted that OF can equal zero when P_{max}=INACID (i.e. no acid production). This is clearly shown in Fig 3.18. Up to 10 g/l nepheline, K1 and K2 (and therefore dP/dt), are zero throughout the fermentation. This is due to the high initial acid concentration (INACID) and corresponding low pH. Above 10 g/l nepheline, the rate of mineral leaching is sufficient to buffer INACID such that dP/dt>0 and a small mass of acid is formed. The rate of acid production increases with NEP until a point is reached where the benefit gained by the buffering action is counterbalanced by the toxicity of dissolved metals. Thereafter, further increases in NEP cause OF to decrease.

Tables 3.11-3.12 give values of $d^2 P/dt^2$, $d^2 (R \times NEP)/dt^2$ for TIME=40 hours, SUG=10 and 30 g/l and NEP=5 to 40 g/l, respectively. It can be seen that all values of $d^2 P/dt^2$ and $d^2 (R \times NEP)/dt^2$ are negative, indicating that the rates of acid biosynthesis and nepheline leaching decrease with time. This is to be expected as x2, R, and K2 decrease with time.

Batch and continuous leaching. Batch and continuous processes should differ in the conditions (optimum values of SUG, NEP and TIME) required for optimum leaching and acid production

From the previous discussion the total mass of acid produced (P_{max}) decreases as the concentration of metal in

TABLE 3.11 VALUES OF NEP, d^2P/dt^2, $d^2(NEPxR)/dt^2$, FOR SUG=10 g/l.

NEP/ gl^{-1}	d^2P/dt^2/ $g^2l^{-2}h^{-2}$	$d^2(NEPxR)/dt^2$/ $g^2l^{-2}h^{-2}$
5	-0.0142	-0.0185
10	-0.0196	-0.0373
15	-0.0175	-0.0559
20	-0.0131	-0.0758
25	-0.0111	-0.0960
30	-0.0110	-0.1100
35	-0.0089	-0.1300
40	-0.0086	-0.1400

TABLE 3.12 VALUES OF NEP, d^2p/dt^2, $d^2(NEPxR)/dt^2$, FOR SUG=30 g/l.

NEP/ gl^{-1}	d^2P/dt^2/ $g^2l^{-2}h^{-2}$	$d^2(NEPxR)/dt^2$/ $g^2l^{-2}h^{-2}$
5	-0.0076	-0.0120
10	-0.0048	-0.0220
15	-0.0039	-0.0240
20	-0.0026	-0.0210
25	-0.0023	-0.0280
30	-0.0029	-0.0340
35	-0.0019	-0.0410
40	-0.0019	-0.0430

TABLE 3.13 A COMPARISON OF PREDICTED AND EXPERIMENTAL VALUES OF THE OPTIMIZATION FACTOR, OF, AS A FUNCTION OF NEP FOR TIME=40 h AND IN AN EXCESS OF SUGAR.

NEP/ g/l	Predicted OF	Experimental OF
6	2.9	3.7
10	4.8	5.2
18	12.8	1.1 (contaminated)
30	16.9	8.8

solution increases. Hence the maximum masses of acid and nepheline, are produced and leached respectively, when the metal concentration in the fermenter is a minimum. Thus, in batch processes, no advantage is gained by adding nepheline before the end of the fermentation. By similar reasoning, in continuous sytems it may be requisite to separate the unit operations of fermentation and leaching. It is of interest (for reference in Chapter 4) to consider the leaching kinetics of such a continuous sytem. A detailed account, based on Figs 3.17-3.18 and Tables 3.9-3.0, follows.

For a continuous sytem, as represented in Fig 3.20, the following mass balance will apply:

$$UC_0 = UC_1 - VdC_1/dt \ . \qquad (3.77)$$

In this equation V is the system volume, U is the material flow rate through the system, C_0 is the concentration of unaltered nepheline at the inlet, C_1 is the concentration of unaltered nepheline at the outlet, and dC_1/dt is obtained by differentiating the Crank equation (Eqn 3.2) noting that $R=(C_0-C_1)/C_0$, as follows.

$$1-2((C_0-C_1)/C_0)/3-(1-((C_0-C_1)/C_0))^{2/3} = Kt$$

$$(2/3C_0-2/3C_0(1-((C_0-C_1)/C_0))^{1/3})dC_1/dt = K$$

$$\text{and} \quad dC_1/dt = 3KC_0(1-R)^{1/3}/2(1-(1-R)^{1/3}). \qquad (3.78)$$

This is substituted into Eqn (3.77), noting that $(C_0-C_1)/C_0=R$,

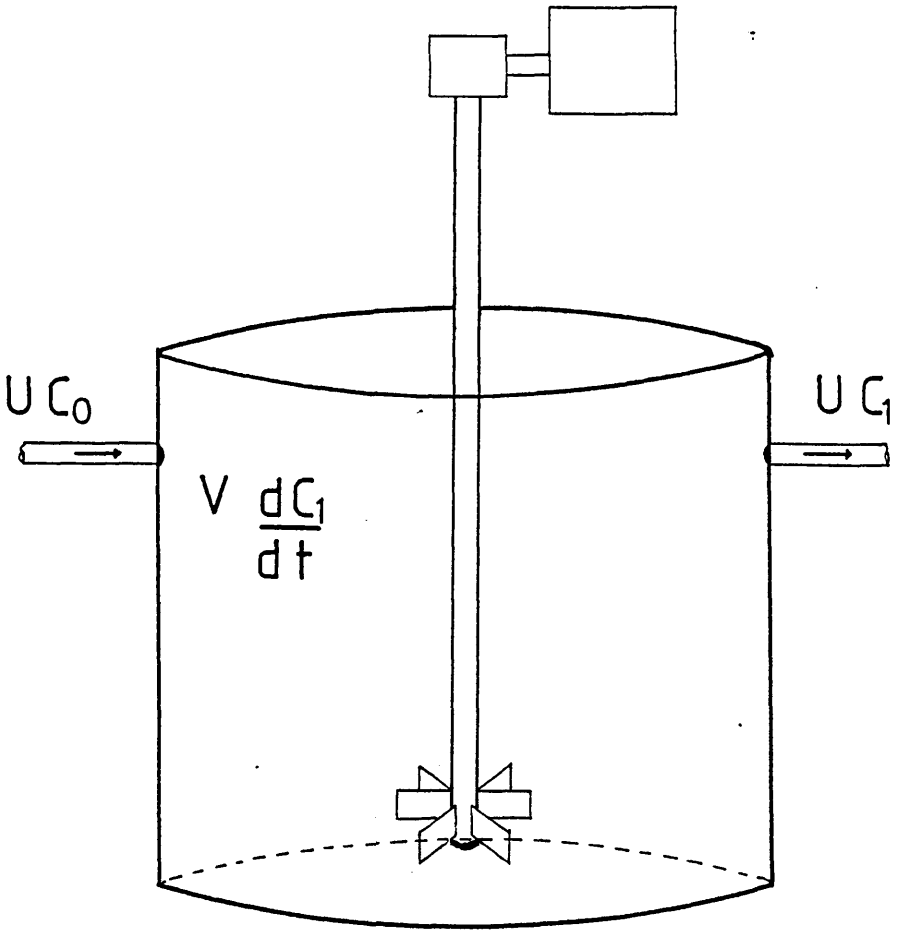


Fig 3.20 Schematic representation of a continuous flow stirred tank reactor (CFSTR).

$$U = 3KV(1-R)^{1/3}/(2R(1-(1-R)^{1/3})). \qquad (3.79)$$

In this equation; when R is zero, U becomes infinity and when R is unity, U becomes zero, which is consistent with practical reality. In order to estimate the material flow rate required, working values of K, R, and V must be estimated. The system volume, V, is known and the leaching rate constant, K, can be found by Eqn (3.6) noting that the pH settles at approximately 3.1± 0.5 during leaching. In continuous systems the Luedking and Piret relationship still applies (as the biochemistry of the system has not changed), but the dimension of time no longer applies and dP/dt, dx2/dt and x2 are constants at the steady state. From Figs 3.17-3.18, over the period of time considered, the average rates of acid production and mineral leaching are a maximum for NEP and SUG = 35 g/l. However, with these conditions dP/dt=0 at or before R=1. So in continuous systems NEP must be substantially lower than 35 g/l to ensure a sufficiently high rate of acid production (i.e. R must be chosen such that $C_0-C_1 << 35$ g/l).

Eqn (3.79) is employed in Chapter 4 to determine the applicability of the model when applied to a continuous system and is not considered further here.

Bases for assumptions used in the model. It will be recalled from Section 3.3.1 that all predictions are based on data of x2 with time for pH 3.3. Therefore it is assumed either that curves of x2 with time do not vary significantly over the envisaged pH range or that the pH remains approximately constant during leaching. It can be

seen from Tables 3.9-3.10 that the pH is constant at approximately 3.1 at the steady state during leaching for 10 g/l. More generally the pH remained between 2.8 and 3.2 for all values of NEP tested. This range was in general agreement with that noted from experimental measurements (Chapters 2-4), thus giving credibility to the use of data for x2 with time for a constant pH of 3.3.

The line represented by Eqn (3.46), of pH as a function of acid molarity, will vary in the presence of cations such as Al^{3+} which complex with the citrate radical, as a result of the release of hydrogen ions from the reaction. However, in the case of nepheline leaching aluminium is the only cation in this category, and , in the range 0-1 g Al^{3+}/l (0-6.15 g total metals/l), the pH increase is assumed to be negligible.

It will be noted that experimental data of K1 and K2 (Tables 3.5-3.6) is only valid for the pH range 2.3-4.3 and metal loading range 0-6.15 g/l, whereas from the earlier discussion of results predictions of K1 and K2 were required for metal loadings up to 35 g/l. Thus, it was necessary to extrapolate the experimental data. The reliability of extrapolated data and the above assumptions were tested by carrying out practical fermentations with a range of nepheline loadings up to the optimum (up to 35 g/l) and comparing experimental data with predicted data from the model. This is considered in detail below.

3.3.3 Fermentations in the presence of nepheline.

Four fermentations, one each containing 6, 10, 18 and

30 g/l nepheline, were carried out under similar conditions (SUG=130 g/l, TIME=40 hours, temperature=26±2°C), in order to determine experimental values of the optimisation factor, OF. These values were compared with those predicted by the computer model for similar conditions of NEP, TIME and SUG. This comparison gave an indication of the accuracy of the model.

Fermentation procedures were as in Section 3.2, but with the following differences. The medium was optimised LM1 (Table 2.14) without supplimentary nutrients (i.e. no extra metal were added). The pH was not controlled and fermentations were open to the atmosphere (i.e. were liable to contamination by airborne microorganisms). Each fermentation was started at the same time and continued under identical conditions for 40 hours. At this time, to one each of the fermentations was added 6.10.18 and 30 g/l nepheline (-30μm), respectively. Liquid samples were taken at frequent intervals (normally 5 minutes) from 40 hours to 40 hours plus 100 minutes, or until R=1. These samples were analysed for the concentrations of acid and sodium by the standard techniques in Section 2.1. The concentration of sodium in solution was use as a measure of R (the fraction of mineral reacted). This element was considered to be the least likely, of those released by nepheline (Al,Na,Si,K), to be adsorbed or absorbed by the fungus.

Values of P and R with time for the four fermentations were used to determine corresponding values of OF. For this purpose a computer program was employed (Appendix). This program operates in an identical manner to that in the main

model for the calculation of OF.

Results and discussion. The results are illustrated in Figs 3.21-3.24 which compare experimental and predicted curves of R and P with time for NEP=6, 10, 18 and 30 g/l respectively, and in Table 3.13 of predicted and experimental values of OF.

From Figs 3.21 and 3.24 it can be seen that the experimental and predicted curves of R and P with time are of the same general form, thus confirming the validity of the model up to NEP=10 g/l. However, from Table 3.13 for NEP=5 and 10 g/l experimental values of OF are greater, by up to 30%, than those predicted by the model. The experimental results for NEP=18 g/l (Fig 3.23-Table 3.13) bear little relationship to the predicted data. In this test it was noted at the time of introduction of nepheline that mycelium was coloured by a orange pigment. After a further three hours, but in the presence of nepheline, the mycelium had changed colour from orange to red. These pigments were absent from the other tests. Based on these observations it was assumed that the discrepency in the results was due to contamination by another organism, possibly Penicillium rubr um (which was present in the laboratory at the time).

For NEP=30 g/l (Fig 3.24), experimental and predicted data are similar up to R=0.35 and P=24 g/l. In the case of the experimental curves, dP/dt decreases to zero after 70-80 minutes (after the introduction of nepheline). At about the same time the acid is exhausted and R becomes constant. On the other hand, predicted curves of R and P

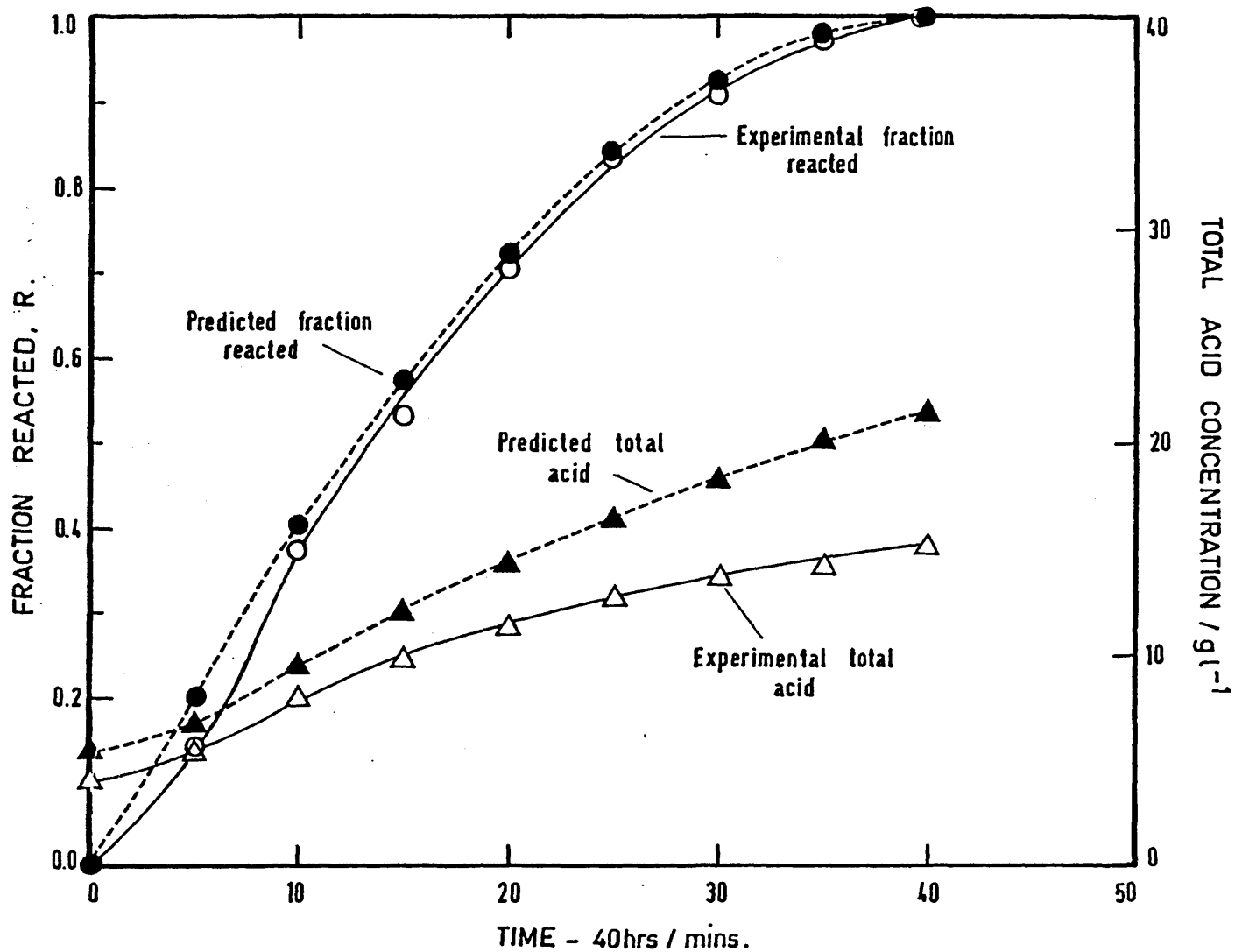


Fig. 3.21: A comparison of predicted and experimental curves of fraction reacted, R, and total acid, P, with time for
= $^{-1}$ = 40hrs in the resence of excess sugar.

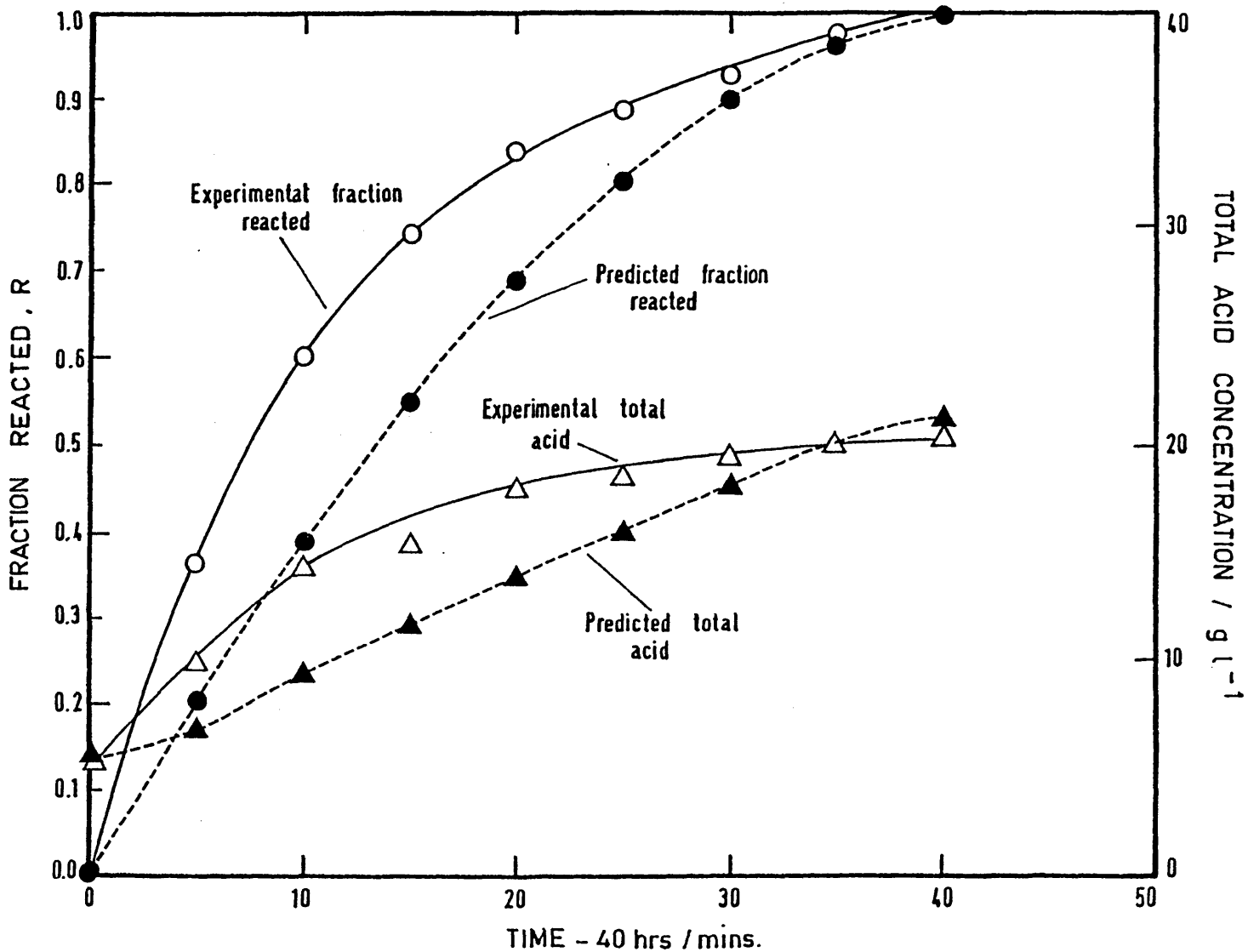


Fig. 3.22: A comparison of predicted and experimental curves of the fraction reacted, R, and total produced, P, with time for NEP = 10 g l^{-1} and TIME = 40 hrs in the presence of excess sugar.

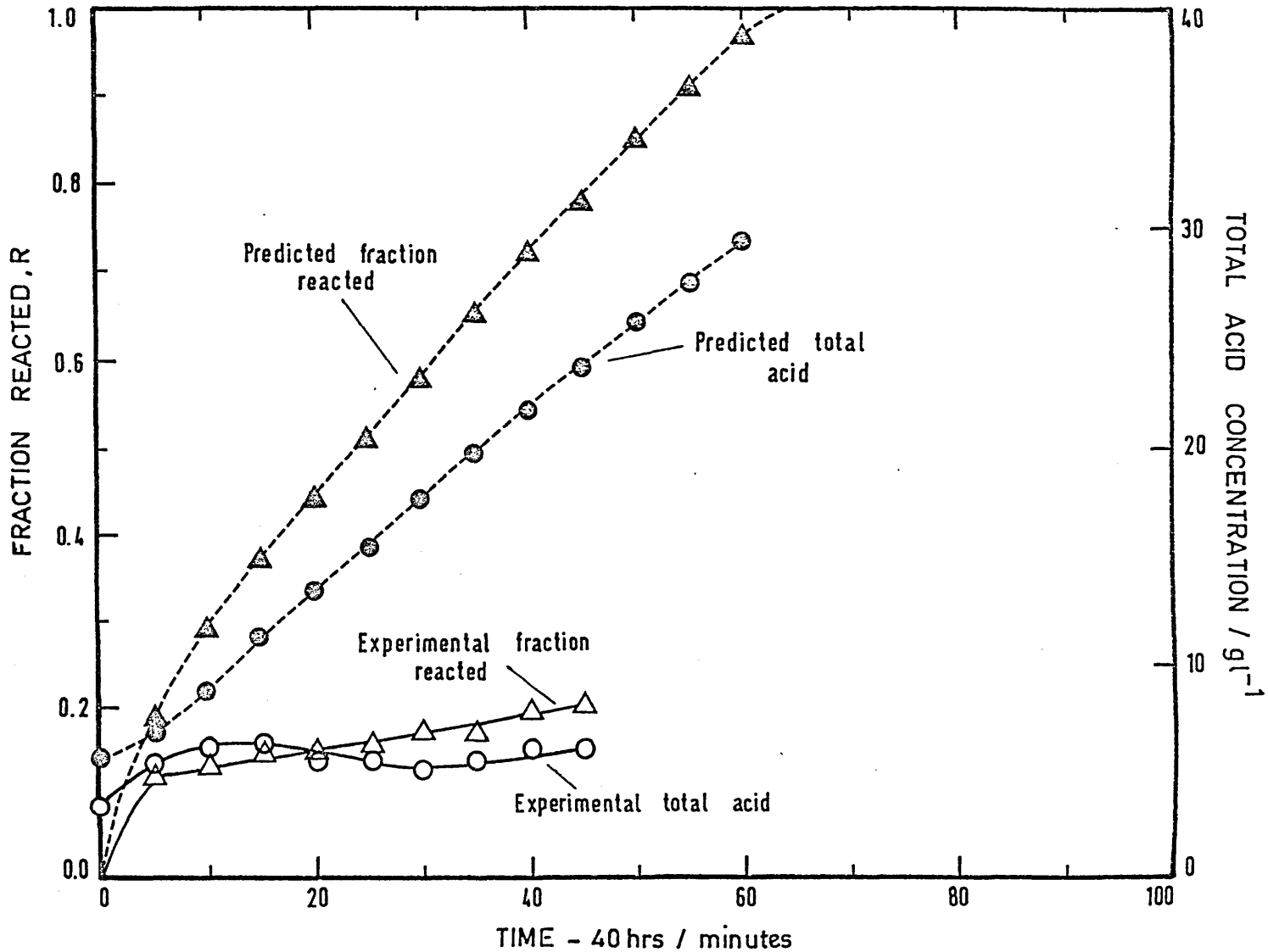


Fig. 3.23: A comparison of predicted and experimental curves of fraction reacted, R, and total acid, P, with time for NEP = 18 $g\,l^{-1}$ and TIME = 40 hr in the presence of excess acid.

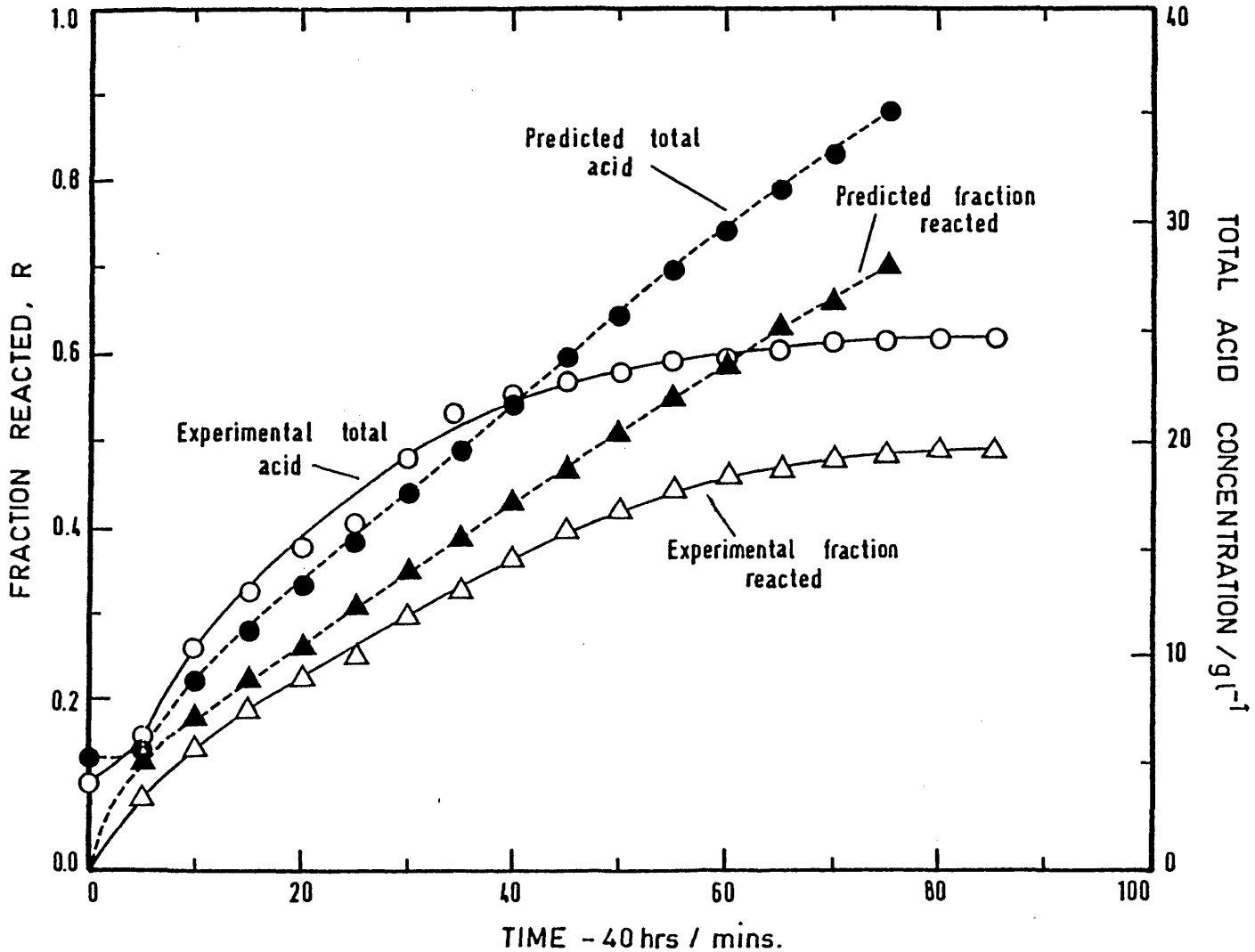


Fig. 3.24: A comparison of predicted and experimental curves of fraction reacted, R, and total acid, P, with time for NEP = 30 g l^{-1} and TIME = 40 hrs in the presence of excess sugar.

with time increase at approximately the same rate until R=0.85. At this point the rate of production of acid is sufficiently low for $R_{m-1} > R_m$ and the computer model stops to calculate OF (see step (15) Section 3.2.1). This results in the abrupt end to the curve in Fig 3.24. Based on these findings, the predictions made by the computer model for metal loadings in excess of 10 g/l become progressively less accurate. This can be explained as follows.

It is evident from the experimental data that the acid rate constants, K1 and K2, become zero when the metals in solution exceeds 15 g/l. However, based on the data in Table 3.6 of K2 as a function of pH and metal loading, and the assumptions derived to allow the extrapolation of this data, it can be shown (by solving Eqns 3.58,3.60 and 3.65 for K2=0 and pH 3.1) that at pH 3.1, K2 is greater than zero (although very small) until the metal loading is of the order of 3000 g/l. This indicates that the equations employed for the extrapolation of data in Tables 3.5-3.6 are inadequate for predictions of K1 and K2 at metal loading in excess of 10 g/l. Further experimental work would be required in order to improve the accuracy of Eqns (3.49-3.66).

It can be concluded that, at best, the model is able to predict values of OF to ±30% up to the limiting metal concentration for acid biosynthesis, which from experimental measurements, is of the order of 14 g/l. For values of NEP> 14 g/l predictions made by the computer model are less accurate due to the lack of experimental data for K1 and K2 in this metal loading range (<14 g/l).

3.4 General Conclusions.

(1) There appears to be little or no advantage in using citric or oxalic acids in place of hydrochloric acid for nepheline leaching. Reaction rates are similar and the ratio of compact to dispersed silica is the same for each acid under the same leaching conditions.

(2) During nepheline leaching by acids there is congruent dissolution of sodium, potassium and aluminium at a rate governed by the hydrogen ion concentration. More generally the rate is controlled by the diffusion of reagents and soluble products through an insoluble layer of silica gel which coats nepheline grains and is formed during the reaction. Under mild conditions of agitation the kinetics of the reaction may be described by the Crank leaching model for diffusion controlled systems.

(3) The inhibitory action of metal and hydrogen ions on acid biosynthesis was adequately described by the Luedking and Piret model. The effect of metals was attributed to the adsorption of charged species into the cell wall.

(4) Total acid yields ranged from 74% (total) - 67% (carbon consumed) for pH 4.3 with no metals to 9.7% (total) - 2.2% (carbon consumed) for pH 2.3 with the maximum metal loading (6.15 g/l). The nitrogen yield factor was apparently unaffected by metals and ranged from 10 to 15. The specific growth rate of growth cells ranged from 0.08 to 0.17 hr^{-1}.

(5) The concentration of oxalic acid decreased with pH

and was always small in comparison to the concentration of citric acid.

(6) The computer model of nepheline leaching by A.niger 31821 could predict the fraction of mineral reacted, pH and acid produced to ±30% for added nepheline concentrations below 14 g/l. Above this value the model broke down due to inadequate data on the variation of the acid rate constants K1 and K2 with metal and hydrogen ion concentrations.

(7) The optimum values of the parameters for average simultaneous acid production and nepheline leaching predicted by the computer model were NEP = 35 g/l, SUG > 35 g/l and TIME = 40 hours. Experimental results indicated that if NEP > 14 g/l acid production ceased.

(8) It was noted that for batch leaching, mineral should be added at the end of the fermentation for optimum acid production and mineral leaching.

CHAPTER 4 SEMI-CONTINUOUS FERMENTATION-LEACHING OF NEPHELINE.

A prerequisite to the successful application of fungi for mineral leaching is the design of suitable equipment for integrated fermentation and leaching. No continuous processes, commercial or experimental, appear to have been reported in the literature. This is hardly surprising bearing in mind that there are few industrial scale fermentations based on filamentous fungi, of any description. Indeed, citric acid is the only major industrial chemical produced solely by fermentation with the aid of filamentous fungi.

Mineral leaching processes based on the oxidation of sulphur compounds by thiobacilli and related bacteria are unsuited to filamentous fungi because of the different morphologies of the two organisms. Whereas bacteria form single cells which are invisible to the naked eye, fungi are clearly visible without the aid of a microscope, and can become attached to submerged or airborne surfaces or form large (0.1-20 mm diameter) mobile pellets and floc particles. One consequence is that solutions containing bacteria sprayed onto a heap or dump readily penetrate and percolate downwards while fungi would soon congregate together and prevent solution flow. Therefore a new approach is required.

The aims of this chapter are to design suitable equipment for the dissolution of nepheline by A.niger; operate this equipment under a range of conditions in order

to assess the practicality and performance of the apparatus; and assess the economics of nepheline bioleaching with particular reference to the production of aluminium or carboxylic acid metal salts.

4.1 Process Appraisal And Equipment Design.

Good preliminary design is a prerequisite to successful process operation. The fungal leaching process was considered in two stages.

(1) A system appraisal based on the advantages and disadvantages of different methods of fermentation, leaching and product recovery.

(2) A design analysis, taking account of the results of (1), of sufficient detail to enable small scale equipment to be built for testwork.

4.1.1. System appraisal.

Fermentation, leaching and product recovery are considered as separate consecutive unit operations connected by a common liquid process stream (Fig 4.1). This is because:

(1) to be commercially viable the system must be continuous, and,

(2) the concentration of metals in the fermenter must be kept to a minimum to ensure sufficient acid is produced for leaching purposes.

The majority of existing commercial processes employing

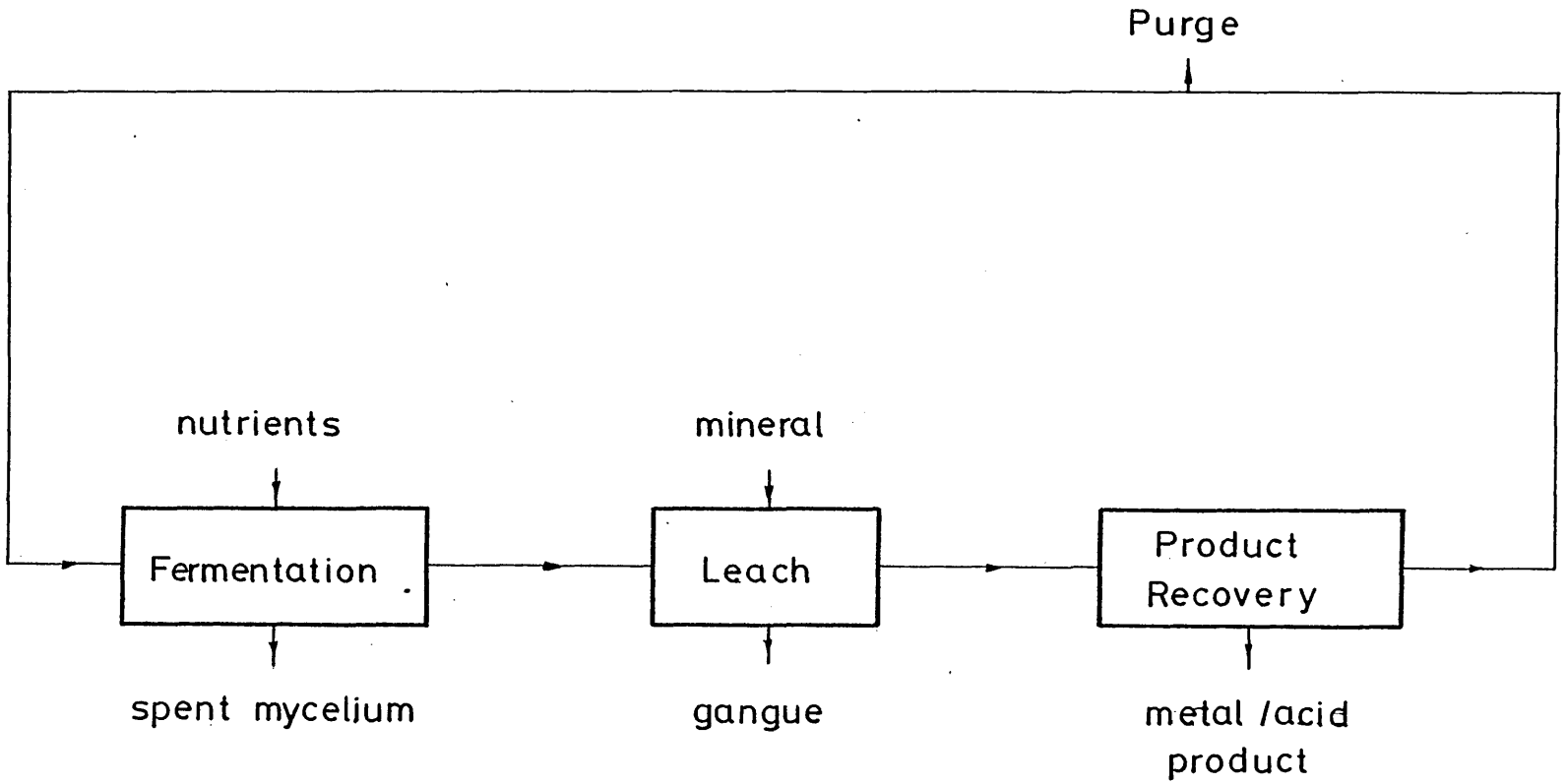


Fig 4.1 Diagram of unit operations required for fungal leaching

microorganisms are operated to produce high specification products suitable for use in the food and pharmaceutical industries. In order to secure high yields of product, and to avoid complex purification procedures, it is necessary to remove competitive microorganisms from the fermenter environment. Equipment having any contact with liquid media are generally sterilised prior to fermentation by means of steam, consequently standard equipment is built to pressure vessel standards and is very expensive (prohibitively so on a scale envisaged for mineral leaching). There is also a reluctance by the fermentation industry to employ continuous fermenters. The reasons for this include the risk of back mutation (thereby causing a loss of efficiency), sterility problems, but mainly the cost of converting current batch to continuous systems. In processes where the profit margin is low (as might be expected for bioleaching processes) and the productivity in continuous culture exceeds that in batch culture (which applies to citric acid fermentations), the advantages of continuous culture outweigh the disadvantages. Thus the process (Fig 4.1) should be oriented to continuous non-sterile operation.

Fermenter. For practicality the fermentation system must conform with the following requirements.

(1) Live fungi must be confined to the fermenter.

(2) The fermenter must be suited to continuous operation and must therefore facilitate the removal of spent mycelium.

Three types of fermenter satisfy (1) above: surface (145), submerged film (266), and fluidized bed (332).

The surface fermenter, discussed in Chapter 1, is a very simple process and probably has the lowest capital cost of any fermenter. However, it can give rise to large numbers of spores, is labour intensive, and is not easy to automate. These disadvantages make it an unlikely candidate in fungal leaching applications. In the submerged film fermenter mycelium is grown as a film on submerged roughened discs in apparatus similar to the rotating disc contactor (331). It has been reported that up to four times more acid can be produced per unit mass of fungus in this type of fermenter as compared to the surface process. However, as far as is known, it is not employed commercially and is difficult to operate continuously over long periods on account of the difficulty of removing spent mycelium from the system.

Although no commercial scale fluidized bed fermenters are known to be operational at the present time, they are most suited to continuous operation. They generally contain high biomass concentrations which are largely independent of throughput and are therefore suitable for high product formation rates. They do not suffer from significant loss of fungus at high liquid throughputs and most systems operate at low viscosities (in comparison with other fermenters) because of the coarse segregation of microbial and fluid phases. The biomass hold up in fluid bed systems can be controlled by using solid support particles with fungus growing on the outside of the support as a film

(332). The film thickness is readily controlled by abrasion which results from the relative movement of particles. In addition, fluidized bed systems are well mixed and therefore have good heat and mass transfer characteristics. Their main disadvantage (as far as commercial citric acid fermentations are concerned) is that they are difficult, but not impossible, to operate under sterile conditions.

The fluidized bed fermenter satisfies both of the conditions and is also suited to application in the process illustrated in Fig 4.1.

Leaching equipment. Citric acid and other 'sugar' acids and their salts (with the exception of oxalic acid) are rapidly degraded by wild populations of microorganisms (Table 4.1). Under non-sterile conditions, therefore, the time between acid production and the recovery of products should be minimised and less than 24 hours. It will be noted from Chapters 2 and 3 that, under constant conditions of temperature and pH, the rate of nepheline leaching is governed by the size of mineral grains, which should be as small as possible, and the degree of agitation in the system, which should be maximized.

These conditions (acid exposure time, mineral grain size and the agitation rate) limit the mineral handling techniques suitable for fungal leaching according to Fig 4.1. Whereas coarse solids can be leached by causing the solvent to pass through a bed of the ore, fine solids offer too high a resistance to flow. Therefore dump and similar large scale percolation methods are unsuitable. Particles

TABLE 4.1 TYPICAL TIMES FOR THE DEGRADATION OF VARIOUS METAL CITRATES BY NATURAL POPULATIONS OF MICROORGANISMS.

Citrate compound	Time/ hrs
citric acid	99% in <2
sodium citrate	99% in <2
aluminium citrate	90% in <8
ferric citrate	90% in <8
cadmium citrate	99% in <24
copper citrate	90% in <24

of less than 50 μm can be maintained in suspension with only a small amount of agitation and as the total surface area is large, an adequate extraction can be effected in a reasonable time. Agitation can be achieved either by the use of a mechanical stirrer or by compressed air. For testwork purposes a combination mechanical/air agitated tank was employed.

Product recovery. There are no reports concerning the recovery of aluminium or aluminium citrate from fermentation media. Two potential methods based on ion exchange or solvent extraction are considered below.

In the published ion exchange method strong base anion exchange resin (Dowex 2-X8 or Amberlite IRA 400) in its citrate form was employed. Aluminium and iron are selectively adsorbed from solutions containing calcium, silicon, manganese, magnesium, sodium and potassium (335). Once the resin has been loaded (by passing the solution containing aluminium through a column packed with the resin) the aluminium is stripped using concentrated hydrochloric acid. Iron, if present in the initial solution, remains on the resin as a chloride complex during the de-adsorption of aluminium and can be stripped in a similar manner by dilute hydrochloric acid. Aluminium could be recovered from the acid solution by the technique proposed for commercial application by the United States Bureau of Mines (336). Provided the leachate was sufficiently concentrated in citric acid and the pH>3, the metal-citrate complexes could be adsorbed directly onto Dowex 2-X8 in its chloride form (Section 4.1.2), thus

avoiding a pretreatment step to convert the resin to its citrate form. Using this method it would be expensive to recover citric acid (which could only be recovered by crystallization of the liquor remaining after the recovery of aluminium).

With the exception of uranium ion-exchange methods are only infrequently used for the large scale recovery of metals from leach solutions. This is partly due to the fact that no truly continuous countercurrent ion-exchange equipment is presently in successful commercial operation, and that more favourable distribution coefficients (mass ratio of extracted metal in the extract to raffinate phases) are obtained with solvent extraction systems. Semi-continuous equipment based on intermittent countercurrent flow are used in the uranium industry but suffer from a number of disadvantages.

(1) The mechanical complexity of the equipment.

(2) The cost of the resin.

(3) The loss of resin by attrition.

However, ion exchange systems offer a major advantage over solvent extraction systems in that they do not toxify/deoxygenate the raffinate which is recycled back to the fermenter (see below).

A number of patents have been issued on behalf of Miles Laboratories (337) for the recovery of citric acid from conventional A.niger fermentation liquors by solvent extraction (338). In this equipment the acid is extracted using conventional countercurrent mixer-settler equipment at room temperature. Citric acid is stripped from the

solvent using similar equipment to that employed for the extraction, with water at 70-80°C. Two solvents have been tested, tridodecylamine and trilaurylamine, with a diluent based on n-octanol and synthetic C_{10}-C_{12} isoparaffinic petroleum hydrocarbons. This process is similar to that reported by Pyatnitskii and Kharchenko (339) for the extraction of anionic metal-citrate complexes with tributylamine and it is possible that the 'Miles' process could be adapted for the simultaneous recovery of aluminium and citric acid provided suitable extractions were obtained in the pH range $2.0 < pH < 3.5$.

A study on the effect of solvent extraction reagents on thiobacilli (340) indicated that dissolved organic solvents decreased the surface tension and oxygen saturation concentration of leach solutions. This caused a decrease in the rate of pyrite oxidation by the bacteria. The following order of inhibition was established for the solvents and modifiers studied: aliquat 336 > nonyl phenol > kerosene 140 > alamine 310 > adogen 381 > di(2-ethylhexyl)phosphoric acid > adogen 365 > tri-n-butyl phosphate > isodecanol > alamine 308 > alamine 336 > alamine 304. bearing in mind the similar oxygen requirement of filamentous fungi and, assuming that the inhibition is related to deoxygenation, this order of inhibition might be expected to apply equally to submerged fermentations.

Considerable preliminary testwork would be required to establish beyond reasonable doubt the viability of the solvent extraction process for the recovery of aluminium citrate from fermentation liquors. On the other hand a

recovery system based on ion exchange could be built and operated on a laboratory scale from current knowledge of the process. Therefore the equipment employed for testwork purposes was based on an ion exchange system.

4.1.2 Design analysis.

Following on from the discussion above a suitable system has the following basic components.

(1) Fluidised bed fermenter.

(2) Recirculation pump.

(3) Continuous agitated tank reactor.

(4) Ion exchange apparatus.

In this equipment units (1) and (3) have been integrated for simplicity and versatility. Each unit is considered below separately with reference to Figs 4.2-4.3, dealing with equipment actually constructed.

Fluidised bed fermenter. The nature of the particles making up the fluidised bed are of paramount importance to the operation of the fermenter. Beads of iron, glass, polyester, wire balls iron or aluminium and compressed aluminium foil have all been tested as supports for fungal growth in fluidised bed fermenters (341). Solid spheres are generally considered to be too dense for the majority of applications. Formers made of compressed wire or foil are less dense and have rougher surfaces which allow rapid attachment of fungus, but metal formers corrode during acid biosynthesis and therefore have a limited life, it was also noted from preliminary tests with the apparatus in Fig 4.3 that foil pellets had a tendency to float due to

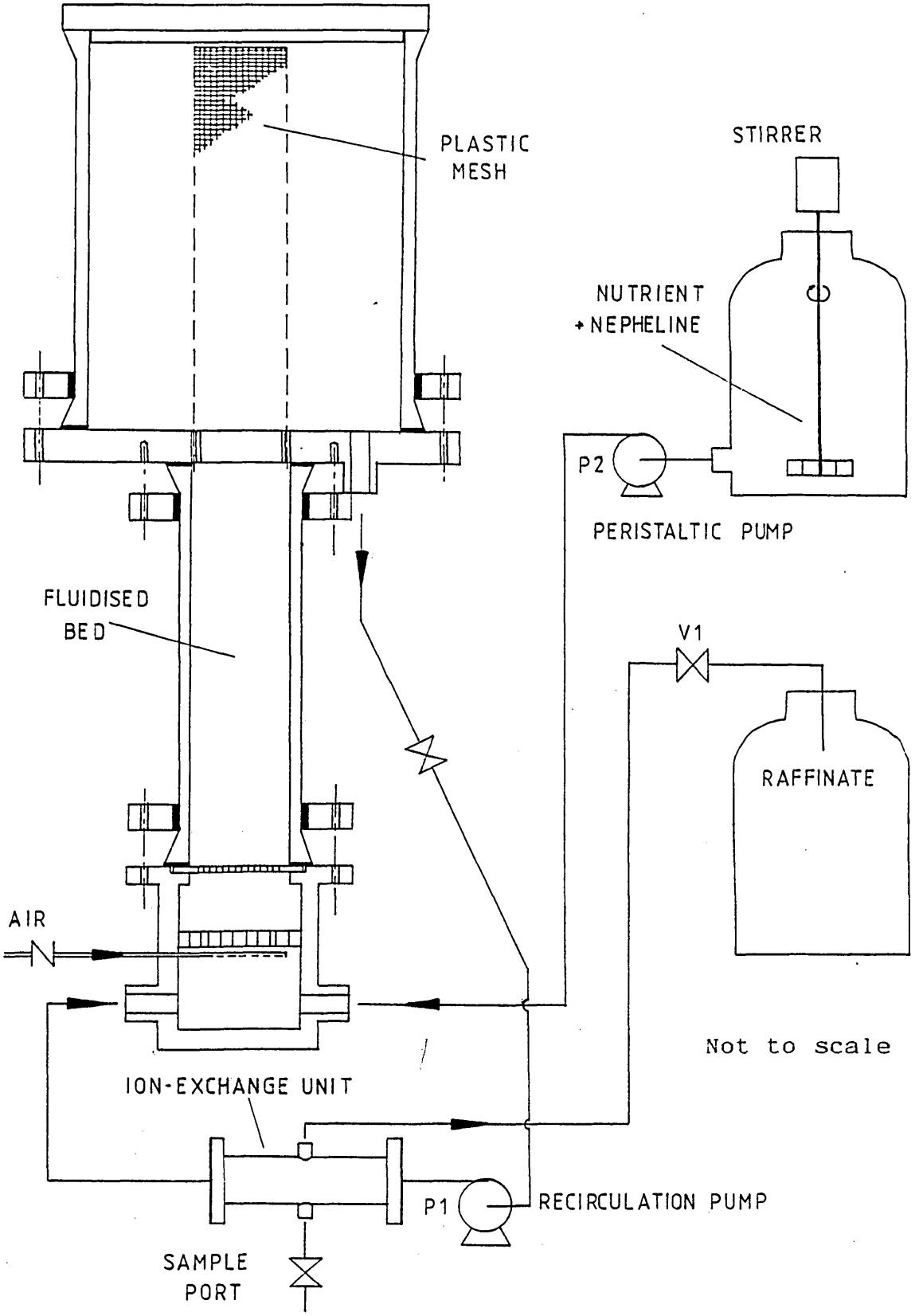


Fig 4.2 Apparatus used for testwork.

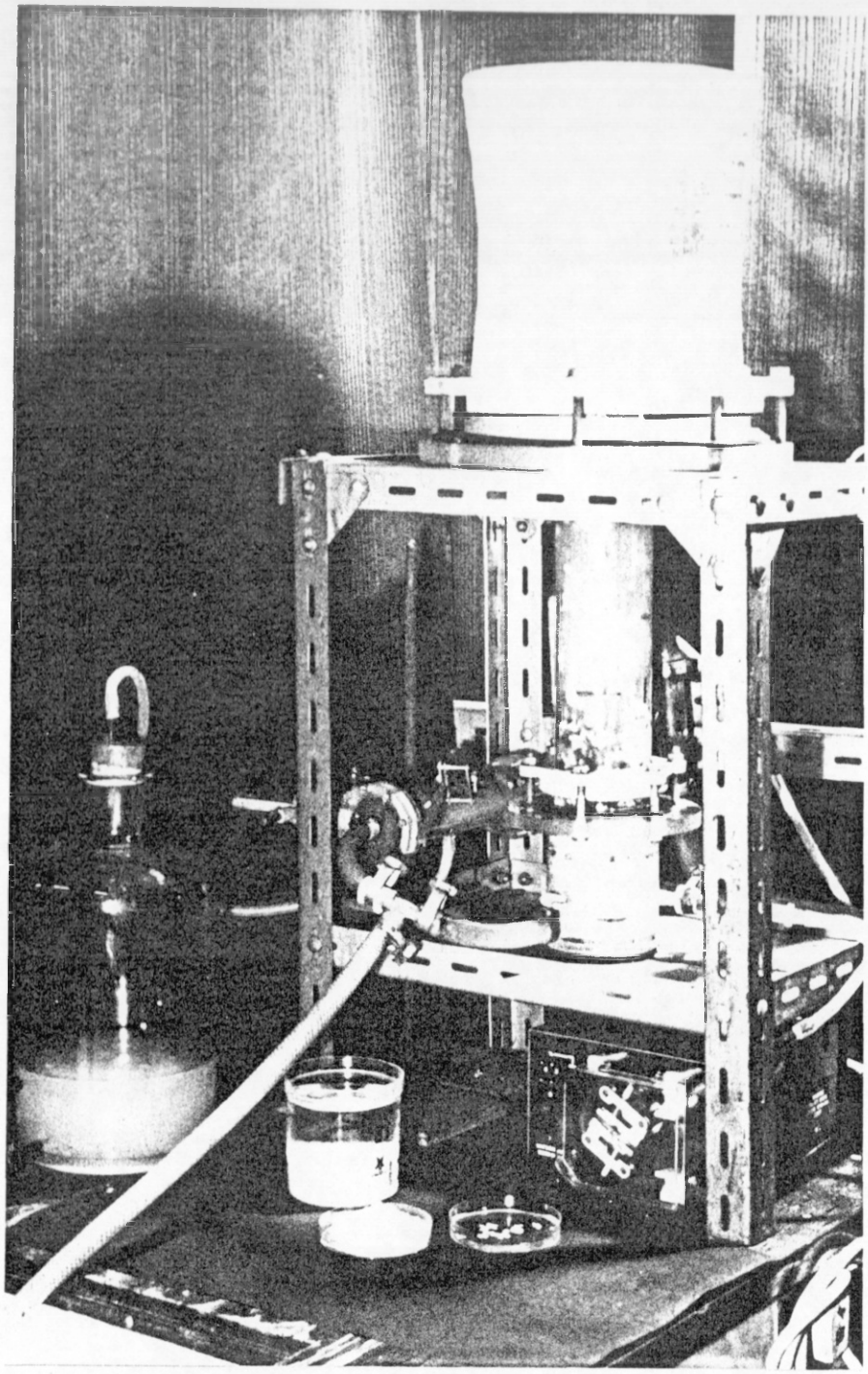


Fig 4.3 Photograph of apparatus in Fig 4.2.

trapped air from the gas sparger. No alternative former materials, with the required properties (inertness, 1<density<3 kg/m^3), have been described. Solid fungus pellets (without a former) satisfy these properties but are not easily abraded during fluidisation. Therefore the biomass hold up could not be controlled in the manner previously described. In order to operate a continuous fermenter based on solid fungus pellets large older pellets would have to be routinely removed from the fluidised bed and replaced with smaller seed pellets. This is a difficult, but not impossible, practical operation on a large scale and in the case of nepheline leaching would serve to remove a major proportion of colloidal silica (which is adsorbed onto mycelium) from the system.

The equipment (Figs 4.2-4.3) is based on a fluidised bed of solid fungus pellets, but excludes equipment for the continuous replacement of old with seed pellets. This operation was carried out by hand in the laboratory process.

The pellets are confined to the fluidised bed chamber by a distribution plate at the bottom of the bed and a tube of plastic mesh, placed at the top of the bed. The distribution plate had 1 mm holes drilled in it in two segments opposite one another as shown in Fig 4.4. This plate was supported on another plate with larger holes (1 cm diameter). Gas was sparged to the system below these plates by a plastic tube (2 mm internal diameter), pierced along its length with pin sized holes. Bubbles produced by this sparger were large (>5 mm) but decreased in size

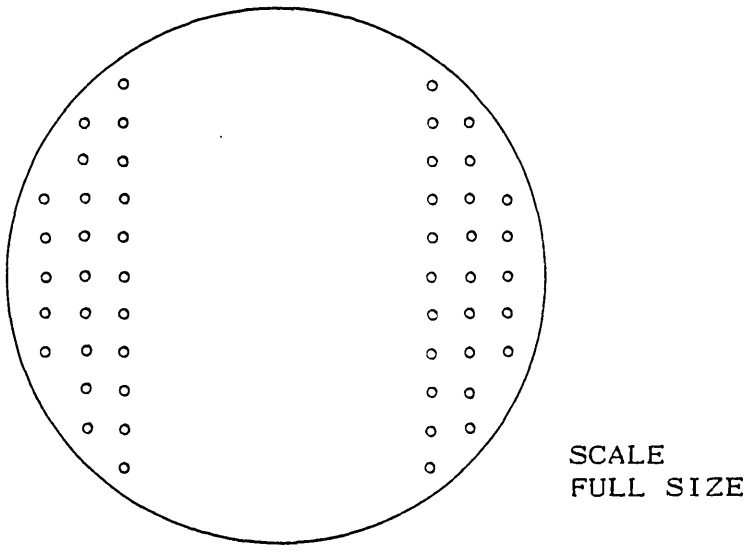


Fig 4.4 Plan of distribution plate.

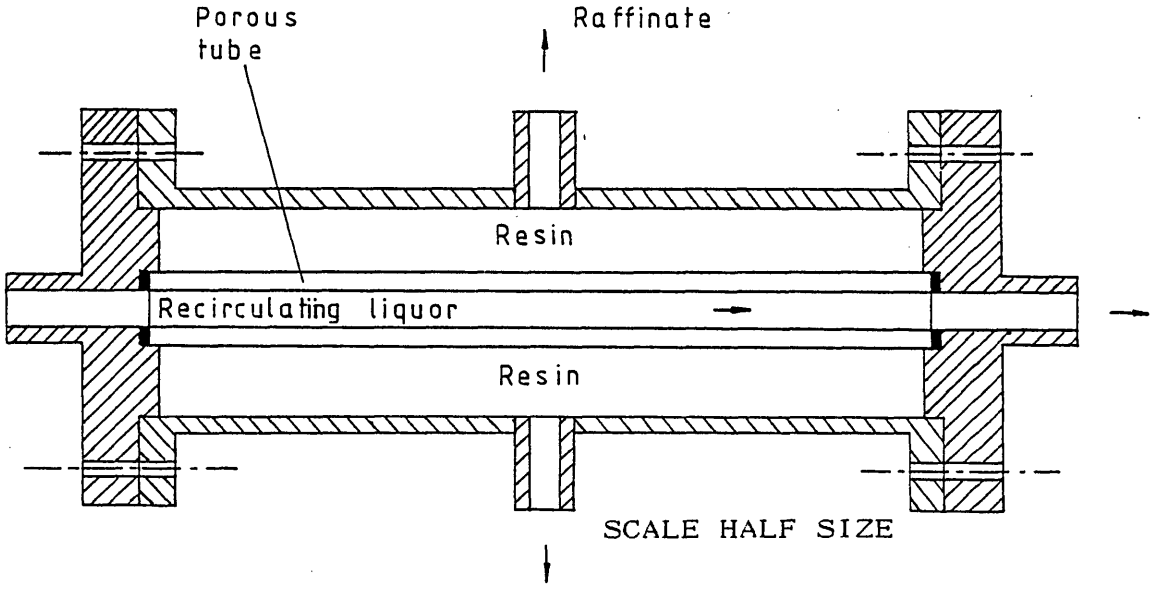


Fig 4.5 Cross section of ion-exchange apparatus.

(< 1 mm) after being forced through the distribution plate with the liquid flowing around the system. Immediately above the distribution plate was a region of turbulence, caused by impinging liquid flows from each segment of the distributor plate. Bubbles, upon entering this region, were seen to be violently agitated, thus promoting the transfer of gas into solution.

The bed volume (~ 4 l) was designed to hold a maximum of 2 Kg of loosely packed fungus pellets, although less than this (0.5-1 Kg) was used for testwork. Pellets can grow >3 cm. In this form the proportion of the total mass which is useful for acid biosynthesis is related to the depth of penetration of nutrients into pellets. In general this is a function of the compactness of the pellets and the degree of turbulence in surrounding liquid. A narrow fluidised bed (aspect ratio 4:1) was employed to give a high liquid velocity through the bed. This ensured that the pellets were sufficently agitated for efficient mass transfer of nutrients to the fungus.

Based on a fluidised bed containing 1 Kg of fungus pellets 2-5 mm in diameter and a typical acid production rate of 0.06-0.1 g citric acid/ g mycelium/ hour (342), in an excess of sugar, the acid production rate might be expected to be 60-100 g citric acid/ hour.

Recirculation pump. The choice of pump was based on the following specification.

(1) All materials having any contact with the fermentation medium should be of chemically resistant plastic (Nylon, Teflon, or Polyethylene), or chromium

stainless steel (suitable for acid environments).

(2) The pump should be able to deliver 20 l water/min (preliminary work showed that this flow was required to fluidise 1 kg of aluminium foil pellets in a 3 inch diameter fluidisation column with the pump elevated in the the center of the column).

(3) The outlet should have an inside diameter no less than 1.5 cm, in order to give a flow velocity great enough to prevent build up of mycelium deposits.

Two pumps were tested - a Micropump Series 101-955 magnetically coupled to a compressed air motor; and a electrically driven washing machine pump. Both were reliable over long operating periods. However, the cooling effect due to the expansion of air through the compressed air motor was sufficient to reduce the temperature of the fermentation media. Therefore the Micropump pump was disgarded in favour of the electrically-driven pump.

Leach (buffer) tank. The top half of the fluidised bed was placed axially inside a larger tank (Fig 4.2). This tank served to increase the liquid capacity of the system (such that the ratio of liquid to fungus was of the order of 5 l fermentation media / 1 Kg of fungus), and under certain conditions to hold mineral to be leached (see below).

Two methods of leaching were considered. For nepheline sized at $>$ 200 μm the mineral was suspended in a porous container (plastic mesh bag) inside the leach tank. Under typical operating conditions (Section 4.1.3) there was sufficient flow of liquid around the leach tank to agitate

the mineral. In tests with nepheline sized below 200 μm the mineral was added to the fermenter continuously in suspension with fresh nutrient medium. Preliminary calculations (Appendix) indicated that if nepheline was to be added from the holding tank T1 (Fig 4.2) it would need to be sized below 10 μm to be maintained in suspension during passage down the pipeline (of internal diameter 0.5 cm), for the minimum flowrate, from T1. Therefore nepheline used for these tests was ground by agate mortar and sized by sedimentation before use.

Ion exchange apparatus. Effluent was stripped of aluminium citrate using Dowex 2-X8 resin in its chloride form (prepared by immersing the fresh resin in an excess of 1 M hydrochloric acid for several hours). The equipment employed is illustrated in Fig 4.5. During operation liquor recirculates around the system as indicated by the arrows in Fig 4.2. Liquid from the main stream, which is under pressure, flows through the porous polythene tube and resin bed into the holding tank T2 at a rate dependent on the setting of the valve V1. Fresh nutrient is pumped into the bottom of the fluidisation bed at the same rate from tank T1, by a Watson Marlow 502 peristaltic pump. Thus, spent liquor is continuously stripped of aluminium citrate and relenished with fresh nutrient. The resin chamber has a volume of approximately 150 cm^3 which is sufficient for the recovery of 200 Meq of aluminium citrate assuming an ionic form $Al(CIT)_2^{3-}$ (the ionic form of aluminium citrate at pH 3.1 is not known. Below pH 5 AlCIT is predominant but above pH 5 $Al(CIT)_2^{3-}$ is the predominant form).

General specification of fermentation/leaching equipment. The fermentation equipment was built of standard Corning 'QVF' borosilicate glass and non-standard Perspex fittings, the latter being manufactured in the MRE Department's workshop. All pipework was of glass fibre reinforced polyethylene or silicone rubber tube. Air from a laboratory ring main was filtered through a packed bed of glass fibre before use. The equipment specification follows.

Fluidised bed	- dimensions	75 mm x 600 mm
	- capacity	≏2.5 l
	- aspect ratio	1:4
	- material	borosilicate glass
Leach tank	- dimensions	225 mm x 300 mm
	- capacity	≏12 l
	- aspect ratio	1:1.25
	- material	borosilicate glass
Ion exchange chamber	- dimensions	55 mm x 200 mm
	- capacity	0.15 l
	- material	perspex
	- resin	Dowex 2-X8
	- porous tube	'fritware' porous polythene, pore size 60 μm.
Recirculation pump	- rating	0.06 Kw
	- capacity	< 30 l/min
Pipework	- bore	> 1 cm
Valves	- material	polyvinyl acetate
	- bore	9.5 mm

	- manufacturer	Fisher
Air rate	-	0.5-3.0 l/min

4.2 Experimental Testwork.

The main aims of the testwork were:

(1) to determine characteristic curves (plots of conversion efficiency, C_1/C_0 , and the RHS of Eqn (3.79), versus dilution rate, F/V), for the system, and thereby comment on the performance of the equipment, and

(2) assess the significance of hyphal activity on silica gel surrounding nepheline grains.

Before considering the typical operating procedure an account is given of the method used to produce fungus pellets for the fermenter.

Preparation of fungus seed pellets. Many workers have described the conditions necessary for pellet growth. A detailed review of standard methods was given by Whitaker and Long (343). Unfortunately equipment was not available to produce the required 0.5-1.0 l pellets in a single batch by the standard technique, so an alternative method was developed. In this method fungus spores were spread over liquid medium LM1 (with 3% methanol to stop sporulation during growth) contained in shallow polythene trays. The total liquid surface area per tray was of the order of 400 cm^2. The trays were incubated at 37° C and left until the fungus had grown to cover the liquid surface. At this point the fungus was carefully removed and cut into 5 mm discs with a cork borer. These discs were gently compressed in DDW to expell air, washed in dilute glucose solution and then used to seed the fermenter. After several days growth the majority could not be distinguished from the pellets produced by the standard method.

4.2.1 Typical operating procedure.

Continuous experiments were carried out as follows. The resin chamber was filled with activated resin in its chloride form (prepared as in Section 4.1.2), taking account of 15% swelling which results from the ion exchange. The fluidisation column was filled to a quarter capacity with LM1. Fungus seed pellets (typically the contents of 1-2 trays) were added and the system was filled to the required capacity (normally 5 l). The gas was turned on and the flow rate adjusted to 0.5 l/min. The recirculation pump was started and adjusted to give a flow of approximately 5 l/min.

After 2-4 days the peristaltic pump, P2, was switched on, the valve V1 (Fig 4.2) opened, and the flows of raffinate and nutrient (LM1 + 8 g/l nepheline) balanced according to the required dilution rate (F/V). At the start this was typically 0.006 hr^{-1}. Samples of liquid (25 ml) were taken from the leach and raffinate tanks (via sample ports) and the pH was measured by placing a pH probe in the leach tank, on a daily basis. These samples were analysed as in Section 2.1 for sodium and aluminium, respectively. The fermentation was continued until the concentration of sodium in the system (which was a measure of R) was approximately constant. At this point the dilution rate was increased to 0.01 hr^{-1} and the fermentation continued (with sampling as above) until a new steady state was achieved (normally after 2-3 days). In this way the dilution rate was increased to 0.02 hr^{-1}, 0.03 hr^{-1}, and finally 0.05 hr^{-1}, each time holding the dilution rate constant

until the concentration of sodium in the system was approximately constant. This procedure was repeated, in a separate fermentation, for an inlet nepheline concentration of 14 g/l.

One additional test was carried out with 500 g nepheline sized between 0.5-3.0 cm. In this test the mineral was placed in a plastic mesh bag suspended by a nylon cord close to the fluidisation column (no pulverised nepheline was added in this test). The fermentation was continued with a dilution rate of 0.006 hr^{-1} for three weeks. At the end of this period samples of mineral were carefully removed and prepared for examination by electron microscopy (as in Section 2.1).

A certain amount of sediment (mainly mica and dead fungi) was formed during the period of leaching. This was removed from the system after each test by flushing the system with high pressure water.

4.2.2. Results and discussion.

Figure 4.6 shows two curves of conversion efficiency, C_1/C_0, versus dilution rate, F/V, for inlet nepheline concentrations of 8 and 14 g/l.

For an inlet concentration of 14 g/l, which is close to the optimum for acid biosynthesis as described in Chapter 3, acid production ceased after the first day. No nepheline was leached, at the steady state, for any dilution rate tested. It appears that a sufficiently toxic environment was created during the early stages of leaching to permanently deactivate the fungus.

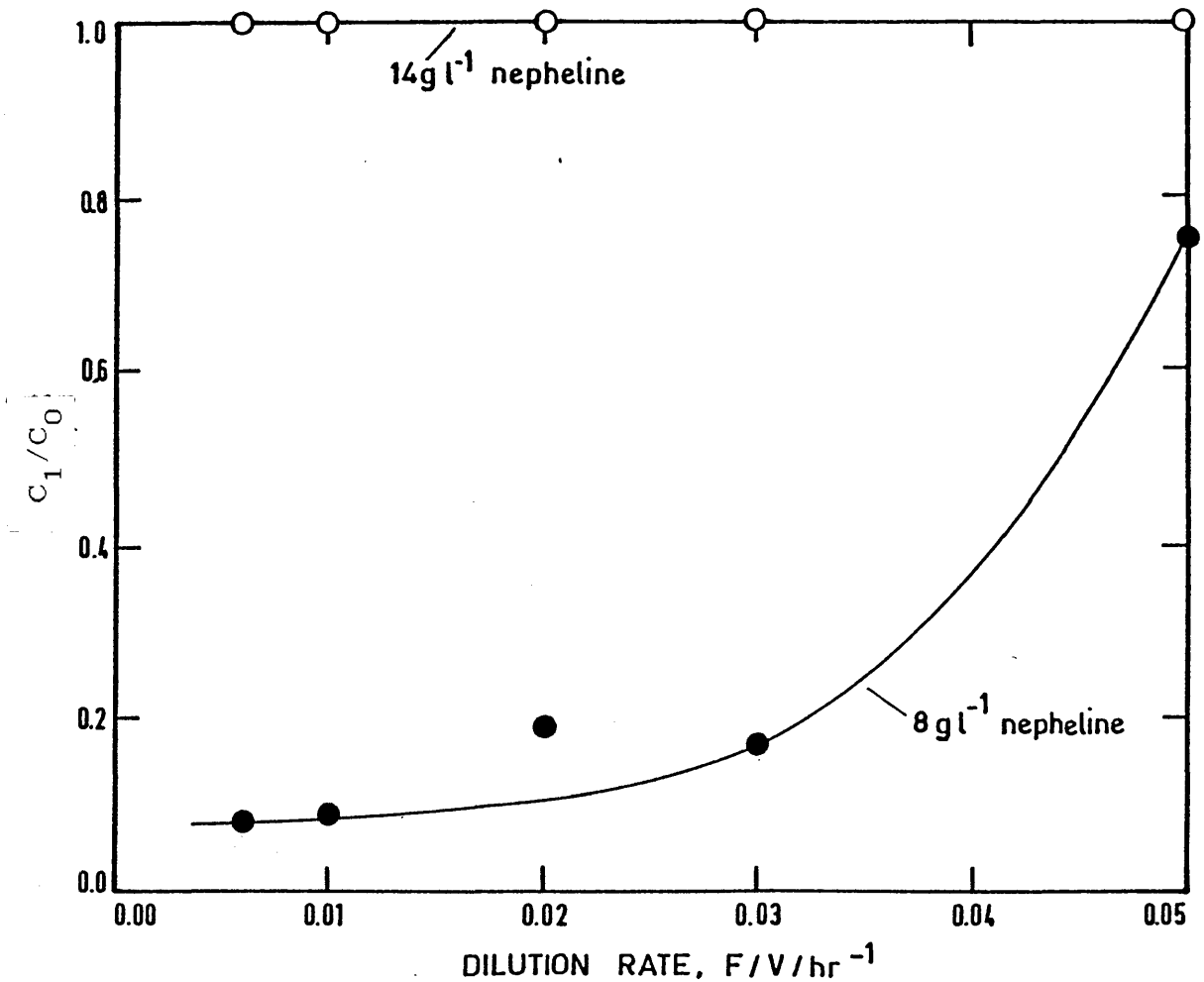


Fig. 4.6: Curves of C_1/C_0 (outlet divided by inlet nepheline concentration) versus dilution rate for inlet nepheline concentrations of 8 and 14 g l^{-1}.

The corresponding data for an inlet concentration of 8 g/l gives a smooth curve. At low dilution rates (i.e., high residence times) approximately 90% of the nepheline was leached. This decreased to approximately 25% for a dilution rate of 0.05 hr^{-1}. This is expected for the following reasons. As the material throughput, or dilution rate, increases the contact time between reactants (mycelium and sucrose, nepheline and acid), decrease. The result is a lower conversion of sucrose to acid, and a corresponding decrease in the fraction of nepheline leached.

Based on stoichiometry and on Fig 4.6, a maximum of 0.8 g acid/hour was consumed during nepheline leaching. The accompanying steady state value of pH (approximately pH 3.0), indicated that acid was mostly consumed. However, analyses of the ion exchange eluate and raffinate in the holding tank, at the end of the fermentation, showed that approximately 11 g acid/hour was produced (which corresponds to a sugar to acid conversion efficiency of 32%). From these observations it is evident that the acid was not buffered by nepheline alone. Further work would be required to establish the cause of this buffering.

A kinetic curve for the system was derived from Eqn (3.79), rearranged in the following form,

$$F/V = 3K(1-R)^{1/3}/2R(1-(1-R)^{1/3}). \qquad (4.1)$$

In this equation the fraction of nepheline reacted, R

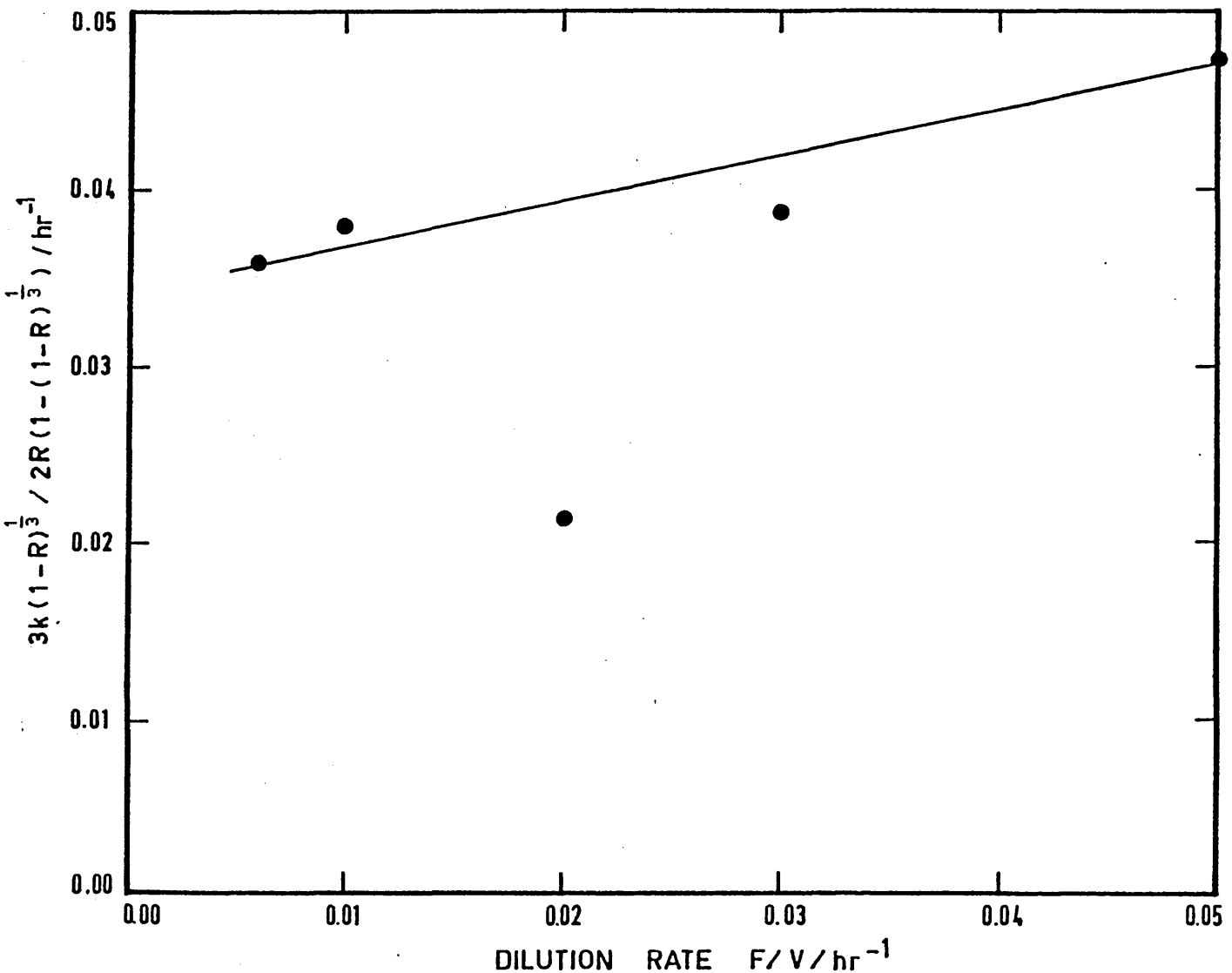


Fig. 4.7: Plot of dilution rate, F/V, versus $3k(1-R)^{\frac{1}{3}} / 2R(1-(1-R)^{\frac{1}{3}})$ for an inlet nepheline concentration of $8\ gl^{-1}$.

$= (C_0 - C_1)/C_0$, is found from experimental measurements of the sodium concentration, and the working value of the leaching rate constant, K, is found form pH measurements by Eqn (3.6) (making adjustments to take account of the smaller grain size and units of hr^{-1}).

Assuming that the level of agitation employed was lower than that required to dislodge the gel layer from the nepheline particles, and bearing in mind the small particle size, Eqn (4.1) should give a straight line. Such a plot is given in Fig 4.7 for an inlet concentration of 8 g/l. Although there is considerable scatter of some data it can be seen that there is a very general linear relationship. The scatter of points probably arises from the turbulent conditions in the fermenter and temperature differences of ±4°C.

Equipment performance. The equipment functioned satisfactorily within constraints imposed by the design. The sucrose to acid conversion efficiency was low (of the order of 30%), as a result of the high metal concentration in the fermenter which resulted from inefficient product recovery (see below). The acid yield might have been improved by the addition of methanol or copper ions but this was not tested in the present work (Section 2.4).

The recovery of aluminium citrate by ion exchange was not as efficient as might have been expected. Based on a maximum exchange capacity of 200 Meq and a complex of the form $Al(CIT)_2^{3-}$, the maximum yield from 150 ml of wet resin should have been of the order of 27 g (under ideal conditions). On average, the actual mass recovered was

approximately 6 g. The low yield was probably pH related as anionic complexes of aluminium citrate only become predominant above pH 5.0 and during fermentation the pH was in the range 3.0-4.5. Bearing in mind that at pH 5.0 the leaching rate constant, K, is negligible, it can be concluded that aluminium citrate cannot be recovered from fermentation liquors, buffered with nepheline, by Dowex 2 resin.

The equipment in Fig 4.3 was designed for manual operation. It is recommended that any future modifications should include a controller to allow for automatic sampling, flow control, temperature control and product recovery. With the exchange of solvent extraction for ion-exchange as a means of recovering aluminium citrate it would also be possible to reduce the concentrations of leach products in the fermenter to acceptable levels.

Physical interaction of hyphae with mineral surfaces. In Chapter 2 (Section 2.3) it was noted that mycelium invariably became physically attached to leaching minerals under conditions of surface mat culture. Observations of nepheline samples recovered from the continuous fermenter (operated with 0.5-3.0 cm lumps) indicated that the fungus was also attracted to nepheline grains under submerged leaching conditions. However, there were significant differences.

Electron and optical micrographs (Figs 4.8-2.23) show that hyphae penetrated and were distributed throughout the gel layer surrounding reacting nepheline grains. These presumably originated as detritus from the fluidised

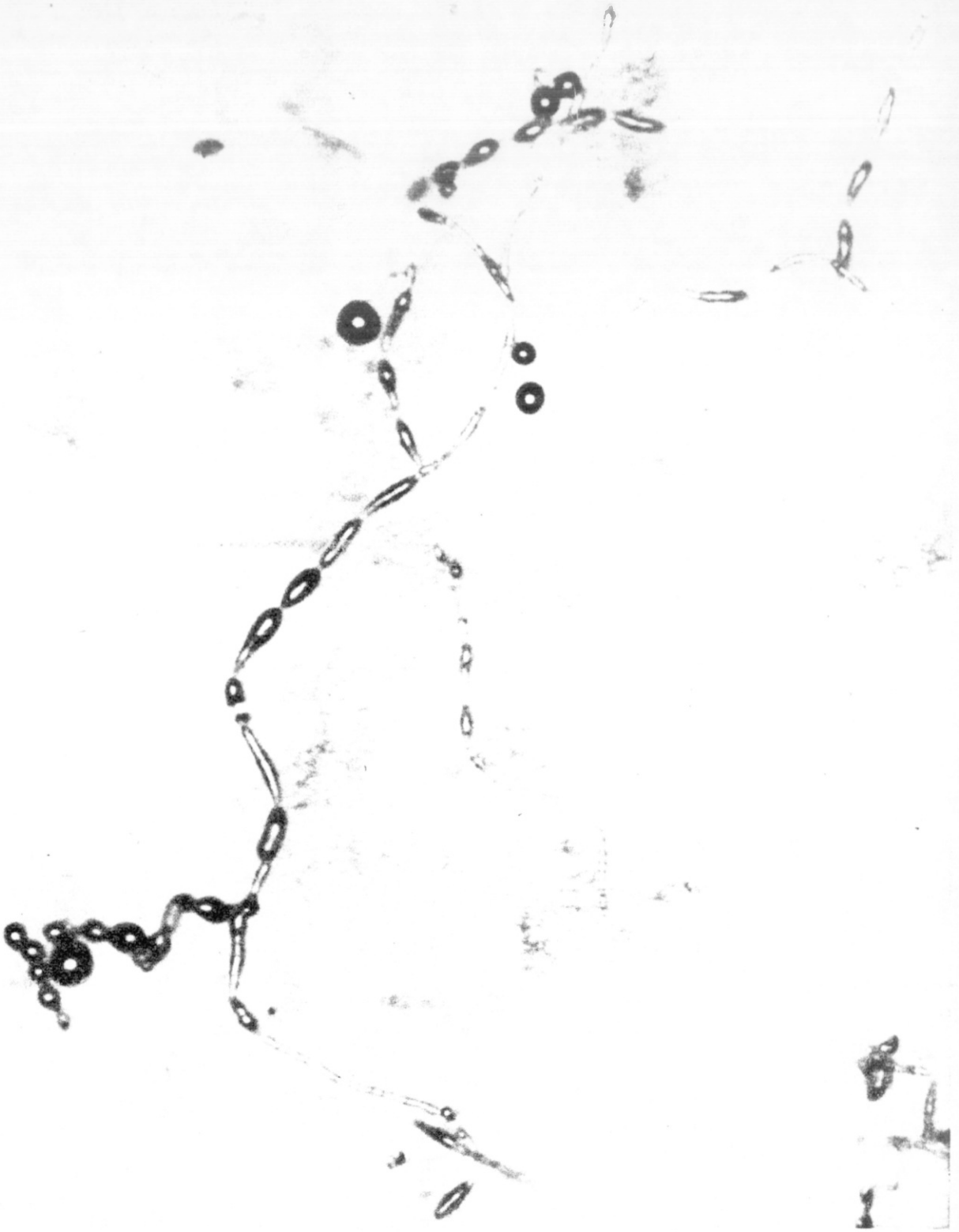


Fig 4.8 Optical photomicrograph of hyphae inside the gel layer of a reacted disc of nepheline (stained with osmium tetroxide) 600×.

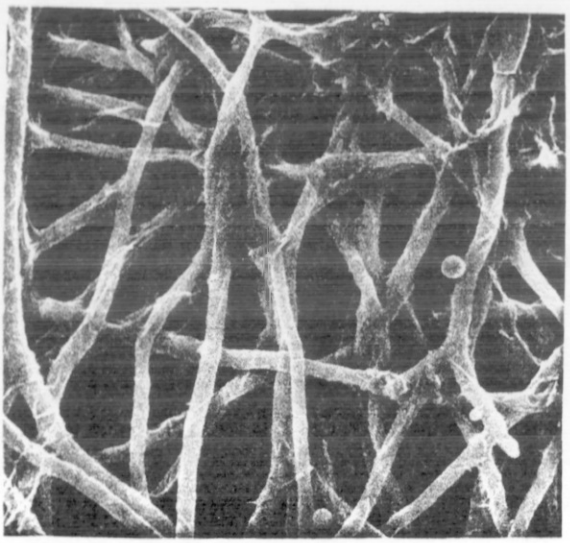


Fig 4.9 Electron photomicrograph showing hyphae typical of fungus pellets 1300×.

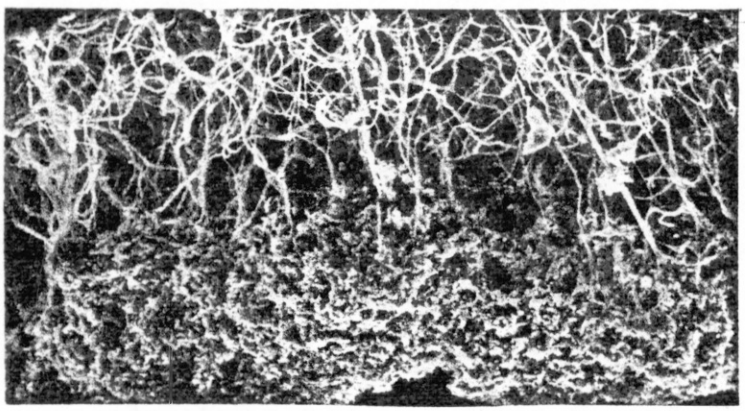


Fig 4.10 Electron photomicrograph showing morphological differences between hyphae in close contact with nepheline (bottom), and hyphae exposed to the air (top) 200×.



Fig 4.11 Electron photomicrograph showing hyphae typical of growth close to reacting nepheline 350×.

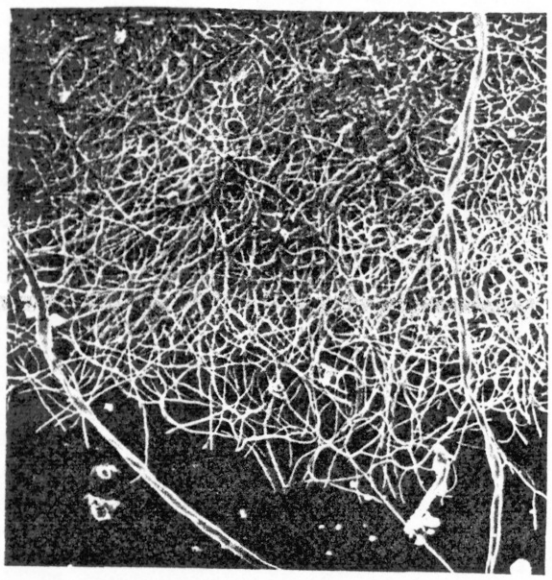


Fig 4.12 Electron photomicrograph showing hyphae typical of growth in the open air 780×.

pellets. Growing hyphae taken from the fluidised bed (electron photomicrograph Fig 4.9), show typical hyphae as long-branched strands of constant diameter ($\simeq$2 μm) and without any obvious abnormalities. Three different forms of hyphae were found around nepheline grains. Hyphae rooted into the silica gel layers around nepheline grains (Fig 4.8) are distorted into bulbous or spherical units. These have a similar structure to yeast cells but can be distinguished by their continuous branched structure. If nepheline and gel plus mycelium are removed, exposed to the air and sprayed continually with a solution of sucrose, a relatively thick fungus mat developed rather like that in surface culture. In cross-section this had a structure as illustrated in Fig 4.10. Hyphae close to the mineral (Fig 4.11) are abnormally short, stubby and forked and form a dense compact structure, whereas hyphae exposed to the air are similar in structure to those found in pellets (Fig 4.12).

It is significant that the abnormal morphological characteristics associated with growth in contact with nepheline are similar to those described by Snell and Schweiger (224) in a patent concerned with the production of citric acid by A.niger ATCC 1015 (the same strain as CMI 31821). 'Hyphae typical of, and required for, an efficient citric acid fermentation are abnormally short, stubby, forked and bulbous with numerous swollen oval to spherical shaped cells well distributed throughout the hyphal structure.'

Over long periods of time and under the conditions

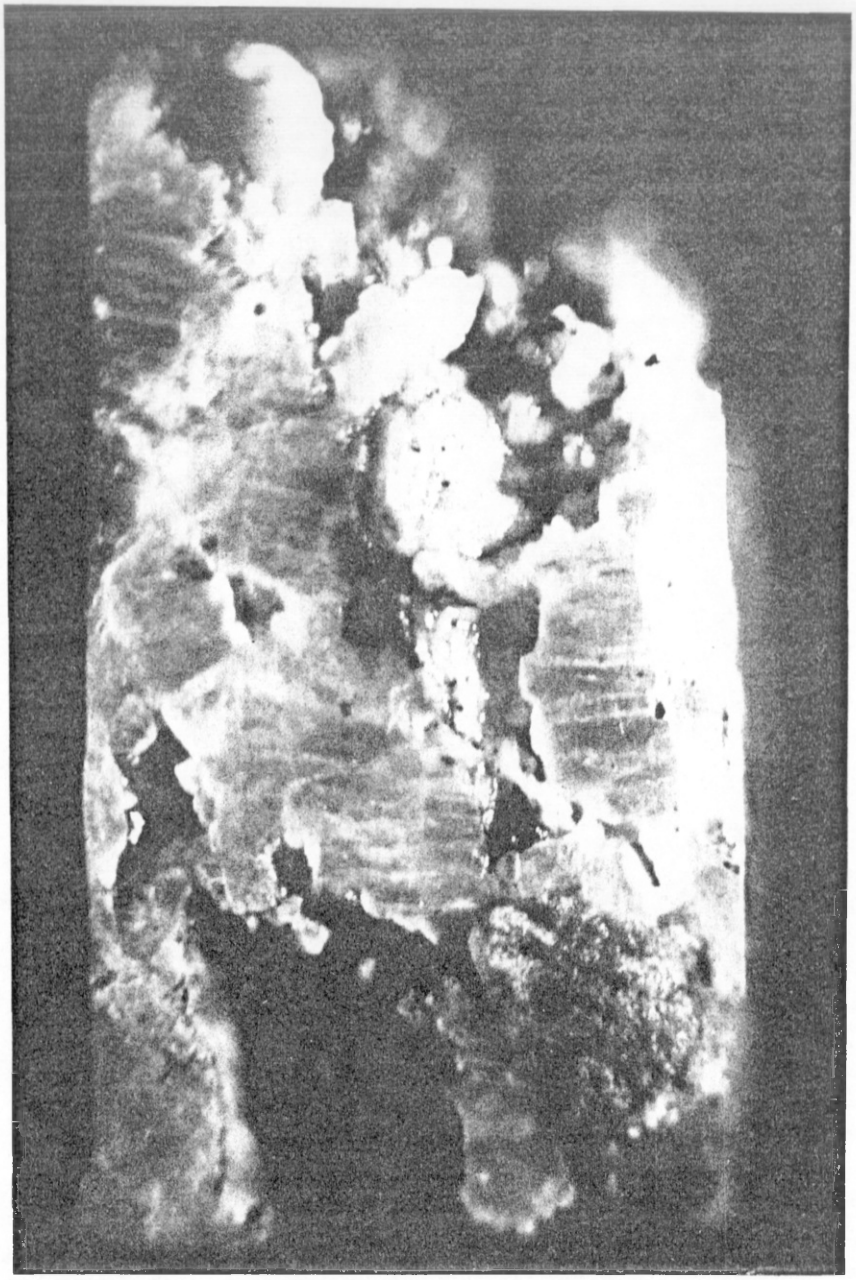


Fig 4.13 Photograph showing mycelium of A.niger (after 8 weeks growth) inside leached cavities of Bancroft nepheline. Unleached mineral is feldspar and the green fungus in the bottom right hand corner is P.purpurogenum 6×.

specified in Section 2.3 the densely packed form of mycelium was particularly aggressive towards nepheline. This is illustrated in Fig 4.13 which is a photomicrograph of a block of nepheline syenite (from preliminary experimental work in Section 2.3). Nepheline crystals have been completely dissolved by fungal action and the cavities remaining have become infilled with fungus. It can be seen that the fungus was bright yellow in colour. This pigmentation frequently appeared when A.niger was grown in the presence of nepheline. Moyer (242) attributed yellow pigmentation in strains of A.niger with high acid yields. These findings suggest that growth of A.niger in close proximity to reacting nepheline grains induces the fungus to produce acid and thereby improve the mineral leaching rate. However, the concentrations of leach products in the gel are likely to be high suggesting that the morphological abnormalities noted above are not, in this case at least, associated with acid biosynthesis.

Insufficient data was available to assess whether hyphal penetration of the silica gel layer enhanced the leaching rate. Such data would be difficult to obtain for practical systems (i.e. those containing nepheline sized at $<50\ \mu m$) due to the relatively rapid reaction of particulate nepheline with acids compared to the slow growth rate of hyphae.

4.2 Economic Evaluaton of Fungal Leaching Processes.

Although the equipment and processes described require much further development work, a preliminary economic assessment can be made. The aims of this section are:

(1) to compare fungal leaching and Bayer processes for producing alumina,

(2) to discuss markets and prices for other products of fungal leaching, e.g. citric acid, metal citrates, and

(3) to estimate capital and operating costs for suitable scaled up versions of equipment in Fig 4.3.

The cost of metallurgical grade alumina from bauxite by the Bayer process is of the order of £210-265/ tonne (344). The equivalent unit cost of alumina (based on raw material costs alone) produced by nepheline bioleaching either of Bancroft nepheline or Norwegian syenite are calculated for comparison in Table 4.2. It can be seen that, neglecting the value of byproducts, alumina produced from nepheline is 2 to 12 times more costly than that produced from bauxite. If processing costs were included bioleaching would compare even less favourably. The process becomes more attractive if byproducts are taken into account. Indeed, based on the values of citric acid, sodium and potassium citrates (see below), it might be better oriented to the production of carboxylic acid metal salts, provided a suitable market exists.

Estimates of the world production and market for citric

TABLE 4.2 RAW MATERIAL COSTS FOR THE PRODUCTION OF ALUMINA FROM BANCROFT NEPHELINE AND NORWEGIAN SYENITE BY FUNGAL LEACHING.

		Bancroft nepheline	Norwegian syenite
Soluble alumina in rock	%	22-28	11-15
Rock required per tonne alumina/	tonnes	3.5-4.5	7-9
Mining and pretreatment costs (i)/	$/tonne	20-65	20-65
Molasses requirement (ii)/	$/tonne nepheline	184-553	184-553
Total cost of raw materials/	$/tonne alumina	578-2258	630-2526
Byproducts (iii)/ tonne	Si	0.47-0.75	0.47-0.75
	Na	0.25-0.43	0.25-0.43
	K	0.16-0.25	0.16-0.25
	citric acid	4.6	4.6
	feldspar	0.38-0.5	3.85-4.95
	mica	0.28-0.36	-
	Dark minerals	-	0.21-0.27

(i) Based on prices quoted in Industrial Minerals Journal (344), for nepheline syenite.

(ii) Calculated assuming:
- (a) 1g of nepheline requires 1.66g citric acid for complete dissolution,
- (b) the sugar to acid conversion efficiency is 30-90%,
- (c) the molasses contains 50% sugars suitable for for acid production, and
- (d) costs £50/tonne.

(iii) The rocks have a composition as in Tables 2.4-2.5.

acid and associated products in 1981 were 300,000 and 175,000 tons, respectively, from sales of $259 million (345,346). About 60% of that sold was used by the food industry where it finds application for pH control (in soft drinks, wines, frozen foods and other products) and as an antioxidant (in fats, oils, sausage and other meat products) (147). There are five major citric acid commodities: citric acid, ammonium citrate, calcium citrate, sodium citrate and potassium citrate. The unit costs of each are compared in Table 4.3. It can be seen from Tables 4.2 and 4.3 that the citric acid produced by nepheline bioleaching has a value of the order of £1700/ tonne of nepheline leached. The acid could be recovered as sodium and potassium citrates but little financial benefit would be gained taking into account the extra processing involved.

Although no uses were found for aluminium citrate this compound might find application as a food or oil additive (347). It is significant that mixtures of water insoluble and soluble aluminosilicates and citric acid have been used in place of phosphates in detergent washing powders to remove hardness (147). The ion exchange and adsorption properties of silica gel coated nepheline grains (which could be produced by the apparatus in Fig 4.3 at high dilution rates to give partial reaction of grains i.e. $R<<1$), are not known. However bearing in mind the reactive nature of nepheline (which incidentally is a source of many natural zeolites tested in detergent formulations), and its ability to adsorb coloured dyes (310), it might be of

TABLE 4.3 UNIT PRICES OF MAJOR CITRIC ACID COMMODITIES.

Compound	Cost/ £/tonne*
citric acid (anhydrous)	1080
citric acid (hydrous)	1024
ammonium citrate	US$ 2.73/kg**
calcium citrate	US$ 4.36/kg**
potassium citrate	1229
sodium citrate	1024

* 1984 UK prices
** 1978 US prices (not available in the UK).

use in detergent applications.

At present many countries allow the use of phosphate in detergents but judging by current European trends (Switzerland has recently banned the use of phosphate based detergents on account of the high level of phosphate in Swiss lakes), and the interest shown in aluminosilicate based detergents by chemical manufacturers in the detergent business (deduced from the numerous patents filed on this subject in recent years), the market for aluminosilicate/ citrate ion exchangers might increase.

Spent mycelium constitutes a major byproduct of citric acid fermentations. It is used as an additive in pet/livestock feedstuffs and there are regulations governing its use in such products (348). It has also been tested as a fertiliser and soil conditioner with some success (349).

Capital and operating costs of leaching equipment.

Typical weekly operating costs of a 25 tonne/ week leaching plant based on the laboratory results, are presented in Table 4.4. These calculations are based on the following assumptions.

(1) The plant comprises 3 x 20 m^3 fermenters which are sufficient to give 4 tonnes citric acid /day based on a production rate of 16 g acid / hour / Kg mycelium.

(2) Liquid is recirculated by 3 4 KW pumps (one for each fermenter); a single 4 KW stirrer is employed for agitation in the leach tank; air is compressed by a 2 KW compressor; and the mycelium production unit required a 4 KW recirculation pump.

TABLE 4.4 ANNUAL OPERATING COSTS FOR A NEPHELINE LEACHING PLANT.

RAW MATERIALS	FLOW/ kg/week	COST/ £/year
molasses	62890	141525
ammonium carbonate	435	24039
potassium phosphate	60	6696
magnesium sulphate	290	7281
mycelium	12000	54000
nepheline	24330	5476
other (copper)	-	1000

PUMPING COSTS	POWER USED kwh/week	COST £/year
recirculation	2016	1000
leach tank	672	300
air	336	150
mycelium production	672	300
maintenance (50% of op costs)		875

Total raw materials + pumping costs	242642
Product recovery (2 ×above total)	485284
Fixed capital + other costs (30% of all other costs)	218378
Total	£ 946304

PRODUCTS	PRODUCTION RATE tonnes/week	REVENUE £/year
sodium citrate	5.76	265410
potassium citrate	2.64	145980
aluminium citrate	20.52	1134810
citric acid	10.92	503235
mycelium	12.00	10800
silica	5.46	1228
other (dark minerals)	0.70	157
Total value of products		£ 2061620

(3) Fermentation, leaching and product recovery are carried out in separate compartments.

(4) Product recovery costs are assumed to be double the sums of raw material and pumping costs for fermentation and leaching.

(5) The cost of the initial charge of liquid to start up the fermenter is neglected.

(6) A dilution rate of 0.024 hr^{-1} is assumed for a conversion of 90%.

(7) Molasses containing 50% fermentable sugars and costing £50/ tonne is employed as the carbon source.

(8) The cost of electricity is 0.2 times the UK domestic rate.

(9) Biomass is changed once per week at a cost of twice its weight in sugar.

(10) Fixed capital and other operating costs are assumed to be 30% of all other costs.

(11) Ammonium carbonate, potassium dihydrogen phosphate and magnesium sulphate are available at 0.5 times the UK price (per tonne) for technical grade chemicals.

(12) The process is situated on a deposit of Bancroft nepheline, containing 70% nepheline and costing £5/ tonne in mining and pretreatment.

(13) The plant operates for 45 weeks per year.

(14) Aluminium citrate has a value of 1.2 times that of citric acid.

(15) Silica has a value of £5/ tonne, mycelium £20/ tonne and other products £5/ tonne.

(16) Copper is added to inhibit growth of other

organisms.

(17) The fermenters operate at atmospheric temperature (26°C).

The results in Table 4.4 indicate an operating profit of £1×10^6/year.

The capital cost is calculated by two different methods. The first is based on West German citric acid fermentation data (Table 4.5), with the following assumptions.

(1) Cost indices for West Germany in 1977 and 1984 are 120 and 155, respectively.

(2) The cost index for the UK in 1984 is 260.

(3) The DM to £ exchange rate for 1984 is 3.7.

(4) A Cran scale up exponent (see below) of 0.8.

The capital cost of a 32 tonne (citric acid)/ week plant now in the UK is of the order of £6×10^5 (excluding leaching and product recovery costs). This could be doubled if leaching and recovery costs are included. It should be noted that using the method proposed by Cran (350) for the scale up (or down) of process plant costs (by a simple equation of the form $C(1)/C(2)=(S(1)/S(2))^n$, where C is the capital cost, S is the plant capacity, n is an exponential index (Lang factor) and the subscripts (1) and (2) refer to plants 1 and 2, respectively), is only accurate (to ± 18%) for ratio's of S(1):S(2)<5. It can be seen that a scale down factor of 15 is used in the above estimation and therefore it can be assumed that errors are >18%. The second method is based on the simple scale up of laboratory equipment costs (£500 for a 5 l fermenter), an the basis of fermenter capacity. Using this method the

TABLE 4.5 WEST GERMAN SUBMERGED CITRIC ACID FERMENTATION COSTS FOR A 72 tonne/day PLANT.

Absolute costs (10 DM/year)	94
Cost breakdown (%)	
Buildings	2
Plant	8
Materials	37
Energy	30
Labour	23

Taken from Schierholt (146).

capital cost is of the order of £1×10^6. In this method a scale up exponent (n) of 15000:1 is employed, therefore it can be assumed that the estimate is less accurate the that determined by the first method.

It can be seen that in spite of the different sources of data used for each method the resulting capital costs are similar in magnitude. Based on a total equipment cost of £1 ×10^6 a payback time (neglecting interest on borrowed capital and assuming a 45 week year), of the order of 1-2 years might be expected. Of course, these results are general in nature and their accuracy should not be expected to be any greater than ±100%, however they illustrate that under certain circumstances the process might by economically viable. In the absence of any up to date comparative data concerning citric acid fermentation equipment and operating costs no further comment can be made.

REFERENCES

1- J. Orcott, New Scientist, 92(1283), 1981, pp 741-747.

2- W.W. Spink, Infectious Diseases, Dawson Publishers, 1st Edn., 1978.

3- M.P. Silverman and H.L. Ehrlich, Advances Appl. Microbiol., 6, 1964, pp 153-206.

4- B. Hartley, Private communication.

5- M.P. Silverman, Biogeochemical Cycling of Mineral Forming Elements, Eds. P.A. Trudinger and D.J. Swaine, Elsevier, 1979, pp 445-465.

6- G.V. Jacks, Science Progress, 41, 1953, pp 301-305.

7- A. Kockova-Kratochvilova, Biotechnology, Eds. H.J. Rehm and G. Reed, Verlag Chemie, 1(1), 1981, p 34.

8- D.P. Kelly, P.R. Norris and C.L. Brierley, Microbial Technology: Current State, Future Prospects, Eds. A.T. Bull, D.C. Ellwood and C. Ratledge, Symp. Soc. Gen. Microbiol., , 1979, pp 265-308.

9- E. Livesley-Goldblatt, T. Tunley and I.F. Nagu, Conference on Bacterial Leaching, Ed. W. Schwartz, GBF Monograph No. 4, Weinheim Verlag Chemie, 1977, pp 175-190.

10- A.L. Demain and N.A. Solomon, Scientific American, 245(3), 1981, pp 43-51.

11- J.V. Beck, Biotech. Bioeng., 9(4), 1967, pp 487-497.

12- C.E. Capes, A.E. McIlhinney, A.F. Sirianni and I.E. Puddington, Can. Min. Metal. Bull., 66(88), 1973, p 91.

13- F. Pooley, Private communication.

14- G.I. Karavaiko and S.A. Pivovaroua, Conference on Bacterial Leaching, Ed. W. Schwartz, GBF Monograph No. 4, Weinhiem Verlag Chemie, 1974, p 40.

15- C.L. Brierley, J.A. Brierley and L.E. Murr, Research and Development, 24, 1973, pp 24-28.

16- V.K. Berry and L.E. Murr, Metallurgical Applications of Bacterial Leaching and Related Microbiological Phenomena, Eds. L.E. Murr, A.E. Torma and J.A. Brierley, Academic Press, 1978, pp 108-136.

17- R.B. Duff, D.M. Webley and R.O. Scott, Soil Science, 95, 1963, pp 105-114.

18- V.G. Aleksandrov, M.I. Tenovkaya and R.N. Blagodyr, Vestn. Sel' Skokhoz. Nauki, 12, 1967, pp 39-42.

19- S. Groudev and F. Grenchev, Proc. Int. Cong. Study Bauxites, Alumina Alumin., 4th Athens, Nat. Tech. Univ. Press, 1, 1978, pp 271-278.

20- Z.P. Testic and M.S. Todorovic, Zemljiste i Biljka, 7, 1959, pp 233-238.

21- D.R. Cullimore and A.E. McCann, Aquatic microbiology, Eds., F.A. Skinner and J.M. Shewan, Academic Press, 1977, pp 219-261.

22- S.R. Rogers and J.J. Anderson, J. Bact., 126, 1976, pp 257-263.

23- R.L. Starkey, Science, 102, 1965, p 531.

24- Y. Pares et al., La solubilisation de l'or par voie bacterienne, Dakar, Bureau de Recherches Geologiques et Minieres, 1965, 10pp.

25- W.S. Rapson, Gold Bull., 15(1), 1982, pp 19-20.

26- G.G. Mineev, T.S. Syttanova and I.K. Skobeev, Soviet Non-Ferrous Met. Res., 5(6), 1977, pp 213-215.

27- C. Thom and K.B. Raper, A Manual of Aspergilli, Williams and Wilkins, Baltimore, 1945, pp 81-91.

28- A.H. Onions, D. Allsop and H.O. Eggins, Smiths Introduction to Mycology, 7th Edn., Edward Arnold Publishers, 1981, p 3.

29- E.A. Gaumann and C.W. Dodge, Comparative Morphology of Fungi, McGraw Hill Publishers, 1st Edn., 1928, p 474.

30- L.B. Lockwood, The Filamentous Fungi; Industrial Mycology, Eds., J.E. Smith and D.R. Berry, Arnold Publishers, Vol 1, 1975, pp 104-119.

31- E. Muller and W. Loeffler, Mykologie, G. Thieme, Stuttgart, 1971.

32- Anon, Catalogue of the Culture Collection of the Commonwealth Institute of Mycology, HMSO, 8th Edn., 1982.

33- A.I. Laskin and H.A. Lechevalier, CRC Handbook of Microbiology, CRC Press, Vol. 3, 1973.

34- P.W. Dacey, D.S. Wakerley and N. Le Roux, The Biodegradation of Rocks and Minerals with particular reference to Silicate Minerals. A Literature Survey, Warren Spring Laboratory Report No. LR 380(ME), 1981.

35- M.A. Batti, British Patent 1145520, 1969.

36- L.Arrieta and R. Grez, App. Microbiol., 22, 1971, pp 487-490.

37- S.R. Dave, K.A. Natarajan and J.V. Bhat, Hydrometallurgy, 7, 1981, pp 235-242.

38- J.R. Boyle and G.K. Voigt, Science, 155, 1967, pp 193-195.

39- G. Rossi, Metallurgical Applications of Bacterial Leaching and Related Microbiological Phenomena, Eds., L.E. Murr, A.E. Torma and J.A. Brierley, Academic Press, 1978, pp 297-320.

40- M.P. Silverman and E.F. Munoz, Science, 169, 1970, pp 985-987.

41- G.M. Wenberg, F.H. Erbisch and M.E. Volin, Trans. of the Soc. Min. Engrs. AIME., 250, 1971, pp 207-212.

42- Y.S. Chiu, Ph.D. thesis, University of Western Ontario, London, Ontario, 1972.

43- M. Tsezos and B. Volesky, Biotech. Bioeng., 23, 1981, pp 584-604.

44- T. Horikoshi, A. Nakajima and T. Sakaguchi, Europ. J. App. Micrbiol. Biotechnol., 12, 1981, pp 90-96.

45- V. Ahmadjian, The Physiology and Biochemistry of Algae, Ed., R. Lewin, Academic Press, 1962.

46- J.C. Madwick and B.J. Ralph, Conference on Bacterial Leaching, Ed. W. Schwartz, GBF Monograph No. 4, Weinheim: Verlag Chemie, 1977, pp 85-91.

47- A.W. Morris and A.J. Bale, Esturine Coastal Mar. Sci., 3(2), 1975, pp 153-164.

48- P.M. Stokes, T.C. Hutchingson and K. Krauter, Can. J. Bot., 51, 1973, pp 2155-2168.

49- T. Sakaguchi et al., Europ. J. Appl. Microbiol. Biotechnol., 8(3), 1979, pp 207-215.

50- D.S. Filip et al., Water Res., 13(3), 1979, pp 305-313.

51- A. Quispel, Rec. Trav. Botan. Neerl., 40, 1943-1945, pp 413-541.

52- D.A. Jenkins and R.I. Davis, Nature, 210, 1966, pp 1296-1297.

53- M.E. Williams and E.D. Rudolph, Mycologia, 66, 1974, pp 648-660.

54- A. Schatz, Naturwissenschaften, 49, 1962, pp 518-519.

55- A. Schatz, J. Agr. Food Chem., 11, 1963, pp 112-118.

56- Anon, Fundamentals of Fungi, Ed. E. Moore-Landecker, Prentice Hall Publishers, Chapter 2, 1972.

57- V.W. Cochrane, Physiology of Fungi, Wiley Publishers, 3rd Edn., 1965, pp 356-386.

58- 29, pp 186-187.

59- M. Zalokar, Am. J. of Bot., 46, 1959, pp 555-556.

60- A.P.J. Trinci, J. of Gen. Microbiol., 81, 1974, pp 225-236.

61- 30, p 3.

62- A.Frey-Wyssling and K.Muhlethaler, Vierteljahresschr Naturforsch Ges. Zurich, 95, 1950, pp 45-52.

63- J.M. Aronson and R.D. Preston, Pro. Roy. Soc., B152, 1960, pp 346-357.

64- G. Setterfield and S.T. Bayley, Ann. Rev. Plant Physiol., 12, 1961, pp 35-62.

65- D. Hunsley and J.H. Burnett, J. of Gen. Microbiol., 62, 1970, pp 203-218.

66- G. Van-Iterson, K.H. Moyer and W. Lotmar, Rec. Trav. Chim., 55, 1936, pp 61-63.

67- M.S. Fuller and I. Barshad, Am. J. of Bot., 47, 1960, pp 105-109.

68- D. Hunsley and G.W. Gooday, Protoplasma, 82, 1974, pp 125-146.

69- A.H. Rose, The Filamentous Fungi, Eds. J.E. Smith and D.R. Berry, Edward Arnold Publishers, 2, Chapter 10, 1976, pp 308-327.

70- A. Beckett, I.B. Heath and D.J. McCaughtin, An atlas of fungal ultrastructure, Longmans Press, 1974.

71- A.S. Sussman, Mycologia, 49, 1957, pp 29-43.

72- S. Bartnicki-Garcia, Symp. Soc. Gen. Microbiol., 23, 1973, pp 245-267.

73- H. Schroder, Z. Allgem. Mikrobiol., 1, 1961, pp 201-202.

74- R.L. Post and C.D. Albright, Membrane Transport and Metabolism, Eds. A. Kleinzeller and A. Kotyk, Academic Press, 1961, pp 219-227.

75- J.C. Skou, Membrane transport and Metabolism, Eds. A. Kleinzeller and A. kotyk, Academic Press, 1961, pp 228-236.

76- M. Burger, E.E. Bacon and J.S.D. Burger, Biochem. J., 78, 1961, pp 504-511.

77- J. Friis and P. Ottolenghi, Comp. Rend. Trav. Lab. Carlsberg., 31, 1959, pp 259-271.

78- B.M. Eberhart, J. Cellular Comp. Physicol., 58, 1961, pp 11-16.

79- J.E. Danielli, Permeability of Natural Membranes, Eds. H. Davson and J.F. Danielli, Cambridge University Press, 1943, pp 341-352.

80- H.W. Doelle, Biotechnology, Eds, H.J. Rehm and G. Reed, Verlag Chemie, 1(3), 1981, p 128.

81- J.G. Horsfall, Principles of Fungicidal Action, Chronica Botanica, Waltham, Massachusetts, 1959.

82- G.C. Polikarpov, Radioecology of Aquatic Organisms, North Holland Publishers, New York, 1966.

83- I. Langmuir. Phys. Rev., 8, 1916, p 149.

84- Y. Tanaka and S. Skoryna, Organic Macromolecular Binders of Metal Ions, Gastrointestinal Research Laboratory of McGill University, Montreal, 1970.

85- E. Somers, Ann. App. Biol., 49, 1961, pp 246-253.

86- I.F. Brown and H.D. Sisler, Phytopathology, 50, 1960, pp 830-839.

87- Anon, Handbook of Enzyme Biotechnology, Ed. A. Wiseman, Wiley Press, 1975, pp 254-255.

88- M.M. Gascoigne and J.A. Gascoigne, Biological Degradation of Cellulose, Eds. J.W. Cook and M. Stacey, Butterworths Press, 1960, pp 53-71.

89- 87, pp 135-136.

90- A. Albert, Selective toxicity with special reference to chemotherapy, Methuen, London; Wiley, New York, 2nd Edn., 1960.

91- B.J. Deverall, The Fungi; an Advanced Treatise, Eds. G.C. Ainsworth and A.S. Sussman, 1, 1965, pp 543-557.

92- P.A. Kitos, J.J.R. Campbell and N. Tomlinson, App. Micrbiol., 1, 1953, pp 156-159.

93- A.P.J. Trinci, Trans. of the Brit. Mycol. Soc., 55, 1969, pp 17-28.

94- G.L. Solomons, Fungal Biotechnology, Eds. J.E. Smith D.R. Berry and B. Kristiansen, The British Mycological Symposium Series No. 3, Academic Press, 1980, pp 55-80.

95- R.A. Steinberg, J. Agr. Res., 59, 1939, pp 749-763.

96- S.J. Pirt and D.S. Callow, J. of Appl. Bacteriol., 23, 1960, pp 87-98.

97- S.J. Pirt, Proc. of the Roy. Soc., B166, 1966, pp 369-373.

98- T. Yano, T. Kodama and K. Yamada, Agr. Biol. Chem., 25, 1961, p 580.

99- 30, pp 86-87.

100- J. Monod, Recherches sur al croissance des cultures bacteriennes, Hernann and CIE, Paris, 1942.

101- H. Moser, Pub No. 614, Washington: Carnegie Institute, 1958.

102- N. Van-Uden, Ann. Rev. of Microbiol., 23, 1969, pp 473-486.

103- D.E. Contois, J. of Gen. Microbiol., 21, 1959, pp 40-50.

104- B. Kristiansen, Ph.D. Thesis, UMIST, 1976, p 164.

105- A. Constantinides, J.L. Spencer and E.L. Gaden, Biotech. Bioeng., 12, 1970, pp 803-830.

106- 30, pp 91-92.

107- C.G. Sinclair and H.H. Topiwala, Biotech. Bioeng., 12, 1970, pp 1069-1079.

108- S.Y. Chiu, L.T. Pan, I.C. Kao and L.E. Erickson, Biotech. Bioeng., 14, 1972, p 129.

109- N.O. Kjeldgaard, O. Maaloe and M. Schaechter, J. of Gen. Microbiol., 19, 1970, pp 607-616.

110- Z. Fencl, Biotech. Bioeng., 12, 1970, p 845.

111- F. Machek and Z. Fencl, Biotech. Bioeng. Sym. No. 4, 1973, pp 129-142.

112- R.D. Megee III, S. Kinoshita, A.G. Fredrickson and H.M. Sushiya, Biotech. Bioeng., 12, 1970, p 771.

113- A.H. Khan and T.K. Ghose, J. Ferm. Tech., 51, 1973, p 734.

114- 104, pp 117-120.

115- R. Luedking and E.L. Piret, J. Biochem. Microbial Tech. Eng., 1, 1959, p 393.

116- T. Kono and T. Asai, Biotech. Bioeng., 11, 1969, p 293.

117- A. Constanides, J.L. Spencer and E.L. Gaden, Biotech. Bioeng., 12, 1970, p 803.

118- P. Shu, J. Biochem. Microbial Tech. Eng., 1, 1959, p 59.

119- H.A. Krebs and H.L. Kornberg, A survey of energy transformations in living matter, Springer-Verlag, Berlin, Gottingen and Heidelberg, 1957, pp 213-215.

120- F. Lipmann, Enzymol., 1, 1941, p 99.

121- H.A. Krebs, Brit. Med. Bull., 9, 1953, p 97.

122- J.D. Bu'lock, Essays in biosynthesis and microbioal development, John Wiley Publishers, 1967.

123- J.D. Bu'lock, The biosynthesis of natural products, McGraw Hill Publishers, 1965.

124- J.N. Currie, J. Biol. Chem., 31, 1917, pp 15-37.

125- S.L. Ranson, Plant Biochemistry, Eds, J. Bonner and J.E. Varner, Academic Press, 1965, pp 493-532.

126- K. Watson and J.E. Smith, Biochem. J., 104, 1967, pp 332-339.

127- H.A. Krebs, Chemical Pathways of Metabolism, Ed. D.M. Greenberg, Academic Press, 1, 1954, p 109.

128- 80, pp 147-149.

129- Anon, The Encyclopedia of Biochemistry, Eds. R.J. Williams and E.M. Lansford, Reinhold Publishers, 1967, pp 541-544.

130- Anon, Outlines of Biochemistry, Eds. E.E. Conn and P.K. Stumpf, 2nd Edn., Wiley Publishers, 1966.

131- W.W. Cleland and M.J. Johnson, J. Biol. Chem., 208, 1954, p 679.

132- P. Shu, A. Funk and A.C. Neish, Can. J. of Biochem and Physiol., 32, 1954, pp 68-80.

133- R.A. Bloomstein and M.J. Johnson, J. Biol. Chem., 198, 1952, p 143.

134- J.M. LaNauze, J. Gen. Microbiol., 44, 1966, pp 73-81.

135- S.A. Ahmed, Ph.D. thesis, University of Strathclyde, 1970.

136- S.A. Ahmed, J.E. Smith and J.G. Anderson, Trans. of the Brit. Mycol. Soc., 59, 1972, pp 51-60.

137- C.V. Ramakrishnan, R. Steel and L.P. Lentz, Arch. Biochem. Biophys., 55, 1955, pp 270-273.

138- F.H. Verhoff and J.E. Spradlin, Biotech. Bioeng., 18, 1976, pp 425-433.

139- Anon, Trace Elements in Biochemistry, Ed. H.J.M. Bowen, Academic Press, 1966, pp 83-84.

140- S.D. Prescott and C.G. Dunn, Industrial Microbiology, McGraw Hill Publishers, 1959.

141- 57, pp 132-135.

142- M. Rohr, C.P. Kubicek and H.J. Kominek, Biotechnology, Eds. H.J. Rehm and G. Reed, Weinheim-Verlag Chemie, 3, 1983, pp 420-454.

143- 142, pp 456-465.

144- K. Bernhauer and H. Thole, Biochem. Z., 287, 1936, pp 167-171.

145- O. Mallea, Industria y. Qiimica (Argentina), 12, 1950, pp 264-280.

146- J. Schierholt, Process Biochem., 12(9), 1977, pp 20-21.

147- Anon, Encyclopedia of Chemical Technology, Eds. H.F. Mark, O.F. Othmer, C.G. Overberger and G.T. Seaborg, 3rd Edn., Wiley Interscience - John Wiley Publishers, 6, 1979, p 156.

148- P. Shu and M.J. Johnson, J. Bact., 58, 1948, p 577.

149- 30, p 148.

150- R.D. Nobel and E.J. Ratajak, US Patent 3044941, 1962.

151- H.T. Herrick and O.E. May, J. of Biol Chem., 77, 1928, pp 185-195.

152- H.T. Herrick and O.E. May, Ind. Eng. Chem., 21, 1929, pp 1198-1203.

153- H.J. Rehm, Industrielle Mikrobiologie, Springer-Verlag, 1967, pp 375-377.

154- S. Kintoshita, O. Terada and K. Oishi, US Patent 2993838, 1961.

155- 30, pp 16-32.

156- J.W. Foster, Chemical Activities of Fungi, Academic Press, 1949.

157- D.S. Clark, K. Ito, and H. Horitsu, Biotech. Bioeng., 8, 1966, p 465.

158- F.G. Davis and M.J. Johnson, J. Bact., 59, 1950, pp 51-60.

159- M.A. Pisano, B.H. Olson and C.L. Clemento, J. Bact., 68, 1954, pp 444-449.

160- R.A. Steinberg, Science, 107, 1948, p 423.

161- W.S. Butkewitsch, Microbiologiga, 3, 1934, pp 574-584.

162- M. Molliard, Compt. Rend. (Paris), 170, 1920, pp 949-951.

163- A. Rippel and G. Behr, Arch. Microbiol., 5, 1934, pp 561-577.

164- H.J. Fielder, Zentr. Bakteriol. Parasitenk. Abt. II, 112, 1959, pp 666-707.

165- F.J. Garnier and L. Kientizler, Bull. Ec. Nat. Sup. Agron., Nancy, 10, 1958, pp 3-6.

166- E.J. Conway and F. Duggan, Biochem. J., 69, 1958, pp 265-274.

167- E.J. Conway, The Biochemistry of Gastric acid Secretion, American Lecture Series, Thomas, Springfield, Illinois, 1953.

168- A. Rothstein, Electrolytes in Biological Systems, Ed. A.M. Shanes, Am. Physiol. Soc., Washington D.C., 1955, pp 65-100.

169- A. Rothstein, Bacteriol. Rev., 23, 1959, pp 175-201.

170- M.A. Batti, US Patent 3355067, 1967.

171- 91, p 435.

172- J.H. Burnett, Fundamentals of Mycology, Edward Arnold Publishers, 1968.

173- D. Bertrand, Comp. Rend., 257, 1963, pp 3057-3059.

174- K. Matsuda and T. Nagata, Nippon Dojo Hiryogaku Zasshi, 28, 1958, pp 405-408.

175- C.B. Sulochana, Proc. Indian Acad. Sci., B36, 1963, pp 19-33.

176- I.D. Chughtai and T.K. Walker, Biochem. J., 48, 1951, p 524.

177- 130, pp 241-247.

178- A. Rothstein, J. Gen. Microbiol., 46, 1963, pp 1075-1085.

179- J.E. Bowen and H.G. Gauch, Plant Physiol., 41, 1966, pp 319-324.

180- R. Ballantine and D.G. Stephens, J. Cellular Comp. Physiol., 37, 1951, pp 369-387.

181- R. Ballantine, J. Cellular Comp. Physiol., 42, 1953, pp 415-426.

182- S.H. Hunter, Ann. Rev of Microbiol., 26, 1972, pp 313-346.

183- D.J.D. Nicholas, Analyst, 77, 1952, pp 629-642.

184- C.G.C. Chesters and G.N. Rolinson, J. Gen. Microbiol., 5, 1951, pp 553-565.

185- R.A. Steinberg and J.D. Bowling, J. Agr. Res., 58, 1939, pp 717-732.

186- R.L. Starkey and S.A. Waksman, J. Bacteriol., 45, 1943, pp 509-519.

187- P. Shu and M.J. Johnson, J. Bacteriol., 54, 1947, p 161.

188- L.B. Schweiger, US Patent 2970084, 1961.

189- Anon, British Patent 742972, 1953.

190- Anon, British Patent 743395, 1953.

191- L.B. Schwieger, US patent 2916420, 1961.

192- A. Narroquin and R.S. Carrieiro, App. Microbiol., 20, 1970, p 888.

193- I.V. Zolchebskaya and I.L. Robotnova, Mikrobiologyia, 35, 1966, pp 1044-1052.

194- S.E.A. McCallan and L.P. Miller, Contrib. Boyce Thompson Institute, 18, 1957, pp 4482-4495.

195- L.J. Ashworth and J.V. Amin, Phytopathology, 54, 1964, pp 1459-1463.

196- D.F. Talburt and G.T. Johnson, Mycologia, 59, 1967, pp 492-503.

197- L.P. Miller, S.E.A. McCallan and R.M. Weed, Contrib. Boyce Thompson Institute, 17, 1953, pp 151-171, 173-195, 283-298.

198- D.J.D. Nicholas, J. Gen. Microbiol., 15, 1956, pp 470-477.

199- D. Perlman, D.A. Kita and W.H. Peterson, Arch. Biochem., 11, 1946, pp 123-129.

200- N. Tomlinson, J.J.R. Campbell and P.C. Trussell, J. Bacteriol., 61, 1951, pp 17-25.

201- J.B. Neilands, Bacter. Rev., 73, 1957, pp 101-111.

202- D.J.D. Nicholas and A.H. Fielding, J. Hort. Sci., 26, 1951, pp 125-147.

203- O. Nowosielski, Roczniki Gleboznawcze, 9, 1960, pp 89-102.

204- K. Zodrow, O. Stefnaiak and J. Januchowski, Chem. Abs., 72, 1970, 75564.

205- O. Kauflmann-Cosla and O. Tudor, Ann. Acad. Romane. Mun. Sect. Stintif, 21 Mem. 6, 1946, p 73.

206- F. Laborey and J. Lavolley, C. R. Acad. Sci. Paris Ser. D, 264, 1967, pp 2937-2940.

207- L.B. Lockwood and M.D. Reeves, Arch. Biochem., 6, 1945, pp 455-469.

208- W. Lohrmann, Arch. Mikrobiol., 11, 1940, pp 329-367.

209- P.B. Marsh, Phytopathology, 45, 1945, pp 676-680.

210- R.A. Macleod and E.E. Snell, Ann. N. Y. Acad. Sci., 52, 1950, pp 1249-1259.

211- C.B. Sulochana and M. Lakshmanan, J. of Gen. Microbiol., 50, 1968, pp 285-293.

212- E.G. Mulder, Plant and Soil, 1, 1948, pp 94-119.

213- N. Raman, S.K, Sastry and P.S Sarma, Biochemica et Biophysica Acta, 56, 1962, pp 195-197.

214- R.A. Steinberg, J. Agr. Res., 52, 1936, pp 439-448.

215- R.A. Steinberg, J. Agr. Res., 55, 1937, pp 891-902.

216- D.J.D. Nicholas, A. Nason and W.D. McElroy, Nature, 172, 1953, p 34.

217- S.Z. Lewin, P.J. Lucchesi and J.E. Vance, J. Am. Chem. Soc., 75, 1953, p 6058.

218- D. Bertrand, Bull. Soc. Chim. Biol., 25, 1943, pp 194-197.

219- C.G.C. Chesters, Biol. Revs. Cambridge Phil. Soc., 26, 1951, pp 239-252.

220- W.S.M. Wold and J. Suzuki, Can. J. of Microbiol., 22, 1976, pp 1093-1101.

221- B.H. Trumpy and N.F. Millis, J. of Gen. Microbiol., 30, 1963, pp 381-393.

222- N.N. Ivanov, V.E. Ivanov and N.N. La Rionova, Arch. Sci. Biol. USSR., 43, 1936, pp 378-381.

223- A.G. Morton and A. MacMillan, J. Exp. Botany, 5, 1954, pp 232-252.

224- R.L. Snell and L.B. Schweiger, British Patent 653808, 1951.

225- M.W. Shepard, US Patent 30831217, 1963.

226- A. Chmiel, Acta Microbiologica Polonica Ser. B, 7(27), 1975, pp 237-242.

227- P. Gerhardt, W.W. Dorrell and I.L. Baldwin, J. Bacteriol., 52. 1946, pp 555-564.

228- P. Gerhardt, W.W. Dorrell and I.L. Baldwin, J. Bacteriol., 62, 1951, p 235.

229- A.W. Dox, J. Biol. Chem., 10, 1911, pp 77-80.

230- K.S. Bhargava, Proc. Indian Acad, Sci., B21, 1945, pp 344-349.

231- S.M. Martin and R. Steel, Can. J. of Microbiol., 1, 1955, p 470.

232- R. Steel, C.P. Lentz and S.M. Martin, Can. J. of Microbiol., 1, 1955, p 299.

233- R.A. Steinberg, J. Agr. Res., 63, 1941, pp 109-127.

234- W.J. Nickerson, Trans. N. Y. Acad. Sci. II, 13, 1951, pp 140-145.

235- S.E.A. McCallan and F. Wilcoxon, Contrib. Boyce Thompson Institute, 3, 1931, pp 13-38.

236- L.J. Sciarini and F.F. Nord, Arch. Biochem., 3, 1943, pp 261-267.

237- M. Zalokar, Arch. Biochem. Biophys., 44, 1953, pp 330-337.

238- E.V. Abbott, Soil Sci., 16, 1923, pp 207-216.

239- F. Challenger and P.T. Charlton, J. Chem. Soc. (London), 1947, pp 424-429.

240- W. Engel and L. Holzapfel, Z. Naturforsch, 9b, 1954, pp 602-606.

241- K. Sakaguchi and S. Baba, J. Agr. Chem. Soc. Japan, 18, 1942, p 1033.

242- A.J. Moyer, J. App. Microbiol., 1, 1953, pp 1-13.

243- E.H. Mosbach, E.F. Phares and S.F Carson, Arch. Biochem. Biophys., 35, 1952, pp 435-442.

244- S. Baba, Bull. Agr. Chem. Soc. Japan, 17, 1941, pp 109-110.

245- M.A. Qadeer, K.M. Khan, M.I.D. Chughtai and M. Ashraf, Pakistan J. of Biochem., 1, 1968, pp 41-48.

246- 57, pp 55-98.

247- W.H. Horr, Plant Physiol., 11, 1936, pp 81-99.

248- J.M. Brannon, Botanical Gazette, 76, 1923, pp 257-273.

249- S.K. Hasija and F.T. Wolf, Mycopathology et Mycologica Applicata, 39, 1970, pp 337-343.

250- M. Kawamura and A. Baba, Shigakenritsu. Tanki Daiaka Gakujutsu Zanshi, 5, 1964, pp 22-29.

251- 147, pp 156-157.

252- A.A. Klyosova and I.V. Churilova, Biokhimiya, 45, 1980, p 1685.

253- W.S. Fong, J.L. Jones and K.T. Semrau, Chem. Proc. Eng., 1980, pp 39-46.

254- G.H. Emert, et al., Chem. Proc. Eng., 1980, pp 47-52.

255- N.D. Millis, B.H. Trumpy and B.M. Palmer, J. of Gen. Microbiol., 30, 1963, pp 365-379.

256- W. Gold and R.J. Kieber, US Patent 3372094, 1968.

257- J. Takahashi and K. Yamada, J. Agr. Chem. Soc. Japan, 32, 1960, pp 310-321.

258- D. Murphy, D.S. Clark and C.P. Lentz, J. Chem. Eng., 1959, pp 157-161.

259- D.D. Jones, M.Sc. thesis, University of Aston in Birmingham, 1972.

260- D.J. Demis, A. Rothstein and R. Meyer, Arch. Biochem. Biophys., 48, 1954, pp 55-62.

261- C.E. Zobell, Advances in Enzymol., 10, 1950, pp 443-486.

262- V. Subramaniam, H.R. Stent and T.K. Walker, J. Chem. Soc., 1929, pp 2485-2492.

263- D. Perlman, Am. J. Bot., 35, 1948, pp 360-363.

264- H. Reischer, Mycologia, 43, 1951, pp 319-328.

265- 57, pp 23.

266- J.A. Blain et al., Biotech. Letters, 1, 1979, pp 269-274.

267- C.G. Sinclair and F. Mauituna, The Filamentous Fungi, Eds. J.E. Smith, D.R. Berry and B. Kristiansen, Edward Arnold Publishers, 4(2), 1983, p 25.

268- S.P.S. Andrew, Trans. Ins. Chem. Engs., 60(1), 1982, pp 3-12.

269- D.H. Philips, Biotech. Bioeng., 8, 1966, pp 456-460.

270- M.Y. Huang and H.R. Bungay, Biotech. Bioeng., 15, 1973, pp 1193-1197.

271- Y. Miura, Advances in Biochemical Engineering Eds. T.K. Ghose, A. Fiecher and N. Blakebrough, Springer-Verlag, Belin, 4, 1976, pp 3-40.

272- E.B. Chain, P. Gvalandi and G. Morisi, Biotech. Bioeng., 8, 1966, pp 595-613.

273- A. Chmiel, Trans. Brit. Mycol. Soc., 68(3), 1977, pp 403-406.

274- A.H. Rose, Chemical Microbiology, Butterworths Press, London, 1968.

275- J. Kovats and L. Sackowska, Przemysl Fermentacyjny I Rolny, 20, 1976, pp 22-25.

276- 57, p 20.

277- Q. Choudhary and S.J. Pirt, J. of Gen. Microbiol., 41, 1965, p 99.

278- J.C. Galbraith and J.E. Smith, Trans. Brit. Mycol. Soc., 52(2), 1969, pp 237-246.

279- 57, p 15.

280- N. Nielsen and D. Dresden, Compt. Rend. Trav. Lab. Carlsberg S'er. Physiol., 22, 1939, pp 287-300.

281- R. Ya. Karlinsh and A.D. Probok, Biosintez organicheskich kislot Riga, Zinatne, 1972.

282- A. Einsele, Process Biochem., 13(7), 1978, pp 13-14.

283- H. Romantschuk and M. Lehtomaki, Process Biochem., 13(3), 1978, pp 16-17.

284- A.B. Metzner et al., Am. Inst. of Chem. Engs. J., 7, 1961, pp 3-9.

285- B.V. Gromov, Microbiologiya, 26, 1959, pp 52-59.

286- 19, pp 272.

287- C.F. Eno and H.W. Reuszer, Soil. Sci., 80, 1955, pp 199-209.

288- G. Muller and I. Forster, Zentralbl. Bakteriol. Parasitenkd., Infeksianskr. Hyg., II Abt., 116, 1963, pp 372-409.

289- L.P. Vokova et al., Izv. Akad. Nauk. SSSR, Ser. Biol., 4, 1977, pp 577-581.

290- F.C. Loughnan, Chemical Weathering of the Silicate Minerals, Elsevier Publishers, 1969.

291- L.A. Matveeva, Kora. Vyvetrivaniya, 14, 1974, pp 227-239.

292- E.B. Schalscha, H. Appall and A. Schatz, Geochim. Cosmochim. Acta, 31, 1967, pp 587-596.

293- R. Schweisfurth, Z. Allg. Mikrobiol., 12(8), 1972, pp 667-671.

294- Anon, Baird Standard Conditions for Atomic Absorption and Flame Emmision Spectroscopy, 1st Edn., 1981.

295- Anon, Esterification and Acylation, Supelco Bull. 721E, 1979.

296- B.D. Cullity, Elements of X-ray Diffraction, 2nd Edn., Addison-Wesley Publishers, 1978.

297- L.V. Azaroff, X-ray Diffraction, McGraw Hill Publishers, 1974.

298- Anon, X-ray Powder Data File, 1-24, Ed. J.V. Smith, ASTM Special Technical Publication 48J, 1960.

299- F. Schneider, Sugar analysis ICUMSA methods, International Commission for Uniform methods of Sugar Analysis, 1979.

300- A. Wohlk, Z. Anal. Chem., 41, 1902, p 91.

301- D. Perlman, H.A. Lardy and M.J. Johnson, Ind. Eng. Chem. Anal. Ed., 16, 1944, p 515.

302- A.I. Vogel, A Textbook of Quantitative Inorganic Analysis, 2nd Edn., Longmans Press, p 248 and 643.

303- W.A. Deer et al., An Introduction to Rock Forming Minerals, 2nd Edn, Longmans Press, 1967.

304- Anon, Can. Min. Metal. Bull., 55(604), 1962, pp 563-570.

305- Anon, Canadian Minerals Yearbook, No. 26, 1976, pp 367-372.

306- J.B. Allen and T.J. Charsley, Nepheline - Syenite and Phonolite, Natural Enviroment Research Council - Institute of Geological Sciences, HMSO, 1968.

307- Anon, Minerals Yearbook, 4, 1963, p 753, 4,1964, p 696.

308- R.M. Levine, Min. J. Ann. Rev., 1983, pp 452-453.

309- E.P. Saggerson, Identification tables for miinerals in thin section, Longmans Press, 1975.

310- M.L. Kieth, Am. Mineral., 24, 1939, p 561.

311- P. Gy, Sampling Nomogram, Minerals et Metaux Societe. Anonyme. Paris.

312- E.J. Pryor, Mineral Processing, 3rd Edn., Elsever Publishers, 1965, pp 571-600.

313- M.L. Wilson, Superconducting Magnets, Oxford, Clarendon, 1983.

314- P. Honig, Principles of Sugar Technology, Elsever Publishers, 3, 1963, p 510.

315- J.P. Cacey, Pulp and Paper Chemistry and Technology, Interscience Publishers, 2nd Edn., 1, 1960, p 210.

316- E.R. Ling, J. Dairy Res., 8, 1937, p 173.

317- W.P. Doelger and S.C. Prescott, Ind. Eng. Chem., 26(11), 1934, pp 1142-1149.

318- K.R.N. Hanson et al., South African National Institute of Metallurgy, Report No. 149(3), 1967.

319- A.M. Ginstling and B.I. Brounshtein, J. Appl. Chem. USSR., 23, 1950, pp 1327-1328.

320- J. Crank, Trans. Faraday Soc., 5, 1957, pp 1083-1091.

321- G. Valensi, Compt. Rend., 202, 1936, pp 309-312.

322- R.E. Treybal, Mass Transfer Operations, McGraw Hill Publishers, 2nd Edn., 1968, p 17.

323- R.E. Carter, Ultrafine Particles, Ed. Kuhn, Wiley Publishers, 1963, pp 419-438.

324- Anon, Encyclopedia of Industrial Chemical Analysis, Eds. F.D. Snell and L.S. Ettre, John Wiley Publishers, 10, 1973, pp 88-89.

325- V.N. Tikhonov, Analytical Chemistry of Aluminium, Halsted Press, John Wiley Publishers, 1973.

326- Anon, Chemical Engineers Handbook, Eds. R.H. Perry and C.H. Chilton, McGraw Hill Publishers, 5th Edn., 1973, 2-54.

327- H.C. Helgeson, Geochim. et Cosmochim. Acta, 35, 1971, pp 421-469.

328- S.J. Pirt, Principles of microbe and cell cultivation, Blackwell, London, 1975.

329- K.A. Andrianova et al., Chem. Abs., 62, 1965, 11846d.

330- 91, pp 451-452.

331- 326, 2-58 to 2-59.

332- B. Atkinson and A.J. Knights, Biotech. Bioeng., 17, 1975, p 1245.

333- 326, 21-24 to 21-25.

334- 147, 6, p 162.

335- O. Samuelson and B. Sjoberg, Ana. Chim. Acta, 14, 1956, pp 121-125.

336- K.B. Bengtson, Alumina process feasibility study and preliminary plant design, US Bureau of Mines Publication, Part 1, 2.1.3, pp 22-23.

337- A.M. Baniel, US Patent 4334095, 1982.

338- Anon, US Govt. Printing Office Code of Federal Regulations, Title 21, 173.280.

339- I.V. Pyatntitskii and V.K. Kharchenko, Ukr. Khim. Zh., 30(1), 1964, pp 311-312.

340- A.E. Torma and I.J. Itzkovitch, Conference on Bacterial Leaching, Ed. W. Schwartz, GBF Monograph No. 4, Weinheim Verlag Chemie, 1977, pp 156-164.

341- B. Atkinson et al., Biotech. Bioeng., 21, 1979, pp 193-200.

342- J.G. Anderson et al., Biotechnology Letters, 2(3), 1980, pp 27-31.

343- A. Whitaker and P.A. Long, Process Biochem., 11, 1973, pp 27-31.

344- Anon, Industrial Minerals, 189, 1984, pp 98-99.

345- 10, p 128.

346- B. Kristiansen and J.D. Bu'lock, Fungal Biotechnology, Eds. J.E. Smith, D.R. Berry and B. Kristiansen, The British Mycological Symposium Series No. 3, Academic Press, 1980, p 24.

347- Pfizer Inc., Private communication.

348- Anon, The Association of American Feed Control Officials, Official Publication, Section 36, 1977, pp 87-88.

349- H.C. DeRoo, The Connecticut Agricultural Experimental Station Bulletin, No. 750, 1975.

350- J. Cran, Proc. Eng., 1978, pp 154-161.

351- F. Habashi, Principles of Extractive Metallurgy, Gordon Breach Science Publishers, Vol 1, 1969, pp 156-165.

352- 30, pp 84-85.

353- 30, pp 41-42.

APPENDIX 1

Computer Programs

All programs are written in superbasic to run on a Sinclair QL microcomputer. A brief description (where necessary) and listing of each program is now given.

Curve fit program. The purpose of this program is to determine the polynomial of any desired degree which best fits a set of experimental data. The program is based on the least squares method of fitting a curve to experimental data that has one independent and one dependent variable.

Given a set of experimental data containing m observations with a weighting factor, independent variable and dependent variable for each observation, the program produces the coefficients of the estimating equation desired, and the standard error of the estimate.

Inputs. The required input data for the program consists of the following.

(a) Number of observations, m, and the degree of polynomial required, n (for m=n+1 a perfect fit ,for the data points in question, is usually obtained).

(b) The number of observations each contains, a weighting factor, w(i), an independent variable, x(i), and a dependent variable, y(i).

Outputs. The coefficients of the estimating equation for the highest degree polynomial desired and the standard error of the estimate, defined by,

$$\text{SEOFE} = \sqrt{\frac{\sum (d_n)^2 w}{\sum w - l1}} \quad ,$$

where d_n is the residual for each observation, w is the weighting factor for each observation, $\sum w$ is the summation of the weighting factors and l1 is equal to the degree of the curve plus 1.

In the listing which follows i,l1,l2,l3,j,k,c,d,s2,s3 t,l,n3,l5,r1 and s4 are working variables; s(100), v(100), b(40,40) are working arrays; the array a(40) holds the coefficients of the estimating equation; and s5 is the standard error of the estimate (SEOFE).

```
5 DIM w(40),x(40),y(40),s(100),v(100),b(40,40)a(40)
6 CLS
10 INPUT "enter number of observations required",m,
"highest degree of polynomial required",n
15 RESTORE
20 IF m>0 THEN GO TO 50
30 PRINT "end of run"
50 LET l1=n+1: LET l2=n+2: LET l3=2*n+1: LET i=0: LET
j=0: LET k=0
70 REM input data x,y,w
90 DATA 0,0.25,1,0.1,0.23,1,0.1,0.07,1,1,0.02,1
100 FOR i=1 TO m
102 READ x(i),y(i),w(i)
110 NEXT i
```

```
250 FOR k=1 TO m
260 LET s(1)=s(1)+w(k)
270 FOR j=2 TO 13
280 LET c=j-1
290 LET s(j)=s(j)+((w(k))*((x(k))^c))
310 NEXT j
330 LET v(1)=v(1)+((w(k))*(y(k)))
350 FOR j=2 TO 11
355 LET c=j-1
360 LET v(j)=v(j)+((w(k))*(y(k))*((x(k))^c))
370 NEXT j
400 NEXT k
430 FOR j=1 TO 11
440 FOR i=1 TO 11
450 LET k=j+i
460 LET b(i,j)=s(k-1)
480 NEXT i
490 NEXT j
530 FOR i=1 TO 11
540 LET b(i,12)=v(i)
550 NEXT i
580 FOR i=1 TO 11
590 LET d=b(i,i)
600 FOR j=i TO 12
610 LET b(i,j)=b(i,j)/d
620 NEXT j
650 LET k=i+1
660 IF k=12 THEN GO TO 810
670 FOR l=k To 11
690 LET t=b(l,i)
700 FOR j=i TO 12
710 LET b(l,j)=b(l,j)-(b(i,j)*t)
720 NEXT j
750 NEXT l
780 NEXT i
810 LET a(11)=b(11,12)
820 LET i=11
830 LET s2=0
840 FOR j=i TO 11
850 LET s2=s2+(b((i-1),j)*a(j))
860 NEXT j
890 LET i=i-1
900 LET a(i)=b(i,12)-s2
910 IF i>1 THEN GO TO 830
915 CLS
930 AT 2,2 :PRINT "number of observations ="! m
940 AT 3,2 :PRINT "degree of polynomial ="! n
945 AT   5,2   :PRINT  "constant"    :AT   5,15   :PRINT
"Coefficients"
950 LINE R 0,0 TO 256,0
960 LET n3=n+1
970 FOR i=1 TO n3
980 LET 15=i+7
990 AT 15,4 :PRINT CHRS$(64+i):AT 15,9 :PRINT a(i)
1000 NEXT i
1900 LET s4=0
1980 FOR k=1 TO m
```

```
1990 LET s3=a(i)
2000 FOR i=1 TO l1
2010 LET c=i-1
2020 LET s3=s3+a(i)*((ABS(x(k))^c))
2030 END FOR i
2060 LET r1=s3-y(k)
2070 LET s4=s4+((ABS(r1))^2)*(w(k))
2090 NEXT k
2099 IF (s(1)-l1)=0 THEN GO TO 2125
2100 LET s5=SQRT (ABS(s4/(s(1)-l1)))
2110 IF  (s4/(s(1)-l1)<0 THEN  PRINT "standard  error of
estimate negative and =",s5
2120 IF  (s4/(s(1)-l1)>=0 THEN PRINT  "standard error of
estimate =",s5
2125 PRINT "perfect fit"
2130 END
```

Program for the prediction of fraction of mineral reacted R, with time. This program is discussed fully in Section 3.1. In the listing which follows m,n and i are counters; t represents time; t1 is the constant time of the introduction of rock; x0,c,b,p and f are working variables; and x1 is the fraction of mineral reacted ,R.

```
5 CLS
10 DIM a(40,2)
15 RESTORE 50
20 FOR m=1 TO 15 :READ a(m,1)
30 INPUT "time between readings mins ",t1
40 CLS
50 DATA   1E-4,2E-4,4E-4,4.5E-4,5.8E-4,6E-4,6.5E-4,7E-4,
7.3E-4,7.5E-4,7.8E-4,7.8E-4,7.8E-4,7.8E-4,7.8E-4,7.8E-4
60 LET n=0:LET t=t1:LET c=0:LET x0=.99
80 FOR n=1 TO 12
90 LET k=a(n,1)
100 LET b=k*t+c
110 LET f=(1-.6666*x0)-((1-x0)^.6666)-b)
120 LET p=(2/3)*((1-((1-x0)^(1/3)))/(1-x0)^(1/3))
130 LET x1=x0-f/p
140 IF ABS(x0-x1)<1E-6 THEN GO TO 170
150 LET x0=x1
155 IF x0>=1 THEN LET x1=1: GO TO 170
160 GO TO 110
165 REM store data
170 LET a(n,2)=x1
175 IF x1=1 THEN GO TO 221
190 LET c=(1-((2/3)*x1)-((1-x1)^(2/3)))
200 LET x0=x1
210 LET t=t+2
215 NEXT n
220 CLS
221 AT  3,2  :PRINT  "time  :AT  3,18  :PRINT  "fraction
reacted"
222 LINE 0,80 TO 200,80
223 FOR i=1 TO 15
234 IF i=1 THEN GO TO 240
```

```
235 IF a((i-1),2)=1 THEN LET a(i,2)=1
240 AT (i+4),2 :PRINT (i*t1):AT (i+4),18 :PRINT a(i,2)
250 NEXT i
260 END
```

Program to determine values of x2 and x3 with time and $kt2_{max}$. This program is discussed fully in Section 3.2. For convenience the curve fit program is integrated into this program to calculate polynomials describing curves of xT at times t and t+ Δt (lines 1070 and 1080, respectively) from experimental data.

In the program that follows i,n and num are counters; txT,tx1,tx2 and tx3 are the total, growth, acid and deactivated cell concentrations, respectively; k2 is $kt2_{max}$; and tx2(50),tx3(50) and tot(50) are working arrays.

```
5 DIM w(40),x(40),y(40),s(100),v(100),b(40,40)a(40)
6 CLS
10 INPUT "enter number of observations required",m,
"highest degree of polynomial required",n
15 RESTORE
20 IF m>0 THEN GO TO 50
30 PRINT "end of run"
50 LET l1=n+1: LET l2=n+2: LET l3=2*n+1: LET i=0: LET
j=0: LET k=0
70 REM input data xT,t,w
90 DATA 20,2.7,1,30,4.7,1,40,6.5,1,50,8,1,60,8.8,1,80,
9.6,1,100,10.07,1,120,10.3,1,140,10.4,1,160,10.54,1,180,
10.64,1,200,10.7,1,220,10.78,1,240,10.82,1,260,10.84,1,
280,10.85,1,300,10.86,1,320,10.88,1
100 FOR i=1 TO m
102 READ x(i),y(i),w(i)
110 NEXT i
250 FOR k=1 TO m
260 LET s(1)=s(1)+w(k)
270 FOR j=2 TO l3
280 LET c=j-1
290 LET s(j)=s(j)+((w(k))*((x(k))^c))
310 NEXT j
330 LET v(1)=v(1)+((w(k))*(y(k)))
350 FOR j=2 TO l1
355 LET c=j-1
360 LET v(j)=v(j)+((w(k))*(y(k))*((x(k))^c))
370 NEXT j
400 NEXT k
430 FOR j=1 TO l1
440 FOR i=1 TO l1
450 LET k=j+i
460 LET b(i,j)=s(k-1)
480 NEXT i
490 NEXT j
530 FOR i=1 TO l1
540 LET b(i,l2)=v(i)
550 NEXT i
580 FOR i=1 TO l1
590 LET d=b(i,i)
```

```
   600 FOR j=i TO 12
   610 LET b(i,j)=b(i,j)/d
   620 NEXT j
   650 LET k=i+1
   660 IF k=12 THEN GO TO 810
   670 FOR l=k To 11
   690 LET t=b(l,i)
   700 FOR j=i TO 12
   710 LET b(l,j)=b(l,j)-(b(i,j)*t)
   720 NEXT j
   750 NEXT l
   780 NEXT i
   810 LET a(11)=b(11,12)
   820 LET i=11
   830 LET s2=0
   840 FOR j=i TO 11
   850 LET s2=s2+(b((i-1),j)*a(j))
   860 NEXT j
   890 LET i=i-1
   900 LET a(i)=b(i,12)-s2
   910 IF i>1 THEN GO TO 830
   1010 DIM tx2(50),tx3(50,tot(10)
   1015 LET txt=0:LET tx2(1)=0:LET tx3(1)=0:LET dxt=10
   1020 LET n=1
   1030 FOR k2=2E-2 TO .1 STEP 5E-2
   1040 LET tx2(1)=0:LET tx3(1)=0
   1050 LET num=1
   1060 FOR time=30 TO 320 STEP 10
   1070 LET xt0=a(1)=a(2)*time+a(3)*(time^2)+a(4)*(time^3)
   +a(5)*(time^4)+a(6)*(time^5)+a(7)*(time^6)+a(8)*(time^7)
   +a(9)*(time^8)+a(10)*(time^9)+a(11)*(time^10)+a(12)*
   (time^11)+a(13)*(time^12)+a(14)*(time^13)+a(15)*
   (time^14)+a(16)*(time^15)+a(17)*(time^16)+a(18)*
   (time^17)
   1080 LET xt0=a(1)=a(2)*(time+10)+a(3)*((time+10)^2)+a(4)
*((time+10)^3)+a(5)*((time+10)^4)+a(6)*((time+10)^5)+a(7) *
((time+10)^6)+a(8)*((time+10)^7)+a(9)*((time+10)^8)+a(10) *
((time+10)^9)+a(11)*((time+10)^10)+a(12)*((time+10)^11)   +
a(13)*((time+10)^12)+a(14)*((time+10)^13)+a(15)*((time+10)
^14)+a(16)*((time+10)^15)+a(17)*((time+10)^16)+a(18)*
((time+10)^17)
   1090 IF  ABS(xT1-xT0)>dxT   AND   (ABS(xT1-xT0)<.4    OR
time>160) THEN GO TO 1095
   1092 LET dxt=ABS(xT1-xT0)
   1095 IF time=30 THEN LET txT=xT0
   1100 IF (time-60)>=10 THEN LET dx1=0: GO TO 1140
   1110 LET x10=5.37-EXP(4.2E-2*(time-30))
   1120 LET x11=5.37-EXP(4.2E-2*(time-20))
   1122 IF time=40 THEN LET x11=0
   1125 IF time=30 THEN LET tx1=x10
   1130 LET dx1=x11-x10
   1140 LET dx2=8
   1143 IF time >65 THEN LET tx1=0
   1150 IF (tx2(num)+dx2)-((txT+dxT)-(tx3(num)+(k2*(.9/(.9+
(1/(dx2/2+tx2(num)))))*(dx2/2+tx2(num))*10))-(tx1+dx1))   >0
THEN LET dx2=dx2-1E-2:GO TO 1145
   1160 LET dx2=dx2+1E-2
```

```
1165 LET tx1=tx1+dx1
1170 LET tx2(num+1)=tx2(num)+dx2
1175 LET dx3=k2*(dx2/2+tx2(num))*10
1178 LET tx3(num+1)=tx3(num)+dx3
1180 LET txT=txT+dxT
1181 LET total=tx2(num+1)+tx3(num+1)+tx1
1182 IF txT=total THEN GO TO 1185
1183 LET tx2(num+1)=tx2(num+1)+((txT-total)/2)
1184 LET tx3(num+1)=tx3(num+1)+((txT-total)/2)
1185 LET total=txT
1186 PRINT time+10, tx2(num+1), dxt
1190 LET num=num+1
1200 NEXT time
1210 LET tot(n)=tx3(num+1)
1220 LET n=n+1
1230 NEXT k2
1240 FOR i=1 TO (num+1)
1250 PRINT tot(i)
1260 NEXT i
1270 END
```

Computer model of fermentation in the presence of nepheline. This program is discussed fully in Section 3.3. In the program that follows t1 is TIME; t2 is the number of minutes in the time increment t; m,j,n,ii and i are counters; fract0 and fract1 are working values of R; v0,v1,v2,v3 and v4 are working variables for numerical integration; u1 is the area under the curve of P with time; u2 is the area under the curve of R with time; rate terms are working variables for the calculation of d^2P/dt^2 and d^2R*NEP/dt^2 ; a limits the time considered after the introduction of mineral; f0,df0,b and c are working variables in the Newton Raphson method; xdif is a working variable in the interpolation of acid cell data; and d and IN are other working variables.

```
130 REMARK Inorder to obtain results of P,R and pH with
time line 1550 should be deleted
140 CLS
150 CLEAR
160 DIM f(2002,2), q(2002,1), ss(200),ff(200),ratq(200),
ratf(200),ratef(200),rateq(200)
170 LET j=1
180 REMARK Set up ranges of nep (mass of nepheline
added), sug (mass of sugar remaining when nepheline is
added) and t1 (time of introduction of nepheline from the
start of fermentation). Note that there is insufficient
memory to include a FOR loop for t1 (TIME), therefore t1 is
incremented in steps of 40 hours by changing its value in
line 190, after each completed cycle of the program (i.e.
when all operations up to line 1880 have been completed)
190 LET a=2000:LET t1=40
200 FOR sug=5 TO 135 STEP 5
210 FOR nep=5 TO 55 STEP 5
220 REMARK Calculate acid concentration and pH at the
outset of fermentation
230 LET inacid=-46.33168 + (1.526094*t1) - (5.914803E-3*
```

```
(t1^2))-(1.767851E-5*(t1^3))+(2.201379E-7*(t1^4))-
(6.62989E-10*(t1^5))+(6.193516E-13*(t1^6))
   240 IF inacid<0 THEN LET pH=1.8
   250 LET pH=((5.3763-LN(inacid/192.1246))/3.829)
   260 IF pH<1.8 THEN LET pH=1.8
   270 LET  R=0:LET  P=inacid:LET  t2=1:LET  f(1,2)=0:  LET
Q(1,1)=inacid:LET fract1=0:LET  f(1,1)=pH:LET  fract0=.9999
:LET remacid=0:LET acid=inacid:LET incacid=0
   280 REMARK Set up time counter
   290 FOR m=t2 TO a STEP t2
   300 IF  P=((.95*sug)+inacid) AND remacid=0  AND j>1 THEN
GO TO 1140
   310 IF R=1 THEN GO TO 570
   320 IF acid+remacid=0 THEN LET pH=6.5: GO TO 340
   330 LET pH  =  (5.3763-LN(((acid+remacid)/2)/192.1246))/
3.829
   340 FOR ii=1 TO 10
   350 REMARK Calculate nepheline rate constant
   360 IF pH>3.82 THEN LET k0=5E-7:GO TO 390
   370 LET k0 =(-3.945098E-5+(1.769306E-3*pH)-(7.838352E-4*
(pH^2))+(8.592752E-5*(pH^3)))
   380 REMARK  Solve  Crank model  for fraction  reacted by
Newton Raphson
   390 IF m=t2 THEN LET c=0:GO TO 410
   400 LET c=1-(2*f((m-1),2)/3)-(1-f((m-1),2)^(2/3))
   410 LET fract0=.99
   420 LET b=k0*m+c
   430 LET f0=(1-(2*fract0/3)-((1-fract0)^(2/3))-b)
   440 LET df0 = (2/3)*((1-((1-fract0)^(1/3)))/((1-fract0)^
(1/3)))
   450 LET fract1=fract0-(fo/df0)
   460 IF ABS(fract0-fract1)<1E-3 THEN GO TO 510
   470 LET fract0=fract1
   480 IF fract0>1 THEN LET fract1=1: GO TO 510
   490 GO TO 430
   500 REMARK Check if all available acid used up
   510 LET f1=P+incacid
   520 IF ((fract1*nep)/.601923)<f1  THEN  LET  remacid=f1-
((fract1*nep)/.601923): GO TO 560
   530 IF ((fract1*nep)>=f1 THEN LET remacid=0
   540 LET R=.99*((f1*.601923)/NEP): GO TO 570
   550 IF R>1 THEN LET R=1
   560 LET R=fract1
   570 REMARK  Calculate  rate  constants  K1  and  K2
corresponding to the current pH and metal loading
   580 LET z1=R*nep
   590 IF  z1<6.15E-2  THEN LET w1=3.23-(z1*1.300813):IF z1
<6.15E-2 THEN LET w2=4.28-(z1*7.642276)
   600 IF z1<.25 THEN LET w3=5.3406-(z1*3.50524)
   610 IF z1>6.15E-2  THEN  LET  w1=3.2055-(2.002002*z1):IF
z1>6.15E-2  THEN LET  w2=3.801666_(z1*4.76086E-2):IF z1>.25
THEN LET w3=4.53106-(z1*.277005)
   620 IF pH<2.3 THEN LET k1=((pH-1.8)*w1)/.5: GO TO 650
   630 IF  pH>2.3 AND pH<3.3  THEN LET k1=((pH-3.3)*(w2-w1)
+w1:GO TO 650
   640 IF   pH>3.3  THEN LET k1=((pH-3.3)*(w3-w2))+w2:GO TO
650
```

```
   650 IF z1<.12 THEN LET w1=.1554-(z1*.2006)
   660 IF z1<.32 THEN LET w2=.18083-(z1*.22542)
   670 IF z1<.25 THEN LET w3=.2018-(z1*.11435)
   680 IF z1>=.12 THEN  LET  w1=.1339-(z1*3.88E-3):IF  z1>=
.32 THEN LET w2=.1086-(z1*9.25E-4):IF z1>= .25 THEN LET w3=
.17458-(z1*1.051E-2)
   690 IF pH<2.3 THEN LET k2=((pH-1.8)*w1)/.5: GO TO 720
   700 IF pH>2.3  AND pH<3.3 THEN LET k2=((pH-2.3)*(w2-w1))
+w1: GO TO 720
   710 IF pH>3.3 THeN LET k2=((pH-3.3)*(w3-w2))+w2
   720 IF k1<0 THEN LET k1=0:IF k2<0 THEN LET k2=0
   730 REMARK  Choose correct curve of x2 vs time according
to pH
   740 LET m1=(t1+m/60)
   750 LET m2=(t1+m/60+t2/60)
   760 IF m1>300 THEN LET incacid=0:GO TO 1100
   770 IF m1>55 THEN GO TO 810
   780 LET x31a=-7.822+(.26345*m1)
   790 LET x32a=-7.822+(.26345*m1)
   800 GO TO 830
   810 LET x31a=1.194903+(.2628295*m1)-(4.137273E-3*(m1^2))
+(2.397898E-5*(m1^3))-(6.057026E-8*(m1^4))+(5.597891E-11*
(m1^5))
   820 LET x31a=1.194903+(.2628295*m2)-(4.137273E-3*(m2^2))
+(2.397898E-5*(m2^3))-(6.057026E-8*(m2^4))+(5.597891E-11*
(m2^5))
   830 IF m1>55 THEN GO TO 870
   840 LET x31b=-14.91261+(.9342592*m1)-(1.706024E-2*(m1^2)
)+(1.42002E-4*(m1^3))
   850 LET x31b=-14.91261+(.9342592*m2)-(1.706024E-2*(m2^2)
)+(1.42002E-4*(m2^3))
   860 LET GO TO 890
   870 LET x31b=35.34877-(.8477324*m1)+(8.638126E-3*(m1^2))
-(4.393358E-5*(m1^3))+(1.090909E-7*(m1^4))-(1.048465E-10*
(m1^5))
   880 LET x31b=35.34877-(.8477324*m2)+(8.638126E-3*(m2^2))
-(4.393358E-5*(m2^3))+(1.090909E-7*(m2^4))-(1.048465E-10*
(m2^5))
   890 IF R>6.15E-2 THEN GO TO 970
   900 LET x31=(16.26016*(x31b-x31a)*R)+x31a
   910 LET x32=(16.26016*(x32b-x32a)*R)+x32a
   920 GO TO 990
   930 IF t1<100 THEN GO TO 970
   940 IF  t1>100 THEN LET xdif=.481-(.5006526-(.3445257*R)
+(.1438126*(R^2))-(2.293981E-2*(R^3))+(1.184741E-3*(R^4)))
   950 LET x31=x31b-xdif:LET x32=x32b-xdif
   960 GO TO 990
   970 LET xdif  =  4.249-(4.241251+(.1711974*R)-(.7496079*
(R^2))+(.2557305*(R^3))-(2.452017E-2*(R^4)))
   980 LET x31=x31b-xdif:LET x32=x32b-xdif
   990 LET xx2=(x31+x32)/2:LET dx2=ABS(x32-x31)
   1000 REMARK Calculate acid  produced  over  the  current
time interval and add to acid left from the last increment
   1010 LET incacid=dx2*k1+xx2*k2
   1020 REMARK  Recalculate average pH  over this increment
and repeat  from  280  until  the  pH  has  converged  (six
increments are normally required)
```

```
   1030 IF (P-inacid)>=(.95*sug) THEN LET incacid=0
   1040 LET pH = (5.3763-LN(((acid + incacid + remacid)/2)/
192.1246))/3.829
   1050 IF pH<1.8 THEN LET pH=1.8
   1060 NEXT ii
   1070 REMARK Check if sugar used up
   1080 IF (P-inacid+incacid)<(.95*sug) THEN LET P=P +
incacid: GO TO 1100
   1090 IF (P-inacid+incacid)>=(.95*sug) THEN LET P=.95*sug
+inacid
   1100 LET IN=((nep*R)+((P-remacid)*.601923))/2
   1110 LET R=IN/nep:LET remacid=P-IN/.601923
   1120 REMARK Store data required
   1130 IF R>=.999 THEN LET R=1
   1140 LET q((m+1),1)=P
   1150 LET f((m+1),2)=R
   1160 LET f((m+1),1)=pH
   1170 IF remacid<=0 THEN LET remacid=0:LET pH=6.5
   1180 LET acid=remacid
   1190 LET remacid=0
   1200 REMARK Check if all nepheline leached, if not
continue to next time increment, otherwise jump out of
cycle
   1210 IF R=1 THEN GO TO 1260
   1220 IF (f((m-1),2)>.99*f(m,2) AND m>10 THEN GO TO 1250
   1230 IF m>150 THEN GO TO 1250
   1240 NEXT m
   1250 IF f((m-1),2)>.99*f(m,2) THEN LET m=m-1
   1260 CLS
   1270 REMARK Calculate areas under curves of acid and
metal leached with time by Simpsons rule
   1280 LET v0=0:LET v1=0:LET v2=0:LET v3=0:LET v4=0:LET
v5=0
   1290 IF INT((m-2)+.1)/2=(m-2)/2 THEN GO TO 1310
   1300 LET m=m-1
   1310 FOR n=2 TO (m-2)
   1320 IF INT((n+.1)/2<>n/2 THEN LET d=4 :GO TO 1340
   1330 LET d=2
   1340 LET v2=v4+(d*(f(n,2)*nep))
   1350 LET v1=v0+(d*(q(n,1)*.601923)
   1360 LET v0=v1:LET v4=v2
   1370 NEXT n
   1380 LET u1 =(v1+q(1,1)*.601923+q((m-1),1)*.601923)*((t2
/60)/3)
   1390 LET u2=(v2+f(1,2)*nep+f((m-1),2)*nep)*((t2/60)/3)
   1400 REMARK Calculate optimisation factor and store the
result
   1410 LET ss(j)=((q(m,1)-inacid)*.601923)/(1+(u1-u2))
   1420 REMARK Calculate d P/dt and d R*nep/dt and store
the results
   1430 LET rate4=0:LET rate6=0
   1440 FOR n=1 TO (m-1)
   1450 LET ratef(n)=(f((n+1),2)-f(n,2))*nep
   1460 LET rateq(n)=q((n+1),1)-q(n,1)-inacid
   1470 NEXT n
   1480 FOR n=1 To m-2
   1490 LET rate3=ratef(n+1)-ratef(n)
```

```
1500 LET rate4=rate4+rate3
1510 LET rate5=rateq(n+1)-rateq(n)
1520 LET rate6=rate6+rate5
1530 NEXT n
1540 LET ratf(j)=rate4/(m-2)
1550 LET ratq(j)=rate6/(m-2)
1560 LET ff(j)=m
1570 PRINT ss(j),ratq(j),ratf(j)
1580 LET j=j+1
1590 GO TO 1800
1600 REMARK Print out values of R, P, and pH with time
1610 INPUT"input to continue",y$
1620 CLS
1630 AT 1,2:PRINT"TIME":AT 1,18:PRINT"FRACTION REACTED"
1640 LINE 0,90 TO 200,90
1650 FOR i=5 TO 80 STEP 5
1660 AT  (i/5+2),4  :PRINT(t1+i/60):AT  (i/5+2),22:PRINT
f(i,2)
1670 NEXT i
1680 INPUT"input to continue",y$
1690 CLS
1700 AT 1,2 :PRINT"ACID":AT 1,18:PRINT"pH"
1710 LINE 0,90 TO 200,90
1720 FOR i=5 TO 80 STEP 5
1730 AT (i/5+2),4  :PRINT  q(i,1):AT  (i/5+2),22  :PRINT
f(i,1)
1740 NEXT i
1750 INPUT"enter to continue",y$
1760 CLS
1770 REMARK Go to next set of conditions
1780 NEXT nep
1790 NEXT sug
1800 REMARK Print out values of optimisation factors,
d^2P/dt^2, d^2R*nep/dt^2 for different conditions tested
1810 FOR i=1 to 200
1820 PRINT ss(i), ff(i)
1830 IF ((i/10)-INT(i/10))=0 THEN INPUT "press key",y$
1840 NEXT i
1850 FOR i=1 TO 200
1860 PRINT ratq(i), ratf(i)
1870 IF ((i/10)-INT(i/10))=0 THEN INPUT "press key",y$
1880 NEXT i
1890 END
```

Program to calculate values of the opimisation factor, OF, from experimental data. This program is identical in structure to lines 1280 to 1410 of the fermentation model, discussed previously. The program is modified so that OF can be calculated directly from experimental data (acid concentration , P, and fraction of nepheline reacted, R).

```
90 RESTORE 160
100 LET nep=6
110 LET m=19
120 LET inacid=3.98
130 DIM q(100),f(100)
140  DATA 4.55,5E-2,5.18,.11,5.96,.17,6.9,.272,7.9,.378,
```

```
8.89,.45,9.65,.545,10.27,.592,10.82,.656,11.4,.715,11.19,
.77,12.4,.815,12.8,.855,13.15,.887,13.5,.913,13.8,.943,14.1
,.966,14.35,.975,14.6,1
   150 FOR i=1 TO 19
   160 READ q(i),f(i)
   170 NEXT i
   180 LET  v0=0: LET v1=0: LET v2=0 :LET v3=0:LET v4=0:LET
v5=0
   190 IF INT((m-2)+.1)/2=(m-2)/2 THEN GO TO 210
   200 LET m=m-1
   210 FOR n=2 TO (m-2)
   220 IF INT((n+.1)/2<>n/2 THEN LET d=4 :GO TO 240
   230 LET d=2
   240 LET v2=v4+(d*(f(n)*nep))
   250 LET v1=v0+(d*(q(n)*.601923)
   260 LET v0=v1:LET v4=v2
   270 NEXT n
   280 LET u1 =(v1+q(1)*.601923+q(m-1)*.601923)*((1/60)/3)
   290 LET u2=(v2+f(1)*nep+f(m-1)*nep)*((1/60)/3)
   300 PRINT (q(m)-inacid)*.601923)/(1+(u1-u2))
```

APPENDIX 2

Estimation of nepheline grain size required for leaching apparatus.

The problem is to estimate the nepheline grain size range which can be maintained in suspension (by the peristaltic pump action) during passage from the liquid holding tank, t1, to the fermenter (down a 0.5 cm diameter pipeline). It is assumed that the viscosity of liquid medium is of the order of 1.4 cp (based on the findings of Solomons (94)), the density of nepheline is approximately 2600 kg/m^3, and the density of the liquid medium is 1000 kg/m^3.

The vertical motion of a spherical particle falling under gravity, and assuming that skin friction is the only resistance, can be described by,

$$y = bt/a + v/a - b/a^2 + (b/a^2 - v/a)e^{-at}$$

where y is the vertical distance moved, a is $18\mu/d^2\rho s$, (where μ is the liquid viscosity, d is the particle diameter and ρs is the solid density), b is $(1-\rho/\rho s)g$ (where ρ is the liquid density and g is the acceleration due to gravity), v is the initial component of velocity in the vertical plane, and t is time. Taking the initial velocity v=0:

$$y = bt/a - b/a^2(1-e^{-at})$$

where $b = 9.81(1 - 1000/2600)$,
$= 6.036$ m/s
and for a 20 µm particle,

$$a = (18\times1.4\times10^{-3})/(20\times10^{-6})\times 2600$$
$$= 20769 \text{ s.}$$

Thus $y = 0.00029t - 1.39\times10^{-8}(1 - e^{-20769t})$
neglecting the exponential term and taking y = 0.5 cm
t = 17 s.

Times for other smaller particles are given below.

Size/ µm	t/ min
2	33.4
5	5.3
10	1.3
20	0.3

At the minimum dilution rate tested (0.006 h^{-1}) for a system capacity of 5 l, and a pipeline (from t1 to the fermenter) 400 cm long and 0.5 cm in diameter, it would take approximately 16 minutes for liquid to travel from t1 to the fermenter. Therefore, on the basis of the above assumptions, nepheline grains should be sized at < 5 µm. Experimental testwork indicated that particles < 10 µm could be adequately suspended for the required 16 minutes.

APPENDIX 3

Estimation of gas flow rate for fermentation.

Oxygen has to be supplied to the fermenter as a gas (compressed air). It is assumed that the fungus oxygen requirement is of the order of 0.2 ml O_2/g fungus/ min, and for a maximum mycelium concentration of 74 g/ 5l medium the supply rate must be 0.33 mmoles/sec.

Neglecting the effects of agitation (gas drag down and turbulence) the mass transfer of gas into solution is given by,

$$N = k_L A (C_G - C_L)$$

where N is the mass flux of oxygen in moles/sec, k_L is the gas-liquid mass transfer coefficient, A is the total interfacial area for mass transfer, C_G is the molar concentration of oxygen in the gas phase and C_L is the molar concentration of oxygen in the liquid phase. Assuming the concentration of oxygen in the air is 20%, C_G is of the order of 8.9×10^{-6} moles/cm^3. According the Andrew (268) the gas-liquid mass transfer coefficient can be described by,

$$k_L a/\varepsilon = 0.4/\mu^{0.5}$$

where a is the interfacial area per unit of liquid volume, ε is the gas-holdup per unit of liquid volume and μ is the liquid viscosity.

Assuming that just sufficient oxygen is to be supplied to satisfy the uptake rate of 74 g of mycelium, i.e. $C_L=0$, and given $C_G = 8.9\times10^{-6}$ moles/cm^3 , $N = 0.33\times10^{-3}$ moles/sec, and μ= 1.3 cp, then,

$$\varepsilon A/a = (0.33\times10^{-3}\times\sqrt{1.3})/(0.4\times8.9\times10^{-6}) = 105.69 \text{ cm}^3 .$$

But note that A=aV (where V is the system volume = 5 l), and for bubbles of radius r,

$$\text{No of bubbles} = 3\varepsilon/4\pi r^3$$

and the area of bubbles per unit liquid volume (a)

$$= 4\pi r^2\times3\varepsilon/4\pi r^3.$$

Thus $aV\varepsilon/a = 105.69 \text{ cm}^3$

and $\varepsilon = 0.02 \text{ cm}^3/\text{cm}^3$.

The average diameter of bubbles produced by the sparger used for testwork was of the order of 0.8 cm, therefore,

$$a = 0.158 \text{ cm}^2/\text{cm}^3 .$$

Under the envisaged fermentation conditions gas flow rates in excess of 0.8 l/min give the required gas hold up. In practice the gas flow rate was maintained at 1-3 l/min.

APPENDIX 4

Operating and capital cost data.

The following data are used to calculate the values in Table 4.5.

Materials required.

Sucrose	inlet concentration	130	kg/m^3
	total fermenter volume	60	m^3
	biomass hold-up	12	tonnes
	dilution rate	0.024	hr^{-1}
	sugar flow	187.2	kg/hr
	molasses flow	374.4	kg/hr
		62.89	tonnes/week

Other materials.

	kg/m^3	tonnes/week	£/tonne
ammonium carbonate	1.8	0.435	1228
potassium phosphate	0.25	0.060	2480
magnesium sulphate	1.2	0.290	558
mycelium		12.000	100

Pumping costs.

	kw	kwh/week
recirculation	4.0×3	2016
leaching	4.0	672
air	2.0	336
mycelium	4.0	672

Capital cost estimation.

From Table 4.6 the capital cost (fermentation only) of a 70 tonne/day citric acid plant is 10% of DM 94×10^6. Therefore a similar fermentation plant built now in the UK would cost,

$$9.4\times10^6\times\frac{155}{120}\times\frac{260}{155}\times\frac{1}{3.7} = £5.5\times10^6$$

where 120, 155 and 260 are the cost indices for West Germany in 1977 and 1984 and the UK in 1984, respectively, and 3.7 is the average 1984 DM to £ exchange rate. Assuming a scale up exponent, n, of 0.8 a 32 tonne/week plant would cost,

$$5.5\times10^6\times\left(\frac{32}{490}\right)^{0.8} = £6.2\times10^5 .$$

Note that this is for fermentation equipment only.

APPENDIX 5

Results of fermentations in the presence of metals.

The following tables give the results of fermentations discussed in Section 3.2.

TABLE A5.1 VALUES OF t1, t2 AND t3 FOR THE DIFFERENT CONDITIONS OF pH AND METAL CONCENTRATIONS TESTED.

pH / metals added/g/l	2.3 t1/ hr	2.3 t2/ hr	2.3 t3/ hr	3.3 t1/ hr	3.3 t2/ hr	3.3 t3/ hr	4.3 t1/ hr	4.3 t2/ hr	4.3 t3/ hr
0.0000	25	35	300	30	55	380	20	52	380
0.0615	25	35	280	25	50	340	20	60	340
0.6160	35	45	220	20	25	300	20	55	320
6.1500	25	35	180	25	80	300	30	65	320

TABLE A5.2 VALUES OF THE NITROGEN YIELD FACTOR FOR THE DIFFERENT CONDITIONS OF pH AND METAL CONCENTRATIONS TESTED.

pH / metals added/g/l	2.3	3.3	4.3
0.0000	12.9	13.8	11.5
0.0615	12.5	14.7	12.5
0.6150	12.1	12.4	9.8
6.1500	11.4	12.1	15.1

TABLE A5.3 VALUES OF TRANSITION CONSTANTS kt1 AND kt2 FOR THE RANGE OF CONDITIONS OF pH AND METAL CONCENTRATIONS TESTED.

pH / metals added/g/l	2.3 kt1/ hr	2.3 kt2/ hr	3.3 kt1/ hr	3.3 kt2/ hr	4.3 kt1/ hr	4.3 kt2/ hr
0.0000	0.146	0.025	0.064	0.025	0.046	0.030
0.0615	0.071	0.040	0.066	0.028	0.038	0.033
0.6150	0.152	0.040	0.061	0.040	0.038	0.020
6.1500	0.135	0.040	0.027	0.030	0.048	0.020

TABLE A5.4 RESULTS OF FERMENTATION IN THE PRESENCE OF METALS FOR pH 2.3 AND 0 g/l METALS.

time/ hr	N/ g/l	xT/ g/l	P/ g/l	1/xT/ l/g	$\dot{x}$T/ g/l/hr	1/$\dot{x}$T/ lhr/g	x1/ g/l	x2/ g/l	x3/ g/l
0	0.29	0.18							
2	0.28	0.20							
4	0.27	0.32							
8	0.25	0.54							
20	0.11	2.17							
25	0.02	3.34		0.29	0.158	6.329	3.34		
30	TR	3.75		0.26	0.108	9.218	2.25		
40		4.34	5.3	0.22	0.048	20.618	0	3.51	0.83
50		4.72	11.4					3.62	1.10
60		5.65	17.0						
70		6.48	21.2						
80		7.30	25.0					3.31	3.99
100		8.00	30.4					2.76	5.24
120		8.24	34.3						
140		8.57	37.5						
150								1.09	7.23
180		8.68	41.6						
200								0.65	7.95
240		8.88	44.7						
250								0.31	8.39
300		8.92	45.5					0	8.92
350		9.11	44.2						
400		8.95	43.7						
450		8.87							
500		8.88							

time/ hr	dP/dt/ g/lhr	dx2/dt/ g/lhr	dP/dt/x2/ 1/lhr	dx2/dt/x2 1/lhr
45	0.61	0.011	0.17	0.003
85	0.41	-0.025	0.127	-0.0078
105	0.32	-0.033	0.123	-0.0126
155	0.136	-0.018	0.117	-0.0153
205	0.066	-0.008	0.109	-0.0139
255	0.030	-0.004	0.110	-0.0137
285	0.020	-0.0025	0.111	-0.0131

TABLE A5.5 RESULTS OF FERMENTATION IN THE PRESENCE OF METALS FOR pH 2.3 AND 0.0615 g/l METALS.

time/ hr	N/ g/l	xT/ g/l	P/ g/l	1/xT/ l/g	$\dot{x}$T/ g/l/hr	1/$\dot{x}$T/ lhr/g	x1/ g/l	x2/ g/l	x3/ g/l
0	0.29	0.14							
2	0.28	0.14							
4	0.27	0.28							
8	0.24	0.50							
20	0.13	1.92							
25	0.03	3.11		0.52	0.181	5.52	3.11		
30	TR	3.62		0.32	0.170	5.88	2.686		
40		4.30	3.8	0.27	0.119	16.66	0		
50		4.82	8.7	0.23				3.705	1.11
60		5.70	14.7	0.20				3.57	2.13
70		6.30	19.0	0.17					
80		7.10	22.5	0.15				3.08	4.01
100		7.72	27.3	0.14				2.47	5.24
120		8.10	30.5	0.13					
140		8.29	32.3	0.12					
150								1.18	7.10
180		8.40	34.2	0.12					
200								0.53	8.07
240		8.73	35.4						
250								0.29	8.45
280								0	8.78
300		8.86	34.7						
350		8.90	33.2						
400		8.72							
450		8.70							
500		8.72							

time/ hr	dP/dt/ g/lhr	dx2/dt/ g/lhr	dP/dt/x2/ 1/lhr	dx2/dt/x2 1/lhr
45	0.88	0.0115	0.236	0.0306
85	0.31	-0.030	0.107	-0.0102
105	0.232	-0.030	0.100	-0.0129
155	0.090	-0.018	0.086	-0.0166
205	0.040	-0.007	0.095	-0.0140
255	0.020	-0.0035	0.101	-0.0125

TABLE A5.6 RESULTS OF FERMENTATION IN THE PRESENCE OF METALS FOR pH 2.3 AND 0.615 g/l METALS.

time/ hr	N/ g/l	xT/ g/l	P/ g/l	1/xT/ l/g	$\dot{x}$T/ g/l/hr	1/$\dot{x}$T/ lhr/g	x1/ g/l	x2/ g/l	x3/ g/l
0	0.29	0.11							
2	0.28	0.12							
4	0.27	0.24							
8	0.24	0.40							
20	0.14	1.78							
25	0.08	2.97		0.56	0.187	5.34	3.60		
30	TR	3.11		0.33	0.133	7.51	2.46		
40	TR	3.92		0.32	0.107	9.34	0		
50		4.54	6.2	0.25	0.07	13.98		3.33	1.21
60		5.37	9.8	0.22	0.07	13.79		2.88	2.48
70		5.81	12.7	0.18	0.06	15.74			
80		6.27	14.9	0.17	0.045	22.20		2.09	4.18
100		6.41	17.6					1.45	4.95
120		6.82	19.0						
140		7.00	20.0						
150								0.57	6.57
180		7.37	21.2						
200								0.19	7.64
220								0	7.52
240		7.52	21.5						
300		7.51	21.5						
350		7.50	21.5						
400		7.52							
450		7.52							
500		7.48							

time/ hr	dP/dt/ g/lhr	dx2/dt/ g/lhr	dP/dt/x2/ 1/lhr	dx2/dt/x2 1/lhr
55	0.272	-0.045	0.088	-0.014
85	0.150	-0.034	0.079	-0.017
105	0.099	-0.025	0.075	-0.018
145	0.044	-0.012	0.070	-0.019
185	0.016	-0.006	0.063	-0.023
205	0.010	-0.004	0.058	-0.022

TABLE A5.7 RESULTS OF FERMENTATION IN THE PRESENCE OF METALS FOR pH 2.3 AND 6.15 g/l METALS.

time/ hr	N/ g/l	xT/ g/l	P/ g/l	1/xT/ l/g	$\dot{x}$T/ g/l/hr	1/$\dot{x}$T/ lhr/g	x1/ g/l	x2/ g/l	x3/ g/l
0	0.29								
2	0.28	0.11							
4	0.27	0.22							
6	0.25	0.38							
8	0.23	0.42							
10	0.21	0.75							
15	0.20	0.80							
20	0.11	1.62							
25	TR	2.89		0.62	0.209	4.78	2.89		
30	TR	3.04		0.34	0.142	7.04	1.92		
40		3.67	0.05	0.32	0.102	9.75	0	2.69	0.97
50		4.02	3.2	0.27	0.049	20.40		2.53	1.49
60		4.92	5.3					2.26	2.66
70		5.34	6.6						
80		5.65	7.6						
100		5.90	8.9					1.06	4.84
120		6.00	9.3						
140		6.15	9.5					0.40	5.75
180		6.20	9.7					0	6.20
240		6.30	9.7						
300		6.30	9.7						
350		6.32	9.7						
400		6.30							
450		6.31							
500		6.28							

time/ hr	dP/dt/ g/lhr	dx2/dt/ g/lhr	dP/dt/x2/ 1/lhr	dx2/dt/x2 1/lhr
45	0.29	-0.0165	0.11	-0.0062
65	0.10	-0.0310	0.05	-0.0146
85	0.09	-0.0300	0.06	-0.0207
105	0.05	-0.0220	0.05	-0.0240
125	0.02	-0.0140	0.04	-0.0240
145	0.02	-0.0080	0.06	-0.0228
165	0.01	-0.0045	0.04	-0.0187

TABLE A5.8 RESULTS OF FERMENTATION IN THE PRESENCE OF METALS FOR pH 3.3 AND 0.0615 g/l METALS.

time/ hr	N/ g/l	xT/ g/l	P/ g/l	1/xT/ l/g	$\dot{x}$T/ g/l/hr	1/$\dot{x}$T/ lhr/g	x1/ g/l	x2/ g/l	x3/ g/l
0	0.29								
2	0.26	0.37							
4	0.25	0.41							
6	0.24	0.57							
8	0.23	0.63							
10	0.22	1.11							
15	0.18	1.70							
20	0.09	2.64		0.37	0.257	3.88			
25	TR	4.28		0.23	0.251	3.98	4.28		
30		5.15		0.19	0.247	4.04	3.88	1.16	0.10
40		7.62	2.0	0.13	0.217	4.59	2.57	4.24	0.81
50		9.50	16.0	0.10	0.119	8.34	0	7.00	2.50
60		10.02	21.4	0.09	0.062	16.00		6.98	3.04
70		10.75	27.7	0.09	0.059	16.95			
80								4.30	6.89
84		11.22	34.3	0.08	0.037	26.66			
100		11.95	40.2	0.08	0.023	37.04		3.04	8.78
112		12.12	43.2	0.08	0.023	42.11			
140		12.55	48.4						
150								1.45	11.44
183		13.20	53.8						
200								0.90	12.60
240		13.95	58.6						
250								0.63	13.35
300		14.05	62.0					0.52	13.53
340								0	14.37
350		14.41	63.0						
400		14.56	62.6						
450		14.50	61.7						
500		14.22	-						

time/ hr	dP/dt/ g/lhr	dx2/dt/ g/lhr	dP/dt/x2/ 1/lhr	dx2/dt/x2 1/lhr
45	1.180	0.276	0.21	0.05
85	0.430	-0.069	0.11	-0.017
105	0.267	-0.049	0.097	-0.017
155	0.183	-0.013	0.133	-0.009
205	0.114	-0.008	0.132	-0.009
255	0.090	-0.003	0.151	-0.005
305	0.050	-0.003	0.135	-0.009

TABLE A5.9 RESULTS OF FERMENTATION IN THE PRESENCE OF METALS FOR pH 3.3 AND 0.615 g/l METALS.

time/ hr	N/ g/l	xT/ g/l	P/ g/l	1/xT/ l/g	$\dot{x}$T/ g/l/hr	1/$\dot{x}$T/ lhr/g	x1/ g/l	x2/ g/l	x3/ g/l
0	0.29								
2	0.28	0.24							
4	0.26	0.43							
6	0.23	0.49							
8	0.22	0.83							
10	0.14	0.94							
15	0.01	2.47		0.41	0.255	3.92			
20	TR	3.60		0.27	0.243	4.14	3.60		
25	TR	4.65							
30		6.00		0.16	0.193	5.19	2.44	2.84	0.72
40		7.13	7.2	0.14	0.095	10.52	0	4.12	3.01
50		7.85	13.2	0.13	0.064	15.62		4.52	3.33
60		8.50	17.0						
70		8.83	19.6	0.11	0.040	25.00			
80								2.35	6.78
84		9.21	22.5						
100		9.82	24.3	0.10	0.035	28.57		1.62	8.20
112		10.30	25.4						
140		11.10	27.3						
150								1.02	10.20
183		11.80	29.0						
200								0.65	11.64
240		12.73	29.7						
250								0.49	12.55
300		13.20	30.0					0	13.20
340									
350		13.58	30.0						
400		13.63	29.6						
450		13.60	-						
500		13.37	-						

time/ hr	dP/dt/ g/lhr	dx2/dt/ g/lhr	dP/dt/x2/ 1/lhr	dx2/dt/x2 1/lhr
40	0.906	0.084	0.22	0.02
80	0.190	-0.049	0.080	-0.021
100	0.087	-0.026	0.053	-0.017
150	0.075	-0.005	0.073	-0.005
200	0.033	-0.007	0.050	-0.010
250	0.020	-0.001	0.041	-0.003

TABLE A5.10 RESULTS OF FERMENTATION IN THE PRESENCE OF METALS FOR pH 3.3 AND 6.15 g/l METALS.

time/ hr	N/ g/l	xT/ g/l	P/ g/l	1/xT/ l/g	$\dot{x}$T/ g/l/hr	1/$\dot{x}$T/ lhr/g	x1/ g/l	x2/ g/l	x3/ g/l
0	0.29								
2	0.28	0.17							
4	0.25	0.36							
6	0.24	0.39							
8	0.23	0.44							
10	0.20	0.56							
15	0.06	1.25							
20	0.02	2.61		0.38	0.189	5.27			
25	TR	3.33		0.28			3.53		
30	TR	3.85		0.26	0.094	10.56	3.38		
40		4.52	5.5	0.22	0.090	11.11	3.02	1.35	0.15
50		5.62	10.5	0.17	0.127	7.84	2.54	2.50	0.58
60		7.30	14.0	0.13			1.91	3.40	1.99
70		8.00	16.8	0.12	0.080	12.50	1.07	4.17	2.76
80							0	4.50	4.13
84		8.51	19.3	0.11	0.031	31.74			
100		9.44	21.0	0.10				3.40	6.04
112		9.78	-						
140		10.39	22.6						
150								1.30	9.23
183		10.84	23.6						
200								0.70	10.40
240		11.37	24.3						
250								0.34	11.07
300		11.81	24.8					0	11.80
340									
350		11.70	24.6						
400		11.86	24.0						
450		12.28	-						
500		12.19	-						

time/ hr	dP/dt/ g/lhr	dx2/dt/ g/lhr	dP/dt/x2/ 1/lhr	dx2/dt/x2 1/lhr
40	0.52	0.109	0.385	0.08
100	0.143	-0.060	0.042	-0.017
150	0.040	-0.027	0.030	-0.020
200	0.038	-0.0096	0.054	-0.013
250	0.010	-0.0070	0.029	-0.020
280	0.008	-0.0032	0.040	-0.016

TABLE A5.11 RESULTS OF FERMENTATION IN THE PRESENCE OF METALS FOR pH 4.3 AND 0 g/l METALS.

time/ hr	N/ g/l	xT/ g/l	P/ g/l	1/xT/ l/g	$\dot{x}$T/ g/l/hr	1/$\dot{x}$T/ lhr/g	x1/ g/l	x2/ g/l	x3/ g/l
0	0.29								
2	0.28	0.28							
4	0.26	0.41							
6	0.24	0.45							
8	0.23	0.79							
10	0.23	0.98							
15	0.15	1.65							
20	0.009	3.32		0.30	0.242	4.12	3.32		
25	TR	4.42							
30		5.82		0.17	0.184	5.43	2.74	2.58	0.49
40		7.01	16.5	0.14	0.134	7.44	1.82	4.24	0.94
50		8.70	27.3	0.11	0.110	9.08	0.37	5.49	2.83
60		9.03	35.0	0.11	0.065	15.18	0	5.19	3.83
70		9.82	39.5	0.10	0.052	19.20			
80								3.75	6.47
84		10.06	44.6	0.09	0.039	25.63			
100		10.68	49.4					2.68	7.99
112		11.22	-						
140		11.86	56.7						
150								1.42	10.66
183		12.60	63.6						
200								0.88	11.97
240		13.32	69.5						
250								0.64	12.58
300		13.95	73.2					0.52	13.43
340									
350		14.10	74.3					0.28	13.82
380								0	14.13
400		14.15	73.8						
450		13.92	72.7						
500		12.01	-						

time/ hr	dP/dt/ g/lhr	dx2/dt/ g/lhr	dP/dt/x2/ 1/lhr	dx2/dt/x2 1/lhr
40	1.65	0.145	0.39	0.034
80	0.42	-0.064	0.112	-0.017
100	0.30	-0.043	0.114	-0.016
150	0.21	-0.014	0.151	-0.0098
200	0.14	-0.0075	0.158	-0.0085
250	0.10	-0.0025	0.161	-0.0039
300	0.08	-0.0040	0.163	-0.0076
350	0.03	-0.0035	0.137	-0.0125

TABLE A5.12 RESULTS OF FERMENTATION IN THE PRESENCE OF METALS FOR pH 4.3 AND 0.0615 g/l METALS.

time/ hr	N/ g/l	xT/ g/l	P/ g/l	1/xT/ l/g	$\dot{x}$T/ g/l/hr	1/$\dot{x}$T/ lhr/g	x1/ g/l	x2/ g/l	x3/ g/l
0	0.29								
2	0.28	0.30							
4	0.27	0.38							
6	0.24	0.47							
8	0.22	0.68							
10	0.11	0.92							
15	0.01	1.30							
20	TR	3.64		0.27	0.352	2.84	3.64		
25		4.32		0.21	0.270	3.70			
30		6.34		0.16	0.193	5.18	3.17	2.38	0.79
40		7.50	14.1	0.13	0.113	8.84	2.48	3.76	1.26
50		8.60	23.0	0.12	0.103	9.70	1.47	4.70	2.43
60		9.56	30.0	0.10	0.079	12.05	0	5.51	4.06
70		10.18	35.0	0.09	0.052	19.23			
80								3.85	6.70
84		10.60	41.0						
100		11.00	45.6					2.61	8.39
120		11.88	49.8						
140		12.20	53.2						
150								1.21	10.87
180		12.90	58.0						
200								0.78	12.32
240		13.20	61.5						
250								0.45	13.23
300		13.85	63.2					0.27	13.40
340									
350		13.82	63.6						
380								0	13.85
400		13.60	62.7						
450		13.58	62.6						
500		13.60	62.7						

time/ hr	dP/dt/ g/lhr	dx2/dt/ g/lhr	dP/dt/x2/ 1/lhr	dx2/dt/x2 1/lhr
40	1.43	0.116	0.38	0.030
80	0.46	-0.073	0.12	-0.019
100	0.26	-0.050	0.10	-0.019
150	0.17	-0.012	0.14	-0.010
200	0.10	-0.008	0.13	-0.010
250	0.06	-0.003	0.15	-0.0077
300	0.02	-0.005	0.09	-0.018

TABLE A5.13 RESULTS OF FERMENTATION IN THE PRESENCE OF METALS FOR pH 4.3 AND 0.615 g/l METALS.

time/ hr	N/ g/l	xT/ g/l	P/ g/l	1/xT/ l/g	$\dot{x}$T/ g/l/hr	1/$\dot{x}$T/ lhr/g	x1/ g/l	x2/ g/l	x3/ g/l
0	0.29								
2	0.26	0.22							
4	0.25	0.28							
6	0.23	0.52							
8	0.21	0.62							
10	0.13	0.87							
15	0.03	1.15							
20	TR	2.85		0.35	0.285	3.50	2.85		
25		4.00		0.25	0.235	4.25			
30		5.20		0.19	0.182	5.47	2.38	2.48	0.40
40		6.50	7.5	0.15	0.140	7.14	1.69	4.25	0.56
50		8.00	15.7	0.13	0.100	9.85	0.67	5.47	1.86
60		8.53	23.6	0.12	0.060	15.53	0	5.89	2.64
70		9.25	30.0						
80								5.00	4.83
84		10.00							
100		10.33	43.3					4.09	6.24
120		10.70	49.0						
140		10.98	53.3						
150								2.02	9.08
180		11.38	60.2						
200								1.04	10.51
240		11.90	65.7						
250								0.56	11.44
300		12.25	67.8					0.30	11.95
340									
350		12.30	66.7						
380								0	12.27
400		12.30	66.3						
450		12.20	-						
500		12.20	-						

time/ hr	dP/dt/ g/lhr	dx2/dt/ g/lhr	dP/dt/x2/ 1/lhr	dx2/dt/x2 1/lhr
40	1.38	0.149	0.32	0.035
80	0.55	-0.045	0.11	-0.009
100	0.44	-0.045	0.108	-0.011
150	0.21	-0.030	0.105	-0.015
200	0.128	-0.010	0.123	-0.012
250	0.066	-0.007	0.119	-0.013
300	0.038	-0.003	0.127	-0.011

TABLE A5.14 RESULTS OF FERMENTATION IN THE PRESENCE OF METALS FOR pH 4.3 AND 6.15 g/l METALS.

time/ hr	N/ g/l	xT/ g/l	P/ g/l	1/xT/ l/g	$\dot{x}$T/ g/l/hr	1/$\dot{x}$T/ lhr/g	x1/ g/l	x2/ g/l	x3/ g/l
0	0.29								
2	0.28	0.20							
4	0.27	0.42							
6	0.24	0.46							
8	0.16	0.57							
10	0.11	0.78							
15	0.03	1.32							
20	TR	2.73							
25		3.84							
30		4.37					4.37		
40		4.62	3.2				3.75		
50		6.00	9.5				2.75	3.00	0.25
60		7.39	17.0	0.16	0.138	7.22	1.14	5.01	1.24
70		8.48	23.6	0.13	0.124	8.06	0		
80		9.05	29.8	0.12	0.083	12.04		5.37	3.68
100		9.97	38.3	0.11	0.064	15.50		4.81	5.16
120		10.10	43.5	0.10	0.026	38.09			
140		10.48	46.7						
150								2.25	8.23
180		10.52	51.0						
200								1.04	9.56
240		10.64	53.6						
250								0.52	10.14
300		10.70	53.8					0	10.70
340									
350		10.65	53.6						
380									
400		10.65	52.7						
450		10.60	-						
500		10.58	-						

time/ hr	dP/dt/ g/lhr	dx2/dt/ g/lhr	dP/dt/x2/ 1/lhr	dx2/dt/x2 1/lhr
50	0.98	0.202	0.30	0.067
80	0.58	-0.038	0.10	-0.006
100	0.41	-0.052	0.08	-0.011
150	0.15	-0.037	0.07	-0.016
200	0.06	-0.015	0.06	-0.014
250	0.036	-0.007	0.07	-0.013
280	0.029	-0.003	0.08	-0.012

Nomenclature

Symbols, definitions and dimensions are given for characters, in most cases as they appear, in Chapters 2-4 only. Units are given, where necessary, in terms of the dimensions time (S), mass (M), temperature (T) and length (L).

$(S_a)_{ave}$	average cross-sectional area of a single spore	L^2
$(S_a/F_a)_{ave}$	or (S/F), average area covered by spores per frame per drop diameter.	L^2
$(S/F_a)_{ave}$	average number of spores per frame per drop.	-
	variance.	-
l	average of major and minor mineral grain dimensions.	L
x	mineral proportion.	-
z'	z number for Gaussian distribution.	-
C(0)	initial metal concentration.	M/L^3
C(*)	equilibrium metal concentration.	M/L^3
V	solvent volume per mass of adsorbant.	L^3/M
k',n'	Freudlich constants.	-
z	$V_p/\alpha V_r$.	-
M_r	molecular weight of reactant.	-
D	diffusion coefficient for the movement of the reagent through silica gel.	L^2/S
C	reagent concentration.	M/L^3
α	stoichiometric factor.	-
ρr	reactant density.	M/L^3
r_0	original radius of mineral grain.	L
R	fraction of mineral reacted.	-
K	reaction rate constant.	S^{-1}

K(ave)	average value of the reaction rate constant.	S^{-}
n,m,N'	are numerical counters.	-
t	represents time.	S
t(n),t(n+1)	times corresponding to n and (n+1), respectively.	S
R(n),R(n+1)	fractions of mineral reacted corresponding to n and (n+1), respectively.	
k''	equilibrium constant.	S^{-}
V_p	specific volume of product.	L^3
V_r	specific volume of reactant.	L^3
x1	mass of growth cells per unit fermentation volume.	M/L
x2	mass of acid cells per unit fermentation volume.	M/L
x3	mass of deactivated cells per unit fermentation volume.	M/L
$\mu 1(max)$,$\mu 1$	maximum and working values of the specific growth rates of growth cells, respectively.	S^{-1}
$\mu 2(max)$,$\mu 2$	maximum and working values of the specific growth rates of acid cells, respectively.	S^{-1}
S	mass of carbon source per unit fermentation volume.	M/L
k	saturation constant for the growth limiting substrate.	S^{-1}
kt1	transition coefficient for the change from growth to acid cells.	S^{-1}
kt2	transition coefficient for the change from acid to deactivated cells.	S^{-}
kt2(max)	maximum value of kt2.	S^{-1}
P	mass of acid products per unit fermentation volume.	M/L
K1	acid rate constant.	-
K2	acid rate constant.	S
xT	total cell mass per unit fermentation volume.	M/L

Ø1	period of time corresponding to the transition from S growth to acid cells.	
Ø2	period of time corresponding to the transition from S acid to deactivated cells.	
t1	time of the start of Ø1 and Ø2.	S
t2	time of the end of Ø1.	S
t3	time of the end of Ø2.	S
x1	mass of growth cells per unit of fermentation volume at t=0.	M/L
N	mass of nitrogen source per unit of fermentation volume.	M/L
kn	saturation constant for nitrogen.	M/L
N(0)	nitrogen concentration at t=0.	M/L
k'''	a constant.	-
x1*	mass of growth cells per unit fermentation volume corresponding to N=kn.	M/L
ks	Contois coefficient.	M/M
x2	dx2/dt.	M/L^3
SUG	mass of sugar per unit fermentation volume at t=t1.	M/L
NEP	mass of nepheline added per unit fermentation volume.	M/
TIME	time of addition of nepheline from t=0.	S
INACID	initial estimate of the mass of acid per unit fermentation volume available for leaching purposes.	M/L
REMACID	estimate of acid remaining at the end of the current time interval.	M/L
XX2	estimate of the average mass of cells per unit fermentation volume present during the current time interval.	M/L

$\Delta x2$	estimate of the difference between the acid cell concentration at the start and end of the current time interval.	M/L
INCACID	estimate of the free acid remaining at the end of the current time interval.	M/L^3
P(max)	the maximum concentration of acid produced.	M/L^3
AREA	area difference between plots of predicted actual and theoretical maximum metal concentrations as functions of time.	L^2
TOT	theoretical maximum mass of nepheline per unit fermentation volume that could be leached by exhausting all available acid.	M/L^3
OF	TOT/AREA (or TOT/(1+AREA))	M/L^3
a,b,c,	polynomial constants.	-
F1	working value of the total acid available for leaching.	M/L^3
z1	working value of aqueous metal concentration.	M/L^3
K1(1)-K1(3)	working values of K1.	-
K2(1)-K2(3)	working values of K2.	S
IN	adjustment variable.	-
R_m, R_{m-1}	values of R corresponding to counters m and (m-1), respectively.	-
h	working variable for numerical integration.	-
U1,U2	areas under the curves of predicted actual and theoretical maximum metal concentrations as functions of time, respectively (note AREA=U1-U2).	L^2
U	material flowrate through system.	M/L^3
V	system volume.	L^3
C0	concentration of unaltered nepheline at the inlet.	M/L^3

C1	concentration of unaltered nepheline at the outlet.	M/L
C(1),C(2)	capital costs of plants 1 and 2, respectively.	£
S(1),S(2)	capacities of plants 1 and 2, respectively.	M/S
n''	Cran scale factor.	-
LM1	Solution corresponding to optimised liquid medium 1.	-